INFORMATION TO USERS

This manuscript has been reproduced from the microfilm master. UMI films the text directly from the original or copy submitted. Thus, some thesis and dissertation copies are in typewriter face, while others may be from any type of computer printer.

The quality of this reproduction is dependent upon the quality of the copy submitted. Broken or indistinct print, colored or poor quality illustrations and photographs, print bleedthrough, substandard margins, and improper alignment can adversely affect reproduction.

In the unlikely event that the author did not send UMI a complete manuscript and there are missing pages, these will be noted. Also, if unauthorized copyright material had to be removed, a note will indicate the deletion.

Oversize materials (e.g., maps, drawings, charts) are reproduced by sectioning the original, beginning at the upper left-hand corner and continuing from left to right in equal sections with small overlaps. Each original is also photographed in one exposure and is included in reduced form at the back of the book.

Photographs included in the original manuscript have been reproduced xerographically in this copy. Higher quality 6" x 9" black and white photographic prints are available for any photographs or illustrations appearing in this copy for an additional charge. Contact UMI directly to order.

UMI®

.

University of Alberta

Defining the Interactions of Troponin-C with Troponin-I by Nuclear

Magnetic Resonance Spectroscopy

By

Ryan Todd McKay   ©

A thesis submitted to the Faculty of Graduate Studies and Research in partial fulfillment

of the requirements for the degree of Doctor of Philosophy

Department of Biochemistry

Edmonton, Alberta

Spring, 1999

Canada

University of Alberta

Library Release Form

Name of Author: Ryan Todd McKay
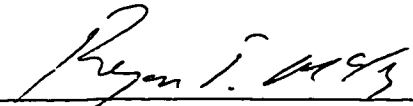
Title of Thesis: Defining the Interactions of Troponin-C with Troponin-I by Nuclear Magnetic Resonance Spectroscopy

Degree: Doctor of Philosophy

Year this Degree Granted: 1999

Permission is hereby granted to the University of Alberta Library to reproduce single copies of this thesis and to lend or sell such copies for private, scholarly, or scientific research purposed only.

The author reserves all other publication and other rights in association with the copyright in the thesis, and except as hereinbefore provided, neither the thesis nor any substantial portion thereof my be printed or otherwise reproduced in any material form whatever without the author's prior written permission.

Signature:_____

Address: 94 Queens Road
Lethbridge, Alberta
Canada, T1K3W3

April 16th, 1999

"… don't give into hate, that leads to the darkside."

Obi-wan Kenobi, 'StarWars – The Empire Strikes Back',

Those who know can not explain,

those who don't can not understand.

Rebar, 10551 Whyte Ave. Ed. AB. 1993-1995

University of Alberta
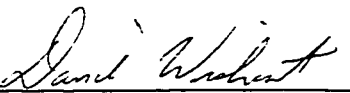
Faculty of Graduate Studies and Research
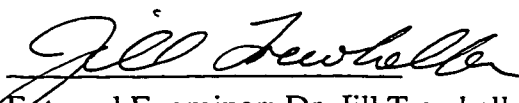
The undersigned certify that they have read, and recommend to the Faculty of Graduate Studies and Research for acceptance, a thesis entitled *'Defining the Interactions of Troponin-C with Troponin-I by Nuclear Magnetic Resonance Spectroscopy'* submitted by *Ryan Todd McKay* in partial fulfillment of the requirements for the degree of *Doctor of Philosophy*.

Supervisor: Dr. Brian D. Sykes

Committee Member: Dr.   Charles Holmes ·

Committee Member: Dr. Paul G. Scott

Committee Member: Dr. David S. Wishart

External Examiner: Dr. Jill Trewhella

Date: April 16, 1999

Abstract

HSQC NMR spectroscopy was used to monitor the resonance frequency changes of the backbone amide groups belonging to ^{15}N-N-TnC upon addition of synthetic skeletal $TnI_{115-131}$. Utilizing the change in amide chemical shifts, the dissociation constant for 1:1 binding of $TnI_{115-131}$ to N-TnC in either low salt, or 100 mM KCl samples was determined to be 28 ± 4 μM and 24 ± 4 μM, respectively. The off rate of $TnI_{115-131}$ was determined to be 300 s^{-1} from observed N-TnC backbone amide HSQC cross-peak line widths, and the binding site on N-TnC was determined to be in the "hydrophobic pocket". The structure of the regulatory domain of chicken skeletal troponin-C (residues 1-90) when complexed with the major inhibitory region (residues 96-148) of TnI was determined. The stoichiometry of the complex was determined to be 1:1, with a dissociation constant in the 1-40 μM range. The structure of troponin-C in the complex was calculated from 1039 NMR distance and 111 dihedral angle restraints, and the binding site was determined to also be in the hydrophobic pocket of calcium saturated troponin-C. TnI_{96-148} was found to bind to the regulatory domain of troponin-C very similarly, but not identically, to $TnI_{115-131}$ thought to represent the major interaction site of troponin-I for this domain of troponin-C. The kinetics and energetics of the binding of three troponin-I peptides, (TnI_{96-131}, TnI_{96-139}, and TnI_{96-148}), to TnC were investigated using NMR spectroscopy. The kinetic off rate and dissociation constants (respectively) for TnI_{96-131} (400 s^{-1}, 32 μM), TnI_{96-139} (65 s^{-1}, < 1 μM) and TnI_{96-148} (45 s^{-1}, < 1 μM) binding to TnC were determined from simulation and analysis of the behavior of HSQC spectra taken during titrations of TnC with these peptides. Two-dimensional ^{15}N-edited TOCSY and NOESY spectroscopy were used to identify 11 C-terminal residues from the

^{15}N-labeled TnI$_{96-148}$ that were unperturbed by TnC binding. TnI$_{96-139}$ labeled with ^{13}C at four positions (Leu^{102}, Leu^{111}, Met^{121}, and Met^{134}) was complexed with TnC and revealed single bound species for Leu^{102}, and Leu^{111}, but multiple bound species for Met^{121} and Met^{134}. TnI$_{115-131}$ was found to bind to calcium-saturated E41A with a K$_d$ of 300 ± 100 mM and changes in chemical shift behavior indicate that calcium binding site I may adopt the calcium bound structure in the presence of peptide.

Preface

My goal in writing this thesis was to concisely communicate the sum of my work here at the University of Alberta, but also to ensure that anyone reading this manuscript would come away with insight into what it was I did for all those years. I did not write this thesis for someone already an expert in the field of NMR or muscle physiology. I wrote this to provide reference for myself in the future (how I did things and why), and to help others move on to the next exciting experiments. I will attempt to describe the tests that did, and did not work so that others can avoid my pitfalls and plights. I hope you come away with a strong and confident understanding of my work, and perhaps even a smile.

Acknowledgements

I also owe a great deal to the following people (presented in order of our first encounter as best I can recall) who had a more personal effect on this thesis: Ron Odagaki (my wingman and co-pilot), Joel Dacks (our bard), Gerald Audette (our gate keeper), Chris Eskiw (confidante and injured reserve), Stacy Stocki (Your OTHER left), Karen Koyko (our Red head), and Andy Agasway (my sensai of 'blad'in), thanks to all of you for soccer, volleyball, R.A.T.T., Rebar, rollerblading, and exploring the world with me. To Heather Berjested for introducing me to the one place where I found the music. To Chantel Deering, Mila Bannerje, and Lynette Bailey for sharing the music. Thank you all for being the few who have "seen what I have seen". Words can't describe what you guys did for me. To Kelsey Douglas Prenevost, for sharing your friendship, family, and life with me since kindergarten. To Deryck Nicholas Hamer Webb for friendship, going through the hell (and back again) of football/highschool, and for entire conversations without a word even being spoken. To Yvonne Stepanov, for saving my life.

Research. Thanks go to each organization for being there in extremely tough economic times.

Table of Contents:

Equations

Figures

Tables

†*Symbols, Nomenclature or Abbreviations*

SR, sarcoplasmic reticulum; **N-terminal**, Amino terminal; **C-terminal**, carboxy-terminal; **TnIp**, inhibitory peptide residues 104-115; **TnC**, Troponin C; **TnI**, Troponin I; **TnT**, Troponin T; **xN-TnC**, N-terminal regulatory domain of chicken skeletal Troponin C residues 1-90 'x' determines skeletal (s) or cardiac (c); **HMJ model**, Herzberg-Moult and James model for calcium saturated conformation of TnC(10); **high salt**, NMR sample containing 100 KCl; **low salt**, NMR sample containing no added KCl; **DSS**, 2,2-dimethyl-2-silapentane-5-sulfonate; **HSQC**, $^1H,^{15}N$-heteronuclear single quantum correlation spectroscopy; $\Delta\delta$, total chemical shift change for an individual backbone NH pair; $\Delta\delta_{Total}$, total chemical shift change for all monitored residues; K_d, dissociation constant; k_{off}, the off rate of $_{TnI115-131}$ in the N-TnC•TnI$_{115-131}$ complex; δ_{obs}, observed chemical shift of cross-peak; P_f, population of free N-TnC; P_b, population of bound N-TnC; δ_f, NMR chemical shift of free N-TnC nucleus; δ_b, NMR chemical shift of bound N-TnC nucleus; Δv_{ex}, line width of a HSQC cross-peak; τ_{ex}, exchange lifetime; Δv_f, NMR line width of unbound N-TnC line width; Δv_b, NMR line width of bound N-TnC; K_{dimer}, dissociation constant of N-TnC dimer; **E41A**, the substitution of Ala for Glu at position 41 of calcium saturated sN-TnC; **C-TnC**, C-terminal domain of troponin-C; **NMR**, nuclear magnetic resonance; **NAD**, the structural unit of N-TnC comprising the N, A and D helices; **BC**, the structural unit made up of the B and C helices; **TnI$_{96-148}$**, troponin-I peptide corresponding to residues 96-148; **NOE**, nuclear Overhauser effect; A_{600}, absorbance at 600 nm; **CSI**, chemical shift index; **A/B**, the angle between the A and B helices; **B/C**, angle between the B and C helices; **C/D**, angle between the C and D

helices; **A/D**, angle between the A and D helices; **TnI$_x$**, synthetic skeletal troponin-I peptide containing residues designated by the subscript value "x"; **TnC•TnI$_{96-131}$**, [U-^{15}N,^{13}C]TnC•TnI$_{96-131}$; **TnC•TnI$_{96-139}$**, [U-^{15}N, ^{13}C-Ala]TnC•TnI$_{96-139}$; (Chapter IV only) **TnC•TnI$_{96-148}$**, [U-^{15}N,^{13}C-Ala]TnC•TnI$_{96-148}$; **^{15}N-TnI$_{96-148}$**, [U-^{15}N]TnI$_{96-148}$; **^{13}C-TnI$_{96-139}$**, [U-^{13}C-(100%)Leu^{102},-(50%)Leu^{111}, ^{13}CH$_3$-(100%)Met^{121},-(50%)Met^{134}]TnI$_{96-139}$; **^{15}N-TnI$_{96-148}$•TnC**, [U-^{2}H]TnC•[U-^{15}N]TnI$_{96-148}$; **^{13}C-TnI$_{96-139}$• TnC**, [U-^{2}H,^{15}N]TnC•[U-^{13}C-(100%)Leu^{102},-(50%)Leu^{111}, ^{13}CH$_3$-(100%)Met^{121},-(50%)Met^{134}]TnI$_{96-139}$; **^{13}C-HSQC**, 2D-^{13}C-edited heteronuclear single quantum correlation NMR spectroscopy; $\Delta G^{\ddagger}_{off}$, activation energy of the reverse reaction.

Chapter I: Introduction[1]

A. Muscle and Contraction

1. Mobility

Motility occurs on many levels including, but not limited to, active membrane

transport, progression of polymerases along DNA, and segregation of replicated

chromosomes. More commonly recognized examples of cellular or macroscopic mobility

include flagella, cilia, and muscle contraction. Muscle contraction is primarily utilized in

higher organisms and is involved in locomotion, eating, and nearly all forms of non-

chemical communication. Corresponding to the different functions there are different

types of muscle tissue. Type I (smooth) or slow twitch contracts slowly but with high

endurance while Type II (skeletal) or fast twitch muscle is only capable of short bursts of

activity, and has a distinct striated appearance when viewed by contrast microscopy.

Skeletal muscle typically lacks a large majority of the mitochondria found in Type I

muscle, and therefore utilizes more anaerobic glucose metabolism. Type I (e.g. intestinal

walls, uterus, and large blood vessels), is characterized by slow, long contractile periods

under phosphorylation dependent regulation, and is involuntary. Smooth muscle includes

cardiac tissue that performs highly aerobic respiration but is striated in appearance like

skeletal. Cardiac also differs from other types of smooth muscle tissue because it does

not appear to be regulated primarily by phosphorylation and is self-stimulated, though the

contractile rate is influenced by external stimuli.

2. The Signal for Contraction

---

[1] General information and figures for the introduction were adapted from (1-3)
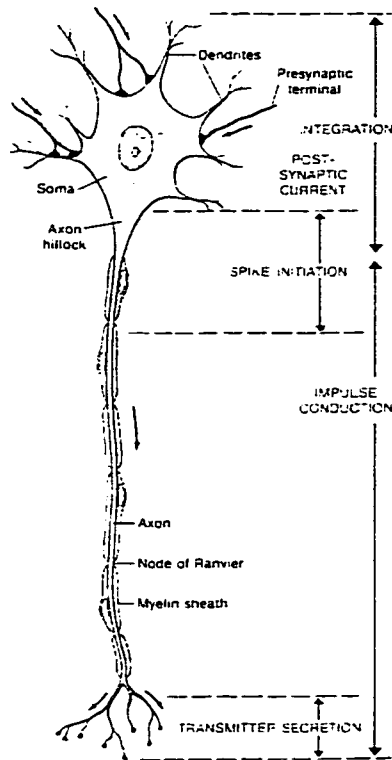
Figure I-1

Vertebrate spinal motor-neuron with the axon and surrounding myelin sheath (Figure adapted from (*3*)).

Skeletal muscle contraction is voluntary and under the control of motor neurons (Figure I-1). Neurotransmission occurs in the form of impulses from the central or autonomic nervous system (*e.g.* jerk reflex). The signal may be passed (usually in a chemical form) from a neuron to other neurons, to glands, or muscle. The signal, or impulse, is electrical in nature and occurs in the form of an ionic concentration wave traveling down the neuron. All cells produce ion gradients across the plasma membrane by ion-specific pumps, and neurons specifically transport K^+ (139 mM in the cell, 4 mM in the extra-cellular space) and Na^+ (12 mM cell, 145 mM outside) into and out of the cell, respectively, in an ATPase dependent manner. The concentration imbalance (a voltage potential referred to as an Action Potential) which is transiently released by removal of the impermeability (opening of membrane channels) to Na^+ followed very quickly by K^+. The voltage changes at the location of the impulse from -81 mV inside the 'resting' cell to approximately +30 mV. The cell membrane quickly (within 0.5 - 1 ms) regains selective, active permeability (*i.e.* pumps K^+ in and Na^+ out) and will not 'fire' again until the pre-signal equilibrium is re-established. For long neurons, several spaced impulses may be traveling down the nerve cell at once. Interestingly the rate of propagation of impulses occurs up to 100 m/s in myelinated (insulated) nerves, and only 10 m/s in non-

myelinated neurons. The type of neuron dictates the maximal rate at which a muscle may

respond to the impulse.

    The ion concentration (electrical) wave arrives at a muscle cell and triggers a

cascade of events. The impulse causes the release of Ca^{2+} from the sarcoplasmic

reticulum (Figure I-2).
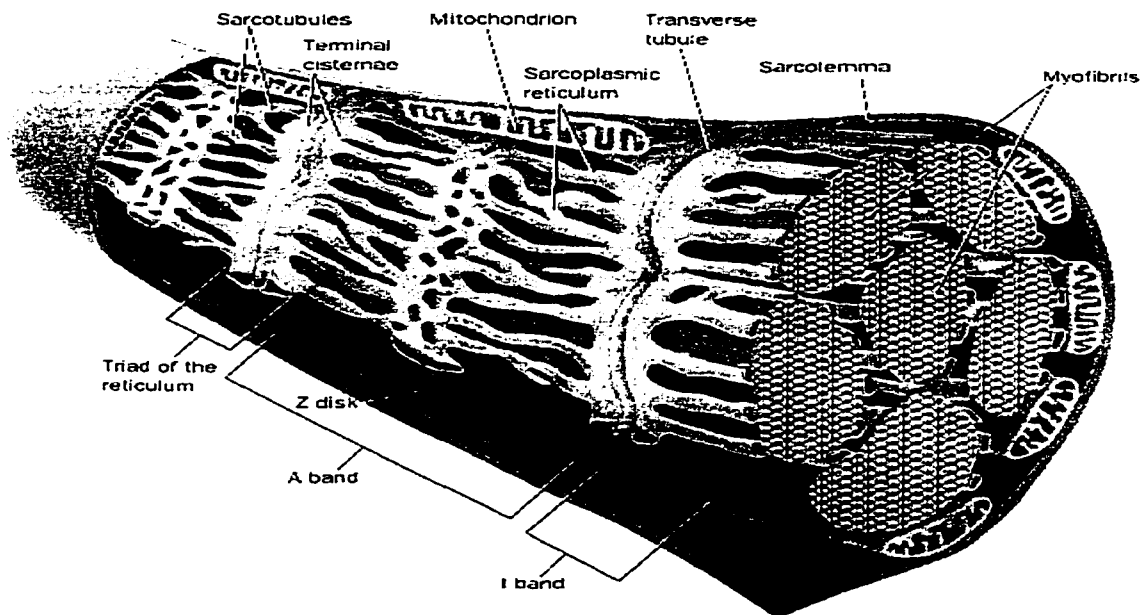
Figure I-2

Cartoon of the myofibrils showing the SR in yellow (adapted from (*1*)).

    The sarcoplasmic reticulum (SR) is derived from the endoplasmic reticulum and

contains ATPase dependent Ca^{2+}-specific pumps that remove Ca^{2+} from the cytosol.

Calcium concentrations in the resting muscle cell are approximately 10^{-7} M while the

concentration inside the SR exceeds 10^{-3} M (see Berridge *et al.* (*4*) for an excellent

review of calcium versatility and utilization). Proteins such as calsequestrin store

calcium in the SR (more than 40 Ca^{2+} molecules are bound by a single calsequestrin

molecule). Aside from the utilization of Ca^{2+} as a signal, intra-cellular Ca^{2+}

concentrations are kept low due to the abundance of various phosphate esters, which

could form low solubility calcium phosphates. The nerve impulse causes the abrupt

transient release of calcium from the SR into the muscle cell. Less than 1 msec is

required for calcium to flood the cell, and in that period cellular Ca^{2+} levels rise from less

than 10^{-7} M to approximately 10^{-5} M.

3. Muscle Cell
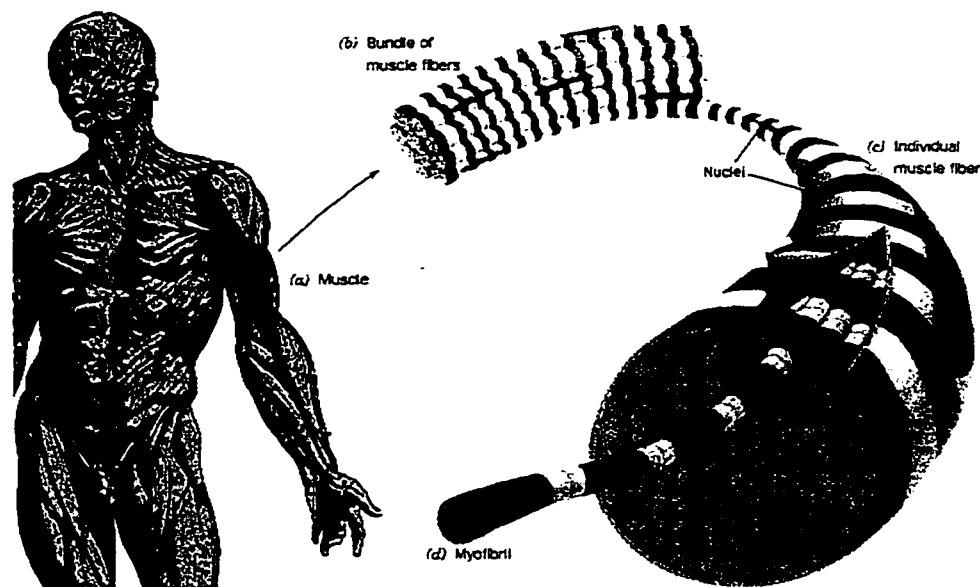
Figure I-3

Organization of skeletal muscle tissue: (a) Muscle, (b) muscle fiber bundles, (c)
multinucleated cells forming a muscle fiber, and (d) myofibrils (figure adapted from (1)).

Skeletal muscle tissue (Figure I-3) is composed of parallel bundles of muscle

fibers. Each individual fiber is a multi-nucleated cell, surrounded by an electrically

excitable plasma membrane, and is composed of parallel packed myofibrils. The striated

appearance of myofibrils (Figure I-3, and I-4) results from the in-register packing of A-

and I-bands making up a single repeating unit called a sarcomere figure I-4). Sarcomere

length shortens upon stimulation, and the macroscopic effect of multiple sarcomere

response is muscle contraction. The different marked zones in Figure I-4 are composed

of interdigitating thick (H zone) and thin filaments (I-band), and each sarcomere is

anchored to the adjacent sarcomere by the "Z-disk". The Z-disk is composed of several

proteins (*e.g.* α–actinin) and links two opposed sets of thin filaments. Other proteins

such as desmin and vimentin are proposed to maintain the myofibrils in register. Titan, a

3600 kDa protein (estimated to be over 33,000 residues!) extends from the thick filament

to the Z-disk through the I-band.
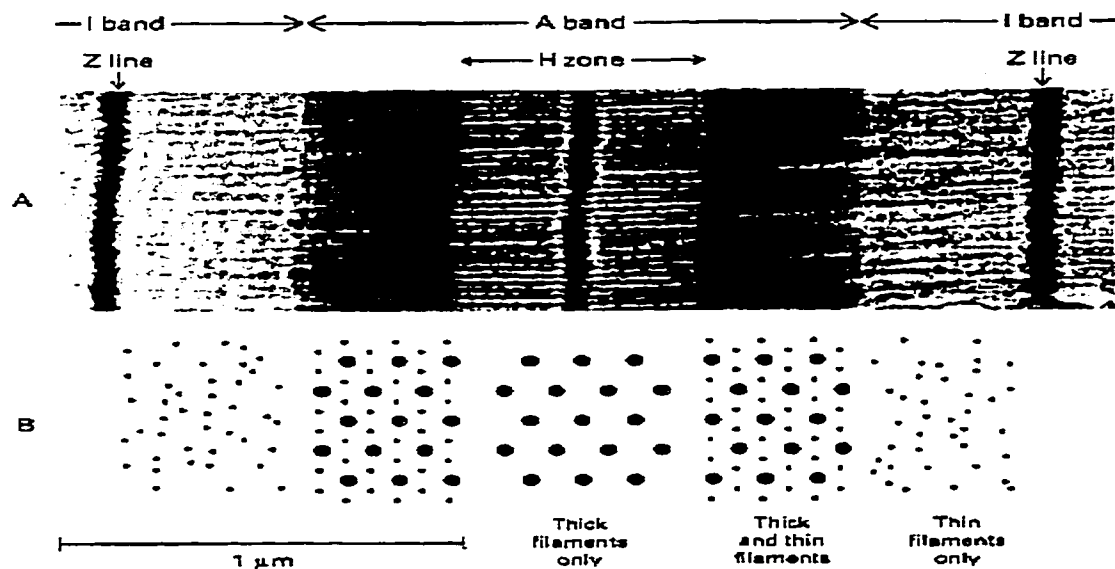
Figure I-4

(A) Electron micrograph of a skeletal muscle myofibril (longitudinal). (B) Diagrams of cross sections corresponding to the micrograph shown above (figure adapted from (2)). The dark line in the H-zone is sometimes referred to as the M-disk.

Titan is thought to function with a spring like mechanism and maintain the thick filament

centered. This may account for the more random cross-sectional appearance of thin

filaments (cross-sectional views, Figure I-4b) which lack a supporting structure. The

thick filaments are also maintained in-register[2] via the 'M-disk' that is composed of two

relatively unstudied molecules called the C- and M-proteins, respectively.

4. Thick filaments
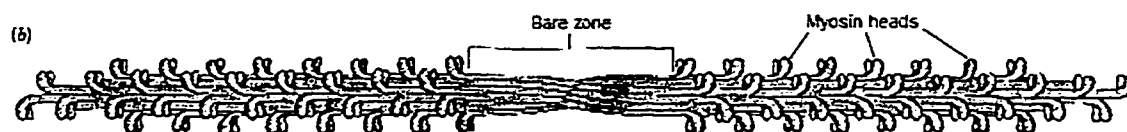
Figure I-5

The thick filament is composed of several hundred myosin molecules in a repeating staggered array (figure adapted from (1)).

a.) Myosin

---
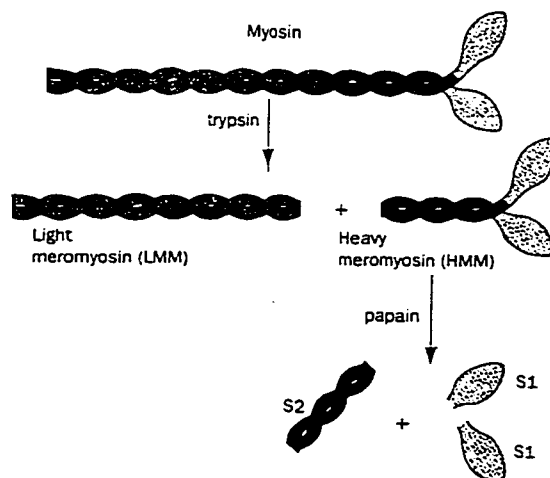
[2] Most electron microscopy showing muscle tissue out of register is an artifact.

Figure I-6

Enzymatic cleavage pattern of myosin showing the S1 globular head (light gray) and coiled coil tail (modified from (*1*)).

The thick filaments are approximately 150 Å in diameter, and composed almost entirely

of myosin (520-540 kDa) protein molecules (Figure I-5). As can be seen in the figure,
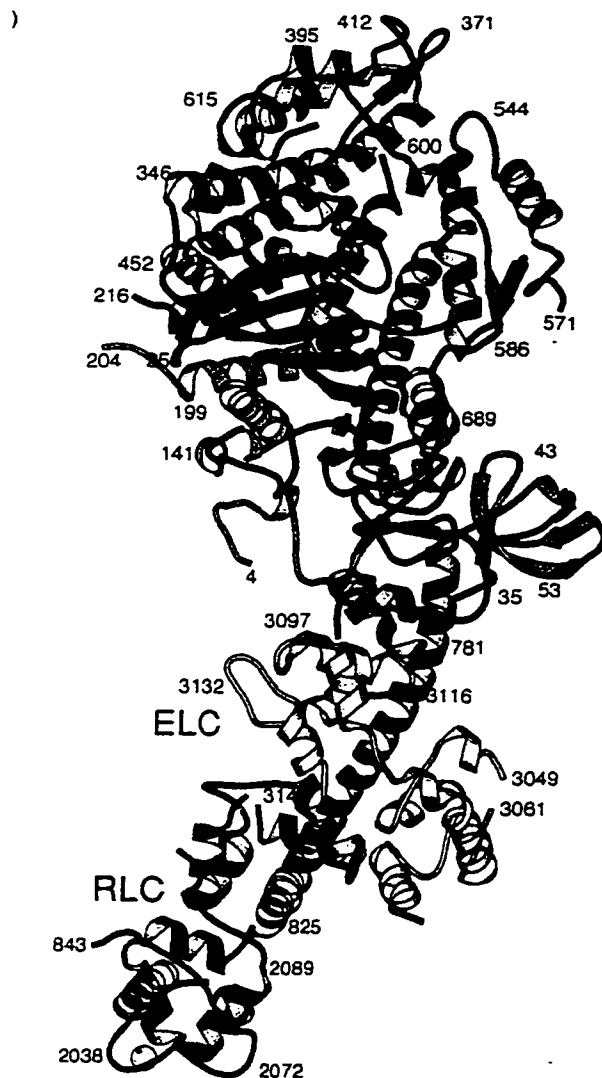
myosin molecules on either side of the Z-disk are in opposite orientations. Myosin is made up of a heavy chain (220 kDa), essential light chain (ELC), and regulatory light chain (RLC, both light chains are ~15-20 kDa), and exists as an α-helical coiled coil with a large globular head (Figure I-6, and I-7). Controlled digestion of myosin with trypsin generates a long coiled coil section (light meromyosin or LMM) and the N-terminal globular section with a coiled coil tail (heavy meromyosin or HMM). Further digestion of HMM with papain will release the globular (S1) head. The S1 region of myosin hydrolyzes ATP and is the force generating subunit for

contraction. Myosin or the isolated S1 region can form cross-bridges with the thin

filament protein actin (A-band to H zone, see *5. Thin filament* below), and hydrolyze

ATP in the absence (albeit slowly), or presence of actin.

Figure I-7

Myosin with the ELC and RLC (yellow and purple, respectively. Modified from (5))

The binding sites for actin and ATP are on opposite sides of the S1 head of myosin.

This requires the transmission of released energy from ATP hydrolysis, and the effects of

actin binding, through the hydrophobic core of myosin. Interestingly, this role of core

involvement in signaling through a protein is becoming recognized in several systems

(*e.g.* muscle regulation (*6,7*), prion strain and cross species susceptibility[3], and certain

types of bacterial pathogenic responses[4] may depend on small equilibrium shifts without

large structural change in core regions to 'activate' responses). Also noteworthy is that

ATP binds to myosin with an association constant of 3×10^{11} M^{-1}, and considering a

diffusion limited on rate constant, this strength of ATP binding corresponds to 5 min per

off event ($k_{off} = 1/300$ s). Once hydrolyzed the resulting ADP has much less affinity.

These kinds of kinetic and energetic details will be the primary focus of chapter V.

b.) The Essential (ELC) and Regulatory Light Chain (RLC) of Skeletal Muscle

The role in skeletal muscle of the light chains in complex with myosin is still

relatively unknown. The presence of the light chains in the S1 head of myosin is not

necessary for regulation or contraction. The light chains do however increase the rate of

sarcomere contraction, but without altering the ATPase activity. This seeming

contradiction is thought to be explained by stabilization of the S1 region of myosin

allowing for a 'longer' power stroke for each ATP molecule expended. The overall

---

[3] Personal communications with C. Dobson, 1998, and R.T.M. candidacy examination.

[4] Regulation of bacterial pathogenic response, Cavanagh, J. personal communication and manuscript(s) in preparation.

homology of the structure and modes of binding of the ELC and RLC when compared to

troponin will be addressed in subsequent chapters.

5. Thin filaments

Figure I-8

X-Ray crystal structure of actin (adapted from Kabsch *et al.* pdb # 1ATN)

a.) Actin

The thin filaments are approximately 90 Å in diameter and primarily composed of

actin (42 kDa). Under low ionic strength conditions the predominant form of actin is

globular (G-actin) and contains one molar equivalent of ATP. With normal cellular salt

concentrations actin: hydrolyzes ATP, has a high affinity for the resulting ADP molecule,

spontaneously polymerizes (filamentous, or F-actin), and the polymers dimerize into a

coiled coil. Each actin monomer in the filamentous form is comprised of 4 sub-domains

with domains 3 and 4 pointing into the helix making contacts with domains 3 and 4 of an

adjacent actin molecule. Myosin and actin alone account for 80-95% (60-70% myosin,

and 20-25% actin) of total skeletal muscle protein. Actin is a fairly ubiquitous protein

and makes up 5-10% of eukaryotic cellular proteins. Non-muscular actin exists in almost

equal portions in the globular and filamentous forms, and plays a role in egg fertilization,

phagocytosis, microvilli, cellular division, and neuronal axon signaling (*i.e.* actin takes

part in signal propagation as well as the mechanical result, albeit in different cells). In

muscle cells the predominant form is F-actin which 2.17 monomers per left handed turn

(i.e. 60 Å rise per turn). Another component of the thin filament is nebulin that is an 800

kDa protein (approximately 7000 residues) and consists of a repeating 35-residue motif.

The motif binds to actin and is thought to control the length of thin filament

polyermization (as might occur with titan and the thick filaments).

b.) Tropomyosin

A major component of the thin filament is tropomyosin. Each tropomyosin

molecule (284 residues, and approximately 70 kDa for the dimer) lays parallel to the thin

filament across seven actin monomers (Figure I-9),

Figure I-9

A model of the thin filament showing actin (string of spheres), Tm (small string of atoms running diagonally from top left to bottom right), and the Tn complex (hammer shaped molecule). Figure adapted from (*1*).

and exists as a homo-dimer. Tropomyosin, like actin, forms an α-helical coiled coil, but with a length of approximately 400 Å. Tropomyosin binds in the groove of the actin-coiled coil (thus winding around actin), overlaps subsequent tropomyosin molecules in a head to tail fashion, and plays a role in regulation that will be discussed in more detail in the following sections.

c.) Troponin

The last component of the thin filament is the troponin complex which, along with tropomyosin, accounts for almost a third of the thin filament's mass. This complex is made up of three proteins named troponin-C (the calcium binding member), troponin-I (the inhibitor of contraction), and troponin-T which is thought to hold the entire complex together, maintain the position of the complex on the thin filament, and accelerate the hydrolysis of ATP by myosin. Troponin-C, -I and their interactions with each other will be the major focus of this thesis, and are discussed in each chapter. The interactions with the rest of the troponin complex will be discussed below.

6. Mechanism of contraction

The globular head of myosin performs the physical work through the release of energy acquired from the hydrolysis of ATP. Myosin turns over ATP at a rate of 0.05 s^{-1}, but the rate increases to 10 s^{-1} in the presence of actin (thus the name **Act**ivator of myos**in**). We also know that myosin forms transient cross-bridges with actin, and that actin does not increase the rate of ATP hydrolysis directly but instead increases the rate of release of the ADP product. The most widely accepted model for the mechanism of contraction is the 'Sliding Filament Model' (Figure I-10). In this model myosin begins bound to actin. The binding of a single molar equivalent of ATP to myosin causes the

dissociation of the acto-myosin complex. The subsequent hydrolysis of ATP causes a

structural change in myosin with the analogy of cocking a hammer on a gun. The release

of the inorganic phosphate molecule allows the re-binding of the now 'cocked' or excited

myosin onto actin. The release of ADP allows the return of myosin to the 'uncocked' or

ground state and the movement of the thick and thin filaments in relation to one another.
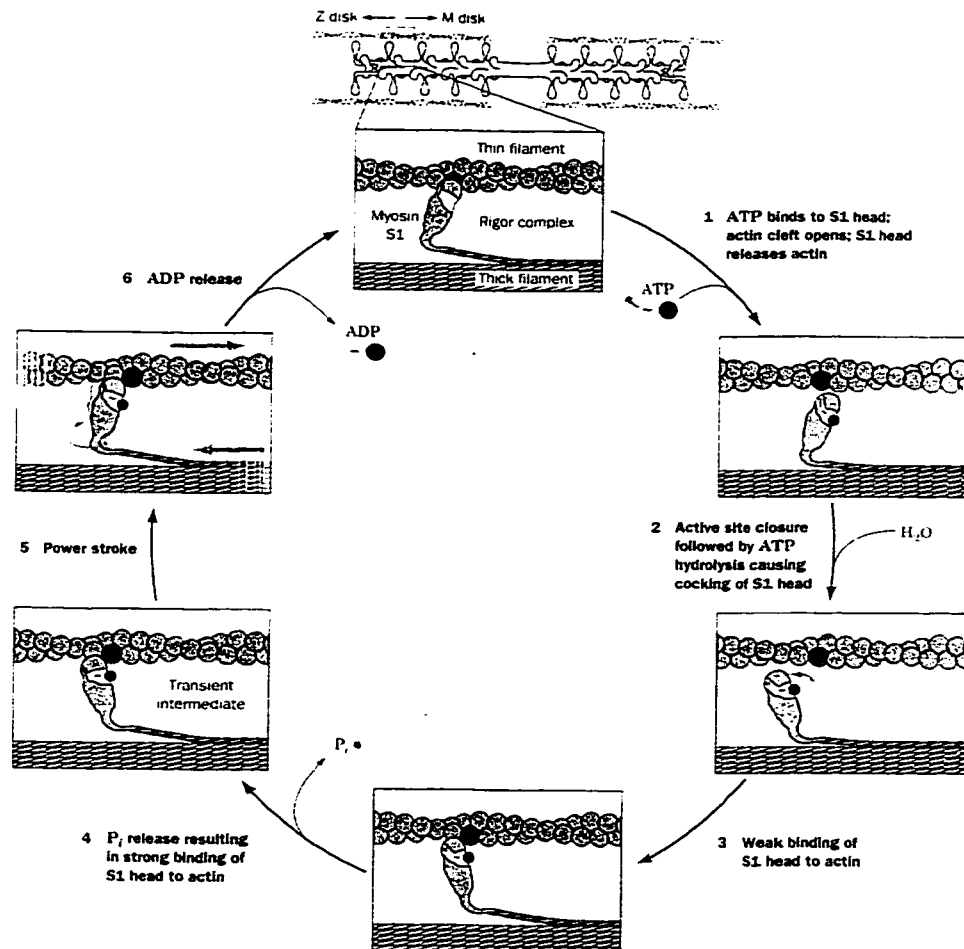
Figure I-10

Proposed model for the generation of force in muscle (adapted from (*1*)).

The repeated release, cocking, re-binding, and firing of multiple myosin molecules (often

thought of as myosin walking along the thin filament) in a single thick filament is thought

to result in the even generation of force throughout the sarcomere, and macroscopically

the muscle. Elucidating the regulation of this 'firing' is the focus of this thesis and

requires a more detailed look at troponin and the present models of regulation.

B. The Troponin Complex

1. Troponin-T

Troponin-T (TnT) is the largest protein in the Tn complex (37 kDa, 263 residues)

and the least studied (see (8,9) for review). Work on TnT has focused on several regions

isolated by chymotryptic and/or cyanogen bromide cleavage. The regions include T1 and

T2 (chymotryptic fragments) comprising residues 1-156 and 157-263, respectively, and

CB1 and CB2 (cyanogen bromide fragments) encompassing residues 1-151, and 71-151,

respectively. The solubility of TnT, or the isolated sub-regions, is highly dependent on

the ionic concentration, and the presence of other members of the troponin complex (e.g.

intact TnT is more soluble in the presence of TnI and TnC). TnT has been shown to

interact with troponin-C (TnT•N-TnC (10), TnT•C-TnC (11), for reviews of TnC•TnT

see (8,12) and references therein), and TnI (via heptad repeating sequences in both TnI.

and TnT (13)), but TnT is mostly known for its interactions with tropomyosin (see

(12,14) and references therein). The amino-terminal region of TnT is helical, interacts

with Tm, and is responsible for heightened activation of actomyosin-ATPase in the

absence of calcium. The C-terminal of TnT is necessary for the proper regulation of

contraction, is thought to adopt a globular structure, and maintains the presence of

TnI•TnC in a calcium-independent fashion on the thin filament. Specifically the last 50

residues of TnT have been shown to interact with the N-terminal region of TnI

(approximately residues 1-96). In addition, residues within the 150-180 region of TnT

appear to interact with Tm residues at the head to tail overlap of Tm (*14,15*).

Interestingly the C-domain of TnT is necessary, but not sufficient, for the full recovery of

contractile velocity. It has been suggested that TnT plays a more active role in calcium

signal transduction to Tm though there is at present minimal supportive evidence for this

hypothesis (see (*16*) and references therein).

2. Troponin-C

Troponin-C (approximately 162 residues totaling 18 kDa) is unlike the other

members of the Tn complex in many ways. For example the high resolution structure of

partially calcium saturated TnC (at pH 5) has been known for quite some time (*17,18*),

while the fully calcium saturated structure has more recently been solved by NMR in

solution (*19,20*) and by x-ray crystallography (*21,22*). TnC is mostly globular, consisting

of two homologous domains supposedly separated by a long rigid helical linker (forming

an overall dumbbell appearance). Low angle x-ray (*23,24*), NMR solution structures on

both cardiac and skeletal TnC (*19,25,26*), and x-ray and solution structures on many

homologous calcium binding proteins (*e.g.* calmodulin (*27-30*), ELC, and RLC (*5*)) have

indicated either that the TnC linker is helical with a kink, or virtually unstructured when

alone in solution or in a binary complex with TnI. Low pH also seems to cause a more

extended structure (*31-33*), and the most recent structural work seems to again suggest

that TnC may be more extended when bound in the Tn complex with Tm (*34*).

a. Domains

The N- and C-terminal domains of TnC are composed of five and four α-helices

(labeled N-, A-, ..., D- for the N-domain, and E-, ..., H- for the C-domain, in order of the

primary amino acid sequence) respectively, and are connected by a short anti-parallel β-

sheet (approximately 3 residues per strand). In addition each domain has two positively

charged metal ion binding sites (highest affinity for calcium with lower affinity for the

smaller magnesium ion, see (6) and reference therein). The two sites have been shown to

bind in either an independent (35) or cooperative (36) fashion, with cooperativity of

binding energy presumably being passed through the interconnecting β-sheet. We know

that the N-domain is required for the proper regulation of contraction and that preventing

the N-TnC from responding to calcium eliminates TnC activity (37). Calcium binding to

C-TnC can be eliminated without affecting TnC regulatory ability, although without

calcium binding in the C-domain of troponin-C is more easily removed from the Tn

complex (see (9) and references therein).

b. EF hand

Each metal binding site in TnC is formed by a helix-loop-helix called an EF hand

motif. The motif was first described by Kretsinger's lab (38) while elucidating a carp

muscle buffering protein named parvalbumin. The EF hand, helix-loop-helix motif is

found in proteins such as calmodulin, troponin, parvalbumin, and S100, and is among the

5 most common protein motifs in animal cells (6). For a full description at the atomic

level of an EF hand motif the reader is directed to the excellent paper by Strynadka et al.

(21). Proteins that bind calcium have been generally classified into two groups. The first

group contains the buffering proteins that have multiple binding sites and maintain a high

affinity of calcium (e.g. calsequestrin). The second group, termed regulatory proteins,

has in general fewer calcium binding sites and the binding of calcium is often associated

with large structural changes. Some proteins have EF hand motifs but are not bound by

calcium in the functional proteins nor do all the sites fulfill a regulatory or even a

functional role. For example, RLC and ELC bind one and zero molar equivalents of calcium, respectively yet still perform their function in myosin. Another example is cardiac TnC that has been shown (as far back as 1977) to bind only three moles of calcium (*39*). In skeletal muscle troponin the binding of calcium in each EF hand is a result of six protein carbonyl groups coordinating to the metal ion with an additional coordination from a solvating water molecule oxygen atom. The large number of coordinating atoms causes cross-linking of different segments of the protein, and can result in large structural re-arrangements. Also, accommodation of the calcium ion causes hydrophobic core rearrangement and reduces the stability of the apo structure (see Chapter V). The smaller size of magnesium results in coordination by only five or six liganding groups in total (*6*).

In TnC there are two pairs of metal binding sites (two in each domain) referred to as sites I+II and III+IV based on the location in the primary amino acid sequence. The first two binding sites located in the N-domain are calcium specific with calcium dissociation constants in the 0.8 - 23 μM range (*35*). The affinity of N-TnC is sensitive to the calcium signal from the SR causing contraction. Sites III and IV (located in the C-domain), bind magnesium ($K_d \sim 10^{-3}$ M) or calcium ($K_d \sim 10^{-7}$), and it is not certain if these sites remain magnesium saturated during the calcium transient.

c. The Hydrophobic Patch

The end result of calcium binding and the corresponding structural changes is the exposure of a group of hydrophobic residues that, in the apo state, are buried inside the hydrophobic core. The secondary structure remains virtual unchanged upon metal binding, and the exposure of hydrophobic residues is the movement (often referred to as

opening) of the B and C helices away from the N, A and D helices (often refered to as the

NAD unit) which remain invariant. This movement of the B and C helices is a result of a

change in inter-helical angle between the B/A and C/D helices. The degree of movement

has been defined and examined elsewhere (40), and it is sufficient to mention here that

there is some debate as to the degree of opening, and to the significance of any

differences found in 'opening'. Interestingly the C-domain of TnC appears to have little

or no definable structure when devoid of metal ions (41), while N-TnC seems to have a

stable three-dimensional structure both apo- and calcium saturated.

The eventual result of calcium binding to TnC is the release of ATPase inhibition

caused by the presence of TnI on actin. The calcium dependent exposure of hydrophobic

surface area on TnC was hypothesized to be the mechanism of regulating the interaction

between TnC and TnI. Specifically, the hydrophobic pocket of calcium saturated TnC

was thought to bind and/or disrupt TnI (e.g. kinetically, structurally, or sterically) in some

fashion thus eventually allowing acto-myosin to hydrolyze ATP and muscle contraction

to occur. Chapters II and III deal specifically with identifying the location(s) of

interaction, and structure of the regulatory domain of TnC while bound to regions of TnI,

while the subject of Chapter IV is the location of TnI interactions on intact TnC.

The hydrophobic patch is also theorized to be the location of dimerization

between N-TnC molecules. Interestingly, the dimerization becomes more pronounced

and calcium independent at low pH (33). This increased dimerization occurs despite the

fact that at low pH N-TnC does not bind calcium and should therefore have less exposed

hydrophobic surface area. The location and extent to which TnC dimerizes can have

strong influences on the measurement of interactions with other members of the Tn

complex and will be discussed in greater detail later.

3. Troponin-I

The inhibitory protein binds to TnC (calcium dependent and independent), TnT,

Tm and actin (calcium dependent only in the presence of TnC). TnI is 24 kDa (182

residues) and very little high-resolution structural information is known about the protein.

Attempts by this author (and several others in the same lab) to acquire information

regarding intact TnI and TnI peptides of several lengths, alone or in the presence of other

members of the Tn complex (over the last five years) have met with very limited success.

TnI (and its interactions) has been dealt with in each of the introductions for the

individual chapters. The following section shall attempt to present an overview of the

published information with an emphasis on the location of interaction between TnC and

TnI.

C. Complexes between TnC and TnI

We know that TnI and TnT interact via heptad repeats that are absent in TnC (*13*),

and that the binary complex of TnI•TnC has affinity for TnT and the actin•Tm complex

but not isolated Tm (*42,43*). The entirety of the binary, and higher order interactions

exceeds the scope of this introduction, and I will instead focus primarily on the TnI•TnC

complex.

Many papers, spanning almost thirty years, have attempted to elucidate the exact

location, mechanism, and strength of interaction(s) between TnC and TnI in the presence

or absence of metal ions. Special care must be taken when comparing measurements of

affinity or sites of interaction since different mutations, substitutions, labels, location of

labels, concentrations, and conditions for complex formation are often used. Amino acid

substitutions have been shown to have surprisingly large effects on calcium binding. For

example, in the homologous protein CaM, the calcium dissociation constant (k_{off}) was

drastically reduced by a single substitution. The substitution caused a **25 fold** increase in

calcium affinity (7). Substitutions can be associated with little, or no, structural change[5]

yet can alter cooperativity ((35) and references therein) and may result in differing

binding affinities of ions and peptides. Another example is F29W and F105W mutants of

TnC or the isolated domains; these probes are thought to be sensitive to peptide binding

in either domain of TnC. Contrary to the previous statement F29W-TnC is oblivious to

the presence or absence of calcium in the C-domain of TnC. This is unexpected because

the presence of calcium is responsible for the structuring of the entire C-domain of TnC

((41,44) and references therein). This suggests either that the probe in the N-domain is

directly perturbed by peptide binding in the C-domain of TnC (contact from the C- to the

N-domain), or that one of the initial statements is untrue (this will be discussed further in

Chapter VI).

The introduction sections of chapters II-IV deal specifically with binary

interactions of TnC with TnI. The next few sections in this chapter will attempt to

concisely summarize interactions of TnI with TnC reported prior to information

contained in this thesis, grouped according to the techniques used and roughly in

chronological order. The sub-sections will be ordered as follows: affinity

chromatography, gel filtration and electrophoresis, ATPase inhibition (often coupled with

affinity chromatography), CD and fluorescence, cross-linking, and finally low angle x-

---

[5] The F29W substitution in N-TnC resulted in only a small change in structure, but caused unfavorable
steric strain on Trp[29], K. Bateman, James Lab, personal communication at the 1998 CFBS meeting.

ray, neutron, and NMR studies. The specific energetics and kinetics of interactions will

be discussed in Chapter V.

1. Chromatography and Gels

One of the first reports of binary interaction(s) between TnC and TnI came from

Head *et al.* in 1974 who utilized gel electrophoresis and affinity chromatography to

demonstrate complex formation (*45*). Similar methodology was used independently by

Weeks *et al.* (*46*) and Leavis *et al.* (*11*) to refine the interaction to the TnC_{83-134} fragment

(in a Ca^{2+} dependent fashion) complexed with TnI, and TnI with Ca^{2+} binding sites I, II

and III, respectively. The Leavis finding was disputed in 1981 when Grabarek *et al.*

(using similar techniques) found that TnC fragments containing Ca^{2+} sites II, III and IV

(not I) formed stable complexes with whole TnI (*10*).

2. ATPase inhibition (introduction of peptides)

The use of ATPase inhibition/recovery yielded several advances in our

understanding of the TnI•TnC complex. Syska *et al.* showed that only a portion of TnI

was needed for inhibition of the acto-myosin ATPase activity (*47*). Specifically they

showed that TnI peptides TnI_{64-133} and TnI_{96-117} were able to inhibit ATPase activity and

that Tm increased the inhibition caused by the peptides. Conversely, addition of Ca^{2+}

saturated TnC reduced the inhibitory effect. The paper also showed that the N-terminal

portion of TnI (residues 1-40) bound tightly to TnC and that TnI_{1-21} also interacted albeit

much more weakly. The introduction of the peptides drastically changed the way in

which interactions were studied mostly by increasing the solubility of the smaller

TnI_x•TnC complexes.

Talbot and Hodges next showed that residues 105-114 of TnI were necessary for inhibition, and that $TnI_{105-114}$ was approximately equally effective as TnI_{96-116} (*48,49*). ATPase studies were continued by Van Eyk *et al.* who showed that residue by residue each amino acid in $TnI_{104-115}$ is needed for binding to TnC (*50*). They also indicated that upon addition of calcium the C-terminal portion of this peptide became more important for binding to TnC and for release of inhibition. The same laboratory later showed (using ATPase inhibition, HPLC, size exclusion, and electrophoresis) that interactions between TnC and TnI peptides corresponding to residues 1-40 (often called Rp), 10-40, and 20-40 were very strong, with Rp the most strongly bound (*51*). Rp was reported to form so tight a complex with TnC that it was capable of displacing whole TnI from TnC (thus the name **R**egulatory **p**eptide), although the ability of Rp to competitively remove TnI from TnC has been disputed (see below).

Farah *et al.* elucidated the orientation of TnI and TnC in 1994 and found that the two proteins interacted in an anti-parallel fashion (*52*). In addition, TnI_{57-182} and $TnI_{103-182}$ were found[6] to regulate ATPase activity, while peptides corresponding to residues 120-182, 1-98 and 1-116 were unable to regulate activity. The inhibitory region of TnI was further refined by Van Eyk who found that $TnI_{104-115}$ was able to yield maximum inhibition (compared to native TnI), but that the peptide TnI_{96-148}, which also caused maximal inhibition, was more fully regulated by the addition of TnC and calcium (*53*). TnI_{1-116} further probed into the N-terminal end of TnI, but responded even less to the presence of calcium saturated TnC than did $TnI_{104-115}$. A recent paper deals specifically with TnI•TnC interactions and has shown that TnI residues 96-131 interact with TnC and

---

[6] ATPase assays, gel electrophoresis and centrifugation were utilized.

residues 140-148 specifically bind to actin (*54*). The study indicated that TnI residues

96-115 bind to C-TnC and actin, residues140-148 only bind actin, and residues 115-131

bind to N-TnC in a calcium-dependent maner. Interestingly this same publication also

shows that the Rp peptide is incapable of displacing TnI_{96-131} and TnI_{96-148} though it is able

to out compete TnI_{96-115}. The finding that these large peptides are not out competed by Rp

draws into question the result of Ngai *et al.* (*51*) in which Rp displaces whole TnI from

TnC[7].

3. CD and Fluorescence

An early report[8] on TnI•TnC was published in 1974 by McCubbin *et al.*, and

showed through CD and fluorescence spectroscopy that a binary interaction between TnI

and TnC existed, and was strengthened in the presence of calcium (*55*). Subsequently,

Cachia *et al.* published some of the only structural information[9] on TnI when they

showed that $TnI_{104-115}$ (also referred to as TnIp) in a complex with TnC was not fully

helical (when compared to mastoparan, an 80% helical peptide) (*56*). Van Eyk *et al.* also

used CD, but in this case to determine the effect of peptide addition on the association

constant for Ca^{2+} binding to TnC (*57*). Very interestingly, they found that the presence of

TnIp <u>reduced</u> the binding of calcium to cardiac TnC, but increased the affinity of skeletal

TnC for calcium. This same article also presents an impressive argument for the binding

of $TnI_{104-115}$ to the C-domain of TnC.

---

[7] The ability of Rp to displace intact TnI from Ca^{2+}-TnC is now considered by the Hodges lab to be uncertain and possibly an artifact. Tripet, B. and Van Eyk, J., personal communication and information presented during discussions at the 1998 Biophysics Society Meeting.
[8] Using heat denaturation, CD and fluorescence.
[9] Circular dichroism results.

Fluorescence has been utilized to augment the secondary structural information provided by CD, with precise[10] binding and dissociation constants. Fluorescence spectroscopy was used[11] to determine the dissociation constant (K_d = 10-14 μM) for $TnI_{104-115} \cdot TnC$ complex (58), and has been utilized to determine the affinity of TnI_{96-116} and TnI_{96-148} to both domains of TnC in isolation or in the intact TnC molecule (44).

4. Cross-linking

Perhaps the most utilized technique for determining direct points of interaction between TnI and TnC is chemical cross-linking. Although great care has been taken to eliminate non-specific cross-linking and use short or 'zero'-length cross-linking molecules, some suspicious contacts have been found for regions of TnC and TnI. It is extremely difficult to form any single conclusion or model from the sum of the cross-linking data.

Tao et al., utilizing the native Cys^{98} in TnC showed early on that binary complexes between TnI·TnT, TnC·TnI, and TnC·TnC were detectable (59). They also demonstrated that the ternary complex of TnC·TnI·TnT could be identified. Refinement continued (using EDC labels) with Leszyk et al., who showed that TnC_{46-78} made contact with TnI within residues 92-167 (60). Another paper by Tao et al., demonstrated very convincingly that Cys^{133} on TnI moved 15 Å closer to Cys^{374} on actin in the absence of calcium, but moved 7 Å closer to Cys^{98} in the presence of calcium (61). They also showed that Cys^{133} of TnI could only be cross-linked to actin in the absence of calcium.

Several cross-linking papers were published in the mid 90's. Ngai et al. again used the TnIp peptide and showed a calcium-dependent interaction to Met^{155} of TnC (62).

---

[10] The accuracy or ability to compare information acquired from the use of primary sequence substitutions, or attachment of bulky spectroscopically active groups to other methods has not been fully elucidated.

Kobayshi *et al.* published two cross-linking studies (*63,64*). The first paper showed that

TnC Ca^{2+} sites II and III interacted with TnI$_{96-145}$ and that TnI$_{96-116}$ cross-linked to <u>both</u>

domains of TnC. The second paper demonstrated that TnC residues 60,61 and 84-94

interact with various TnI peptides. Jha *et al.* showed that TnC labeled at 8 cysteine

positions (1 native, 7 introduced by substitution), only formed cross-links with TnI when

cysteine was present at TnC positions 57, 98 (native), 133, and 158. These residues of

TnC formed cross-links to both the N-terminal <u>and</u> C-terminal residues of TnI.

5. X-ray/Neutron, NMR and Resonance energy transfer.

The only structural data for intact TnI has came from Olah *et al.*, who in 1994

published two papers regarding low angle x-ray and neutron scattering experiments on

the TnC•TnI complex (*65,66*). They discovered TnI binding to a TnC molecule that

resembled the crystal structure of the isolated and partially calcium saturated TnC. The

structure of TnC while bound with TnI was found to have a radius of gyration of 23.9 ±

0.5 Å and a linear dimension of approximately 72 Å. TnI was found to be even more

extended with a maximal linear dimension of 118 Å (radius of gyration 41 ± 2 Å). The

centers of mass of the two components and their long axes were essentially coincident

(within experimental resolution). The second paper dealt more with how the results

pertained to regulation of contraction (see section C.). Structural data were modeled and

showed TnI wrapping around TnC. TnI appeared helical and interacted with TnC

through the hydrophobic pockets of each domain of TnC. Based on the structural

information the sum of reported experiments, Olah *et al.* proposed a molecular switching

mechanism for regulation of contraction (see below).

---

[11] Using an AEDANS label.

A recent low angle x-ray and neutron scattering study has found the structure of TnI to be separated into two ellipsoids while in complex with TnC and TnT (*34*). This publication has also found that TnI in the complex appears to compact upon addition of calcium while TnC remains virtually unperturbed.

Investigation into the structure of TnI peptides has also been performed by NMR. Campbell *et al.* published three papers between 1991 and 1992 regarding the structure of $TnI_{104-115}$ (or an analog) complexed to either skeletal or cardiac TnC. Campbell found that the peptide adopted a mostly helical structure with a kink at the two-proline residues. The peptide was docked into the C-domain of TnC and the resulting structure reported (*67*). NMR was also used to investigate the interactions of $TnI_{104-115}$ with the synthetic C-domain molecule composed of two peptides mimicking TnC calcium binding sites III and IV (called the III/IV hetero-dimer) (*68*). It was found previously that the two peptides associated in the presence of calcium to form a molecule resembling that of C-TnC. This study found perturbations to residues: Phe 102, 112, 151, 154; Ile 104, 113, 121,149, and Asp^{150} upon addition of $TnI_{104-115}$.

Taken together the sum of the interaction data suggests that TnI and TnC are involved in multiple, largely hydrophobic, both calcium dependent and independent interactions. There is no single clear picture, but several models for the interactions of the troponin complex and how they apply to regulation of contraction have been suggested.

C. Regulation of Contraction[12]

---

[12] The information for this section was taken from (*69*), (*9*), (*70*) and references therein.

The most predominant model for the regulation of contraction is the Steric

Blocking model (for an excellent review see (*69*)) and will be the focus for this section of

the introduction. Although other related models have been proposed, the complexity,

length, and the problems surrounding them exceed the space limits of this introduction

(see (*70-72*)). In this section a short summary of the basic steric blocking model and

some modifications proposed will be provided.

In the original description of the steric blocking model components of the thin

filament move physically on actin (*73*). The resulting movement was under an unknown

mechanism of calcium control (direct or indirect), and blocked the myosin-binding site

on actin under relaxed muscular conditions. Tn responded to the calcium signal and was

obviously involved in the control of myosin/actin interaction. One of the earliest

problems was how could Tn regulate myosin interaction with actin when there was only

one Tn complex for every 385 Å (seven actin monomers) of actin length. Immediately

Tm was considered to play a role since it covered the seven intervening actin monomers,

interacted directly with Tn, and also made contacts with the preceding and subsequent

Tm/actin units on the thin filament (a possible mechanism of cooperativity). Modern

versions of the basic model are presented in Figure I-11.
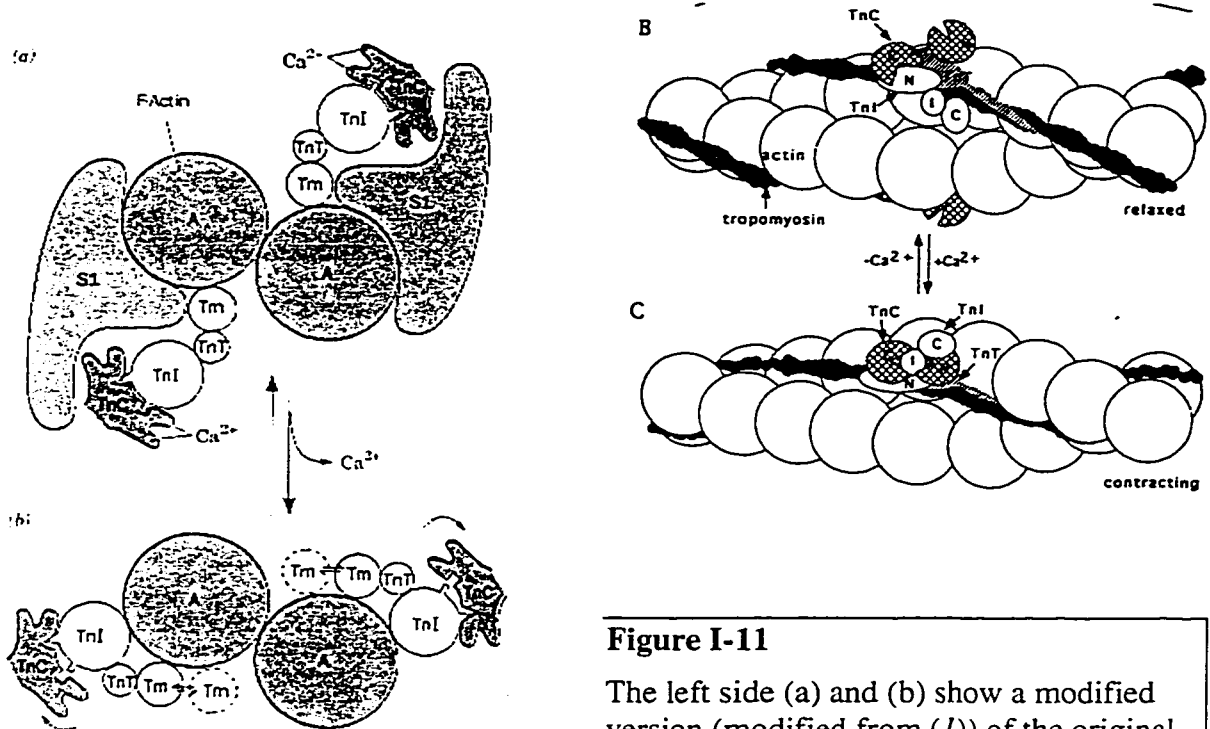
Figure I-11

The left side (a) and (b) show a modified version (modified from (*1*)) of the original steric blocking model proposed by Zot and Potter, *Annu. Rev. Biophys. Biophys. Chem.* **16**, 555 (1987). The model centers on the movement of TnI and Tm under control of calcium. The right side (B) and (C) is taken from Farah *et al.* (*9*), and shows a 3D version of the Tm movement.

These figures show the movement of Tm 10 Å deeper into the actin coiled coil groove allowing myosin to interact with actin and hydrolyze ATP, and the dissociation of TnI•actin by calcium saturated TnC. An important point not made in the figure is that the removal of TnI/Tm inhibition may be cooperative with myosin binding (*i.e.* myosin may push Tm, TnI or both out of the way under calcium saturating conditions). It is actually unlikely that the interactions can be anything other than cooperative (either positive or negative) since this is a closely linked and regulated system dependent on many factors.

The idea of Tm movement was a result of modeling x-ray diffraction and neutron

scattering of the thin filament with Tn and electron micrographs of F-actin and Tm. A

change in the diffraction pattern was noticed from the calcium to apo states. This change

has been attributed to the movement of Actin, Tm, Tn, or a combination of the thin

filament components.

[1] SIMPLE THREE-STATE SCHEME

STATE 1: TM 'blocked'   STATE 2: TM 'cocked'   STATE 3: TM 'open'

[2] DYNAMIC TWO-STATE SCHEME

STATE 1: TM 'blocked'   (equilibrium)   STATE 2: TM 'open'
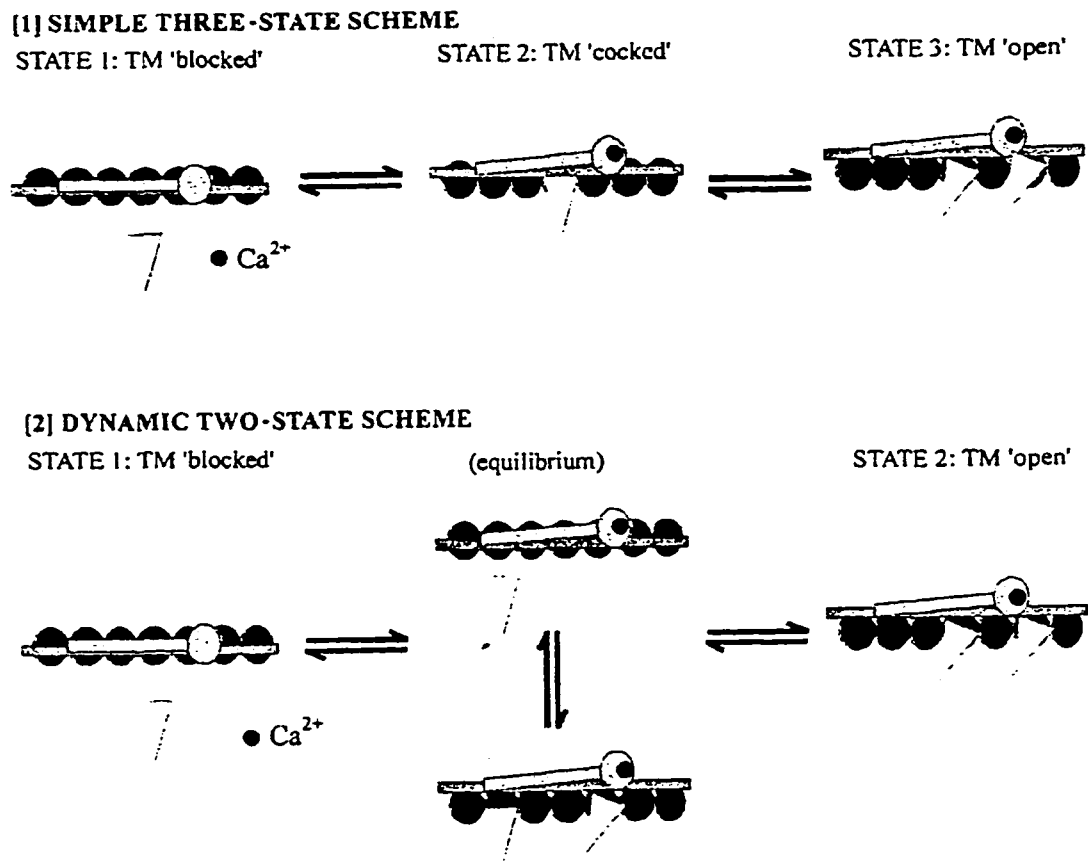
Figure I-12

Illustrations of two thin filament regulation schemes. Actin is shown as the dark spheres, Tm the horizontal dark gray bar, and the Tn complex as the lolly-pop in light gray (figure adapted from (69))

Further support came from Holmes *et al.* who found that S1 bound mainly to

domain 1 of an individual actin monomer close to the Tm binding site (74). Early x-ray

work indicated that two positions for Tm on actin with one predominating in the resting

muscle and a different orientation in the rigor state.

Several factors have suggested modification to the original model (see (75) and

references therein), and one of the latest ideas is that of a "three state" model (76-78). In

this model the first state is termed 'off' or blocked and myosin binds only transiently to

actin with little or no force generation. The second state is 'closed' where calcium is

present but myosin still only forms weak interactions. The final state is 'on' or open, and

strong interactions of acto-myosin are observed with large force generation. An

interesting point from the authors is that the three states may be represented by only two

structures or positions of Tm (Figure I-12). The closed to open transition not only

requires calcium but the presence of "cocked" myosin to essentially shove the Tm/Tn

complex deeper into the actin grove. Calcium in this case would control the proportions

of the blocked to closed equilibrium.

The most recent information has again both challenged (75), and strongly

supported (61,79,80) the steric model. Interestingly Miki et al. mention the Lehman

paper (79) that disagrees with their results but offer no explanation as to why their

reported fluorescence resonance energy transfer (FRET) measurements differ from

several electron microscopy reports. Miki et al. also present one of their abundant

models (Figure I-13, for other models from this lab see (81), (82), and (83)).
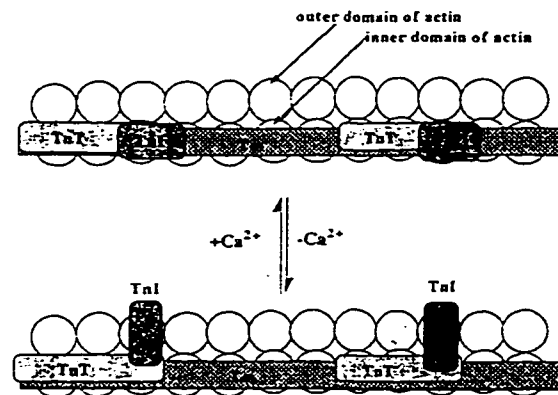
Figure I-13

Proposed model for the regulation of the thin filament with no change in Tm position in the presence or absence of calcium. In this model only individual TnI proteins move and (somehow) each TnI controls a 385 Å length of actin (adapted from Fig.6 (75))

The model (Figure I-13) is reasonable except that it fails in the same manner as the first steric blocking picture in that a majority of the actin monomers are exposed for interaction with myosin.

Malnic *et al.* have also presented a model for Tn•Tm interaction (Figure I-14). While this model does not go so far as to explain how the calcium signal is relayed to myosin/actin it does summarize the information available, up to but not including this thesis, on how members of the troponin complex interact with the thin filament. In addition it will focus the reader on the area addressed in the following three chapters (*i.e.* how TnI and TnC interact in the presence of calcium).
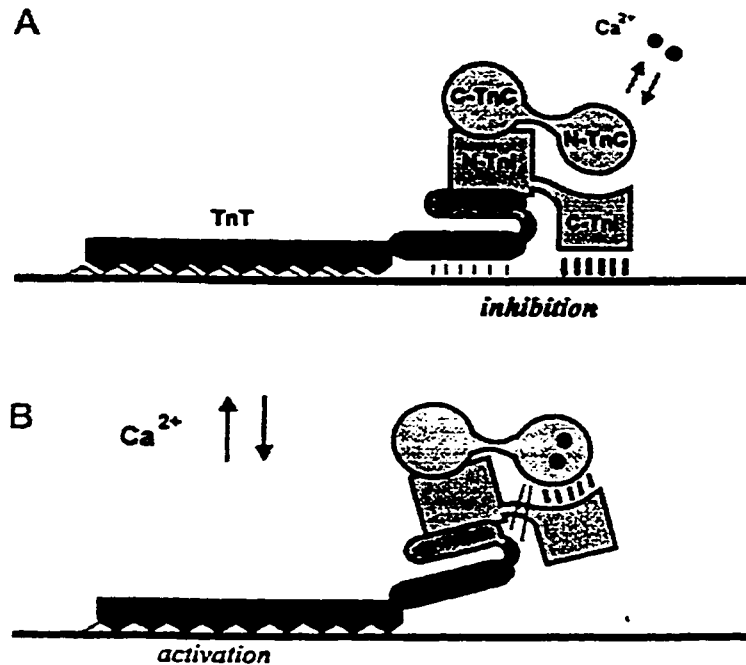
Figure I-14

The figure shows the most up to date information regarding the interactions of the thin filament regulatory proteins (modified from (*12*)). The "thin filament" is shown as the black line on the bottom of (A) and (B). Malnic *et al.* use the black line to inter-changeably represent actin and/or Tm. The thick and thin vertical lines indicate strong (*e.g.* C-TnI and N-TnC, apo) and weak interactions (*e.g.* N-TnC and TnT, apo), respectively.

The figure demonstrates how TnC alters interactions with TnI and indirectly with the thin filament depending on calcium. A unique aspect of this figure is the regulation of TnT interactions with the thin filament not seen in other models. The switching motion of TnI has been presented before (*9,54,66*) and will be discussed in several of the other chapters.

D. NMR

Over the past decade NMR has developed as a useful technique for determination of high-resolution enzyme structures. Many excellent publications (*20,84-87*) are available to fully describe the techniques and results of 1D, 2D, 3D and even higher order protein NMR spectroscopy and structure determination (*e.g.* chapter III), and is well

beyond the intended scope of this thesis to be repeated here. I would like to focus the

remainder of the introduction to relatively new material not well described in general

texts.

For example, a relatively new development in NMR structure determination is the

use of random fractional deuteration of proteins (chapter III). This technique has become

widely used during the period of this thesis work. For a full description of the advantages

and disadvantages of deuterium incorporation the reader is directed to the excellent paper

by LeMaster (see (88) and references therein). The practical advantages of deuteration

can be seen in chapter III and without which the structure would not have been solved.

NMR also has the ability to yield kinetic and energetic information on a system.

Although this is not a new area of NMR it is one that has, until recently, been mostly

under utilized. The next two sections of this introduction will give a brief summary of

how NMR cross-peak line shape can be used to determine kinetics rate constants, and a

brief review of the type of energetics discussed in the next chapters. The very last section

will describe how direct inter-molecular NOEs between TnC and TnI peptides were

acquired.

1. Analysis of TnC•TnI peptide NMR Cross-peaks yields exchange kinetics.

Line width analysis is starting to be used for rate determination of biological

events ((89) and chapters II, and IV). One of the best descriptions of NMR spectra under

the influence of exchange was done by I. Sutherland (90). The article very clearly

describes the derivation of NMR 1D line-shape in the rotating frame using the Bloch

equations. If a single molecule experiences exchange between two conformations then

the resonance frequency of each individual atom in the molecule responds to that change.

The magnitude of the change in backbone amide resonance and the rate of exchange between the two environments determines the characteristic of observed NMR signal. For example, a system exchanging very rapidly on the NMR time scale ($k_{ex} \gg 2\pi\,\Delta\delta$) shows an averaged NMR resonance. The position of the resonance peak will be a weighted average based on the ratio of the two populations. If the exchange is slow on the NMR time-scale then each of the two species are observed with the amplitude of each species proportional to the populations. For NMR spectra of a species experiencing intermediate exchange approaching the NMR time scale a much more complicated spectral result occurs (see chapter II and IV). Sutherland has presented the equation describing the observed spectral magnitude as a function of frequency for an exchanging system (Equation I-1).

(Eq. I-1.)

$$G = G_A + G_B = -iC\frac{[\tau_A + \tau_B + \tau_A\tau_B(\alpha_A p_B + \alpha_B p_A)]}{(1 + \alpha_A\tau_A)(1 + \alpha_B\tau_B) - 1}$$

$$C = \gamma H_1 M_o$$
$$\alpha_A = 1/T_{2A} - 2\pi i(v_A - v)$$
$$\alpha_B = 1/T_{2B} - 2\pi i(v_B - v)$$

$$A \underset{\tau_B}{\overset{\tau_A}{\rightleftharpoons}} B$$
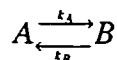
In this equation, G is the total observable magnetization which is the sum of the magnetization from species A (G_A) and B (G_B). H_1 (often seen as B_1), γ, v_A, v_B and M_o represent the applied magnetic field, gyromagnetic ratio, resonance frequency (v) of species A (Hz), resonance frequency of B (Hz), and the original net magnetization (M_o), respectively. The theoretical lineshape may be obtained by plotting the imaginary component of G (Im(G)) against v (normalization is usual done). To speed up

calculations, Sutherland has supplied the extracted imaginary portion of equation I-1

(Equation I-2).

(Eq. I-2.)

$$\text{Im}(G) = \frac{-C\{P[1 + \tau(p_B / T_{2A} + p_A / T_{2B})] + QR\}}{P^2 + R^2}$$

$$\tau = p_B \tau_A \qquad \qquad \delta v = v_A - v_B \qquad \qquad \Delta v = \tfrac{1}{2}(v_A + v_B) - v$$

$$P = \tau\left[\frac{1}{T_{2A}T_{2B}} - 4\pi^2\Delta v^2 + \pi^2\delta v^2\right] + \frac{p_B}{T_{2B}} + \frac{p_A}{T_{2A}}$$

$$Q = \tau\left[2\pi\Delta v - \pi\delta v(p_A - p_B)\right]$$

$$R = 2\pi\Delta v\left[1 + \tau(1/T_{2A} + 1/T_{2B}\right] + \pi\delta v\tau(1/T_{2B} - 1/T_{2A}) + \pi\delta v(p_A - p_B)$$

The parameters v_A, v_B, p_A, p_B, T_{2A}, and T_{2B} are: resonance frequency for the free, resonance frequency for the bound, fraction of the total population free, fraction of the total population bound, transverse relaxation time for the free, and transverse relaxation time for the bound species, respectively. T_2 for the free and bound species is approximated to be $1/\pi\omega$ where ω is the peak width at half height for each species, respectively (see also Appendix 2).

The above isolated equation, although possibly intimidating, allows rapid

simulation of NMR spectra. The value for the dissociation constant (k_B) can be

determined from the formula, when the remaining parameters are known (k_{on} is assumed

to be diffusion limited), in an iterative manner by comparing resulting simulated spectra

to experimental data (e.g. Figure II-3, and Figure IV-3). The above formula has been

used with the program Mathematica (91) and the scripts for line width simulation are

shown in Appendix 2.

2. Basic Energetic/Kinetics of ligand binding

The energetics we will be discussing are extremely simple, and assume that with

mM (often even lower) concentrations that the concentration dependence of free energy

is negligible. We will be using the following formula for the reaction of protein with

peptide:

(Eq. I-3.)

$$\text{Protein} + peptide \underset{t_{off}}{\overset{t_{on}}{\longrightarrow}} complex$$

$$= yTnC + TnI_x \underset{t_{off}}{\overset{t_{on}}{\longrightarrow}} yTnC \bullet TnI_x$$
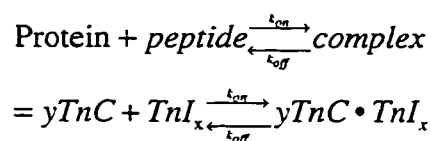
In this reaction 'y' can denote either the N- or C-domain of TnC (TnC by itself indicates

the intact molecule) and 'x' indicates the corresponding residues of the TnI peptide. The

off rate constant is determined by comparing simulated line shapes to experimental NMR

amide backbone cross-peaks (see above). The on rate constant is usually estimated to be

equal to or less than the diffusion limit (i.e. $\sim 1 \times 10^8 - 1 \times 10^9$).

In a few cases we will also be discussing the possibility of more than a single

peptide binding at one time, and the reaction will take the form below.

(Eq. I-4.)

$$yTnC \bullet TnI_x + TnI_x \longleftrightarrow yTnC \bullet 2TnI_x$$
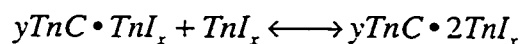
The dissociation constant is determined as described in chapters II-IV and Appendix 1.

Some common formulas, constants, and conversions that are often used are

presented below for quick reference.

$$\Delta G^{\circ} = -RT \ln K_{eq}$$

$$K_{eq} = 1/K_d = k_{on}/k_{off}$$

$$\ln K_{eq} = \frac{-\Delta H^{\circ}}{R}\frac{1}{T} + \frac{\Delta S^{\circ}}{R}$$

$$\Delta G^{\ddagger}_{off} = -RT \ln \frac{k_{off} h}{k_b T}$$

$$h = 6.626 \mathrm{Lx} 10^{-34} J \sec$$

$$R = 8.3145 1 Jmol^{-1} K^{-1}$$

$$4.1855 J = 1 cal$$

$$k_b = 1.3807 x 10^{-23} J \cdot K^{-1}$$

Determined energetics values are presented in kcal/mol instead of the more modern

kJ/mol for easier comparison to the majority of published values.

The derivation of $\Delta G^{\ddagger}_{off}$ makes a few assumptions that are important to point out,

and shall be briefly summarized below from Voet &Voet (pg. 349-350 (*1*)).

(Eq. I-5.)

$$protein + peptide \xrightleftharpoons{\quad K^{\ddagger} \quad} X^{\ddagger} \xrightarrow{\quad k_1 \quad} Complex$$
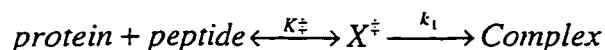
Where $K^{\ddagger}$ is the equilibrium constant between the 'substrates' and the transition state, and

k_1 is the rate constant for the decomposition of transition state 'bonds' to the complex.

The rate of change of complex is:

(Eq I-6.)

$$\frac{d[complex]}{dt} = k_1 e^{\left(\frac{-\Delta G^{\ddagger}}{RT}\right)}[protein][peptide] = k_1[X^{\ddagger}]$$

$$= k_{forward}[protein][peptide]$$

$$K^{\ddagger} = \frac{X^{\ddagger}}{[protein][peptide]}$$

$$-RT \ln K^{\ddagger} = \Delta G^{\ddagger}$$

The rate constant for the decomposition (k_1) is equal to the product of the transmission

coefficient (κ) and the vibrational frequency (v) of the transient bonds forming $X^{\ddagger}$. The

forward rate constant ($k_{forward}$) is for the overall reaction and not just for the change to the

transition state (this is critical, see below).

$$k_1 = \kappa \nu$$

κ represents the probability of transition state break down in the forward direction and is commonly estimated to be between 0.5 and 1 (most assume 1 as will be the case here) for a large favorable $\Delta G°$ in the forward direction[13]. All that is left is to determine the value of k_1 in more useful terms.

$$\nu = \frac{\varepsilon}{h}$$

$$\varepsilon = k_b T$$

$$\therefore k_1 = \frac{\kappa k_b T}{h}$$

Remembering that κ is assumed to be 1, and substituting the final portion of Eq. I-8 into I-6 yields:

$$\frac{\kappa k_b T}{h} e\left(\frac{-\Delta G^{\ddagger}}{RT}\right)[protein][peptide] = k_{forward}[protein][peptide]$$

$$\therefore k_{forward} = \frac{k_b T}{h} e\left(\frac{-\Delta G^{\ddagger}}{RT}\right)$$

Since the off rate constant is measured Eq. I-9 can be used to determine the activation energy of the reverse reaction.

---

[13] It may be important to note here that all calculations of $\Delta G^{\ddagger}$ done in chapter II-V were done on k_{off}. Therefore we are calculating a $\Delta G^{\ddagger}_{rev}$ and the assumption that κ will be between 0.5 and 1 may not be entirely accurate, although as long as a consistent value is used for κ the measurements should still be comparable.

$$k_{off} = \frac{k_b T}{h} e\left(\frac{-\Delta G_{rev}^{\ddagger}}{RT}\right)$$

Some important information that this equation yields is that the rate of reaction will be

inversely proportional to the activation energy and proportional to the temperature of the

system (independent of $\Delta G°$ of the system).

3. Filter/Edit and Edit/Filter intermolecular NOEs.

When determining the structure of labeled N-TnC in the presence of unlabeled

TnI peptide several NOE cross-peaks were found that could not be accounted for as intra-

molecular (*i.e.* N-TnC). These inter-molecular cross-peaks made the task of identifying

N-TnC to N-TnC long-range contacts (necessary for N-TnC structure calculations)

difficult due to the added complexity. Over the course of attempting to devise a means of

eliminating these peaks it was realized that the inter-molecular NOEs were perhaps of

even <u>greater</u> biological interest than the structure determination itself. It was expected

from the small magnitude of chemical shift changes (*i.e.* compared to the changes in N-

TnC caused by calcium binding, see chapter IV) to N-TnC upon binding of TnI

peptide(s) that there would not be large structural changes to N-TnC. Determining

exactly which N-TnC residues were involved in contacts to the peptide, and possibly

identifying the TnI residues in contact became an even larger priority. To do this NMR

pulse sequences were used that specifically selected for magnetization originating on the

^{15}N-, ^{13}C-labeled molecule (in this case N-TnC) and then ended up (via the NOE) on the

unlabeled peptide (Figure I-15). This was called an Edit/Filter NOE experiment. The

opposite path of magnetization transfer has also been used (*i.e.* starting on the peptide and

ending up on the protein and no change to labeling) and has been termed a Filter/Edit

NOESY experiment.
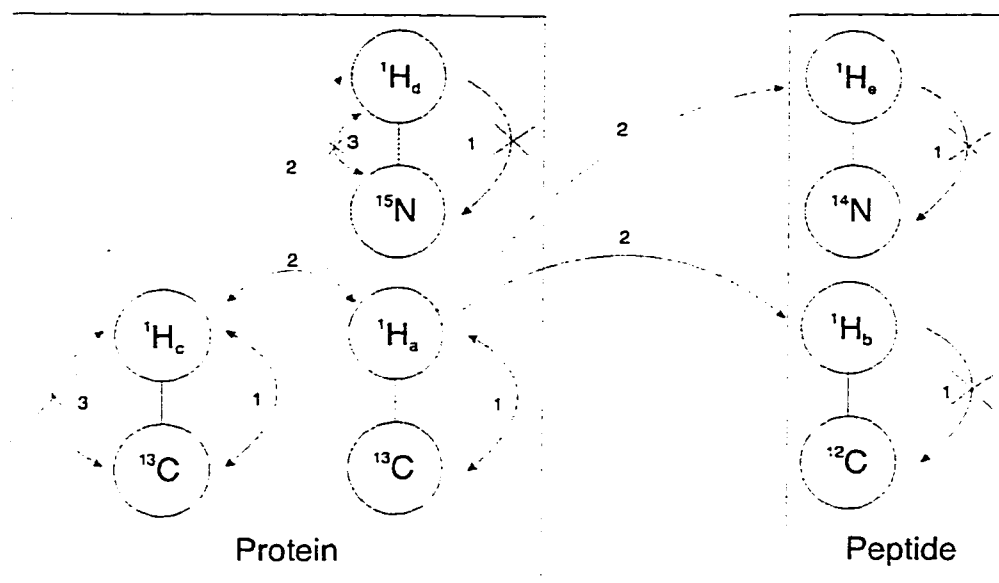
Figure I-15

Model of the magnetization pathway for an Edit/Filter NOESY NMR experiment. The editing portion of the experiment (pathways marked 1) picks up spin information for both the ^{13}-C atom (t_1), and attached hydrogen atom (t_2) while de-phasing any magnetization not originating from a ^{1}H-^{13}C pair (1 crossed out). The surviving spin information is then passed (via the NOE) to neighboring hydrogen atoms (2). The final stage is the Filtering, in which magnetization ending up on a ^{1}H-^{15}N, or ^{1}H-^{13}C system is de-phased (3 crossed out) and therefore removed from direct detection (t_3). The only surviving spin information started from a hydrogen atom on ^{13}C (protein), and ending up on unlabeled ^{12}C or ^{14}N (peptide).

An important point to note here is that the filtering portion (Figure I-15, step 3) of the

experiments is not perfect (Chapter III-B4). Some magnetization originating and ending

up on methyl groups from the labeled protein, due to their relative intensity, may be able

to survive the filtering portion of the experiment. Therefore extra measures have been

taken to eliminate from consideration those peaks which may have been intra- rather than

inter-molecular in origin (see chapter III, results and discussion).

The chapters to follow describe the use of NMR spectroscopy to elucidate the interactions of N-TnC with two TnI peptides of different lengths. Chapter IV broadens the experiments to intact TnC and longer TnI peptides. Chapter V deals with energetics of TnI/TnC interactions, and how a mutant of the N-domain (E41A) reveals more energetics information regarding opening of TnC and regulation of contraction.

The purpose of this thesis was to elucidate the interaction of calcium saturated TnC with several regions of TnI. We proposed that the TnI•TnC interacts via the calcium regulated hydrophobic pockets in each domain of TnC. We also proposed that the use of different length TnI peptides would affect the location, energetics and kinetics of the interaction. In the final section we proposed that the use of a mutant N-TnC molecule would yield the energetic contribution to opening for one of the liganding residues to calcium.

E. References

1.   Voet, D., and Voet, J. G. (1995) in *Biochemistry*, 2nd Ed., pp. 500-502, 1234-1252, John Wiley & Sons, Inc., Toronto

2.   Stryer, L. (1995) in *Biochemistry*, 4th Ed., pp. 347-350, 391-404, W.H Freeman and Company, New York

3.   Eckert, R. (1988) in *Animal Physiology*, 3rd Ed., pp. 136, 329-367, W.H. Freeman and Company, New York

4.   Berridge, M. J., Bootman, M. D., and Lipp, P. (1998) *Nature* **395**, 645-8

5.   Rayment, I., Rypniewski, W. R., Schmidt-Base, K., Smith, R., Tomchick, D. R., Benning, M. M., Winkelmann, D. A., Wesenberg, G., and Holden, H. M. (1993) *Science* **261**, 50-58

6.   Malmendal, A., Evenas, J., Thulin, E., Gippert, G. P., Drakenberg, T., and Forsen, S. (1998) *J Biol Chem* **273**, 28994-9001

7.   Kragelund, B. B., Jonsson, M., Bifulco, G., Chazin, W. J., Nilsson, H., Finn, B. E., and Linse, S. (1998) *Biochemistry* **37**, 8926-8937

8.   Pearlstone, J. R., and Smillie, L. B. (1978) *Can J Biochem* **56**, 521-7

9.   Farah, C. S., and Reinach, F. C. (1995) *FASEB J.* **9**, 755-767

10.   Grabarek, Z., and Drabikowski, W. (1981) *J. Biol. Chem.* **256**, 13121-13127

11.   Leavis, P. C., Rosenfeld, S. S., and Gergely, J. (1978) *J. Biol. Chem.* **253**, 5452-5459

12.   Malnic, B., Farah, C. S., and Reinach, F. C. (1998) *J Biol Chem* **273**, 10594-601

13.   Stefancsik, R., Jha, P. K., and Sarkar, S. (1998) *Proc Natl Acad Sci U S A* **95**, 957-62

14.   Pearlstone, J. R., and Smillie, L. B. (1982) *J Biol Chem* **257**, 10587-92

15.   Mak, A. S., and Smillie, L. B. (1981) *J Mol Biol* **149**, 541-50

16.   Potter, J. D., Sheng, Z., Pan, B. S., and Zhao, J. (1995) *J Biol Chem* **270**, 2557-62

17.   Herzberg, O., and James, M. N. G. (1988) *J. Mol. Biol.* **203**, 761-779

18.   Satyshur, K. A., Rao, S. T., Pyzalska, D., Drendal, W., Greaser, M., and
       Sundaralingam, M. (1988) *J. Biol. Chem.* **263**, 1628-1647

19.   Slupsky, C. M., and Sykes, B. D. (1995) *Biochemistry* **34**, 15953-15964

20.   Slupsky, C. M. (1995) *The NMR Solution Structure of Calcium-Saturated Skeletal
       Muscle Troponin C.,* PhD Thesis, University of Alberta. pgs. 352

21.   Strynadka, N. C. J., Cherney, M., Sielecki, A. R., Li, M. X., Smillie, L. B., and
       James, M. N. G. (1997) *J. Mol. Biol.* **273**, 238-255

22.   Houdusse, A., Love, M. L., Dominguez, R., Grabarek, Z., and Cohen, C. (1997)
       Structure **5**, 1695-1711

23.   Wachtel, E. J., Sverbilova, T., McCubbin, W. D., and Kay, C. M. (1989) *Biochem
       J* **261**, 1043-6

24.   Heidorn, D. B., and Trewhella, J. (1988) *Biochemistry* **27**, 909-15

25.   Slupsky, C. M., Reinach, F. C., Smillie, L. B., and Sykes, B. D. (1995) *Protein
       Sci.* **4**, 1279-1290

26.   Sia, S. K., Li, M. X., Spyracopoulos, L., Gagné, S. M., Liu, W., Putkey, J. A., and
       Sykes, B. D. (1997) *J. Biol. Chem.* **272**, 18216-18221

27.   Kretsinger, R. H., Rudnick, S. E., and Weissman, L. J. (1986) *J. Inorg. Biochem.*
       28, 289-302

28.   Babu, Y. S., Bugg, C. E., and Cook, W. J. (1988) *J. Mol. Biol.* **204**, 191-204

29. Ikura, M., Clore, G. M., Gronenborn, A. M., Zhu, G., Klee, C. B., and Bax, A. (1992) *Science* **256,** 632-638

30. Wriggers, W., Mehler, E., Pitici, F., Weinstein, H., and Schulten, K. (1998) *Biophys J* **74,** 1622-39

31. McCubbin, W. D., and Kay, C., M. (1990) *Chemtracts - Biochemistry and Molecular Biology* **1,** 511-513

32. Wang, C. L., Zhan, Q., Tao, T., and Gergely, J. (1987) *J Biol Chem* **262,** 9636-40

33. Wang, C. K., Lebowitz, J., and Cheung, H. C. (1989) *Proteins* **6,** 424-30

34. Stone, D. B., Timmins, P. A., Schneider, D. K., Krylova, I., Ramos, C. H. I., Reinach, F. C., and Mendelson, R. A. (1998) *J Mol Biol* **281,** 689-704

35. Li, M. X., Gagné, S. M., Tsuda, S., Kay, C. M., Smillie, L. B., and Sykes, B. D. (1995) *Biochemistry* **34,** 8330-8340

36. Pearlstone, J. R., Borgford, T., Chandra, M., Oikawa, K., Kay, C. M., Herzberg, O., Moult, J., Herklotz, A., Reinach, F. C., and Smillie, L. B. (1992) *Biochemistry* **31,** 6545-6553

37. Grabarek, Z., Tan, R. Y., Wang, J., Tao, T., and Gergely, J. (1990) *Nature* **345,** 132-5

38. Swain, A. L., Kretsinger, R. H., and Amma, E. L. (1989) *J Biol Chem* **264,** 16620-8

39. Burtnick, L. D., and Kay, C. M. (1977) *FEBS Lett* **75,** 105-10

40. Gagné, S. M., Li, M. X., McKay, R. T., and Sykes, B. D. (1998) *Biochem. Cell Biol.* **76,** 301-12

41. Fredricksen, S. R., and Swenson, C. A. (1996) *Biochemistry* **35,** 14012-14026

42.   Van Eyk, J. E., Strauss, J. D., Hodges, R. S., and Rüegg, J. C. (1993) *FEBS. Let.* **323,** 223-228

43.   Pearlstone, J. R., and Smillie, L. B. (1983) *J Biol Chem* **258,** 2534-42

44.   Pearlstone, J. R., Sykes, B. D., and Smillie, L. B. (1997) *Biochemistry* **36,** 7601-7606

45.   Head, J. F., and Perry, S. V. (1974) *Biochem. J.* **137,** 145-154

46.   Weeks, R. A., and Perry, S. V. (1978) *Biochem. J.* **173,** 449-457

47.   Syska, H., Wilkinson, J. M., Grand, R. J. A., and Perry, S. V. (1976) *Biochem. J.* **153,** 375-387

48.   Talbot, J. A., and Hodges, R. S. (1979) *J. Biol. Chem.* **254,** 3720-3723

49.   Talbot, J. A., and Hodges, R. S. (1981) *J. Biol. Chem.* **256,** 2798-2802

50.   Van Eyk, J. E., and Hodges, R. S. (1988) *J. Biol. Chem.* **263,** 1726-1732

51.   Ngai, S.-M., and Hodges, R. S. (1992) *J. Biol. Chem.* **267,** 15715-15720

52.   Farah, C. S., Miyamoto, C. A., Ramos, C. H. I., da Silva, A. C. R., Quaggio, R. B., Fujimori, K., Smillie, L. B., and Reinach, F. C. (1994) *J. Biol. Chem.* **269,** 5230-5240

53.   Van Eyk, J. E., Thomas, L. T., Tripet, B. P., Wiesner, R. J., Pearlstone, J. R., Farah, C. S., Reinach, F. C., and Hodges, R. S. (1997) *J. Biol. Chem.* **272,** 10529-10537

54.   Tripet, B. P., Van Eyk, J. E., and Hodges, R. S. (1997) *J. Mol. Biol.* **271,** 728-750

55.   McCubbin, W. D., Mani, R. S., and Kay, C. M. (1974) *Biochemistry* **13,** 2689-94

56.   Cachia, P. J., Van Eyk, J., Ingraham, R. H., McCubbin, W. D., Kay, C. M., and Hodges, R. S. (1986) *Biochemistry* **25,** 3553-62

57.		Van Eyk, J. E., Kay, C. M., and Hodges, R. S. (1991) *Biochemistry* **30**, 9974-9981

58.		Lan, J., Albaugh, S., and Steiner, R. F. (1989) *Biochemistry* **28**, 7380-7385

59.		Tao, T., Scheiner, C. J., and Lamkin, M. (1986) *Biochemistry* **25**, 7633-7639

60.		Leszyk, J., Grabarek, Z., Gergely, J., and Collins, J. H. (1990) *Biochemistry* **29**, 299-304

61.		Tao, T., Gong, B. J., and Leavis, P. C. (1990) *Science* **247**, 1339-41

62.		Ngai, S.-M., Sönnichsen, F. D., and Hodges, R. S. (1994) *J. Biol. Chem.* **269**, 2165-2172

63.		Kobayashi, T., Grabarek, Z., Gergely, J., and Collins, J. H. (1995) *Biochemistry* **34**, 10946-10952

64.		Kobayashi, T., Leavis, P. C., and Collins, J. H. (1996) *Biochim. Biophys. Acta* **1294**, 25-30

65.		Olah, G. A., Rokop, S. E., Wang, C.-L. A., Blechner, S. L., and Trewhella, J. (1994) *Biochemistry* **33**, 8233-8239

66.		Olah, G. A., and Trewhella, J. (1994) *Biochemistry* **33**, 12800-12806

67.		Campbell, A. P., Cachia, P. J., and Sykes, B. D. (1991) *Biochem. Cell Biol.* **69**, 674-681

68.		Slupsky, C. M., Shaw, G. S., Campbell, A. P., and Sykes, B. D. (1992) *Protein Sci.* **1**, 1595-1603

69.		Squire, J. M., and Morris, E. P. (1998) *Faseb J* **12**, 761-71

70.		Tobacman, L. S. (1996) *Annu. Rev. Physiol.* **58**, 447-481

71.		Chalovich, J. M. (1992) *Pharmacol Ther* **55**, 95-148

72.		Leavis, P. C., and Gergely, J. (1984) *CRC Crit. Rev. Biochem.* **16**, 235-305

73.   Hitchcock, S. E., Huxley, H. E., and Szent-Gyorgyi, A. G. (1973) *J Mol Biol* **80,**
       825-36

74.   Holmes, K. C. (1996) *Curr Opin Struct Biol* **6,** 781-9

75.   Miki, M., Miura, T., Sano, K., Kimura, H., Kondo, H., Ishida, H., and Maeda, Y.
       (1998) *J Biochem (Tokyo)* **123,** 1104-11

76.   McKillop, D. F., and Geeves, M. A. (1993) *Biophys J* **65,** 693-701

77.   Head, J. G., Ritchie, M. D., and Geeves, M. A. (1995) *Eur J Biochem* **227,** 694-9

78.   Schaertl, S., Lehrer, S. S., and Geeves, M. A. (1995) *Biochemistry* **34,** 15890-4

79.   Lehman, W., Vibert, P., Uman, P., and Craig, R. (1995) *J Mol Biol* **251,** 191-6

80.   Luo, Y., Wu, J. L., Gergely, J., and Tao, T. (1998) *Biophys J* **74,** 3111-9

81.   Takeda, S., Kobayashi, T., Taniguchi, H., Hayashi, H., and Maéda, Y. (1997) *Eur.
       J. Biochem.* **246,** 611-617

82.   Vassylyev, D. G., Takeda, S., Wakatsuki, S., Maeda, K., and Maeda, Y. (1998)
       Biophys. J. **74,** A53

83.   Vassylyev, D. G., Takeda, S., Wakatsuki, S., Maeda, K., and Maeda, Y. (1998)
       Proc Natl Acad Sci U S A **95,** 4847-52

84.   Homans, S. W. (1995) *A dictionary of concepts in NMR*, revised Ed. Biophysical
       Techniques Series (Dwek, R. A., Ed.), Clarendon Press, Oxford

85.   Evans, J. N. S. (1995) *Biomolecular NMR Spectroscopy*, Oxford University Press,
       Oxford

86.   Cavanagh, J., Fairbrother, W. J., Palmer III, A. G., and Skelton, N. J. (1996)
       Protein NMR Spectrscopy: Principles and Practice, 1st Ed., Academic Pres,
       Toronto

87.   Wüthrich, K. (1986) *NMR of proteins and nucleic acids.*, John Wiley & Sons, New York

88.   LeMaster, D. M. (1990) *Quart. Rev. Biophys.* **23**, 133-174

89.   Forsén, S., Vogel, H. J., and Drakenberg, T. (1986) in *Calcium and Cell Function* Vol. VI, pp. 113-157, Academic Pres, Inc.

90.   Sutherland, I. O. (1971) in *Annual Reports on NMR spectroscopy* (Mooney, E. F., ed) Vol. 4, pp. 71-223, Academic Press, London and New York

91.   Wolfram, S. (1996) *The Mathematica Book*, 3rd Ed. (Walsh, J., Beck, G., and Grohens, J., Eds.), Wolfram Media/Cambridge University Press, Cambridge

Chapter II: Interaction of the Second Inhibitory Region of Troponin I with the Regulatory Domain of Skeletal Muscle Troponin C as Determined by NMR Spectroscopy[1]

A. Introduction

One of the first intra-cellular steps required for skeletal muscle contraction is release of Ca^{2+} ions in the muscle cell, leading to a protein-protein interaction cascade and sliding of the thin and thick filaments past one another in the contractile or power stroke (for reviews see Refs. 1-3). Cardiac and skeletal muscle cells have similar cascades, though the individual proteins involved and the molecular mechanism of regulation differ. The target for calcium is the troponin complex consisting of Troponin C (TnC)†, Troponin I (TnI), and Troponin T (TnT). TnC is the calcium binding component and the best characterized member of the Troponin complex. TnI inhibits the ATPase activity of myosin, while TnT is thought to anchor the complex to actin/tropomyosin. Calcium binding alters the interaction amongst the components of the troponin complex and with other proteins in the thin filament (4). Calcium saturated TnC binds to TnI relieving the inhibition of muscle contraction (Refs. 5 and 6 and references therein).

The crystal structures of TnC revealed a dumbbell shaped molecule with two distinct domains joined by a helical linker (7,8). TnC contains four EF hand calcium binding motifs, two in each of the N and C-terminal domains (9). The N-terminal or regulatory domain of TnC (N-TnC) was devoid of calcium under the crystallization conditions and showed a 'closed' structure. This domain was postulated in the Herzberg-Moult and James model (HMJ model) to open upon calcium binding, exposing nonpolar residues and creating a hydrophobic pocket (10). The opening of the regulatory domain in response to calcium binding was demonstrated by the NMR solution structures of the

calcium saturated N-domain, and whole TnC molecules (11,12). Comparison of these structures demonstrated that isolation of the N-domain does not significantly alter the effects of Ca^{2+} binding. Interestingly calcium saturated cardiac N-TnC remains in the closed conformation (13).

Although there have been several studies investigating the interaction of TnC and TnI, no high resolution three dimensional structures of TnI or the TnC•TnI complex are available (3,14-26). We know TnI binds TnC and actin, and inhibits the actomyosin ATPase in the absence of calcium. However, it was not known exactly which residues of TnI bind to TnC, nor where this complex occurs on TnC. Mutation studies (23), cross-linking experiments (17,18,22,24,27), and low angle x-ray diffraction structures (15) have suggested that the exposed TnC hydrophobic pockets are the site of TnC•TnI interaction. Interestingly the TnC•TnI complex formation was insensitive to calcium unless Tropomyosin and other members of the Troponin complex were present, although calcium was found to stabilize the isolated TnC•TnI complex (6,28). Farah *et al.* used deletion mutants to determine that TnC and TnI bind in an anti-parallel fashion (29).

In regards to TnI, Syska *et al.* showed that TnI bound actin and were the first to show that only a portion of TnI (specifically region 96-117) was needed for full inhibition of ATPase activity (5). Subsequently, synthetic TnI peptides provided an attractive alternative to the use of highly insoluble whole TnI in studies of muscle protein interactions. Talbot and Hodges showed that the synthetic TnI peptide corresponding to region 96-116 behaved identically to the cyanogen bromide cleaved fragment (26). Talbot and Hodges also identified the TnIp peptide (TnI residues 104-115), which was the minimum length inhibitory peptide of TnI still regulated by TnC, and able to inhibit ATPase activity (30). Campbell *et al.* solved the structures of the synthetic TnIp peptide while bound to intact skeletal and cardiac TnC using the transferred NOE technique (16,31). TnIp had an amphiphilic α-helical structure distorted around the central proline residues in both cases. Ngai *et al.* determined that the TnIp fragment cross-linked to C-

terminal domain of TnC, and modeled the NMR derived TnIp structure into the TnC

crystal structure (17).

Recently Tripet *et. al.* have mapped a second TnC binding site on TnI and

postulated that the region, corresponding to residues 115-131 ($TnI_{115-131}$), interacts with

the N-domain of TnC in the Ca^{2+} regulated hydrophobic pocket (19). In this paper the

interaction of calcium saturated N-TnC with $TnI_{115-131}$ was explored with multinuclear,

multi-dimensional NMR spectroscopy. We monitored ^{15}N-labeled N-TnC upon addition

of $TnI_{115-131}$ to determine the stoichiometry of binding, dissociation constant of the

complex, and location of chemical shifts induced in the N-TnC molecule. We have

mapped those chemical shift changes on to the structure of Ca^{2+} bound N-TnC. Further

we monitored the change in cross-peak line width to determine the reaction rate

constants. These results provide direct evidence for TnI binding in the hydrophobic

pocket of the regulatory domain, and have implications for the kinetic competence of the

complex with respect to muscle contraction.

B. Experimental Procedures

1. Proteins and Peptides

The cloning, expression, and purification of 50% deuterated, uniformly ^{15}N-labeled N-TnC was done by modifying the protocols described in Gagné et al. (32) for non-deuterated N-TnC (see Chapter III, Experimental Procedures). The synthetic N^{α}-acetyl-TnI-(115-131)-amide rabbit skeletal peptide was prepared as described previously (19), and lyophilized repeatedly to remove residual organic solvents. The sequence was confirmed by amino acid analysis, and the mass was verified by electrospray mass spectrometry.

2. NMR Sample Preparation

Two NMR samples (500 µL) of [U-^{15}N; 50% ^{2}H]-N-TnC were prepared for titration with the TnI$_{115\text{-}131}$ peptide differing only in the concentration of added KCl. The first sample (designated high salt) contained 100 mM KCl, while the second had no added KCl (low salt). The N-TnC was dissolved in a buffer containing 90% H_2O, 10% D_2O, and 10 mM deuterated Imidazole, with 0.1 mM DSS (2,2-dimethyl-2-silapentane-5-sulfonate) as an internal reference. The only other salts were slight amounts of HCl or NaOH necessary to pH the samples to 6.85.

The concentrations of N-TnC and TnI$_{115\text{-}131}$ were determined by amino acid analysis performed in triplicate. The initial concentration of the high salt sample was 1.54 ± 0.1 mM N-TnC, while the low salt sample was 1.36 ± 0.03 mM N-TnC. The concentration of $CaCl_2$ for the high and low salt samples was 6 mM and 5.4 mM, respectively.

3. NMR Spectroscopy

All experiments were conducted at 31°C on a Varian Unity-600 spectrometer. The HSQC spectra of the high salt sample were acquired with a sweep width of 8000 Hz ^{1}H (512 complex t_2 points), and 1650.2 Hz for ^{15}N (128 complex t_1 points) with 64

transients per increment, while the low salt HSQC spectra were performed using a sweep

width of 8000 Hz for ^{1}H (512 complex t_2 points), and 1800 Hz for ^{15}N (128 complex t_1

points) with 28 transients per increment. Acquisition time was approximately 4.5 hours

per spectra. All experiments were processed using the software package NMRPipe (33)

and analyzed using the program PIPP (34). Data were zero filled in t_2 to 1024 complex

points. The t_1 points were increased by linear prediction to 256 complex points, and then

zero filled to 512 complex points. Spectra were apodized using a shifted sine bell before

Fourier transformation.

4. TnI$_{115-131}$ Titrations (K$_d$)

TnI$_{115-131}$ was added in 5 µL aliquots to 500 µL N-TnC samples to final TnI$_{115-}$

$_{131}$•N-TnC ratios of 1.7:1 and 1.4:1 for the high and low salt samples, respectively. Two

dimensional ^{1}H, ^{15}N-Heteronuclear single quantum correlation spectra (HSQC) (34,35)

were acquired at TnI$_{115-131}$•N-TnC ratios of 0, 0.3, 0.7 1, 1.4, and 1.7 for the high salt

sample and ratios of 0, 0.1, 0.3, 0.5, 0.6, 0.8, 1, 1.1, 1.3, and 1.4 for the low salt sample.

TnI$_{115-131}$ was dissolved in the same stock buffer as N-TnC, and the pH of the NMR

sample was checked after each addition. N-TnC backbone amide HSQC cross-peaks

were followed during each point of the titration and the total chemical shift change ($\Delta\delta$)

was determined as in Equation II-1:

(Eq. II-1.)

$$\Delta\delta_j = ((\Delta\delta_{^{15}N})^2 + (\Delta\delta_{^1H})^2)^{1/2}$$

where $\Delta\delta_{^{15}N}$ and $\Delta\delta_{^1H}$ are the ^{15}N and ^{1}H chemical shift changes (Hz) for a particular

backbone amide residue j. The total chemical shift change for the N-TnC molecule

($\Delta\delta_{Total}$) is shown in Equation II-2:

<div align="right">(Eq. II-2.)</div>

$$\Delta\delta_{Total} = \sum_{j=1}^{n} \Delta\delta_j$$

and the summation is over all residues followed (n).

5. Calculation of Dissociation Constants

The dissociation constant (K_d see Appendix 1) for the reaction:

<div align="right">(Eq. II-3.)</div>

$$P + L \underset{t_{on}}{\overset{t_{off}}{\rightleftharpoons}} PL$$
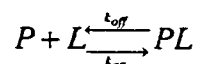
was determined from the $\Delta\delta_{Total}$ by an iterative nonlinear least-squares analysis (25,36 and

Appendix I) using the program Xcrvfit (available at www.pence.ualberta.ca). In

Equation II-3, P is the free N-TnC protein, L is the free $TnI_{115-131}$ peptide, and PL is the

complex. The fit of the results also establishes the stoichiometry of the reaction.

6. Off rate constant (k_{off}) determination

Two-backbone amide cross-peaks were selected from the low salt titration

spectra. They were selected because their shifts were parallel to the ^1H NMR axis, and

therefore traces through the cross-peaks demonstrated lineshape changes and were not

complicated by unresolved splittings in the 50% ^2H N-TnC sample. Methionine 46 was

chosen because it showed one of the largest $\Delta\delta$ of ~130 Hz, while Asparagine 52 was

selected because it showed a smaller change of ~30 Hz. The program Mathematica (37)

(see Appendix 2) was used to simulate the spectral line shapes for various values of k_{off}.

Input parameters included the determined K_d, protein and ligand concentrations, free and

bound chemical shifts, and free and bound line widths for each set of peaks, using the

equations for the effect of site exchange on NMR spectra (38). From these simulations

the off rate for the $TnI_{115-131}$ peptide, in the TnI115-131•N-TnC complex, was determined.

C. Results

1. Titrations

The interaction of $TnI_{115-131}$ with calcium saturated N-TnC was studied using 2D

$^1H,^{15}N$-HSQC NMR spectroscopy. The $TnI_{115-131}$ was unlabeled, whereas the N-TnC was

uniformly ^{15}N labeled, allowing for specific monitoring of the N-TnC component of the

complex without interference from TnI signals. N-TnC was partially deuterated (50%) to

reduce the line width of the observed cross-peaks. HSQC spectra show approximately 90

backbone amide and 6 Asn/Gln NH_2 side chain cross-peaks that can be used to follow the

titration in great detail. Each cross-peak responds to changes in the corresponding atom's

local environment, and this allows sensitive monitoring of each amino acid.

Contour plots of an expanded region of the HSQC spectra taken during the

titration are shown in Fig. II-1 (A and B) for the high salt and low salt samples,

respectively. Some N-TnC amide resonances are not affected by the addition of $TnI_{115-131}$

(e.g. Gly^{33}, Asp^{36}) while other resonances are significantly altered in either the ^1H, ^{15}N, or

both dimensions (e.g. Met^{46}, Gly^{50}, and Met^{82}). Virtually all amide resonances shift very

similarly in both samples. To a first approximation (see detailed lineshape analysis

below) these spectra are in the NMR intermediate-fast exchange limit. Only a single

resonance peak is observed for each amide whose position is the weighted average of the

free and bound chemical shifts (Equation II-4):

(Eq. II-4.)

$$\delta_{obs} = P_f \delta_f + P_b \delta_b = (1 - P_b)\delta_f + P_b \delta_b$$
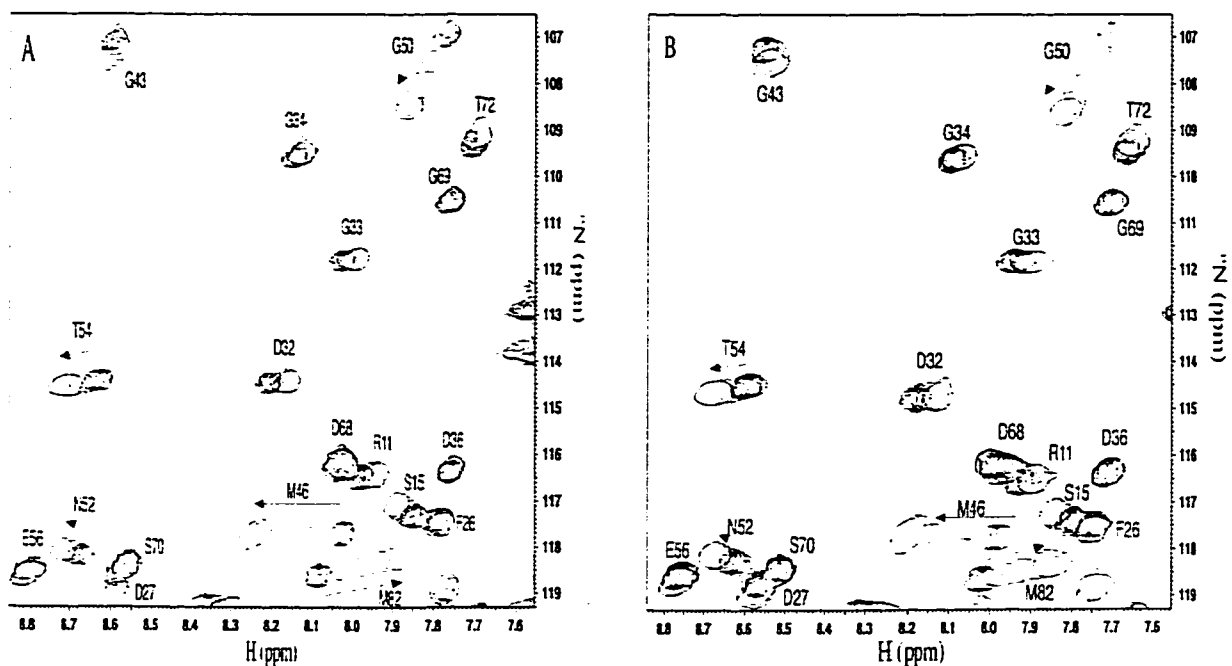
Figure II-1

Contour plots showing an expanded region of the 2D ^{1}H,^{15}N-HSQC NMR spectra of N-TnC monitoring the titration with TnI$_{115-131}$. (A) displays the spectra for the 100 mM KCl sample at additions of 0, 0.3, 0.7 1, 1.4, and 1.7 molar equivalents of TnI$_{115-131}$, and (B) shows the spectra for the sample without added KCl at additions of 0, 0.3, 0.6, 1, 1.3, and 1.4 molar equivalents of TnI$_{115-131}$. Several cross-peaks have arrows indicating the change in chemical shift during the titration (e.g. G50, M82). Some resonances (e.g. M46, G50) are more sensitive to TnI$_{115-131}$ addition than others (e.g. G43 or G34). Splitting in some of the cross-peaks (e.g. M46 ^{15}N dimension) is due to deuteration of neighboring C$_\alpha$ hydrogen sites in 50% of the species present in solution. Uncomplexed N-TnC cross-peaks have more contours while overlaying peaks that appear hollow (single contour) show the effect of the addition TnI$_{115-131}$ peptide to solution during the titration.

where δ_{obs} is the observed chemical shift of the backbone amide cross-peak, P_f and P_b are

the fraction free and fraction bound of N-TnC respectively, and δ_f and δ_b are the

chemical shifts for the free and bound species, respectively.

2. Chemical Shift Analysis and determination of dissociation constants.

A total of 77 N-TnC backbone amide nitrogen and hydrogen pairs were followed

throughout the $TnI_{115-131}$ titration of the high salt sample. The NMR chemical shift

change was calculated for each amide for each point in the titration, and individual $\Delta\delta$

values were summed yielding the $\Delta\delta_{Total}$. Initial assignments of N-TnC backbone amide

nitrogen and hydrogen atoms to be followed through the titration were taken from Gagné

et. al (32). Residues Ala^1, Ser^2, Met^3, Ala^{25}, Met^{28}, Glu^{57}, Phe^{78}, and Leu^{79} were not

followed throughout the titration due to rapid amide exchange or resonance overlap.

Pro^{53} lacks a backbone amide hydrogen atom and thus does not show a cross-peak in the

HSQC spectra. Thr^4 resonated in a crowded region in the high salt sample, and was

therefore not included in the titration. Asp^{66} and Leu^{49} were not assigned in the original

N-TnC NMR spectra. An attempt was made to assign these two residues in the

$TnI_{115-131}$•N-TnC complex and interpolate back to where the cross-peak originated from in

the free N-TnC spectra. Subsequently it was determined that extrapolation of Ala^{25}

overestimated the degree of $\Delta\delta$ for that residue (see Chapter III-Discussion). From

$\Delta\delta_{Total}$ values acquired during the titration a K_d of 24 ± 4 μM was determined for a 1:1

binding complex (Fig. II-2A).
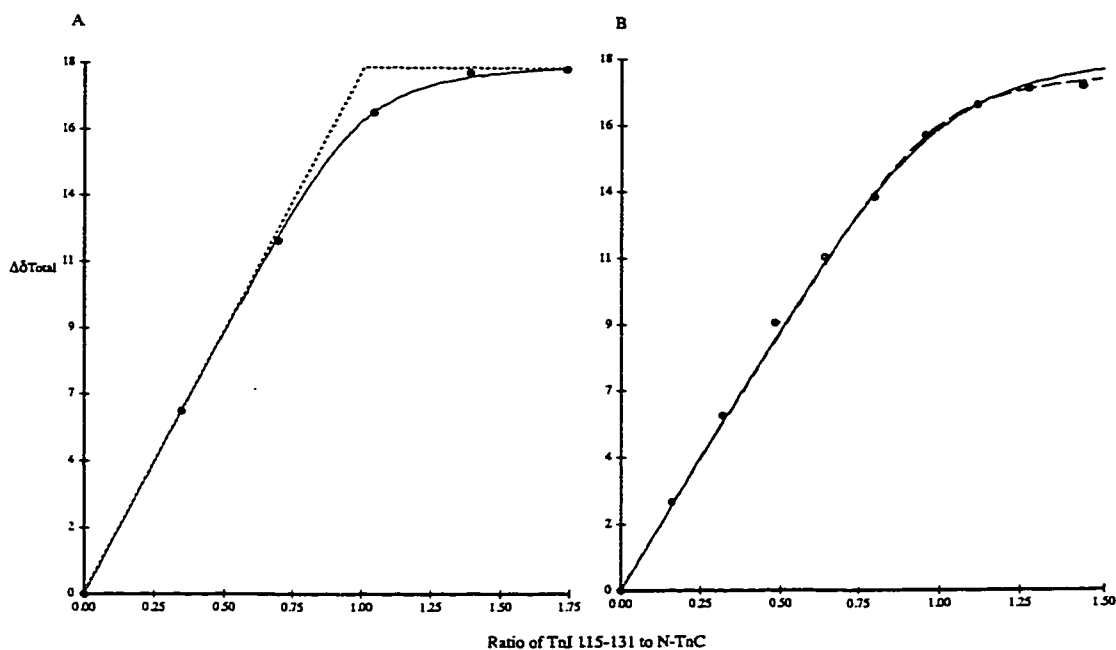
Figure II-2

Binding curves derived from 2D HSQC NMR spectra for the titration of N-TnC with TnI$_{115-131}$. The $\Delta\delta_{Total}$ for the 77 monitored backbone amide pairs during the titration of the high salt sample is shown in (A). The molar ratio of TnI$_{115-131}$: N-TnC added during the titration is shown along the x-axis. The dotted line indicates what a theoretical infinitely tight binding curve would look like while the solid line shows the best fit for the experimental data. (B) displays the summation of the 78 amide cross-peaks followed for the 0 added KCl sample, and the best fit (solid line). The dashed line in (B) shows the fit with the curve maximum locked to a $\Delta\delta_{Total}$ of 18.22 (see text).

The low salt N-TnC titration was analyzed as described above, but a total of 78

peaks were followed. In the low salt sample Thr^4 was isolated enough to follow through

half the titration and did not shift upon TnI$_{115-131}$ addition. A K$_d$ of 40 ± 23 μM for a 1:1

complex was obtained (Fig. II-2B). Because the titration did not go beyond a

TnI$_{115-131}$•N-TnC ratio of 1.4, the fitting was repeated with the maximum shift held

constant at 18.22 (the result of the high salt titration). A K$_d$ of 28 ± 4 μM for a 1:1

complex (Fig. II-2B, *dashed line*) was obtained. This assumption was considered

reasonable because both samples had almost identical responses to binding of the peptide

and the same backbone amide groups were followed throughout. The only exception is

threonine 4, which was followed for the low salt sample; however Thr[4] did not alter the binding data because it does not shift during the titration. The completeness of the titration is evident since a majority of the peaks ceased chemical shift changes before the end of the titration.

3. Lineshape analysis and determination of exchange rates.

Closer inspection of individual HSQC NMR cross-peaks during the titration reveals differential broadening of resonances (for examples see Fig. II-1, A and B, residue Gly[50](G50)), indicating exchange broadening. One-dimensional traces through the cross-peaks of N-TnC residues Met[46] and Asn[52] are shown in Fig. II-3 (A and E, respectively) to display the effect of exchange at various points during the addition of peptide. For Asn[52], where the $\Delta\delta_{^1H}$ was 30 Hz, the line shape only slightly broadens during the titration. On the other hand Met[46], which has a $\Delta\delta_{^1H}$ of 130 Hz, broadens substantially during the titration and then sharpens dramatically at the end. Different broadening is expected because the effect of chemical exchange on line width in the intermediate exchange limit has a dependence on the chemical shift difference between the free and bound species:

(Eq. II-5.)

$$\Delta v_{ex} = P_f P_b \tau_{ex} (\Delta\delta^i)^2$$

where Δv_{ex} is the observed line width, P_f and P_b are the populations of free and bound N-TnC, and τ_{ex} is the exchange lifetime defined as $(\tau_f \tau_b)/(\tau_f + \tau_b)$. The line widths of the free (Δv_f) and bound (Δv_b) N-TnC, and the starting (δ_f) and final (δ_b) resonance positions were determined from the NMR spectra without TnI$_{115-131}$.
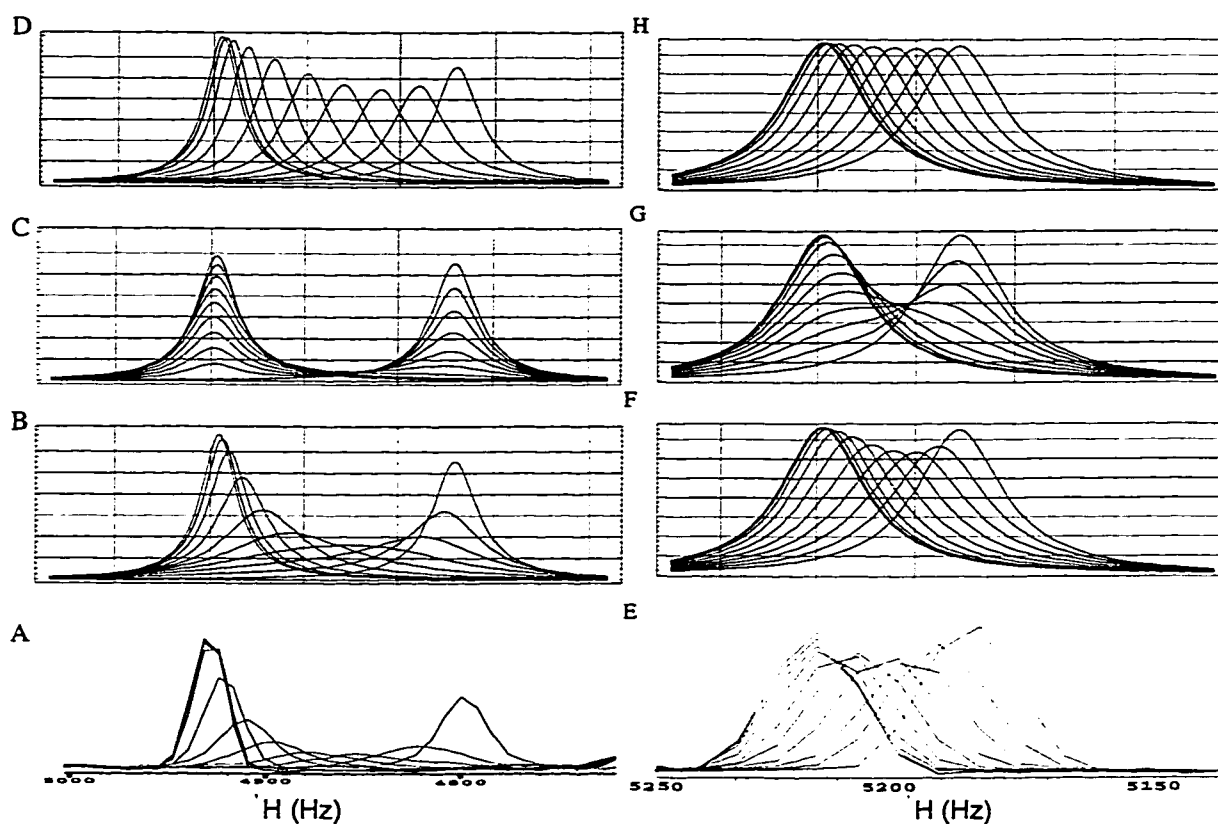
Figure II-3

Traces taken through the HSQC cross-peaks of M46 and N52 (high salt sample) during the titration are shown in (A) and (E) respectively. (B-D) are computer simulations of M46, and (F-H) are similar simulations of N52, both made using k_{off} rates of 350 (B,F), 35 (C,G) and 3500 (D,H) s^{-1}. Broader upfield peaks for both M46 and N52 show the N-TnC alone in solution (dimerized), and both sets of peaks move from right to left upon addition of $TnI_{115-131}$. Ratios of $TnI_{115-131}$:N-TnC used in the simulations are identical to each titration.

and at the highest $TnI_{115-131}$ to N-TnC ratio used. The starting line width of the free N-TnC of 24 Hz (Fig. II-3A, *right peak*) sharpens to 20 Hz (Fig. II-3A, *left peak*) for the bound complex.

A

B
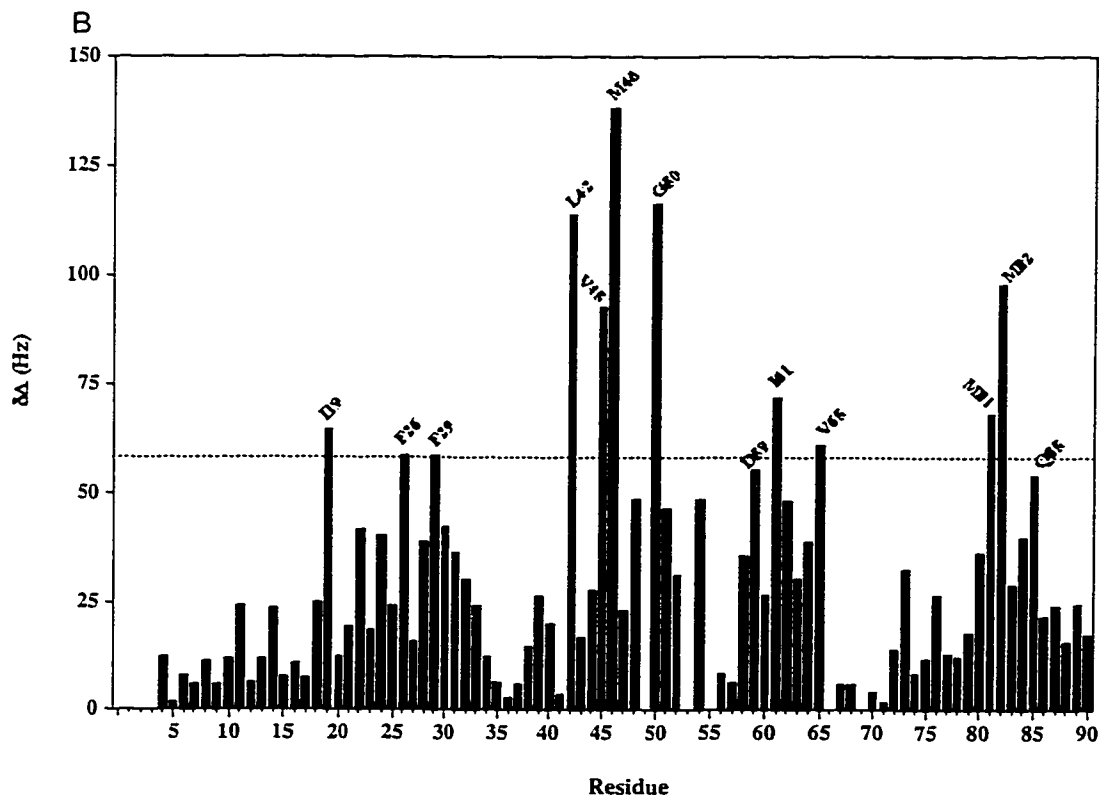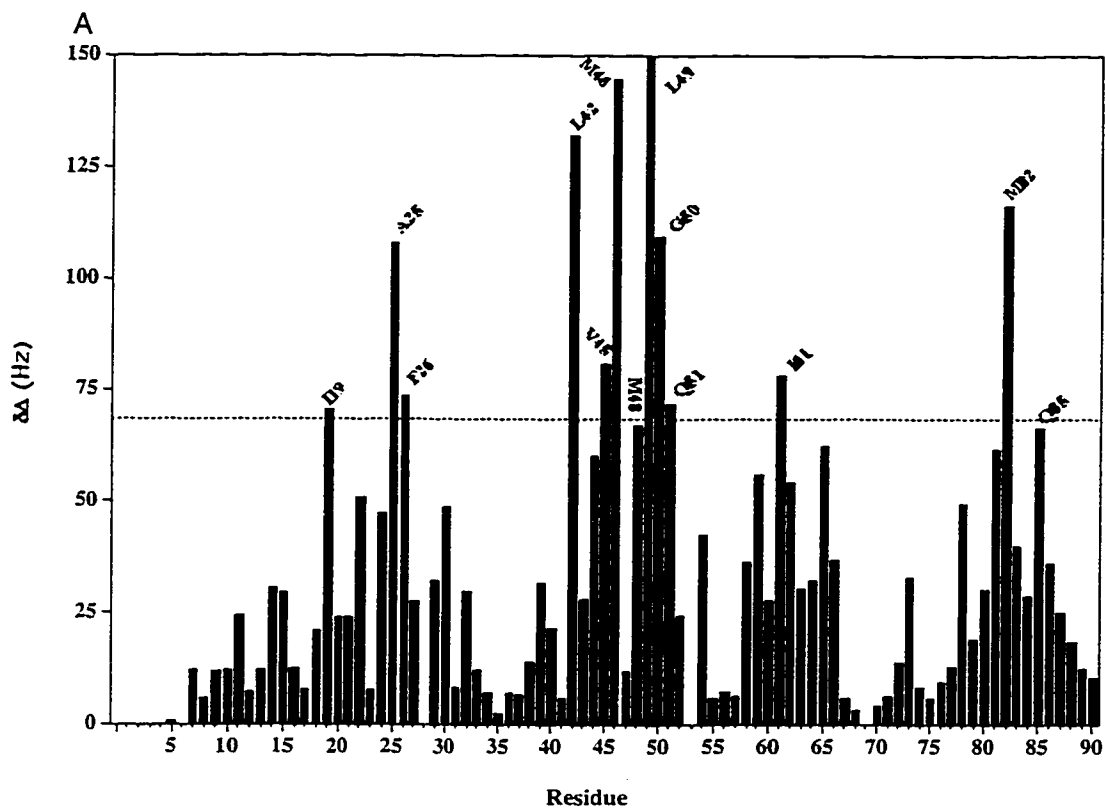
Figure II-4

The $\Delta\delta$ for each individual backbone amide of N-TnC upon addition of $TnI_{115-131}$. The 100 mM KCl sample is shown in (A) while the 0 mM KCl sample is shown in (B). Residues Thr^4, Gln^6, Ala^{25}, Leu^{49}, Asp^{66} in the high salt sample were not followed over the entire titration and the values shown are either extrapolated based on the data acquired (e.g. D66, L49, A25) or shown for as far as they were followed in the titration. For (B) no residues were extrapolated. Residues Thr4, Ala20, Ala25, Thr44, Gln51, Leu79in (B) with an asterisk were followed until lost in the titration and the chemical shift magnitude indicates the last known chemical shift position. The dashed lines in (A) and (B) indicate the mean chemical shift change plus one standard deviation.

This results because N-TnC transfers from a weak dimer to a tighter TnI•TnC complex

(39). Line shapes were simulated using the experimentally derived values for Δv_f, Δv_b,

δ_f, δ_b, K_d and adjusting k_{off}. The results of using k_{off} rates of 350, 35, and 3500 s^{-1} were

shown in Fig. II-3 (B-D and F-H) for Met^{46} and Asn^{52}, respectively. A k_{off} of ~3 x 10^2 s^{-1}

(Fig. II-3, B and F) provides the closest fit to the experimental data (Fig. II-3, A and E)

for both residues.

4. Identification of $TnI_{115-131}$ binding site on N-TnC

The binding site of $TnI_{115-131}$ on N-TnC was mapped by following backbone amide

chemical shift changes during the titration. The maximum $\Delta\delta$ was obtained for each

residue at saturating $TnI_{115-131}$ under both salt conditions, and is presented in Fig. II-4 (A

and B). The average $\Delta\delta$ was 35 Hz and 29 Hz for the high and low salt samples,

respectively. A standard deviation of 38 Hz and 27 Hz was calculated for the $\Delta\delta$ of the

high salt and low salt samples, respectively. Values of $\Delta\delta$ greater than, or approximately

equal (within the digital resolution) to one standard deviation above the mean $\Delta\delta$ were

considered to be statistically significant (Fig. II-4, A and B, dotted line). In the high salt

sample residues Ile^{19}, Ala^{25}, Phe^{26}, Leu^{42}, Val^{45}, Met^{46}, Met^{48}, Leu^{49}, Gly^{50}, Gln^{51}, Ile^{61},

Val^{65}, Met^{82}, and Gln^{85} showed statistically different $\Delta\delta$, while residues Ile^{19}, Phe^{26}, Phe^{29},

Leu^{42}, Val^{45}, Met^{46}, Gly^{50}, Asp^{59}, Ile^{61}, Val^{65}, Met^{81}, Met^{82}, and Asn^{85} changed significantly

in the low salt sample. N-TnC resonances that show a significant change in chemical

shift upon addition of $TnI_{115-131}$ are shown in Fig. II-5. The structure used is that of Ca^{2+}

saturated N-TnC (11). N-TnC residues that have a significant $\Delta\delta$ are shown in *red* and

line the hydrophobic pocket.
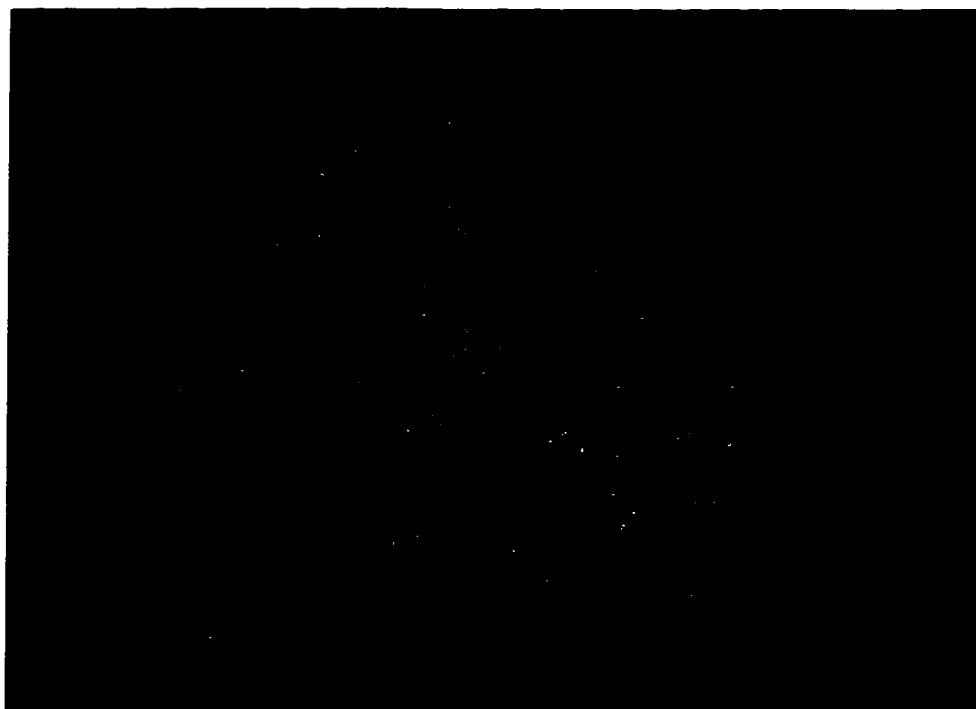
Figure II-1

Space filling model (green or light grey) of N-TnC(11) with the residues most effected by $TnI_{115-131}$ binding shown in red (or dark grey for non-color copies) (Ile^{19}, Ala^{25}, Phe^{26}, Phe^{29}, Leu^{42}, Val^{45}, Met^{46}, Met^{48}, Leu^{49}, Gly^{50}, Gln^{51}, Asp^{59}, Ile^{61}, Val^{65}, Met^{81}, Met^{82} and Gln^{85}). The structure represents N-TnC by itself in solution not the structure of N-TnC while bound, nor is the $TnI_{115-131}$ shown. These marked residues clearly indicate that binding occurs in the hydrophobic pocket of N-TnC.

D. Discussion

We have used HSQC NMR spectroscopy to show that the peptide $TnI_{115-131}$ binds

N-TnC with 1:1 stoichiometry under both high salt and low salt conditions, to measure

the dissociation and off rate constants for the complex, and to demonstrate that binding

occurs in the hydrophobic pocket of N-TnC (10,11). The high-resolution HSQC spectra

provide a unique tool to monitor each individual residue in the protein. This allows one

to observe protein complex formation in solution, without the potential hazards of

introducing a chemical modification, or sequence mutation in the protein which are used

to introduce a localized, single spectrographic probe.

Interestingly the high and low salt samples showed similar values for K_d. A

previous study had shown that salt concentrations played a part in TnI•TnC affinity

chromatography (19). Further Van Eyk *et al.* showed the importance of basic residues in

their TnI_p•cardiac TnC affinity studies (40), and therefore high salt was expected to

screen electrostatic interactions and decrease complex affinity (19,41). However, this

was not observed. A possible explanation for the difference in results may be that high

salt concentrations disrupt nonspecific interactions occurring in the affinity

chromatography.

Dimerization of N-TnC was a concern in affinity calculations because Slupsky *et*

al. had shown previously that the dimerization interface occurred in the hydrophobic

pocket of N-TnC (39). To test this hypothesis we simulated binding curves with

increasing dimerization strength (Fig. II-6). The first two simulations with dimerization

dissociation constants (K_{dimer}) of 100 mM and 10 mM indicated that K_{dimer} in this range

would be insufficient to affect calculated protein•peptide complex dissociation constants.

For a K_{dimer} of 1 mM there was a slight reduction in the observed K_d. For example an

apparent K_d of 22 µM would actually correlate to a K_d of approximately 16 µM. Slupsky

et al. showed a K_{dimer} of approximately 1 mM at 30°C for intact TnC, and our lineshape

analysis indicated an N-TnC dimerization dissociation for N-TnC of $\sim$ 3 mM[1]. Therefore

the reported K_ds for the $TnI_{115-131}\cdot$N-TnC complex are probably closer to the lower

experimental value reported.
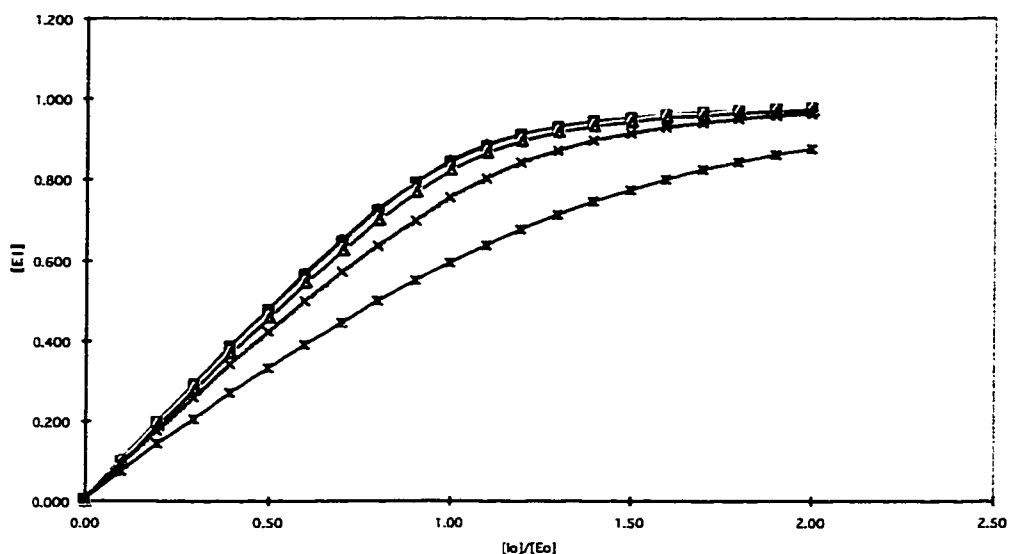
Figure II-1

Theoretical effect of several N-TnC dimerization strengths on the observed dissociation constant of $TnI_{115-131}\cdot$N-TnC. The calculations were done assuming an actual peptide•protein K_d of 30 μM, and that the N-TnC dimerization site is the location of TnI peptide interaction. The observed binding coordinate for N-TnC dimers of 10 μM, 100 μM, 1mM, 10 mM, and 100 mM are represented by the blue 'x', green 'x', yellow 'Δ', purple '', and blue '◊'. For grey scale images the curves are in order, from bottom to top, for lowest Kd to highest, respectively.

We used the chemical shift changes of the backbone amide resonances to demonstrate the

position of the TnI peptide binding. This technique has been used to identify extremely

specific and tight binding compounds for enzyme active sites (42). Cross-peaks which

shifted more than one standard deviation from the mean chemical

---

[1] The K_{dimer} was determined using the observed line width for both the $TnI_{115-131}\cdot$N-TnC complex and partially dimerized N-TnC molecule, and assuming that the fully dimerized N-TnC would have a line width

shift change were marked in Fig. II-4 (A and B), and shown on the N-TnC structure in

Fig. II-5. These residues are predominantly hydrophobic and line the N-TnC

hydrophobic pocket. These results agree with mutational studies that demonstrated that

residues such as M48, and M46 were critical for proper regulation of muscle contraction

(43,44). In addition our results agree with cross-linking studies that showed the TnI•TnC

interface consisted of the interactions TnI 96-145 to whole TnC (22,24,45). More

specifically TnIp was shown to cross-link to TnC residues 84-94 and either 60 or 61.

The interaction of TnIp with the C-terminal domain of TnC (17), and $TnI_{115-131}$

with N-TnC (19) supports the anti-parallel model of Farah et al. (3). The lack of an

extended spacer between the two TnI binding regions suggests a more compact bound

TnC structure than indicated by low resolution neutron scattering experiments (14,15).

A compact bound TnC structure would also agree with the homologous Calmodulin

(46,47), and Myosin (e.g. RLC, ELC) crystal structures (48,49).

We determined off-rate constants from detailed lineshape analysis of HSQC

cross-peaks. The simulations of cross-peak traces (Fig. II-3, B-D and F-G) show that one

can easily distinguish between k_{off} rates differing by a factor of ten. However, the

precision is limited to approximately ± 100 s^{-1}. Lineshape was sensitive to both k_{off} and

K_d. A limitation of the lineshape fitting procedure was the quality of the spectra obtained

as traces through HSQC spectra. There are issues such as limiting spectral resolution,

and also the varying T_2 during the intermediate sections of the titration, which leads to

small differential intensities in the cross-peaks.

The measured k_{off} is fast enough to be kinetically competent for muscle

contraction. For example, the contraction frequency of insect flight muscle can be as fast

as 600-1000 Hz (50). Interestingly the k_{off} for our complex is of the same order as the k_{off}

double that of the monomer.

for calcium (Ref. 51 and references therein), implying that the steps of calcium binding, opening of the hydrophobic pocket, and TnI binding all occur on similar time scales.

This study offers a unique starting point for kinetic analysis of other Troponin interactions. These values will be compared with future kinetic work on even larger TnC and/or TnI protein fragments, and is only the beginning of fully dissecting the molecular kinetics of muscle contraction.

E. References

1.   Tobacman, L. S. (1996) *Annual Review of Physiology* **58**, 447-481

2.   Leavis, P. C., and Gergely, J. (1984) *CRC Critical Reviews in Biochemistry.* **16**(3), 235-305

3.   Farah, C. S., and Reinach, F. C. (1995) *FASEB J.* **9**(9), 755-767

4.   Heeley, D. H., Golosinska, K., and Smillie, L. B. (1987) *J. Biol. Chem.* **262**(21), 9971-9978

5.   Syska, H., Wilkinson, J. M., Grand, R. J. A., and Perry, S. V. (1976) *Biochem J.* **153**, 375-387

6.   Head, J. F., and Perry, S. V. (1974) *Biochem J.* **137**, 145-154

7.   Herzberg, O., and James, M. N. G. (1988) *J. Mol. Biol.* **203**, 761-779

8.   Satyshur, K. A., Rao, S. T., Pyzalska, D., Drendal, W., Greaser, M., and Sundaralingham, M. (1988) *J. Biol. Chem.* **263**, 1628-1647

9.   Leavis, P. C., Rosenfeld, S. S., and Gergely, J. (1978) *J. Biol. Chem.* **253**(15), 5452-5459

10. Herzberg, O., Moult, J., and James, M. N. G. (1986) *J. Biol. Chem.* **261**, 2638-2644

11. Gagné, S. M., Tsuda, S., Li, M. X., Smillie, L. B., and Sykes, B. D. (1995) *Nature Struct. Biol.* **2**(9), 784-789

12. Slupsky, C. M., and Sykes, B. D. (1995) *Biochem.* **34**, 15953-15964

13. Sia, S. K., Li, M. X., Spryacopoulos, L., and Gagné, S. M. (1997) *J. Biol. Chem.* **272**, 18216-12221

14. Olah, G. A., Rokop, S. E., Wang, C.-L. A., Blechner, S. L., and Trewhella, J. (1994) *Biochem.* **33**, 8233-8239

15. Olah, G. A., and Trewhella, J. (1994) *Biochem.* **33**, 12800-12806

16. Campbell, A. P., and Sykes, B. D. (1991) *J. Mol. Biol.* **222**, 405-421

17.   Ngai, S.-M., Sönnichsen, F. D., and Hodges, R. S. (1994) *J. Biol. Chem.* **269,** 2165-2172

18.   Tao, T., Scheiner, C. J., and Lamkin, M. (1986) *Biochem.* **25,** 7633-7639

19.   Tripet, B. P., Van Eyk, J. E., and Hodges, R. S. (1997) *J. Mol. Biol.* **271,** 728-750

20.   Pearlstone, J. R., and Smillie, L. B. (1995) *Biophys. J.* **68,** A166

21.   Pearlstone, J. R., and Smillie, L. B. (1997) *Biophys. J.* **72,** A331

22.   Kobayashi, T., Grabarek, Z., Gergely, J., and Collins, J. H. (1995) *Biochem.* **34,** 10946-10952

23.   Pearlstone, J. R., and Smillie, L. B. (1995) *Biochem.* **34,** 6932-6940

24.   Leszyk, J., Grabarek, Z., Gergely, J., and Collins, J. H. (1990) *Biochem.* **29,** 299-304

25.   Slupsky, C. M., Shaw, G. S., Campbell, A. P., and Sykes, B. D. (1992) *Prot. Sci.* **1,** 1595-1603

26.   Talbot, J. A., and Hodges, R. S. (1979) *J. Biol. Chem.* **254,** 3720-3723

27.   Jha, P. K., Mao, C., and Sarkar, S. (1996) *Biochem.* **35,** 11026-11035

28.   Van Eyk, J. E., and Hodges, R. S. (1988) *J. Biol. Chem.* **263**(4), 1726-1732

29.   Farah, C. S., Miyamoto, C. A., Ramos, C. H. I., da Silva, A. C. R., Quaggio, R. B., Fujimori, K., Smillie, L. B., and Reinach, F. C. (1994) *J. Biol. Chem.* **269**(7), 5230-5240

30.   Talbot, J. A., and Hodges, R. S. (1981) *J. Biol. Chem.* **256**(6), 2798-2802

31.   Campbell, A. P., Van Eyk, J. E., Hodges, R. S., and Sykes, B. D. (1992) *Bioch Biophys Acta* **1160,** 35-54

32.   Gagné, S. M., Tsuda, S., Li, M. X., Chandra, M., Smillie, L. B., and Sykes, B. D. (1994) *Prot. Sci.* **3,** 1961-1974

33.   Delaglio, F., Grzesiek, S., Vuister, G. W., Zhu, G., Pfeifer, J., and Bax, A. (1995) *J. Biomol. NMR* **6,** 277-293

34.   Garrett, D. S., Powers, R., Gronenborn, A. M., and Clore, G. M. (1991) *J. Magn. Reson.* **95**, 214-220

35.   Kay, L. E., Keifer, P., and Saarinen, T. (1992) *J. Am. Chem. Soc.* **114**, 10663-10665

36.   Shaw, G. S., Golden, L. F., Hodges, R. S., and Sykes, B. D. (1991) *J. Am. Chem. Soc.* **113**, 5557-5562

37.   Wolfram, S. (1996) *The Mathematica Book*, 3rd Ed., Wolfram Media/Cambridge University Press, Cambridge

38.   Sutherland, I. O. (1971) in *Annual Reports on NMR spectroscopy* (Mooney, E. F., ed) Vol. 4, pp. 71-223, Academic Press, London and New York

39.   Slupsky, C. M., Kay, C. M., Reinach, F. C., Smillie, L. B., and Sykes, B. D. (1995) *Biochem.* **34**, 7365-7375

40.   Van Eyk, J. E., Kay, C. M., and Hodges, R. S. (1991) *Biochem.* **30**, 9974-9981

41.   Pearlstone, J. R., Sykes, B. D., and Smillie, L. B. (1997) *Biochem.* **36**(24), 7601-7606

42.   Shuker, S. B., Hajduk, P. J., Meadows, R. P., and Fesik, S. W. (1996) *Science* **274**, 1531-1534

43.   Pearlstone, J. R., McCubbin, W. D., Kay, C. M., Sykes, B. D., and Smillie, L. B. (1992) *Biochem.* **31**, 9703-9708

44.   Pearlstone, J. R., Borgford, T., Chandra, M., Oikawa, K., Kay, C. M., Herzberg, O., Moult, J., Herklotz, A., Reinach, F. C., and Smillie, L. B. (1992) *Biochem.* **31**, 6545-6553

45.   Kobayashi, T., Leavis, P. C., and Collins, J. H. (1996) *Bioch Biophys Acta* **1294**, 25-30

46.   Ikura, M., Clore, G. M., Gronenborn, A. M., Zhu, G., Klee, C. B., and Bax, A. (1992) *Science* **256**, 632-638

47.   Houdusse, A., and Cohen, C. (1995) *Proc. Natl. Acad. Sci. U.S.A.* **92,** 10644-

       10647

48.   Rayment, I., Rypniewski, W. R., Schmidt-Base, K., Smith, R., Tomchick, D. R.,

       Benning, M. M., Winkelmann, D. A., Wesenberg, G., and Holden, H. M. (1993)

       Science **261,** 50-58

49.   Rayment, I., Holden, H. M., Whittaker, M., Yohn, C. B., Lorenz, M., Holmes, K.

       C., and Milligan, R. A. (1993) *Science* **261,** 58-65

50.   Baker, J. R. (1996) in *The Academic American Encyclopedia* Vol. Version 8.0.3,

       Grolier, Inc., Danbry, CT.

51.   Potter, J. D., and Johnson, J. D. (1982) in *Calcium and Cell Function* (Cheung,

       W. Y., ed) Vol. 2, pp. 145-169, Academic Press, Inc.

Chapter III: *Structure and Interaction Site of the Regulatory Domain of Troponin-C when Complexed with the 96-148 Region of Troponin-I[1]*

A. Introduction

Muscle contraction involves a neural signal cascade resulting in an increased cytosolic calcium concentration. Sliding of the thin filaments (containing actin, tropomyosin and the troponin complex) past the thick filaments (mostly composed of myosin) constitutes the actual muscular contraction. The myosin heads on the surface of the thick filaments do the physical work of contraction by utilizing energy from the hydrolysis of ATP. The troponin complex is the critical unit for calcium regulation of contraction and consists of troponin-C (TnC), TnI, and troponin-T. In the complex troponin-T is postulated to anchor the complex to actin/tropomyosin, TnI inhibits the ATPase activity of myosin, and TnC is the calcium binding protein. Calcium binding to TnC alters its interaction with TnI, which in turn restores the actomyosin ATPase activity.

The X-ray structure of skeletal TnC revealed a dumbbell shaped molecule with two EF hand calcium-binding sites in each of its two separate domains (*1,2*). In the crystal structure the two domains are connected by a helical linker; however, NMR solution structures have shown the linker to be unstructured and the two domains to be relatively independent of each other (*3,4*). C-TnC contains the high affinity calcium/magnesium sites that are occupied under physiological conditions. N-TnC contains the low affinity calcium specific sites which respond to the changes in calcium

---

levels during neuronal signaling (5-9). Presently there are X-ray structures of N-TnC and whole TnC under different conditions and with several different metal ion replacements (1,2,10-12), and NMR structures of apo and Ca^{2+} saturated skeletal N-TnC (13), Ca^{2+} saturated skeletal E41A N-TnC (14), Ca^{2+} saturated skeletal TnC (3), apo and Ca^{2+} saturated cardiac N-TnC (15), and Ca^{2+} saturated cardiac TnC (4). N-TnC functions similarly to whole TnC when comparing Ca^{2+} binding affinities (16) and overall structure, although isolation of the N terminal domain subtly affects its stability (17). The structures of other homologous proteins such as the myosin light chain (18-21) and calmodulin (22-24) have also given insight into the structure and function of troponin-C.

These structures are important in exhibiting how the binding of calcium to TnC affects the physical properties of these proteins, and ultimately how calcium regulates the interaction of the thick and thin filaments. At present, no high resolution 3D structure of the TnC•TnI complex exists, but 3D structural information for the TnC•TnI complex includes small angle X-ray scattering experiments (25,26), two NMR structures of small synthetic TnI peptides bound to TnC (27,28), and a model based on cross-linking data (29). The experimental X-ray scattering data has been fit with a model which shows an elongated TnC complexed with a 'helical' central region of TnI. The TnI interacts with the hydrophobic pockets of both the C- and N-terminal domains of TnC. Significant portions of TnI (~50 residues) were distributed at the two ends of the structure. The scattering data shows that the centers of mass of TnC and TnI are coincident within experimental error but does not distinguish between parallel versus anti-parallel orientations of TnC and TnI, or establish the precise interfacial contacts in the complex. The elongated TnC structure contrasts with the more compact structures of the regulatory and essential light chains of myosin bound to a portion of the heavy chain (19-21). In addition, recent work by Luo et al. (30) using resonance energy transfer to determine the distance between probes attached to Cys^{48} and Cys^{133} of TnI when complexed to TnC

found a much shorter distance (41 Å) than would have been expected from the scattering

model (70 Å).

The exact regions of TnI that contact TnC in the complex are beginning to be

elucidated. Recent studies have shown that TnC and TnI bind in an anti-parallel fashion

(5,31-33). In this model, C-TnC interacts with the N-domain of TnI, and N-TnC makes

calcium sensitive contacts with both the inhibitory domain (residues 96-116) (34) and C-

domain (residues 117-182) (35) of TnI. C-TnC and N-TnC have been found to bind to

adjacent segments of TnI (36-38). McKay et al. have measured the stoichiometry,

affinity, and kinetics of the interaction of N-TnC with residues 115-131 of TnI, and have

shown that this complex is kinetically competent to be on the mechanistic pathway for

muscle contraction (39).

Other regions of troponin-C also contribute to regulation of contraction. The

central helix of TnC appears to be important in the formation of the biologically active

TnC•TnI complex (40,41). Recently C-TnC has been shown to competitively bind

residues 1-40 and 104-115 of TnI, and also troponin-T (5,29,36-38,42). Preliminary

structures of the C-terminal domain of cardiac and skeletal TnC while bound to the N-

terminal domain of cardiac and skeletal TnI respectively have been presented (43,44).

These combined data suggest that C-TnC might play a more active role in the release of

ATPase inhibition.

An important question to address is the structure of N-TnC in complex with TnI.

NMR (3,13) and x-ray (10) structures of N-TnC in the apo and calcium saturated states

revealed large changes in interhelical angles between the NAD and BC structural units

upon calcium binding (e.g. ~40° for the A/B angle and ~60° for the C/D angle) which

result in the exposure of the hydrophobic pocket. A recent x-ray structure (11) confirms

that global changes in structure occur although the extent of the change is now under

scrutiny (see (45) and references therein for review). The hydrophobic pocket has been

shown to bind the TnI peptide fragment corresponding to regions 115-131 (36,38,39). It

is not known whether this domain opens further in the presence of TnI, or closes around

the TnI in some fashion. The structure would be of general interest for other proteins as

well, such as calmodulin and the myosin light chains in which homologous domains have

been shown to bind helical peptides in a variety of states including closed, semi-open,

and open (*18*). Surprisingly the structure of the highly homologous N-domain of cardiac

TnC is closed in the calcium bound form (*4,15*). The determination of the TnC•TnI

complex structure is necessary to fully elucidate the mechanism of regulation.

The focus of this work was to determine the structure of skeletal chicken N-TnC

in the presence of calcium when bound to skeletal chicken (S96N mutation) TnI_{96-148} and

to explore the interaction(s) between the two proteins. It has been shown that the TnI_{96-148}

fragment is highly soluble, binds tightly to N-TnC, and retains the full, regulated

inhibitory activity of intact TnI (*37,38*). Comparisons of the affinities of several TnI

peptides for calcium-saturated, intact TnC or N-TnC indicate that residues within the 96-

116 and 117-148 regions are primarily responsible for binding to C-TnC and N-TnC,

respectively (*36,38*). In this study we have determined the NMR solution structure of N-

TnC while bound with TnI_{96-148}, examined the change in N-TnC structure upon peptide

binding, and compared the binding of this fragment with that of the shorter TnI peptide

corresponding to region 115-131(*39*). The location of the peptide binding site on N-TnC

was also resolved by monitoring the change in chemical shift of the backbone N-TnC

atoms, and by utilizing specifically designed NMR experiments to isolate contacts

between the protein and peptide.

B. Experimental Procedures

1. Proteins

The cloning, expression, and purification of N-TnC was performed as described

previously (*46*), and TnI$_{96-148}$ was prepared as described by Pearlstone *et al.* (*38*).

Deuterated N-TnC samples were prepared in the same manner as non-deuterated samples

except for preconditioning of expressing cells for growth in M9 limited media containing

80% D$_2$O(Cambridge Isotopes Inc.) and 20% v/v H$_2$O. Cell conditioning involved

growing transformed cells at 36 °C to a high A$_{600}$ on enriched media. These cells were

used to inoculate similar media containing 45% D$_2$O and grown to an approximate A$_{600}$

of one, and then subsequently used to inoculate 80% D$_2$O media, and again grown to an

A$_{600}$ of one. Cells were then suspended in 30% v/v glycerol, stored frozen at -80 °C

and/or used to inoculate media of higher D$_2$O concentrations. Deuteration levels of 88%

for N-TnC were determined by mass spectrometry assuming 98% uniform ^{13}C and ^{15}N

labeling. The composition and concentration was confirmed by amino acid analysis in

triplicate (*47*). Protein purity was confirmed by analytical HPLC and SDS-PAGE.

2. NMR Sample Preparation

NMR samples (500 μl) used for structure determination consisted of 0.7 mM N-

TnC uniformly labeled with ^{15}N, or ^{15}N and ^{13}C, or ^{15}N and ^{2}H (88%), 0.9 mM unlabeled

TnI$_{96-148}$, 90% H$_2$O, 10% D$_2$O, pH of 6.8 (uncorrected for the deuterium isotope effect),

0.1 mM 2,2-dimethyl-2-silapentane-5-sulfonate as an internal standard, 100 mM KCl, 10

mM imidazole, and 2.8 mM CaCl$_2$.

3. NMR Experiments

The titration of ^{15}N labeled N-TnC upon successive 0.3 molar equivalent additions

of unlabeled TnI$_{96-148}$ to a final ratio of 1.5:1 TnI$_{96-148}$ to N-TnC was followed using 2D

^{1}H,^{15}N-HMQC NMR spectroscopy at 30 °C. Resonance frequency assignments of ^{1}H,

^{13}C, and ^{15}N, and NOE interproton distance restraints for N-TnC were determined using

2D and 3D NMR experiments as described in Table III-1. Experiments were conducted

on a Varian Unity-600 except for the Edit/Filter NOESY experiment which was acquired

on a Varian Inova 500 NMR spectrometer.

All experiments were processed using the software package NMRPipe (*48*) and

analyzed using the program PIPP (*49*). Linear prediction was used to increase the

number of points in the indirectly detected dimensions by up to half the number of

acquired points. Directly and indirectly detected data were then zero filled to twice the

number of acquired plus predicted points. Spectra were apodized using a shifted sine bell

before Fourier transformation.

4. Intramolecular NOE Filtering

A sample containing [U-^{13}C] alanine, ^{12}C valine, and 2-^{13}C-serine was used to test

filtering efficiency of the intermolecular NOE experiments. The efficiency was

determined by the relative suppression of the ^{13}C-alanine and ^{12}C valine NOE peaks

compared to the intramolecular β–^{13}C to α–^{12}C serine cross-peak. The delay periods for

the 2 purge pulses were set for proton-carbon coupling constants of 125 Hz and 140 Hz,

to give a broader range of filtering efficiency.

Table III-1

NMR spectra acquired and experimental conditions used to obtain assignments and NOE restraints.

Exp. Name	Nuclei[a]	nt[b]	x-pts[c]	y-pts	z-pts	x-sw	y-sw	z-sw	Mix[d]	Ref.
^{15}N-HMQC	^{1}H,^{15}N	96	1024	128	-	8000	3000	-	-	(72)
^{15}N-HSQC	^{1}H,^{15}N	32	512	256	-	8000	1647	-	-	(58,73)
TOCSY-HMQC	^{1}H,^{1}H,^{15}N	16	512	128	32	8000	8000	1800	75	(74)
HCCH-TOCSY	^{1}H,^{1}H,^{13}C	32	512	136	32	8000	4000	3165	-	(75)
CBCA(CO)NNH	^{1}H,^{13}C,^{15}N	40	512	50	30	8000	9174	1650	-	(58)
^{15}N-NOESY HMQC	^{1}H,^{1}H,^{15}N	16	512	118	32	8000	8000	1800	150	(76)
^{15}N-NOESY HSQC[e]	^{1}H,^{1}H,^{15}N	20	512	108	32	8000	3003	1650	175	(77)
^{15}N-NOESY HSQC	^{1}H,^{1}H,^{15}N	24	512	128	32	8000	7000	1650	70	(77)
^{13}C,^{15}N-NOESY[f]	^{1}H,^{1}H,^{13}C/^{15}N	32	704	128	32	8000	7000	3164	150	(78)
HNCO	^{1}H,^{13}C(O),^{15}N	24	512	48	32	8000	1800	1650	-	(58)
HNCA	^{1}H,^{13}C,^{15}N	32	512	46	32	8000	3922	1650	-	(79)
HCACO	^{1}H,^{13}C,^{13}C(O)	64	256	30	48	3000	4566	1818	-	(80)
Filter/Edit NOESY[g]	^{1}H(^{12}C,^{14}N),^{1}H,^{13}C	32	512	96	24	8000	7000	3164	200	(78)
Edit/Filter NOESY	^{1}H,^{1}H(^{12}C,^{14}N),^{13}C	32	512	84	26	8000	5000	3000	110	(81)

[a] the nucleus acquired in each dimension (e.g. ^{1}H,^{15}N indicates proton x, nitrogen y). [b] the number of transients acquired for each FID. [c] 'x,y,z'-pts and 'sw' is the number of complex points and sweep width in each respective dimension (x is the directly detected dimension). [d] mixing times are given in milliseconds. [e] executed on an 88% deuterated, uniformly ^{15}N labeled N-TnC sample. [f] ^{13}C,^{15}N-NOESY or "Mother Noesy" is a simultaneously acquired ^{13}C, and ^{15}N-edited-NOESY. [g] see 'Results' for details on the Filter/Edit and Edit/Filter NOESY experiments.

5. NOE Distance Restraints

Only the NOE contacts with the highest assignment confidence were utilized in the structural calculations. This resulted in many observed, ambiguous NOE contacts being abandoned. More ambiguity exists in the spectrum of the N-TnC•TnI$_{96-148}$ complex than for isolated N-TnC because of unassigned NOE cross-peaks from TnI$_{96-148}$. Peptide resonances were observed to be broad and overlapping. NOE intensities were not classified into calibrated distance restraints due to spin diffusion. A distance restraint of 1.8 to 5 Å was used in the structure calculations for all assigned NOE contacts except for the upper bound of methyl or pseudoatom methylene groups which was extended by 1 Å.

6. Dihedral Angle Restraints

All non-glycine residues (N-TnC region 4-87) were given a ϕ restraint of -90 ± 90° unless the CSI (50-52) values, and $d_{NHH\alpha}(i,i-3)$ NOEs (53) indicated a definable secondary structure. For regions of alpha helical structure determined by the CSI and NOE measurements, the ϕ angle was restricted during calculations to -50 ± 40°. For beta sheet regions, the ϕ restraint was set to -120 ± 40°.

The ψ angle restraints were based on the ratio between the backbone amide to intraresidue H_α NOE and the backbone amide to inter-residue H_α NOE (46). If the intensity of the intraresidue-amide to H_α contact was greater than the amide to the preceding $H_{\alpha(i-1)}$ (ratio of ≥ 1.1) then the secondary structure was considered to be helical and the ψ angle was restricted to -30 ± 100°. On the other hand if the ratio was less than 0.9 then the ψ was restricted to -120 ± 100°. Ratios between 1.1 and 0.9 were considered indeterminable and no ψ restriction was imposed.

7. Structure Calculations

Thirty structures of N-TnC were generated with the simulated annealing protocol in XPLOR (*54*), using 18000 high temperature steps (90 ps), and 9000 cooling steps (45 ps). The solution structure of calcium-saturated N-TnC (*13*) was used as a starting structure since TnI was expected to bind the "open" TnC conformation. The calculated structures represent N-TnC while bound to TnI$_{96-148}$, but no structural NMR data was included for the peptide.

C. Results

In this paper we have studied the interaction of the regulatory calcium-binding

domain of troponin-C with the major inhibitory region of troponin-I using a variety of

2D/3D multi-nuclear NMR experiments. N-TnC was uniformly labeled with ^{15}N or

^{15}N/^{13}C whereas the TnI_{96-148} was unlabeled. This allowed for the selection of NMR

information pertaining to N-TnC in the complex so that we could determine its structure

and any resulting changes induced by the binding of the peptide. Initially, N-TnC was
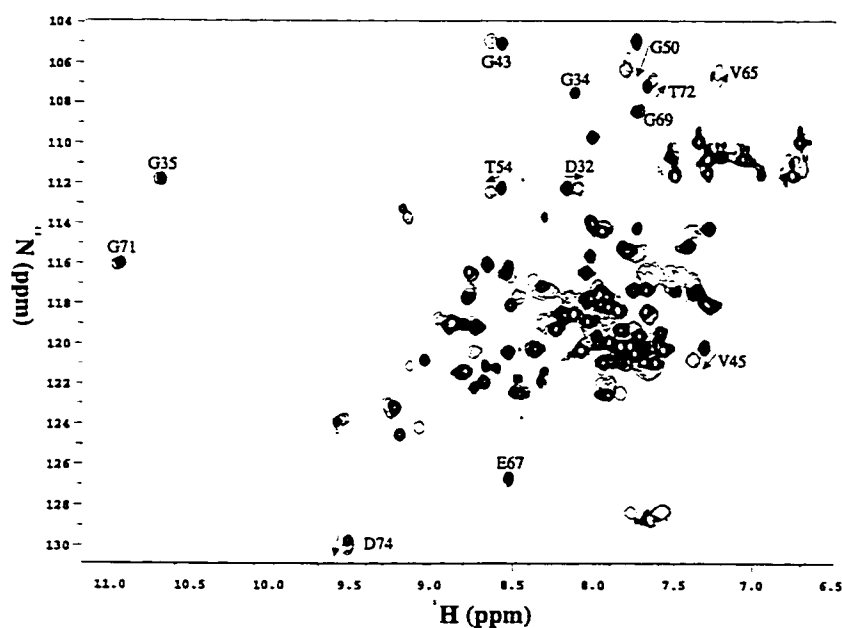
titrated with TnI_{96-148} and the chemical shift changes of N-TnC ^{15}N-HMQC cross-peaks were monitored during the titration (Figure III-1).

Figure III-1

Contour plots of the 2D ^{1}H,^{15}N-heteronuclear multiple quantum correlation NMR spectra of N-TnC showing the titration with TnI_{96-148}. The spectra show 0, 0.37, 0.67, and 1 molar equivalents of TnI_{96-148}. Uncomplexed N-TnC cross-peaks are plotted with more contours, while overlaying peaks that appear hollow (single contour) demonstrate the effect of peptide addition during the titration.

A 1:1 stoichiometry of binding was determined with a dissociation constant on the order

of 1-40 μM (data not shown). The spectra in Figure III-1 indicate intermediate-fast

exchange on the NMR timescale as expected for a K_d in the reported range (*39*).

Exchange broadening of cross-peaks made following chemical shifts difficult in a few

cases (e.g. Phe[26]). The protein•peptide complex was found to precipitate above a

concentration of 0.7 mM as determined by amino acid analysis of the pellet and

supernatant. The complex was less soluble in water below a pH of 6.5, and interestingly

was much less soluble in D_2O. Similar solubility limits in D_2O for intact TnC and TnI

have been observed by Olah et al. (25).

1. TnC•TnI Binding studies

Previous binding studies of TnI_{96-148} to troponin-C (38) have used fluorescence

spectroscopy to follow N-TnC with a single site (F29W) tryptophan mutation (55).

Attempts to follow the titration of F29W N-TnC with TnI_{96-148} using NMR under identical

sample conditions and concentrations as for the wild type N-TnC (see Experimental

Procedures), were not successful due to insolubility of the F29W N-TnC•TnI_{96-148}

complex. Starting concentrations as low as 0.2 mM F29W N-TnC were utilized, but

even at these relatively low concentrations no detectable F29W N-TnC NMR signals

remained at a 1:1 ratio of TnI_{96-148} to F29W N-TnC, and no backbone amide chemical

shift changes of F29W N-TnC were observed during the titration. The fluorescence

spectroscopy binding studies utilizing F29W N-TnC reported no solubility problems in

the μM concentration range.

2. NMR

One of the major obstacles in determining a protein solution structure using NMR

is the molecular weight limit. This limit is dependent, amongst other things, on how fast

the molecule in question undergoes rotational diffusion in solution. The larger the

molecule the slower the rotational tumbling, resulting in broadened NMR resonances. A

slowly tumbling protein also allows cross relaxation to occur more rapidly between spins

making accurate distance measurements more difficult. The width at half height of an

NMR resonance $(\Delta v_{1/2})$ is inversely proportional to the relaxation time (T_2) which

characterizes the decay of an NMR signal during multipulse experiments, which is in

turn proportional to the rotation time (τ_{Rot}):

(Eq. III-1)

$$\Delta v_{1/2} = \frac{1}{\pi T_2} \propto \tau_{Rot}$$

We have determined the ^{15}N T_2 for most of the backbone nitrogen nuclei in N-

TnC while complexed to TnI_{96-148} (Figure III-2A). The average backbone ^{15}N T_2

relaxation time for N-TnC in the complex was 93 ms. Apo N-TnC (56) and the highly

homologous apo N-domain of cardiac TnC (~10 kDa each) showed average T_2's of 154,

and 148 ms, respectively[2]. The expected T_2 for a 16.2 kDa protein at 30 °C is calculated

to be 94 ms either by extrapolation from 10 to 16.2 kDa using the average T_2 values of

the apo proteins or calculated from standard relaxation theory (57). This value agrees

well with the observed value. The apparent ^1H NMR line widths of the amide hydrogen

nuclei observed for cross-peaks in the HSQC spectra were 28-32 Hz. These are in the

expected range for a 16.2 kDa complex by extrapolation from the apparent ~20 Hz line

widths observed in HSQC spectra of N-TnC complexed with a smaller TnI peptide

(residues 115-131) with a combined molecular weight of ~12 kDa. Thus, the N-

$TnC \bullet TnI_{96-148}$ complex appears monomeric in solution. Nonetheless the effect of the

shortened T_2's is propagated exponentially through multi-delay NMR experiments,

drastically reducing signal intensity. The loss of NMR signal resulting from the

---

[2] Spyracopoulos, Leo, Gagné, Stéphane M., Li, Monica X., and Sykes, Brian D. "Dynamics and Energetics of the apo and Ca^{2+}-saturated States of the Regulatory Domain of Cardiac Troponin C". In press Biochemistry.
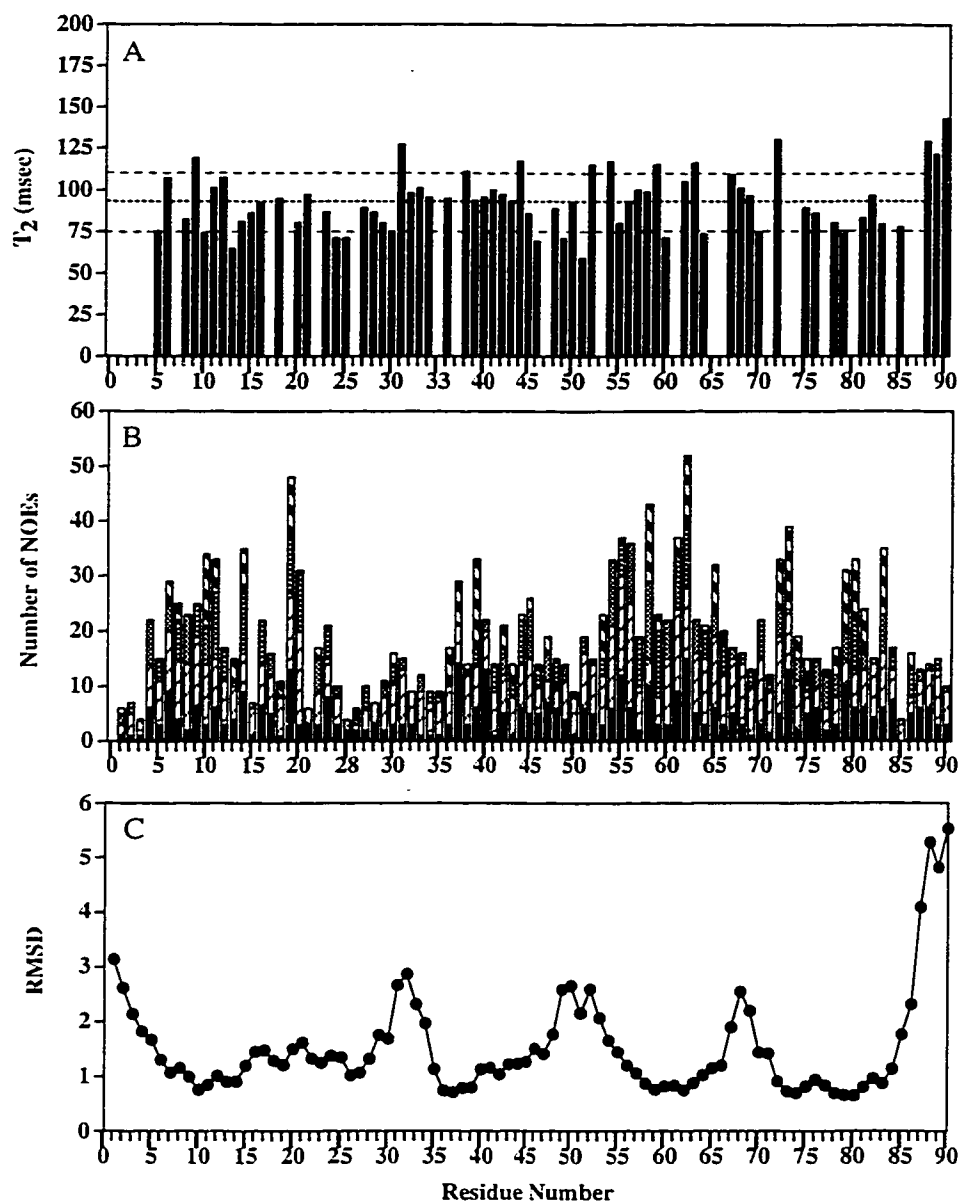
increased signal decay, coupled with limited solubility of the complex, was most

noticeable in the HNCACB and HNHA experiments (58-60).

Figure III-2

(A) Backbone nitrogen T_2 relaxation time (ms) for each of the N-TnC residues subsequently monitored during titration with TnI_{96-148}. The average relaxation time (dotted line) was 93 ms with a standard deviation (dashed lines) of 17 ms. A value of zero for Phe[26], and Asp[66] indicates that the residue could not be followed due to spectral overlap. (B) Distribution of NOEs on a per residue basis used in the structural calculations. Intraresidue, sequential, medium, and long range contacts are described by

solid, dotted cross-hatched, shaded, and thick cross-hatched columns respectively. (C) Atomic RMSDs (Å) of backbone atoms (N,C_α,C') for the 30 generated structures. The average RMSD was 1.55 ± 0.35 angstroms for all regions and the RMSD was 1.11 ± 0.25 Å for the well defined (helices and β-sheet) areas.

3. Deuteration of Proteins

To help alleviate the spectroscopic problems associated with the large size of the complex, random fractional deuteration of the non-exchangeable protons of N-TnC hydrogen atoms (up to levels of 88%) was employed to increase signal to noise and spectral resolution (61,62). The resulting molecular weight of ^{2}H, ^{13}C, ^{15}N protein was 10898 ± 2. The deuterated amide groups were back exchanged with hydrogen atoms from the solvent to allow NMR detection of the residues in question. Figure III-3A and 3B demonstrates the increase in cross-peak intensity of the 2D ^{15}N-HSQC NMR spectra for the approximately 96 backbone and side chain amide groups of N-TnC upon deuteration. The average signal to noise based on peak height increased by a factor of ~1.6 while the line widths of the upfield glycine residues narrowed by an average of 5 Hz. Improvement in resolution is a direct result of the extended T_2 relaxation times of the deuterated molecule (61,63). Comparison of a single nitrogen plane of the 3D ^{15}N-edited-NOESY spectra of deuterated and non-deuterated samples (Figure III-3 C,D with 1D trace shown overlaid) clearly shows the improvement in signal to noise and resolution. The use of deuterated protein allows the collection of a smaller sweep width and therefore improved spectral resolution. The enhanced spectral resolution and signal to noise of the deuterated N-TnC in the complex facilitated the identification of more than 90% of all assignable atoms.
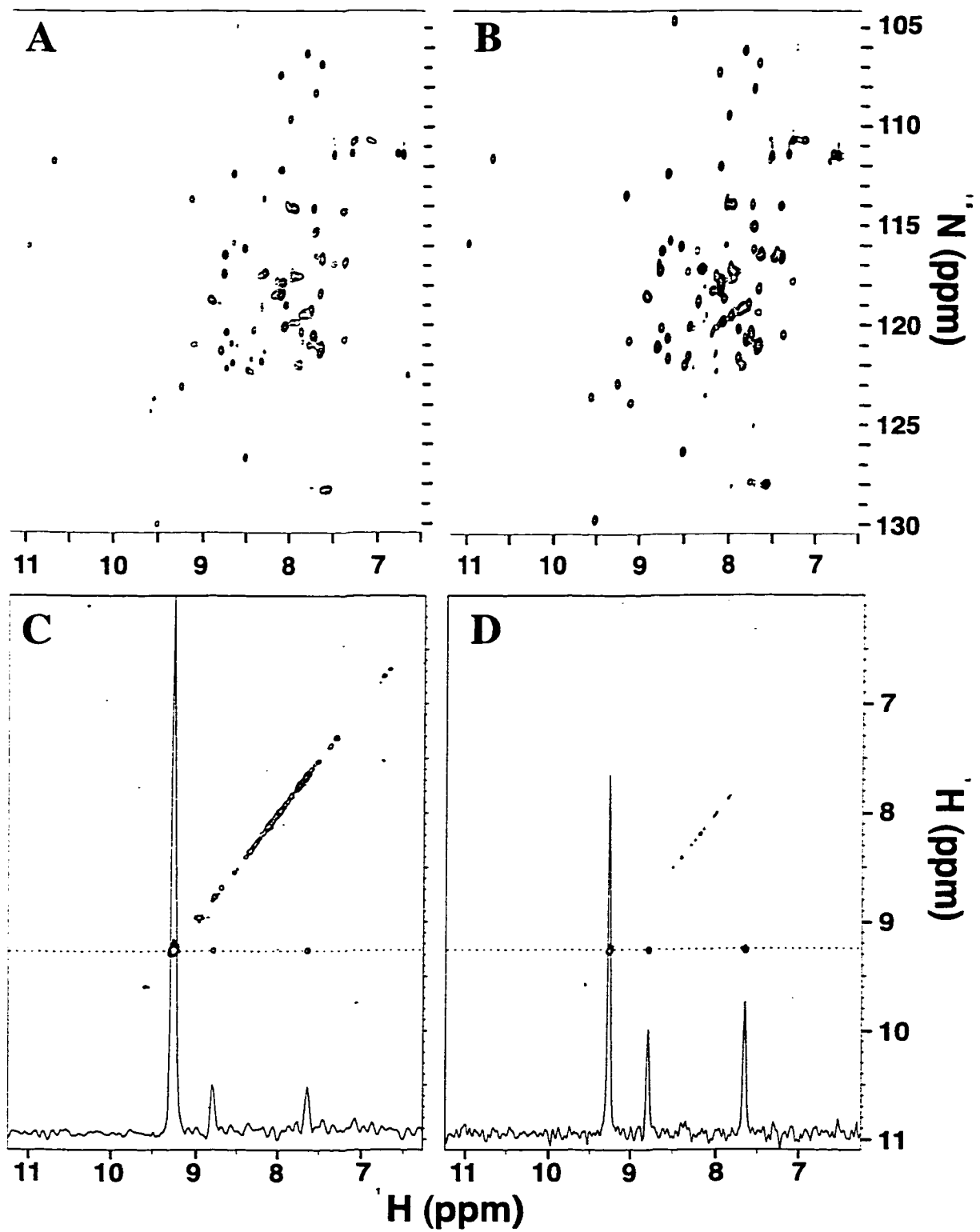
Figure III-3

Spectra of protonated (A, C), and 88% randomly deuterated (B, D) N-TnC while bound to TnI_{96-148} from (A, B) 2D-^{1}H,^{15}N-HSQC, and (C,D) a single ^{15}N spectral plane from a 3D ^{15}N-noesyhsqc. The backbone amide deuterium atoms were back exchanged for hydrogen in the solvent to be visible by NMR in this experiment. In the HSQC spectra, the deuterated sample (B) was on average 1.6 times higher in signal to noise than the non-deuterated sample (A). There are several cross-peaks that are too weak to be visible in the protonated sample (e.g. V65 in the up field portion of the HSQC). The deuterated HSQC was acquired with 8000 Hz (512 t_2 complex points) and 1650 Hz (256 t_1 complex points) sweep widths for hydrogen and nitrogen respectively with 64 transients per FID. Only the first 128 t_1 complex points from the spectra of the deuterated sample were processed to make the digital resolution equivalent to the protonated sample. The non-deuterated sample was acquired with a sweep width of 8000 Hz (512 t_2 complex points) and 1800 Hz (128 t_1 complex) for hydrogen and nitrogen respectively with 32 transients per FID. Both experiments were processed using a $\pi/3$ shifted sinebell, zero filled to 1024 t_2 complex points and 512 t_1 complex points, and both samples were approximately 0.7 mM (complex). The difference in the number of transients per acquisition was also compensated in the presentation of the spectra. (C,D) A single plane of the 3D-^{15}N-noesyhsqc experiments with the 1D trace corresponding to Val^{45} (dotted line) shown overlapping in both spectra for ease of comparison is presented. (D) shows an example of the improvement in spectra for sequential assignment that can be obtained by acquiring a narrower (i.e. 3000 Hz for the deuterated sample as compared to the 8000 Hz for the protonated sample) sweep width in the deuterated sample without overlap from upfield aliphatic resonances (see Table III-1 for experimental details).

Resonance frequencies and interproton NOEs were assigned and analyzed from the eleven NMR experiments shown in Table III-1 using protocols described previously ((64) and references therein). The total number of assigned short, medium, and long range NOEs are given in Figure III-2B. Utilizing the program XPLOR (54), a total of 30 structures were generated using 1039 NOE and 111 dihedral angle restraints. The structural statistics are presented in Table III-2. The N, A, B, C, and D helices and the β-sheet (residues 6-14, 16-29, 39-47, 55-65, 76-86, and 36-38 /72-74 respectively) are similar in sequence location and structure to those reported by Gagné et al. (46).

Table III-2

Structural statistics for N-TnC in complex with TnI$_{96-148}$.

NOE restraints	
Total	1039
Intra-residue ·	411
Sequential (|i-j| = 1)	303
Medium range (2 ≤ |i-j| ≤ 4)	201
Long range (|i-j| ≥ 5)	124
Dihedral Restraints	
Total	111
φ	77
ψ	34
RMSD to average structure (Å)	
Well defined regions[a] (N,C$_\alpha$,C)	1.11 ± 0.25
All regions[b](N,C$_\alpha$,C)	1.55 ± 0.35
Heavy atoms	2.05 ± 0.31
N-helix (residues 6-14)	0.33 ± 0.08
A-helix (16-29) ·	0.67 ± 0.28
B-helix (39-47)	0.53 ± 0.20
C-helix (55-65)	0.36 ± 0.14
D-helix (76-86)	0.61 ± 0.23
β-sheet (36-38, 72-74)	0.35 ± 0.14
Energies[c] (kcal mol^{-1})	
E$_{total}$.	81 ± 18
E$_{NOE}$	8 ± 5
E$_{Dihedral}$	6 ± 4
φ,ψ in core or allowed regions	95%

[a] N-D helices, and β-sheet. [b] residues 4-87. [c] the three highest energy structures were removed from the ensemble of thirty structures.

In the bound structure the N- and C-terminal residues, as well as the linker regions, are less well defined. The backbone RMSD for all 30 structures is shown in Figure III-2C with an average RMSD of 1.55 ± 0.35 Å. The average RMSD includes all regions of the structure. If the well defined regions (helices and β-sheet) are superimposed then the RMSD is 1.11 ± 0.25 Å. The structures were evaluated with the program PROCHECK (65), and showed 75% of the backbone dihedral φ and ψ angles (30 structures) in the most favored regions with another 21% in the additionally allowed regions. The average structure had 76% of the backbone dihedral angles in the most favored region and 22% in additionally allowed regions. The RMSDs and PROCHECK results indicate that the structure is of medium resolution, and therefore only backbone changes will be evaluated.
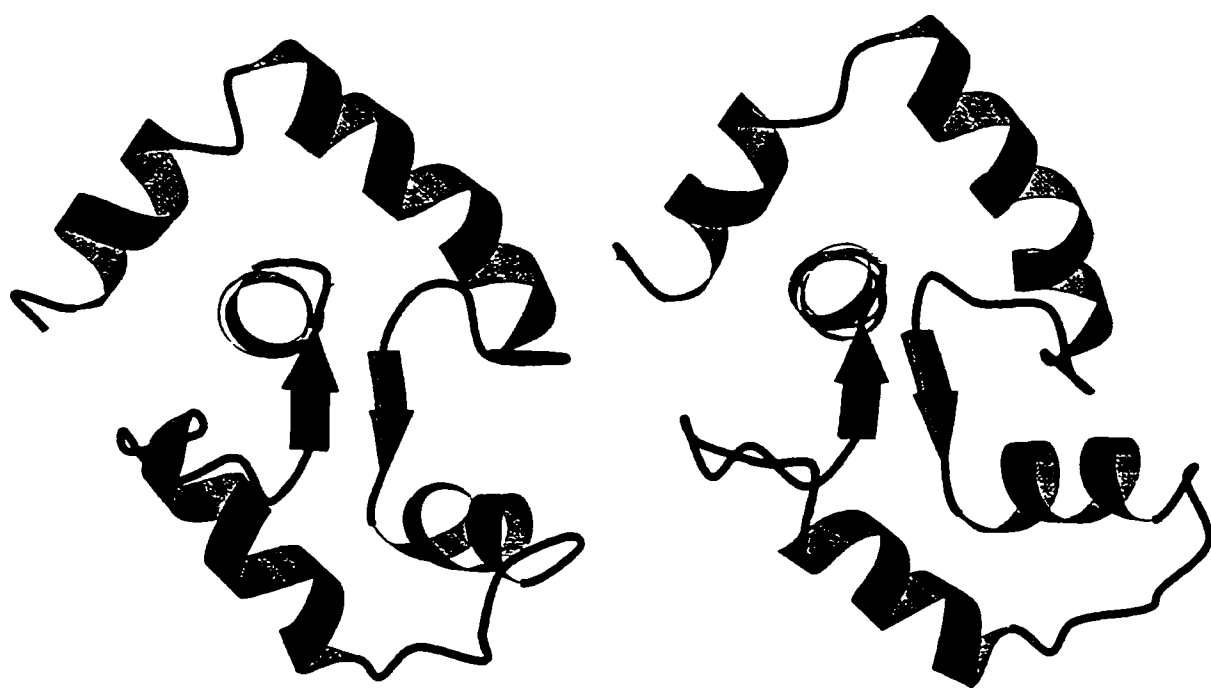

Figure III-4

Ribbon diagrams showing a comparison of the average, TnI peptide bound, backbone N-TnC structure (left) with that of the calcium-saturated N-TnC structure (right). The diagrams were generated using the program Molscript (82).

Figure III-4 shows the ribbon diagram of the average N-TnC structure bound to

TnI_{96-148} and the unbound calcium-saturated N-TnC structure (*13*) for comparison. The

interhelical angles (residues 6-13, 16-28, 42-48, 55-64 and 75-85 were used for helices

N, A, B, C and D respectively) for N-TnC bound to TnI_{96-148} are A/B: 92° ± 11, B/C: 116°

± 12, C/D 88° ± 6, and A/D 114° ± 6. Interestingly, the B-C linker (residues 48-54)

appears to be slightly more closed than does the NMR and x-ray calcium bound N-TnC

structures (*10,11,13*)[3]. Comparison of the average calcium saturated and peptide bound

N-TnC structures show an alteration in the C/D angle, which changes from 68° ± 5

without peptide to 88° ± 6 when bound. This indicates a slight closing of the

hydrophobic pocket upon binding[4,5]. The other interhelical angles (*e.g.* A/B) remain

relatively unchanged upon peptide binding within experimental error but do appear to

more closely resemble the recent x-ray structures. A recent review has examined the

interhelical angles of the x-ray and NMR structures of troponin-C, and has addressed the

structural and energetic implications of the reported differences (*45*).

In addition to determining the N-TnC structure in the complex, the location of

interaction between N-TnC and the TnI peptide was also investigated. The region of

interaction was first identified by analyzing the change in chemical shift (*39*) for each N-

TnC backbone amide pair upon the addition of TnI_{96-148}. The $\Delta\delta$ for each of the

monitored N-TnC residues is presented in Figure III-5A. N-TnC backbone amide pairs

showing chemical shifts changes upon peptide addition greater than one standard

deviation (thin dashed line) above the average $\Delta\delta$ (thick dotted line) are labeled in the

figure and are considered to be statistically different. The residues include Ala^{20}, Phe^{22},

Ala^{25}, Met^{28}, Leu^{42}, Val^{45}, Met^{48}, Gly^{50}, Gln^{51}, Asp^{59}, Ile^{61}, Glu^{64}, and Lys^{87} and thus

---

[3] Proper comparison of interhelical angles requires that helix definitions are consistent, and that the same program is used for calculations. Coordinates and definitions were not available from Houdusse *et al.* (1997) at the time of writing this paper.

[4] An angle of 180° would indicate two helices lying anti-parallel with respect to one another.

[5] The PDB file has been assigned the Brookhaven Protein Data Bank accession no. 1BLQ.

should represent amino acids directly involved with binding the TnI_{96-148} peptide, immediate neighbors, or residues in the structural hinge regions (66). These residues are not all inclusive, and represent only those for which we have the strongest confidence based on chemical shift mapping. Some residues in the molecule could not be followed during the entire titration and therefore do not appear (e.g. Phe^{26}, Leu^{49}, and Asp^{66}), while others (e.g. Ala^{24}, Ala^{25}, and Lys^{87}) may have been underestimated (i.e. followed for only part of the titration).
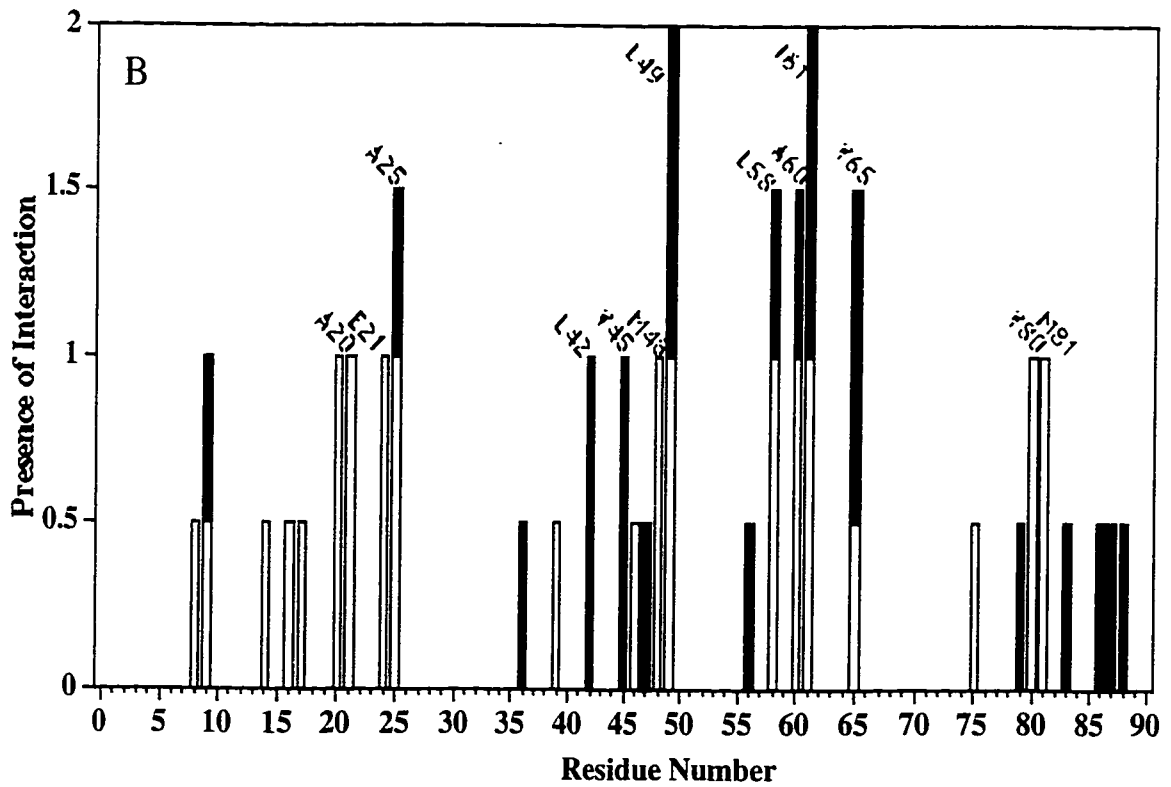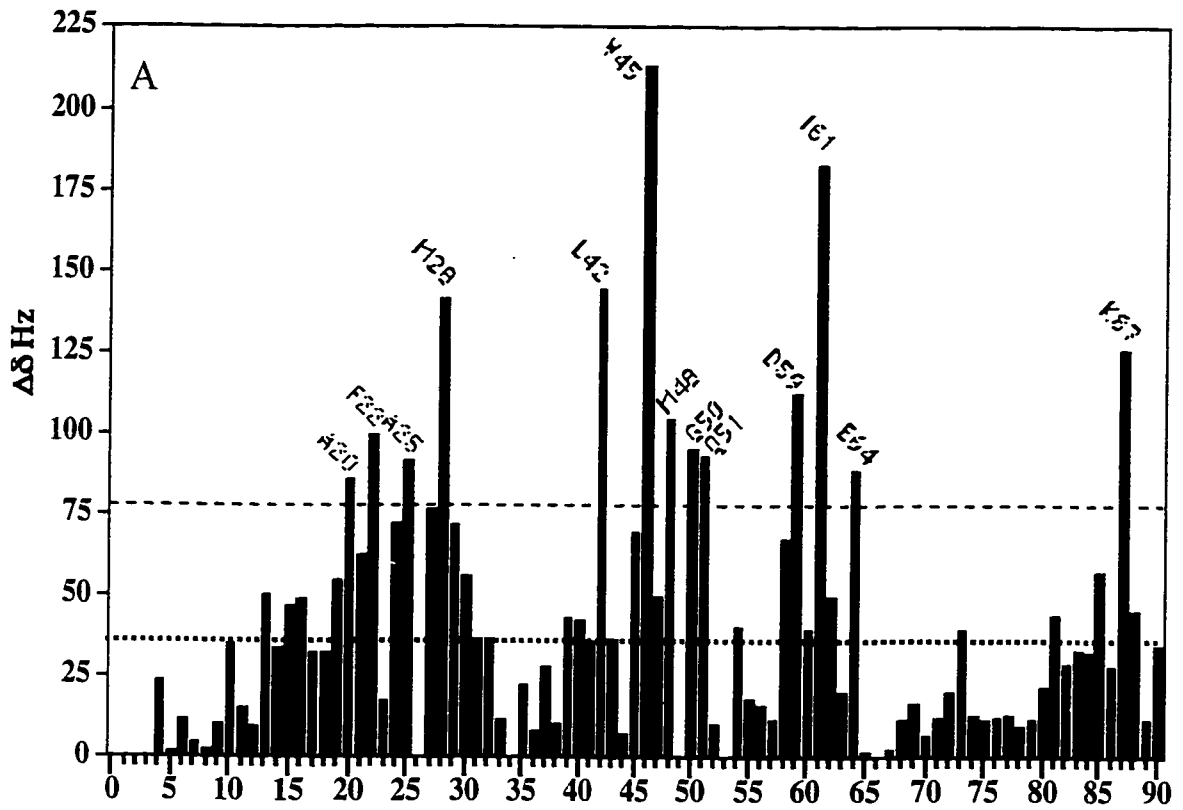

Figure III-5

    (A) The change in chemical shift ($\Delta\delta$) for each backbone amide pair in N-TnC upon binding of TnI_{96-148}. The thin dashed line indicates one standard deviation (41 Hz) above the average (thick dotted line, 39 Hz) $\Delta\delta$. Residues Ala^{20}, Phe^{22}, Ala^{25}, Met^{28}, Leu^{42}, Val^{45}, Met^{48}, Gly^{50}, Gln^{51}, Asp^{59}, Ile^{61}, Glu^{64}, and Lys^{87} demonstrating statistically different $\Delta\delta$ are labeled. Residues Ala^{1}, Ser^{2}, Met^{3}, Phe^{26}, Gly^{34}, Leu^{49}, and Asp^{66} were not followed due to spectral overlap while residues such as Ala^{24}, Ala^{25}, and Lys^{87} may be underestimated (see text). (B) Intermolecular NOEs between TnI_{96-148} and each residue of N-TnC. Residues Ala^{20}, Glu^{21}, Ala^{24}, Ala^{25}, Leu^{42}, Val^{45}, Met^{48}, Leu^{49}, Leu^{58}, Ala^{60}, Ile^{61}, Val^{65}, Val^{80}, and Met^{81} which have unambiguous contacts to the peptide are labeled. A value of 1 indicates an unambiguous contact with the peptide while a value of 0.5 indicates ambiguous contacts. The unshaded columns indicate the Filter/Edit-NOESY experiment while the black columns represent the Edit/Filter experiment.

To further investigate the site of interaction and support the chemical shift information we performed two sets of filter/edit NOESY experiments. These experiments select for intermolecular NOE contacts, and therefore identify N-TnC hydrogen atoms within 5 Å of TnI_{96-148} peptide hydrogens. The first NOE experiment (Filter/Edit) involves filtering out magnetization originating on hydrogen atoms attached to ^{13}C, thus selecting for hydrogen atoms on the peptide (i.e. protons attached to ^{14}N and ^{12}C). The surviving magnetization is then passed, *via* the NOE, to other protons and standard heteronuclear editing procedures are used to detect only hydrogens attached to ^{13}C. The results of this experiment were scrutinized for any contact that could be intra-molecular. For example, if a side chain showed few contacts (i.e. β-protons showed contacts but protons further along the side chain showed no interactions), and/or if the assignment of the particular N-TnC atom was in a crowded spectral region (higher ambiguity), then this contact was considered of lower confidence and not considered for presentation in Figure III-5B. Most often a cross-peak was eliminated from consideration if it corresponded to an N-TnC methyl group showing contacts in the filtered experiments to a "methyl group" presumably on the peptide whose resonance frequency was degenerate with an N-TnC methyl group less than 5 Å away. In this case there exists the possibility, that the observed cross-peak might be a leak in the filtering

process. Therefore only NOE cross peaks with the highest confidence which could only

be intermolecular contacts (*i.e.* no N-TnC neighbors could account for the contact) were

assigned. A second NOE experiment (Edit/Filter) was performed to verify the contacts

identified above. The second experiment was similar to the first, but selected

magnetization (editing) from protons attached to ^{13}C, and then transferred to hydrogen on

^{12}C. An important advantage of this experiment was that ^{13}C was not decoupled during

acquisition; therefore any "leaks" in the pulse sequence filter were more identifiable by

their carbon-proton splitting of ~150 Hz. The results of both the filter/edit experiment

and the edit/filter experiments are shown in Figure III-5B. From these two experiments

residues Ala^{20}, Glu^{21}, Ala^{24}, Ala^{25}, Leu^{42}, Val^{45}, Met^{48}, Leu^{49}, Leu^{58}, Ala^{60}, Ile^{61}, Val^{65},

Val^{80}, and Met^{81} were unambiguously seen to be in close contact to as yet unassigned

TnI_{96-148} hydrogen atoms. Residues which showed contacts but were eliminated based on

the above mentioned criteria include Ala^{8}, Glu^{9}, Leu^{14}, Glu^{16}, Glu^{17}, Asp^{36}, Thr^{39}, Met^{46},

Arg^{47}, Glu^{56}, Phe^{75}, Leu^{79}, Val^{83}, Met^{86}, Lys^{87}, and Glu^{88}. These residues are reported to

show that the list of highest confidence contacts is by no means all inclusive.

To better illustrate the spatial relation of interacting residues within the 3D

structure, residues of N-TnC which are now thought to be involved in binding TnI_{96-148}

are highlighted in Figure III-6. The N-TnC molecule is shown in green and residues

displaying significant $\Delta\delta$ and/or unambiguous NOE contacts are colored in red. From

the $\Delta\delta$ values and the two intermolecular selective NOE experiments we have strong

evidence that TnI_{96-148} binds in the hydrophobic pocket (*67*) of N-TnC. These

experiments also draw attention to the predominantly hydrophobic nature of the residues

responding to the binding of TnI.
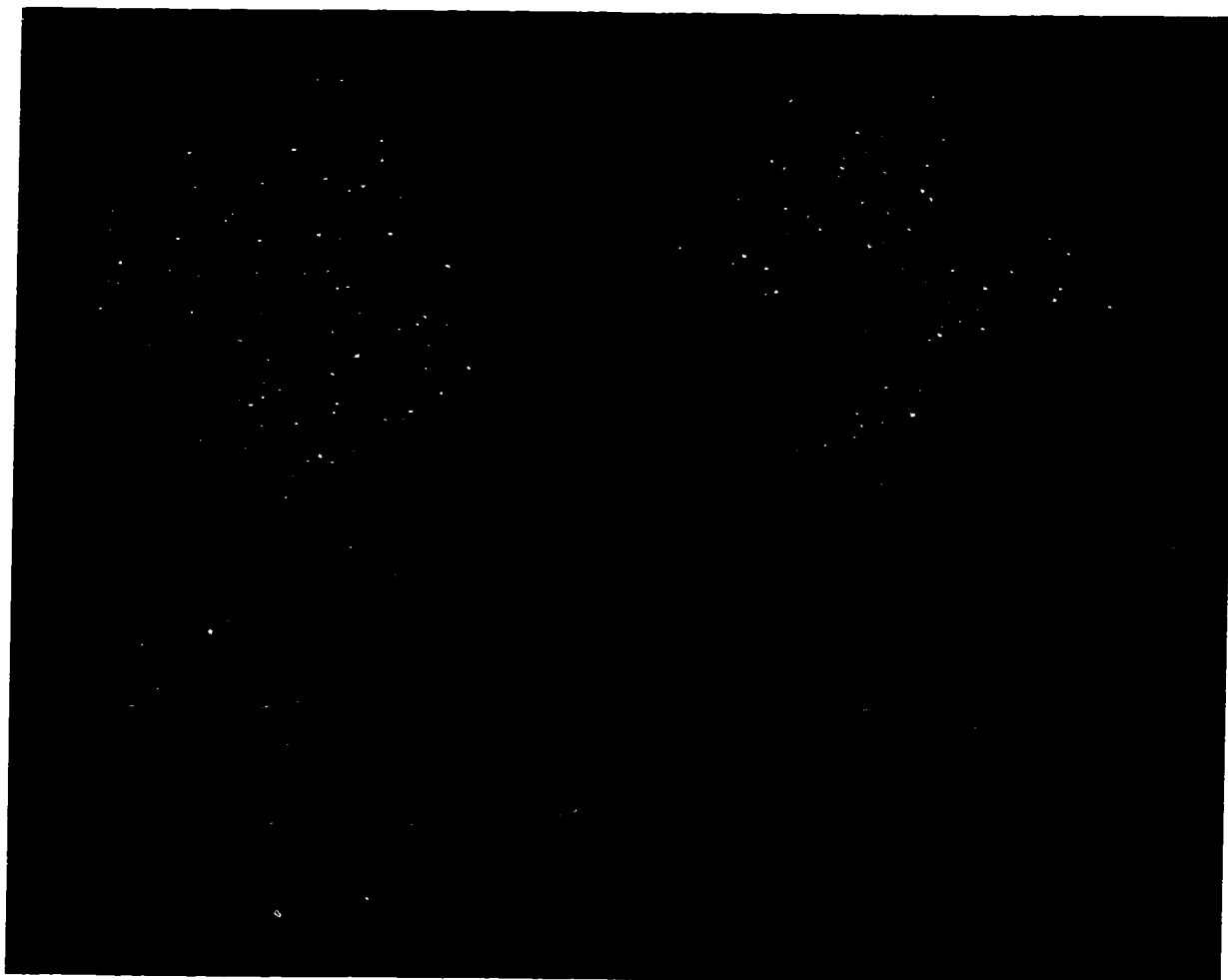
Figure III-1

Space filling model of N-TnC (green) while bound to TnI$_{96-148}$. Residues Ala^{20}, Glu^{21}, Phe^{22}, Ala^{24}, Ala^{25}, Met^{28}, Leu^{42}, Val^{45}, Met^{48}, Leu^{49}, Gly^{50}, Gln^{51}, Leu^{58}, Asp^{59}, Ala^{60}, Ile^{61}, Glu^{64}, Val^{65}, Val^{80}, Met^{81} and Lys^{87} which showed statistically different changes in Δδ and/or intermolecular NOEs are shown in red. The two images are rotated approximately 90 degrees to one another, and the average backbone orientation corresponding to each space filling model was included (bottom) for easier viewer orientation. The binding site is a channel formed by the hydrophobic pocket running laterally across the protein.

D. Discussion

In this paper we followed the titration of labeled N-TnC with unlabeled TnI_{96-148} by $^1H,^{15}N$-HMQC NMR spectroscopy. The TnI_{96-148} fragment was chosen for its high solubility and full inhibitory effect on the actomyosin complex (*37,38*). The spectra seen in these experiments were similar to the spectra seen with the shorter TnI (region 115-131) peptide (*39*). The additional residues in the 96-148 TnI peptide compared to 115-131 peptide apparently (within experimental error) do not alter the interaction strength of the complex. The dissociation constants reported by Pearlstone *et al.* (*38*) using a mutant N-TnC (F29W) (*55*) are smaller than we have observed. The difference in the reported K_d values may be due to the F29W mutation and/or different sample concentrations between the fluorescence and NMR experiments.

1. Comparison of Peptide Binding

It is interesting to compare the effects induced in N-TnC upon binding of TnI_{96-148} in this study with those of a smaller peptide $TnI_{115-131}$ presented previously (*39*). The shorter peptide is thought to comprise the N-TnC binding site (*36*), but it is not known if the two peptides bind in an identical fashion or if the extra residues in the longer peptide also interact with N-TnC. Comparison of the induced chemical shift changes observed for the two peptides shows that similar but not identical changes are caused by the TnI peptides. In Figure III-7A, the chemical shift changes induced by TnI_{96-148} are plotted versus those induced by $TnI_{115-131}$. Not all residues fall on the diagonal demonstrating that they have experienced different shifts from the two peptides. The difference in induced $\Delta\delta$ versus sequence position is plotted in Figure III-7B. There does not appear to be an isolated region in the sequence responding differently to either peptide. To

evaluate whether these differences are real, or a reflection of experimental errors,

previously published data for $TnI_{115-131}$ at two salt concentrations are plotted in Figure III-7C.

$\Delta\delta$ of sN-TnC•TnI $_{115-131}$ high salt (Hz)
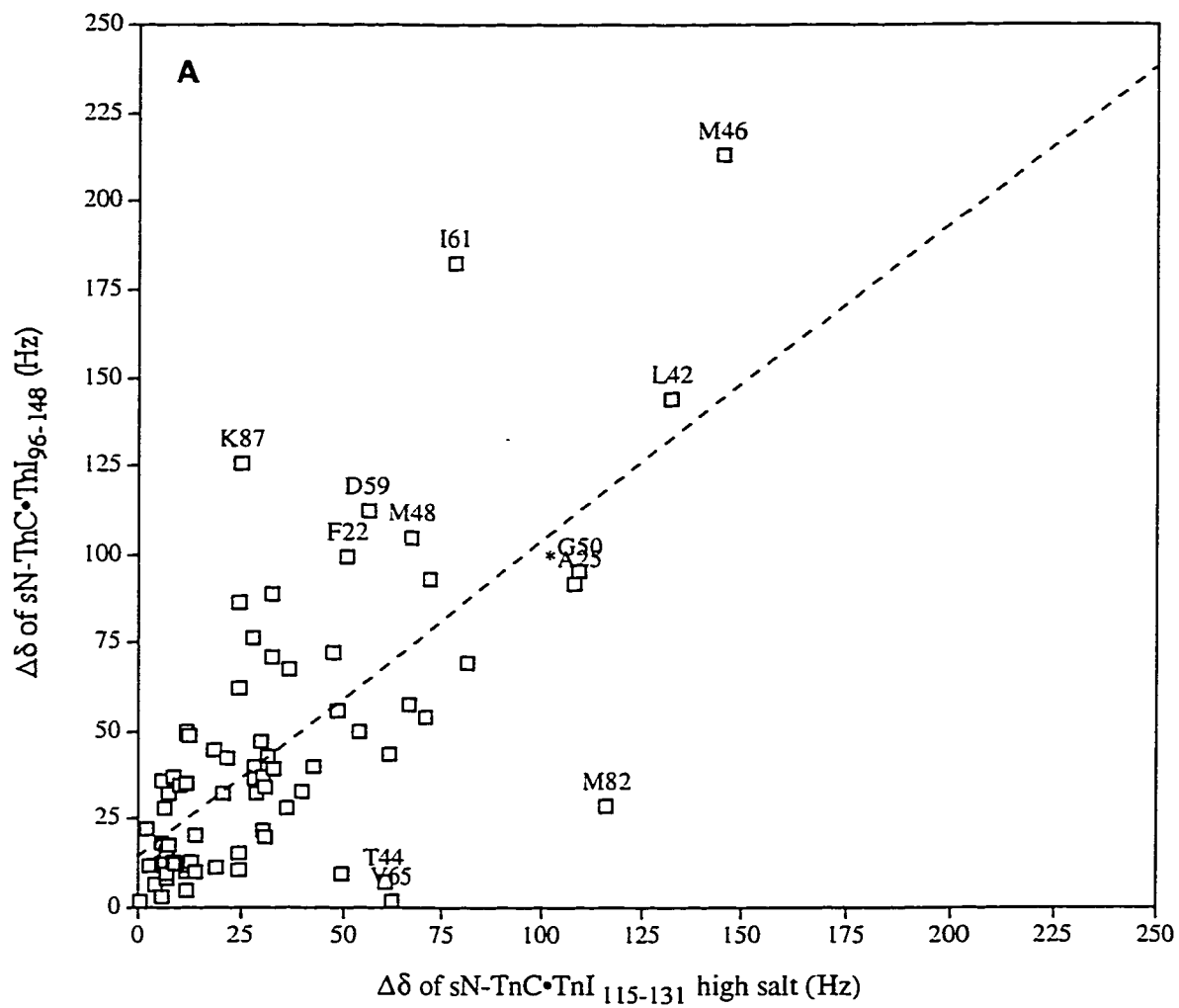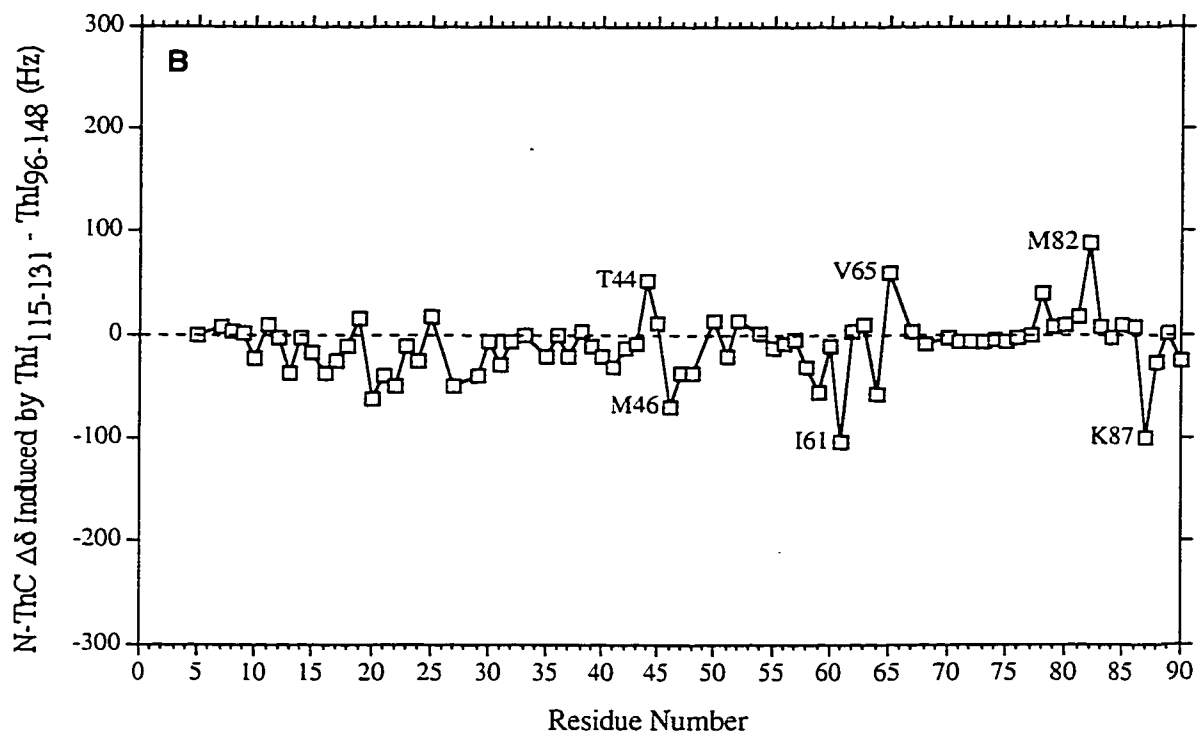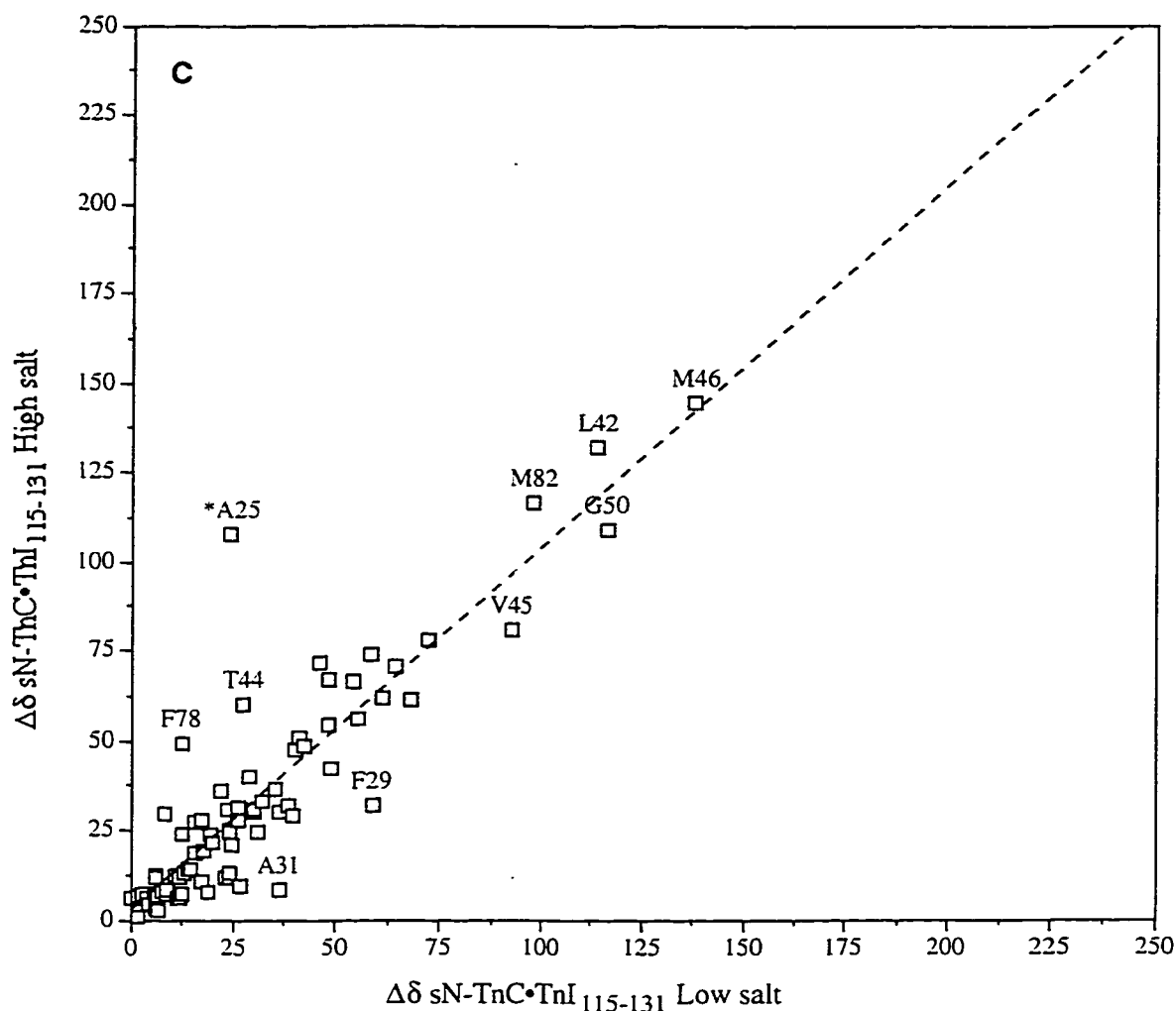
Figure III-7

Comparison of the change in chemical shift induced in N-TnC residues upon TnI peptide binding. (A) Comparison of TnI_{96-148} (y-axis) binding induced N-TnC chemical shift changes when plotted against the changes caused by $TnI_{115-131}$ (x-axis) in high salt. The least squares fit (dashed line) showed a slope of 0.90 and a y-intercept of 14. (B) Shows the difference ($\Delta\delta$ induced by $TnI_{115-131}$ - $\Delta\delta$ induced by TnI_{96-148}) in $\Delta\delta$ for each N-TnC residue followed when comparing $TnI_{115-131}$ to TnI_{96-148} binding. (C) The change in chemical shift for N-TnC residues upon binding of $TnI_{115-131}$ in high salt (y-axis) plotted versus the change caused by $TnI_{115-131}$ in low salt (x-axis) for comparison. A least squares fit (dashed line) showed a slope of 1.01 and a y-intercept of 2.6 implying very similar induced changes.

While the difference shown might still be real they are much less than when comparing the two different length peptides. This implies that $TnI_{115-131}$ binds similarly at the two

different ionic strengths and also provides an approximation of the experimental error.

Interestingly Ala[25] (Fig. III-7C) which was extrapolated (39) in the high salt sample

stands out when compared with the second $TnI_{115-131}$ titration (low salt) induced shifts

revealing the relatively large experimental error associated with that residue. When

comparing the two different length peptides residues such as Met[46], Ile[61], and Lys[87] show

larger chemical shift changes upon addition of TnI_{96-148} while Phe[26], Thr[44], Val[65], and

Met[82] respond more to the smaller peptide. The differences in $\Delta\delta$, despite the similar

dissociation constants, indicate that the two peptides do not interact in identical ways

though both peptides do interact in the same area and with virtually the same residues.

The difference is most likely a result of the additional residues in the larger peptide. This

may cause a small change in average secondary structure of the terminal binding peptide

residues, and/or an entropic barrier to binding of the larger peptide that may be over come

with a slightly larger, stable binding region. In any event the changes are small when

compared to the experimental error and digital resolution of the experiments.

2. Bound Structure

A goal of this paper was to determine the 3D NMR solution structure of skeletal

N-TnC while bound to TnI_{96-148}. We have presented an NMR solution structure with a

backbone RMSD of 1.5 Å for all regions of N-TnC and 1.1 Å for the well defined

regions. The bound and unbound N-TnC structures are similar except for the BC linker

(residues 49-54) and the C/D interhelical angle (bound: 88° ± 6, unbound: 68° ± 5). The

difference results in a slight closing of the BC helices and therefore a slight reduction in

the surface area of the hydrophobic pocket. This suggests that the N-TnC may "clamp"

down on the TnI peptide; however the change is small in comparison to the changes of N-

TnC from apo to the calcium saturated state (*13*). Interestingly the recently reported apo

and calcium saturated cardiac N-TnC (*15*) and calcium saturated whole cardiac TnC (*4*)

structures do not exhibit the expected opening of the hydrophobic pocket. Identifying the

exact location of TnI_{96-148} binding has become even more important in light of this new

structural information.

3. Location of Binding

Another goal was to identify the location of TnI_{96-148} binding on N-TnC. The

combined use of chemical shift mapping which indicates alterations in the local magnetic

environment, and the intermolecular NOE experiments which provide direct

intermolecular hydrogen contacts within 5 Å, allow an efficient method for identifying

which hydrogen atoms are involved in intermolecular van der Waals contact. The

binding of TnI_{96-148} presumably disrupts the TnC dimer (~30% dimerized at 1 mM

(*13,68*)) in solution which may account for some of the difference seen in the unbound

versus bound structures. This is especially relevant since dimerization was shown to

occur primarily in the N-domain (*3*). We have attempted to select residues experiencing

functionally relevant changes by highlighting only those with statistically different shifts

(i.e. the selection of one standard deviation above the average). We are therefore

attempting to discern between primary effects of binding and secondary effects of small

remote changes in the environment.

Our results agree with previously reported crosslinking studies (*33,69,70*).

Mutational work by Pearlstone *et al.* (*55,71*) that identified residues making up the

hydrophobic pocket match those residues found in our study which bind to TnI_{96-148}. The

present study has not yet identified which TnI_{96-148} residues are involved in binding to

N-TnC. However, primary sequence inspection of TnI revealed a common characteristic

between TnI regions 108-115 and 137-144 (*5*). Later a three fold repeated sequence

(designated α, β, and γ) which is highly conserved among species involving residues

~101-114, ~121-132, and ~135-146 was reported (*38*). In recent reports (*36,39*) residues

115-131 were shown to be involved in binding to the hydrophobic patch of N-TnC and

residues 140-148 were identified as playing a crucial role in inhibition of actomyosin S1

ATPase (*37*). Coupled with abundant evidence (summarized in (*36*)) for C-TnC and the

central helix interaction with TnI residues 96-115, the present data indicates strongly that

the 96-131 region of TnI is intimately involved in binding to the hydrophobic patch

regions of both C- and N-TnC.

We have determined the structure of N-TnC while bound to TnI_{96-148}, and the site

of interaction between N-TnC and TnI_{96-148} using the $\Delta\delta$ and intermolecular NOE

experiments. This paper has shown that TnI_{96-148} and N-TnC interact through the calcium

regulated hydrophobic pocket of N-TnC. The lack of significant structural changes in

N-TnC also indicates that the binding of calcium and the exposure of the hydrophobic

pocket is sufficient to prepare N-TnC for interaction with the TnI peptide. Future work

will logically lead to determining the structure of the TnI peptide while bound to the N-

domain and eventually to the structure of the intact TnC•TnI complex.

E. References

1.   Herzberg, O., and James, M. N. G. (1988) *J. Mol. Biol.* **203**, 761-779

2.   Satyshur, K. A., Rao, S. T., Pyzalska, D., Drendal, W., Greaser, M., and
      Sundaralingham, M. (1988) *J. Biol. Chem.* **263**, 1628-1647

3.   Slupsky, C. M., and Sykes, B. D. (1995) *Biochemistry* **34**, 15953-15964

4.   Sia, S. K., Li, M. X., Spyracopoulos, L., Gagné, S. M., Liu, W., Putkey, J. A., and
      Sykes, B. D. (1997) *J. Biol. Chem.* **272**, 18216-18221

5.   Farah, C. S., and Reinach, F. C. (1995) *FASEB J.* **9**, 755-767

6.   Li, M. X., Gagné, S. M., Tsuda, S., Kay, C. M., Smillie, L. B., and Sykes, B. D.
      (1995) *Biochemistry* **34**, 8330-8340

7.   Head, J. F., and Perry, S. V. (1974) *Biochem. J.* **137**, 145-154

8.   Weeks, R. A., and Perry, S. V. (1978) *Biochem. J.* **173**, 449-457

9.   Potter, J. D., and Johnson, J. D. (1982) in *Calcium and Cell Function* (Cheung,
      W. Y., ed) Vol. 2, pp. 145-169, Academic Press, Inc.

10.   Strynadka, N. C. J., Cherney, M., Sielecki, A. R., Li, M. X., Smillie, L. B., and
      James, M. N. G. (1997) *J. Mol. Biol.* **273**, 238-255

11.   Houdusse, A., Love, M. L., Dominguez, R., Grabarek, Z., and Cohen, C. (1997)
      Structure **5**, 1695-1711

12.   Rao, S. T., Satyshur, K. A., Greaser, M. L., and Sundaralingam, M. (1996) *Acta
      Crystallographica Section D* **52**, 916-922

13.   Gagné, S. M., Tsuda, S., Li, M. X., Smillie, L. B., and Sykes, B. D. (1995) *Nature
      Struct. Biol.* **2**, 784-789

14.   Gagné, S. M., Li, M. X., and Sykes, B. D. (1997) *Biochemistry* **36**, 4386-4392

15.   Spyracopoulos, L., Li, M. X., Sia, S. K., Gagné, S. M., Chandra, M., Solaro, R. J.,
      and Sykes, B. D. (1997) *Biochemistry* **36**, 12138-12146

16.   Li, M. X., Chandra, M., Pearlstone, J. R., Racher, K. I., Trigo-Gonzalez, G.,
      Borgford, T., Kay, C. M., and Smillie, L. B. (1994) *Biochemistry* **33**, 917-925

17.   Fredricksen, S. R., and Swenson, C. A. (1996) *Biochemistry* **35**, 14012-14026

18.   Houdusse, A., and Cohen, C. (1995) *Proc. Natl. Acad. Sci. U.S.A.* **92**, 10644-10647

19.   Xie, X., Harrison, D. H., Schlichting, I., Sweet, R. M., Kalabokis, V. N., Szent-Gyorgyi, A. G., and Cohen, C. (1994) *Nature* **368**, 306-312

20.   Rayment, I., Holden, H. M., Whittaker, M., Yohn, C. B., Lorenz, M., Holmes, K. C., and Milligan, R. A. (1993) *Science* **261**, 58-65

21.   Rayment, I., Rypniewski, W. R., Schmidt-Base, K., Smith, R., Tomchick, D. R., Benning, M. M., Winkelmann, D. A., Wesenberg, G., and Holden, H. M. (1993) *Science* **261**, 50-58

22.   Babu, Y. S., Bugg, C. E., and Cook, W. J. (1988) *J. Mol. Biol.* **204**, 191-204

23.   Kretsinger, R. H., Rudnick, S. E., and Weissman, L. J. (1986) *J. Inorg. Biochem.* **28**, 289-302

24.   Ikura, M., Clore, G. M., Gronenborn, A. M., Zhu, G., Klee, C. B., and Bax, A. (1992) *Science* **256**, 632-638 .

25.   Olah, G. A., Rokop, S. E., Wang, C.-L. A., Blechner, S. L., and Trewhella, J. (1994) *Biochemistry* **33**, 8233-8239

26.   Olah, G. A., and Trewhella, J. (1994) *Biochemistry* **33**, 12800-12806

27.   Campbell, A. P., and Sykes, B. D. (1991) *J. Mol. Biol.* **222**, 405-421

28.   Campbell, A. P., Van Eyk, J. E., Hodges, R. S., and Sykes, B. D. (1992) *Biochim. Biophys. Acta* **1160**, 35-54

29.   Ngai, S.-M., Sönnichsen, F. D., and Hodges, R. S. (1994) *J. Biol. Chem.* **269**, 2165-2172

30.   Luo, Y., Wu, J.-L., Gergely, J., and Tao, T. (1997) *Biochemistry* **36**, 11027-11035

31.   Sheng, Z., Pan, B. S., Miller, T. E., and Potter, J. D. (1992) *J. Biol. Chem.* **267**, 25407-25413

32.   Krudy, G. A., Kleerekoper, Q., Guo, X., Howarth, J. W., Solaro, R. J., and
       Rosevear, P. R. (1994) *J. Biol. Chem.* **269**, 23731-23735

33.   Kobayashi, T., Grabarek, Z., Gergely, J., and Collins, J. H. (1995) *Biochemistry*
       34, 10946-10952

34.   Talbot, J. A., and Hodges, R. S. (1981) *J. Biol. Chem.* **256**, 2798-2802

35.   Farah, C. S., Miyamoto, C. A., Ramos, C. H. I., da Silva, A. C. R., Quaggio, R.
       B., Fujimori, K., Smillie, L. B., and Reinach, F. C. (1994) *J. Biol. Chem.* **269**,
       5230-5240

36.   Tripet, B. P., Van Eyk, J. E., and Hodges, R. S. (1997) *J. Mol. Biol.* **271**, 728-750

37.   Van Eyk, J. E., Thomas, L. T., Tripet, B. P., Wiesner, R. J., Pearlstone, J. R.,
       Farah, C. S., Reinach, F. C., and Hodges, R. S. (1997) *J. Biol. Chem.* **272**, 10529-
       10537

38.   Pearlstone, J. R., Sykes, B. D., and Smillie, L. B. (1997) *Biochemistry* **36**, 7601-
       7606

39.   McKay, R. T., Tripet, B. P., Hodges, R. S., and Sykes, B. D. (1997) *J. Biol.
       Chem.* **272**, 28494-28500

40.   Ramakrishnan, S., and Hitchcock-DeGregori, S. E. (1996) *Biochemistry* **35**,
       15515-15521

41.   Jha, P. K., Mao, C., and Sarkar, S. (1996) *Biochemistry* **35**, 11026-11035

42.   Pearlstone, J. R., and Smillie, L. B. (1995) *Biochemistry* **34**, 6932-6940

43.   Gasmi-Seabrook, G., Howarth, J. W., Finley, N., Abbott, M. B., Brito, R. M., and
       Rosevear, P. R. (1998) *Biophys. J.* **74**, A299

44.   Vassylyev, D. G., Takeda, S., Wakatuski, S., Maeda, K., and Maeda, Y. (1998)
       Biophys. J. **74**, A53

45.   Gagné, S. M., Li, M. X., McKay, R. T., and Sykes, B. D. (1998) *Biochem. Cell
       Biol.* **Manuscript in Review**

46. Gagné, S. M., Tsuda, S., Li, M. X., Chandra, M., Smillie, L. B., and Sykes, B. D. (1994) *Prot. Sci.* **3**, 1961-1974

47. Zhou, N. E., Kay, C. M., and Hodges, R. S. (1994) *Protein Eng.* **7**, 1365-1372

48. Delaglio, F., Grzesiek, S., Vuister, G. W., Zhu, G., Pfeifer, J., and Bax, A. (1995) *J. Biomol. NMR* **6**, 277-293

49. Garrett, D. S., Powers, R., Gronenborn, A. M., and Clore, G. M. (1991) *J. Magn. Reson.* **95**, 214-220

50. Wishart, D. S., and Sykes, B. D. (1994) *Methods Enzymol.* **239**, 363-392

51. Wishart, D. S., and Sykes, B. D. (1994) *J. Biomol. NMR* **4**, 171-180

52. Wishart, D. S., Sykes, B. D., and Richards, F. M. (1991) *J. Mol. Biol.* **222**, 311-333

53. Wüthrich, K. (1986) *NMR of proteins and nucleic acids.*, John Wiley & Sons, New York

54. Brünger, A. T. (1992) *X-PLOR Version 3.1 A system for X-ray Crystallography and NMR*, Yale University Press, New Haven

55. Pearlstone, J. R., Borgford, T., Chandra, M., Oikawa, K., Kay, C. M., Herzberg, O., Moult, J., Herklotz, A., Reinach, F. C., and Smillie, L. B. (1992) *Biochemistry* **31**, 6545-6553

56. Gagné, S. M., Tsuda, S., Spyracopoulos, L., Kay, L. E., and Sykes, B. D. (1997) *J. Mol. Biol., in press*

57. Abragam, A. (1961) *Principles of Nuclear Magnetism.* International Series on Monographs on Physics (Adair, R. K., Edwards, S. F., Ehrenreich, H., Llewellyn Smith, C. H., and Rees, M., Eds.), 32, Oxford University Press, Toronto

58. Muhandiram, D. R., and Kay, L. E. (1994) *J. Magn. Reson.* **B103**, 203-216

59. Wittekind, M., and Mueller, L. (1993) *J. Magn. Reson.* **B 101**, 201-205

60. Vuister, G. W., and Bax, A. (1993) *J. Am. Chem. Soc.* **115**, 7772-7777

61. LeMaster, D. M. (1990) *Quart. Rev. Biophys.* **23**, 133-174

62. Grzesiek, S., Wingfield, P., Stahl, S., Kaufman, J. D., and Bax, A. (1995) *J. Am. Chem. Soc.* **117**, 9594-9595

63. Grzesiek, S., Anglister, J., Ren, H., and Bax, A. (1993) *J. Am. Chem. Soc.* **115**, 4369-4370

64. Slupsky, C. M. (1995) in *Thesis: Biochemistry*, University of Alberta, Edmonton

65. Laskowski, R. A., MacArthur, M. W., Moss, D. S., and Thorton, J. M. (1993) *Journal of Applied Crystallography* **26**, 283-290

66. Shuker, S. B., Hajduk, P. J., Meadows, R. P., and Fesik, S. W. (1996) *Science* **274**, 1531-1534

67. Herzberg, O., Moult, J., and James, M. N. G. (1986) *J. Biol. Chem.* **261**, 2638-2644

68. Slupsky, C. M., Kay, C. M., Reinach, F. C., Smillie, L. B., and Sykes, B. D. (1995) *Biochemistry* **34**, 7365-7375

69. Leszyk, J., Grabarek, Z., Gergely, J., and Collins, J. H. (1990) *Biochemistry* **29**, 299-304

70. Kobayashi, T., Leavis, P. C., and Collins, J. H. (1996) *Biochim. Biophys. Acta* **1294**, 25-30

71. Pearlstone, J. R., McCubbin, W. D., Kay, C. M., Sykes, B. D., and Smillie, L. B. (1992) *Biochemistry* **31**, 9703-9708

72. Bax, A., Griffey, R.H., and Hawkins, B.L. (1983) J. of Magn. Reson. **55**, 301-315

73. Kay, L. E., Keifer, P., and Saarinen, T. (1992) *J. Am. Chem. Soc.* **114**, 10663-10665

74. Marion, D. C., Driscoll, P. C., Kay, L. E., Wingfield, P. T., Bax, A., Gronenborn, A. M., and Clore, G. M. (1989) *Biochemistry* **28**, 6150-6156

75. Kay, L. E., Xu, G. Y., Singer, A. U., Muhandiram, D. R., and Forman-Kay, J. D. (1993) *J. Magn. Reson.* **B101**, 333-337

76.   Kay, L. E., Marion, D., and Bax, A. (1989) *J. Magn. Reson.* **84,** 72-84

77.   Zhang, O., Kay, L. E., Olivier, J. P., and Forman-Kay, J. D. (1994) *J. Biomol.*
       NMR **4,** 845-858

78.   Pascal, S. M., Muhandiram, D. R., Yamazaki, T., Forman-Kay, J. D., and Kay, L.
       E. (1994) *J. Magn. Reson.* **B103,** 197-201

79.   Grzesiek, S., and Bax, A. (1992) *J. Magn. Reson.* **96,** 432-440

80.   Powers, R., Gronenborn, A. M., Clore, G. M., and Bax, A. (1991) *J. Magn.*
       Reson. **94,** 209-213

81.   Lee, W., Revington, M. J., Arrowsmith, C., and Kay, L. E. (1994) *FEBS. Let.* **350,**
       87-90

82.   Kraulis, P. J. (1991) *Journal of Applied Crystallography* **24,** 946-950

Chapter IV: *Defining the Region of Troponin-I that Binds to Troponin-C[1]*

A. Introduction

The transient release of calcium in a muscle cell in response to a neural signal results in a cascade of changing protein-protein interactions and eventually muscle contraction (for review see (1-4)). The sliding of the thick and thin filaments past one another constitutes the actual physical mechanism of contraction produced as a result of the hydrolysis of ATP by myosin. The regulatory target for calcium in skeletal muscle cells is the troponin complex consisting of troponin-C (TnC)[†], troponin-I, and troponin-T. TnC is the calcium-binding component and is the only member of the complex presently resolved at an atomic level. TnI inhibits the ability of myosin to hydrolyze ATP thus preventing muscle contraction. Troponin-T anchors the troponin complex to actin/tropomyosin, interacts with TnC directly, and is involved in the activation of contraction in the presence of calcium (see (5) and references therein). Once calcium is released in the cell, the three-dimensional structure of TnC and subsequent protein/protein interactions are altered. Specifically, TnC in the presence of calcium interacts with TnI more strongly and allows muscle contraction to occur (see (1,2,6,7) and references therein). However, the exact mechanism of how TnI inhibits contraction in the absence of calcium, and conversely participates in the activation of the actomyosin complex in the presence of calcium, is not presently understood.

TnC is an 18 kDa protein of 162 amino acids comprising 2 separate domains (N and C domains each ~80 amino acids) covalently attached by a flexible 'helical' linker (residues ~ 80-95). Both the C- and N-terminal domains are predominantly α-helical

with each individual domain containing two EF hand calcium binding sites that interact through a short bisecting β-sheet. The calcium binding sites are labeled sequentially I-IV based on their respective positions in the primary amino acid sequence of the protein. The C-terminal sites have a higher affinity for Ca^{2+} than the N-terminal sites, and the C-terminal sites also have affinity for Mg^{2+} while the N-terminal sites are calcium specific. Sites I and II have calcium affinities ($\sim7\times10^4$ and 5×10^5 M^{-1} for K_a, respectively) in the range of the transient Ca^{2+} signal (8). It has not been determined if the C-terminal sites are bound with Mg^{2+} at all times, or if the Ca^{2+} signal is of sufficient duration to displace Mg^{2+} in the contractile state.

There is presently no high-resolution structure for TnC with Mg^{2+} bound in sites III and IV, but there are several crystal structures of skeletal TnC with calcium present in the C-domain, and absent from (9,10) or present in the N-domain (11-13). NMR solution structures include that of apo and Ca^{2+} saturated N-TnC (14), Ca^{2+} saturated E41A N-TnC (15), Ca^{2+} saturated TnC (16), both apo and Ca^{2+} saturated cardiac N-TnC (17), cardiac TnC (18), and Ca^{2+} saturated N-TnC while bound to TnI_{96-148} (19) (see (20) for an overall review and comparison of the solution and x-ray troponin-C structures). The structures have revealed important information regarding the mechanism of both cardiac and skeletal muscle regulation. In the skeletal system the binding of calcium in the low affinity sites causes the movement of the B and C helices away from the N, A and D helices (14), exposing a hydrophobic pocket that has been shown to bind TnI (19,21). Interestingly, this large structural change is not observed in cardiac TnC upon binding calcium. Recently, the X-ray crystal structure of $2Ca^{2+}$ (sites III and IV occupied) skeletal TnC while bound with a TnI peptide (residues 1-47) was reported (22,23).

Calmodulin and the myosin light chains are very highly homologous, multiple EF hand motif containing, dumbbell shaped, calcium binding proteins that have also been resolved at an atomic level (see (24) for review). The structures of CaM bound to: skeletal or smooth muscle myosin light chain kinase peptides (25,26), a brain CaM-

dependant protein kinase IIα peptide (27), and the regulatory and essential light chains of

myosin bound to a portion of the heavy chain (28), have revealed different manners in

which the N- and C-terminal domains of calcium regulatory proteins interact with protein

targets (see (29) and references therein). These structures and other experiments

involving various target peptides suggest that calcium-binding proteins may be able to

bind using both domains in an extended structure, or both domains in a collapsed

orientation to grasp target peptides.

Despite the structural information presently available for TnC and the

homologous CaM and myosin systems, there is relatively little known about TnI either in

isolation or in complex with TnC and/or TnT. We do not know exactly which residues of

TnI interact with TnC under conditions normally associated with the contractile or

relaxed states, nor do we fully understand the mechanism or nature of the interaction.

However, based on a variety of experimental approaches, evidence for an anti-parallel

arrangement of TnC and TnI molecules (2) in either an extended, partially extended, or

compact structure has been deduced (23,30-32) and a number of interaction sites

identified (see below). Studies have included cross-linking (33-38), low-angle X-ray

diffraction of TnC•TnI (30,39,40), ATPase assays of various combinations of both intact

proteins and their fragments in the presence or absence of Ca^{2+} (41-43), and binding

studies of intact TnC, N-TnC, C-TnC with TnI and its peptide fragments (i.e. proteolytic,

synthetic or recombinant) by gel electrophoresis, fluorescence, and NMR measurements

(19,21,44-48).

These studies have identified two regions (1-21 and 96-148) of the TnI

polypeptide chain important in Ca^{2+}-dependent interaction with TnC. TnI residues 1-40

appeared to bind exclusively to the C-domain of TnC with a low dissociation constant

($K_d < 10^{-7}$ M) in the presence of Ca^{2+} (49). This affinity is weakened when Ca^{2+} is

replaced by Mg^{2+} (50). These observations are consistent with other studies (5,41) using

longer fragments of TnI (i.e. residues 1-98 and 1-116). The recently reported 2.3 Å X-

ray structure of 2 Ca^{2+} TnC in complex with TnI_{1-47} shows a 'compact' TnC structure with

multiple proposed contacts from both N- and C-terminal domains of TnC to the peptide.

On the basis of their structure and other data they have proposed a model. It is presently

unclear how representative this model is of the complex of calcium saturated TnC with

intact TnI (or fragments derived from its central and/or C-terminal regions).

The latter segments of TnI are the major focus of this present investigation.

Residues 96-116 have long been recognized as containing the major inhibitory activity of

TnI (i.e. residues 104-115 known as the inhibitory region) (7,51,52). Interaction of the

inhibitory region with TnC has been localized to the C-domain and possibly the linker

(i.e. the D/E helix in x-ray structure) between the N- and C-domains. More recently a

section of TnI (i.e. residues ~ 115-148) has been recognized as contributing significantly

to inhibition and to Ca^{2+}-sensitivity of the ATPase activity in the reconstituted

troponin•tropomyosin actomyosin system (41,43). In a comparison of binding affinities

of TnI_{96-116} and TnI_{96-148} to calcium saturated TnC and its isolated N- and C-domains, the

binding to the N-domain of TnC was significantly increased with the extended fragment,

and a three-fold repeated sequence motif has been reported, specifically involving TnI

residues 101-114, 121-132, and 135-146 (47). Using a variety of synthetic peptides

encompassing residues 96-148, Tripet et al. (32) have demonstrated the importance of

lysine residues 141, 144 and 145 for full inhibitory activity (i.e. binding to

tropomyosin/actin), and the importance of the 116-126 region in binding to TnC. Two

models have been suggested. The first contains a "switching mechanism" that is

dependent on the presence of calcium in the N-domain of TnC ((30), (32) and references

therein), while the second model has the N-terminal TnI residues (~ 1-47) specifically

involved in calcium independent binding to the hydrophobic pocket of C-TnC (22,23).

There is presently no definitive experiment to decide between either model.

In an attempt to provide more detailed information on the interface between the

two components of the TnC•TnI complex, this laboratory has applied multinuclear,

multidimensional NMR spectroscopy to the interaction of TnC with TnI peptides,

specifically in the 96-148 region. Studies to date have provided dissociation constants for

TnI115-131 and TnI96-148 in complex with calcium saturated N-TnC, and identified

residues perturbed by binding of these peptides (19,21). The data confirm that TnI

peptide binding involves interactions with residues in the hydrophobic pocket of N-TnC.

The present report extends these studies to a comparison of the binding kinetics and

energetics of TnI96-131, TnI96-139, and TnI96-148 to calcium saturated, intact TnC. In

addition to providing the dissociation and kinetic off rates for these peptides, the NMR

spectral data of the labeled TnI peptide show that residues 97-136 are the residues within

the 96-148 region primarily involved in binding to calcium saturated TnC. Also, a

specifically13C- labeled TnI96-139 peptide when complexed to TnC indicates that the N-

terminal region of the TnI peptide appears to bind in a single orientation (presumably to

the C-domain of TnC), while the C-terminal region of TnI assumes multiple bound

conformations.

B. Experimental Procedures

1. Proteins and Peptides

The cloning, expression, and purification of [U-^{15}N,^{13}C-Ala] TnC, [U-^{15}N,^{13}C]

TnC and [U-^{2}H (88%)] TnC were performed as described previously (21,53). Synthetic

N$^{\alpha}$-acetyl- peptides corresponding to rabbit skeletal troponin-I regions 96-131, 96-139,

and 96-148 were prepared as described by Tripet et al. (32). Synthetic N$^{\alpha}$-acetyl TnI$_{96-139}$

incorporating [U-^{13}C]-L-leucine (residues 102, and 111) and [^{13}CH$_3$]-L-methionine

(residues 121, and 134) was prepared as the other peptides except for manual synthesis

runs at each labeled position. Leucine at position 102 was 100% labeled while the

synthesis of position 111 was performed with only 50% labeled leucine, as was the case

for methionine positions 121 (100%) and 134 (50%), respectively. The uniformly ^{15}N-

labeled TnI$_{96-148}$ peptide was produced from the cloning and transformation of

pAED4.TnI$_{96-148}$ into E. coli strain BL21.DE3.pLysS (Novagen) for inducible protein

expression with 0.4mM IPTG. The purification of expressed TnI$_{96-148}$ from an extract of

dried acetone powder cell pellet, on a CM-cellulose column at pH 7.5, has been described

previously (47). To produce uniformly ^{15}N labeled protein, cells were initially grown in

ZB medium (54) supplemented with ampicillin and chloramphenicol (both at 0.1 mg/ml)

to A$_{600}$ ≈ 0.7. Ten ml of this culture was inoculated into each of four, 1 L volumes of M9

medium (55), in which NH$_4$Cl was replaced with 99.4% ^{15}N-enriched (NH$_4$)$_2$SO$_4$ (Isotec

Inc.). The M9 minimal medium was supplemented with filter-sterilized solutions of

minerals (final concentration of 2 mM MgSO$_4$, 1 μM FeCl$_3$, 25 μM ZnSO$_4$, and 0.1 mM

CaCl$_2$), ampicillin, chloramphenicol, and vitamins (1 mg each of D-biotin, choline

chloride, folic acid, niacimamide, D-pantothenic acid, pyridoxine, and 5 mg thiamine and

0.1 mg riboflavin per liter). The concentration and primary sequence of proteins and peptides was confirmed by amino acid analysis done in quadruplicate, the correct mass verified by electrospray mass spectrometry, and the overall purity confirmed by reverse phase HPLC.

2. NMR sample Preparation

NMR samples were prepared for each of the $[U^{-15}N,^{13}C]TnC \cdot TnI_{96-131}$, $[U^{-15}N,$ ^{13}C-Ala$]TnC \cdot TnI_{96-139}$, $[U^{-15}N,^{13}C$-Ala$]TnC \cdot TnI_{96-148}$, $[U^{-2}H]TnC \cdot [U^{-15}N]TnI_{96-148}$, and $[U$-$^{2}H,^{15}N]TnC \cdot [U^{-13}C$-(100%)$Leu^{102}$, -(50%)$Leu^{111}$, $^{13}CH_3$-(100%)Met^{121}, -(50%)$Met^{134}]TnI_{96-139}$ complexes. All titration samples started with 500 µL volumes. The $[U^{-2}H]TnC \cdot [U^{-15}N]TnI_{96-148}$ complex sample had a volume of 500 µL with peptide and protein concentrations of $5x10^{-4}$ M and $6x10^{-4}$ M, respectively. The ^{13}C-$TnI_{96-139} \cdot TnC$ complex sample had a volume of 500 µL with peptide and protein concentrations of 1.2 mM each. All NMR samples consisted of 90% H_2O, 10% D_2O, 10 mM deuterated imidazole, 100 mM KCl, 0.1 mM 2,2-dimethyl-2-silapentane-5-sulfonate as an internal reference standard, and slight amounts of HCl and/or NaOH as necessary to pH the samples to a level of 6.8 (uncorrected for isotope effects). Each sample contained 8 equivalents of calcium per molecule of TnC (i.e. 2 moles per Ca^{2+} binding site). Imidazole has been calibrated and was used as an internal pH reference standard (data not shown).

3. Titrations of TnC with TnI peptides

Three separate titrations were performed. In each case TnC was titrated with the addition of a TnI peptide, and 2D-$^{1}H,^{15}N$-HSQC NMR spectra were taken at each point. In the first titration 5 µL of stock TnI_{96-131} ($5.1x10^{-8}$ moles/addition) were added to 500 µL

of TnC (0.65 mM) achieving a final ratio of 1.54 to 1, peptide to TnC. The second

titration involved adding 5 μL of stock TnI_{96-139} (6.3×10^{-8} moles/addition) to 500 μL of

TnC (0.85 mM) to a final ratio of 1.48 to 1, peptide to TnC. In the first two titrations the

final addition of peptide was only 4 μL because 1 μL had been set aside for amino acid

analysis. The third titration employing the TnI_{96-148} peptide was found to have

precipitated upon complex formation, and therefore amino acid analysis was performed

before and after titration. Stock TnI_{96-148} was added ten times in 5 μL aliquots (2.25×10^{-8}

moles/addition) to 500 μL of TnC (0.4 mM) to a final ratio of 1.1 to 1, peptide to protein.

4. NMR Spectroscopy and Assignment

Experiments were conducted on a Varian Unity-600 (titrations, TOCSY and

NOESY) or an Inova 500 (^{13}C-HSQC) spectrometer, and spectra were referenced

according to Wishart et al. (56). The HSQC (57,58) spectra for the $TnC \cdot TnI_{96-131}$,

$TnC \cdot TnI_{96-139}$, and $TnC \cdot TnI_{96-148}$ titrations were acquired at 31°C with sweep widths of

8000 Hz (all spectra acquired at 512 complex t_2 points) and 1650.2 Hz (128, 96, and 96

complex t_1 points for the first through third titrations, respectively) for the direct and

indirectly detected dimensions, respectively, and with 24 transients/increment. The 2D-

^{15}N-edited-TOCSY-HSQC (59) spectra collected on the ^{15}N-$TnI_{96-148} \cdot TnC$ complex was

acquired at 25°C with 6500 Hz sweep widths in the indirectly (352 complex t_1 points) and

directly (512 complex t_2 points) detected dimensions, respectively, and with 256

transients/increment. Both the 150 ms and 75 ms mixing time 2D-^{15}N-edited-noesyhsqc

(59) experiments were collected at 25°C with 7000 Hz sweep widths in both the directly

and indirectly detected dimensions. The 75 ms mixing time NOESY-HSQC had 512

complex points in both dimensions with 80 transients/increment while the 150 ms

experiment had 256 t_1 complex points, 512 t_2 complex points, and 256

transients/increment. The ^{13}C-HSQCs for the ^{13}C-TnI$_{96-139}$ peptide, and ^{13}C-TnI$_{96-139}$•TnC

complex were done at 31°C, and had 7000 Hz (2048 t_2 complex points) and 5500 Hz

sweep widths (1536 t_2 complex points) for the directly detected dimension, respectively.

Both ^{13}C-HSQCs were acquired with a sweep width of 2000 Hz (56 complex t_1 points)

for the indirectly detected dimension, and mirror-image linear prediction was used to

double the number of complex points. Carbon decoupling was not performed during the

extended, directly detected acquisition period (293 ms) to prevent probe damage.

All directly and indirectly detected data sets were zero filled to twice the number

of acquired (plus predicted when used) points and spectra were apodized using a shifted

sine bell before Fourier transformation. The acquisition time for HSQC experiments was

approximately 4 hrs while ~1.5 days was required for each of the TOCSY and NOESY

experiments. All experiments were processed and analyzed using the software package

NMRPipe and NMRDraw (60). Assignment of the TOCSY and NOESY experiments

was performed as described previously (61,62).

5. Dissociation Constants

Two procedures were used to determine the equilibrium dissociation constants for

the reaction of TnC with the TnI peptides. For TnI$_{96-131}$ the total chemical shift change of

the well-resolved amide proton HSQC cross-peaks was monitored during the titration as a

function of added TnI$_{96-131}$. The changes were fit to both simple 1:1 binding,

(Eq.IV-1.)

$$P + L \underset{k_{off}}{\overset{k_{on}}{\rightleftharpoons}} PL$$
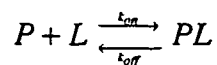
<div align="right">(Eq. IV-2.)</div>

$$K_d = \frac{k_{off}}{k_{on}}$$

and to the case where two peptides bind to TnC,

<div align="right">(Eq. IV-3.)</div>

$$P + L \underset{k_{on}}{\overset{k_{off}}{\rightleftarrows}} PL + L \underset{k_{off2}}{\overset{k_{on2}}{\rightleftarrows}} PL_2$$
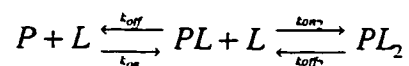
where P designates TnC, L the TnI peptide ligand, and PL and PL_2 stand for the

protein•peptide and protein•2peptide complexes, respectively. Fitting was performed

using a non-linear least squares technique (see (21) and references therein). For the TnI_{96-}

$_{139}$ and TnI_{96-148} titrations the chemical shift changes were not in the intermediate-fast

NMR chemical exchange limit required for this approach.

For the longer peptides, spectra taken during the titrations were analyzed using a

full lineshape analysis (see below) to determine the dissociation rate constant (under an

assumption of 1:1 binding). The dissociation constant is a parameter of this fitting

process. However, because of the relatively high concentrations used for NMR

spectroscopy, the fitting is not sensitive to the value of K_d once the dissociation constant

is tighter than approximately 1 μM. This is the case for the TnI_{96-139} and TnI_{96-148} titrations

and thus only an upper limit for the K_d is determined. A lower limit for K_d can be

determined from the fitted value of k_{off} and an upper-limit for the value of k_{on} ($\leq 1 \times 10^8$

$M^{-1}s^{-1}$, see (63-65) and references therein) using Equation IV-2.

6. Line Shape Analysis

The ^{15}N-labeled TnC was monitored by 2D-^{15}N,^{1}H-HSQC NMR spectroscopy

during each point of the titration, for each of the different TnI peptides. Spectral cross-

peaks of backbone amides were then analyzed for changes in chemical shift and

lineshape during the titrations. Residues from each of the N- and C-terminal domains of

troponin-C (Asp^{32} and Lys^{107}, respectively) were chosen that specifically had chemical

shift changes only in the proton dimension. The lack of chemical shift changes in the

nitrogen dimension allowed for easier cross-peak simulation and cross-peak display. The

program Mathematica (66) was used as previously described (21) to simulate the spectral

line shapes of the selected residues during each titration, except that the script file was

modified from the previous study to better simulate the effect of dilution on TnC peak

intensity^{2}. The k_{off} was modified manually in an iterative manner until the best

observable fit was obtained. The backbone amide cross-peaks for Glu^{16}, Val^{65}, and Gly^{119}

were also checked (data not shown), to insure that the line width behavior was consistent

with other residues.

---

^{2}The new and previous Mathematica scripts used are available upon request from brian.sykes@ualberta.ca, or ryan.mckay@ualberta.ca and see Appendix 2.

C. Results

1. Spectroscopy

Two-dimensional ^1H, ^{15}N-HSQC NMR spectroscopy was used to elucidate the

interaction of three different length TnI peptides with labeled, calcium-saturated chicken

skeletal TnC. The three TnI peptides corresponded to regions 96-131, 96-139, and 96-

148, respectively. Initially the TnI peptides were unlabeled, while the TnC protein was

^{15}N labeled. This was done to allow the specific NMR observation of TnC in the

complex without interference from TnI resonances. The HSQC NMR spectra display

backbone and side chain amide cross-peaks that are sensitive to changes in their local

environment and thus allow the monitoring of the titration at the amino acid residue level

of resolution. Subsequently, ^{15}N-labeling was incorporated into the TnI_{96-148} peptide,

while the TnC was deuterated to minimize signal loss and focus on peptide residues. In

the case of the ^{15}N-labeled TnI_{96-148}, 2D ^{15}N edited-TOCSY and NOESY NMR

spectroscopy was used to identify peptide amino acid spin systems after addition of one

equivalent of deuterated TnC. A TnI_{96-139} peptide (^{13}C-TnI_{96-139}) was synthesized

incorporating uniformly ^{13}C-labeled leucine (position 102 and 111 at 100% and 50%

label, respectively), and ^{13}C-methyl-labeled methionine (positions 121 and 134 at 100%

and 50% label, respectively). ^{13}C-HSQC was used to monitor the effect of TnC addition

to the ^{13}C-TnI_{96-139} peptide.

2. TnI•TnC complexes

Titrations of TnC with TnI_{96-131}, TnI_{96-139}, and TnI_{96-148} are shown in Figure IV-1

panels A-C, respectively, using contour representations of HSQC spectra. Not all cross-

peaks are affected equally indicating that some TnC residues have a greater change in
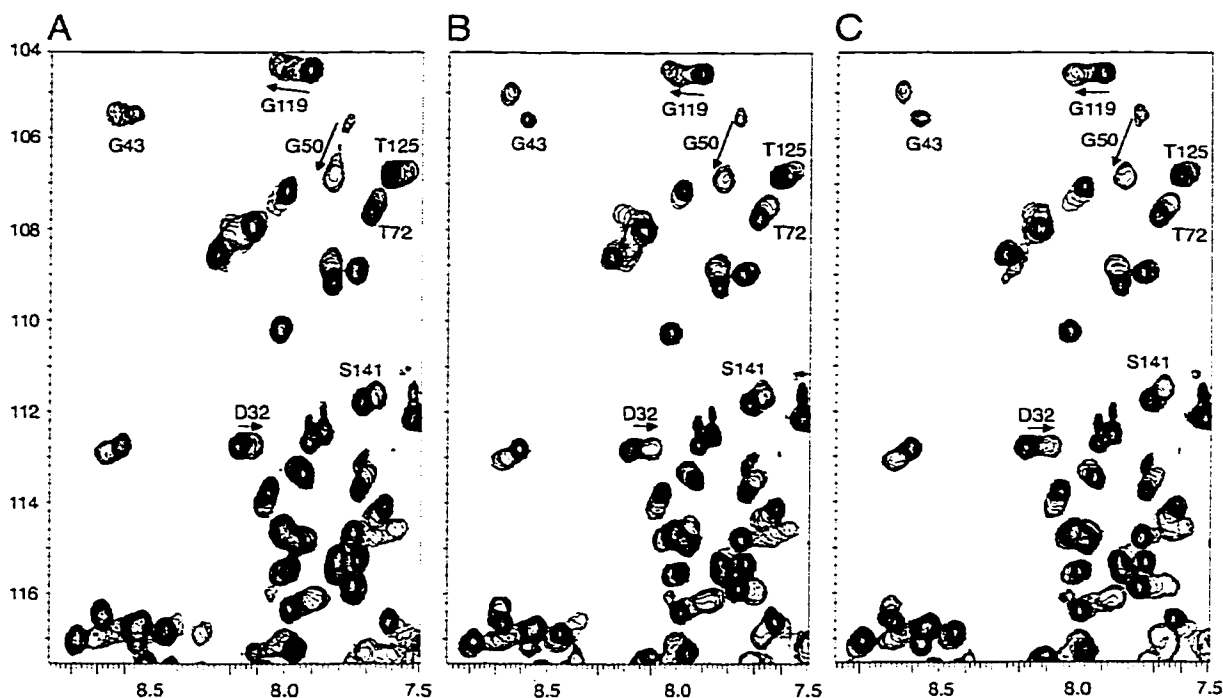
Figure IV-1

Contour plots of an expanded region of the 2D-^{1}H,^{15}N-HSQC NMR spectra taken of ^{15}N-labeled TnC upon titration with unlabeled peptide; (A) TnI$_{96-131}$, (B) TnI$_{96-139}$, and (C) TnI$_{96-148}$, respectively. (A) shows the addition of 0, 0.2, 0.3, 0.5, 0.6, 0.8, 1.0, 1.1, 1.3, 1.4, and 1.5 molar equivalents of TnI$_{96-131}$, (B) shows addition of 0, 0.1, 0.3, 0.4, 0.6, 0.7, 0.9, 1.0, 1.2, 1.3, and 1.5 molar equivalents of TnI$_{96-139}$, and (C) shows the addition of 0, 0.1, 0.2, 0.3, 0.45, 0.6, 0.7, 0.8, 0.9, 1.1 molar equivalents of TnI$_{96-148}$. Uncomplexed TnC cross-peaks are plotted with more contours while overlaying single contour cross-peaks show the effect of peptide addition. The different effect on cross-peaks experiencing fast-intermediate or slow exchange is very evident in residues such as Gly^{43}, Asp^{32} and Gly^{50} when comparing the addition of TnI$_{96-131}$ (A) and the two larger peptides (B) and (C). Residues experience similar changes of magnitude and direction to the their amide chemical shift in all three titrations. The one letter code is used for marked residues in the figure.

their local environment than others; however, changes experienced by individual cross-peaks are very similar when comparing the effect of different peptides. The spectral changes induced in the N-domain of intact TnC upon addition of the TnI$_{96-131}$ peptide resemble quite closely spectra seen for the TnI$_{115-131}$ and TnI$_{96-148}$ peptides when added to

the isolated N-terminal domain of troponin-C (*19,21*). The largest difference between the

three titrations shown in Figure IV-1 is the change in NMR cross-peak behavior from

intermediate-fast exchange with the TnI_{96-131} peptide, to intermediate-slow exchange with

the TnI_{96-139} and TnI_{96-148} peptides. In the NMR fast exchange limit a single cross-peak is

observed with a chemical shift that is a weighted average of the free and bound chemical

shifts. In the slow exchange limit two cross-peaks are observed, one with the chemical

shift of the free species and one with the chemical shift of the bound species. In the slow

limit the intensity of each peak represents the relative abundance of each species. We do

not observe spectra in either the extreme slow or fast exchange limits (see detailed

lineshape and chemical shift analysis below), but instead see a mixture dependent upon

the total chemical shift and respective rates of complex dissociation.

3. Chemical shift analysis and determination of dissociation constants

The observed total chemical shift change (*21*) was used to determine a

dissociation constant for the reaction of TnI_{96-131} with TnC. This titration exhibited

spectra in the intermediate-fast exchange limit. Chemical shift assignments for TnC were

taken from Slupsky *et al.* (*67*). A total of 85 backbone amide HSQC cross-peaks (out of

162 possible) were followed during each point of the titration (Figure IV-2) from which

$\Delta\delta_{total}$ (*21*) was determined. Figure IV-2, panels A and B show the best fit for a 1:1 and

1:2 binding of TnC to TnI_{96-131}, respectively. The 1:1 binding was best fit with a K_d of 32

$\pm$ 16 μM, while the 1:2 binding analysis yielded a K_{d1} of 1-50 μM and a K_{d2} of ~2 mM.

The binding of two peptides to TnC was considered because a second binding event was

observed when excess peptide was added (Figure IV-3). In Figure IV-3 (especially Panel

G) initial peptide binding (i.e. cross-peak broadening) can be seen.
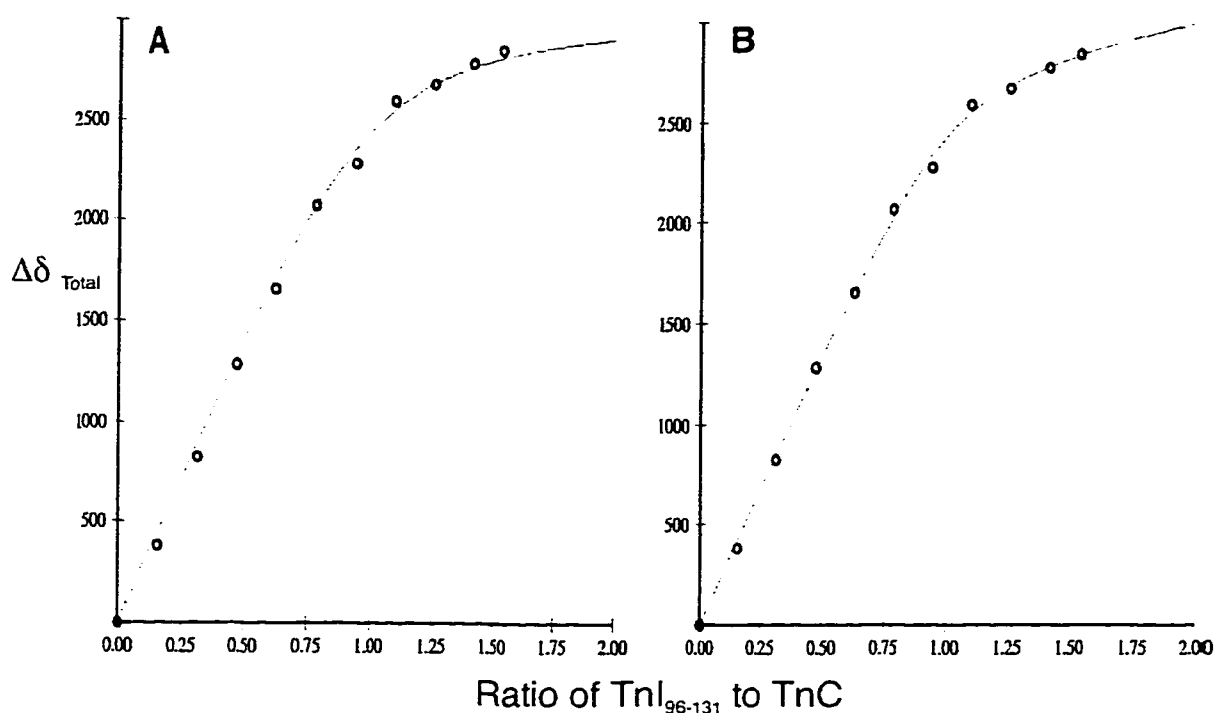
Figure IV-2

Binding curves derived from the 2D-^{1}H,^{15}N-HSQC spectra of labeled TnC upon addition of TnI$_{96-131}$. The $\Delta\delta_{total}$ for the 85 TnC backbone amide pairs that were monitored throughout the TnI$_{96-131}$ titration as a function of the molar ratio of TnI$_{96-131}$•TnC with a 1:1 binding curve fit analysis (see text) is shown in (A), while (B) is the same data fit with a 1:2 binding of TnC to TnI$_{96-131}$.

Subsequently, coupling of peptide binding and breakup of the TnC dimer results in sharpening of the N-TnC cross-peak line width up to a 1:1 ratio. In the presence of excess TnI peptide, TnC cross-peaks again broaden. This is probably due to competition for both the N- and C-terminal TnC domains by more than one TnI peptide. Since the initial binding event is so much stronger (*i.e.* K$_{d1}$ << K$_{d2}$), the second event can be assumed to be negligible and a value of 32 μM was used during the lineshape analyses (see below).

4. Line shape analysis and determination of exchange rates

The dissociation rate constants for all three complexes were determined from a

detailed lineshape analysis at each point of the titration, of an amide proton spectral

cross-peak corresponding to an amino acid in both the N- and C-terminal domain of TnC.

For the TnI_{96-139} and TnI_{96-148} titrations, the K_ds were also estimated from these simulations

since chemical shifts could not be used directly. Analysis of cross-peaks at each addition

is critical to properly simulate the effect on cross-peak line width. Residues Asp^{32} and

Lys^{107} (from the N- and C-terminal domains respectively) were chosen for analysis

because they display different degrees of chemical shift changes (*e.g.* ~30 Hz for Asp^{32},

and ~55Hz for Lys^{107}) and because both changed primarily in the ^1H dimension. This

made simulation of the cross-peaks solely dependent on one nuclei's chemical shift

change, and display of the cross-peaks far easier (*i.e.* traces corresponding to a single ^{15}N

spectral frequency could be displayed throughout). A comparison of experimentally

observed and mathematically simulated one-dimensional traces through the backbone

amide cross-peaks of Asp^{32} and Lys^{107}, at each point of all three TnI peptide titrations, is

shown in Figure IV-3, panels A-C. D-F, respectively. The experimental one-dimensional

traces (stacked and overlaid) are presented above the simulated spectra. The two residues

of TnC monitored during the TnI_{96-131} titration show intermediate-fast exchange, with

Lys^{107} displaying more broadening (due its larger chemical shift change) than Asp^{32}.

When the same residues are compared for the TnI_{96-139} and TnI_{96-148} titrations, virtually

identical intermediate-slow exchange broadening and chemical shift changes are

observed, indicating similar dissociation rate constants for both larger TnI fragments.

This indicates that binding of the longer two TnI peptides is much tighter to intact TnC

than that of TnI_{96-131}.

A

B

C
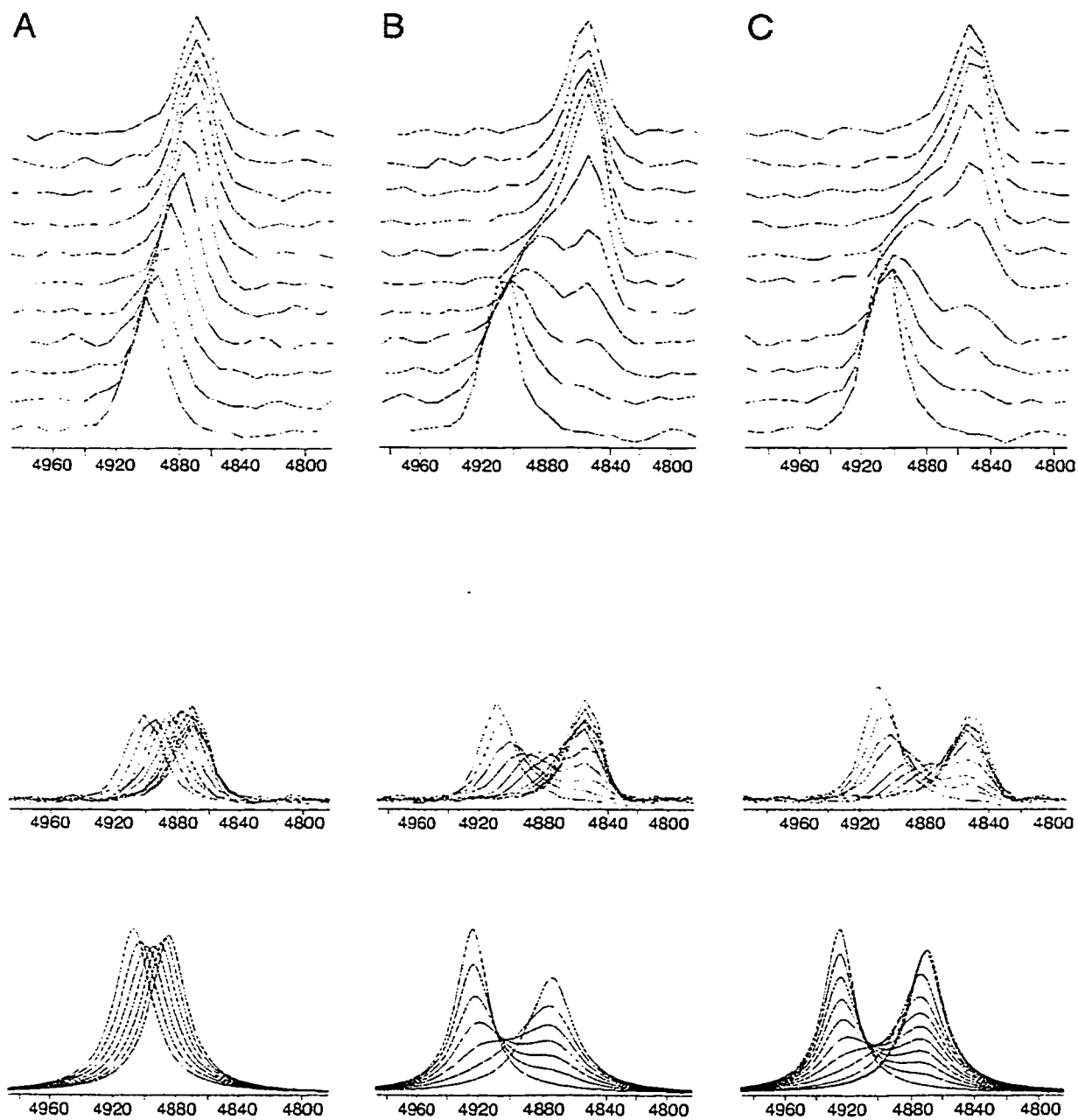
Figure IV-3

One dimensional traces from HSQC cross-peaks of TnC residues Asp^{32} (A-C) and Lys^{107} (D-F) during each point of addition of TnI_{96-131} (A,D), TnI_{96-139} (B,E), and TnI_{96-148} (C,F), respectively. The effect of N-domain dimerization is evident from the broader line widths of Asp^{32} when compared to the Lys^{107}. Spectra for the fourth addition of TnI_{96-148} to TnC (C and F) were not saved properly and a gap is left in the display to better compare with the other traces. (D, E and F continued on next page), Stacked experimental, overlaid experimental, and overlaid simulated spectra are shown from the top to the bottom, respectively.

D

E

F
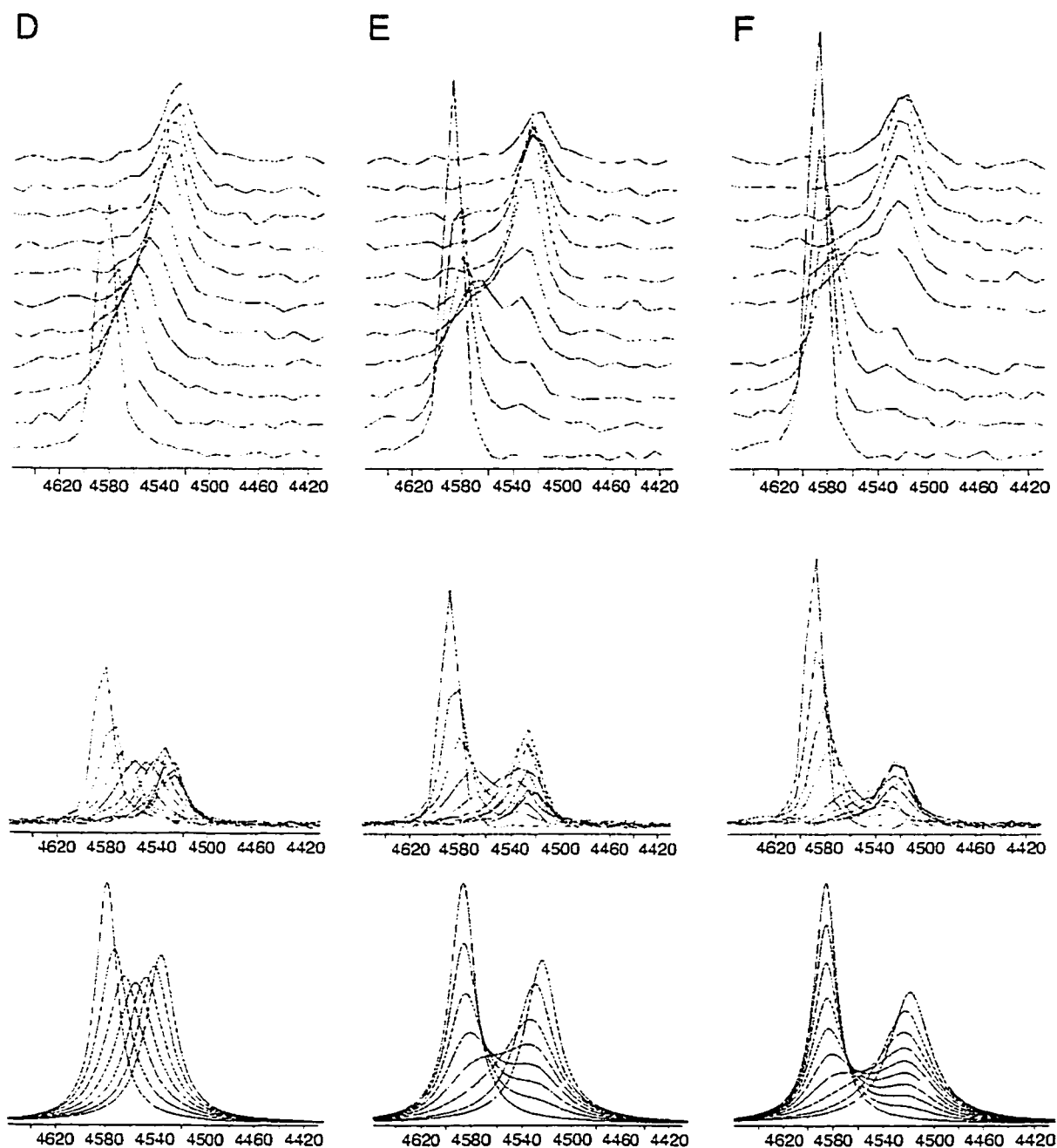
(Figure IV-3 cont.) (G) shows the same data as (A middle), but with a horizontal offset for each titration point to better demonstrate the effect of peptide addition after a 1:1 ratio. The initial broadening due to binding of peptide, and subsequent line width narrowing due to break up of the N-domain dimer is visible up to a ratio of 1:1 (peptide to protein). Issues such as differential relaxation perturb intensities in HSQC spectra and preclude detailed least squares analysis. However, only one parameter (k_{off}) was varied in the fit, and the optimum value was easily identified. When excess peptide is added a second binding event is observed resulting in rapid line broadening (G is shown on the next page).

G

Ratio of TnI_{96-131}:wTnC
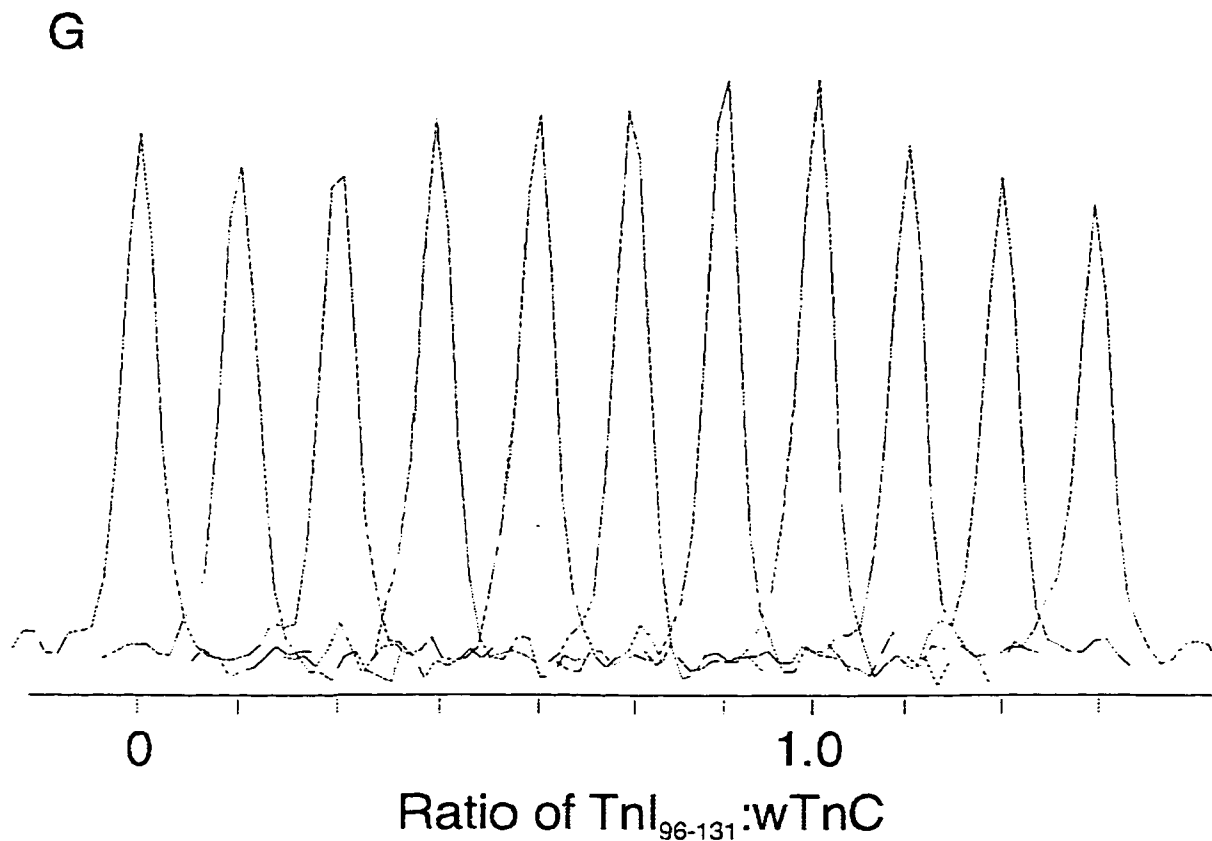
5. Kinetics and Energetics

The determined off rate constants, dissociation equilibrium constants, free energy of binding, and free energy of reverse-activation for all three titrations are shown in Table IV-1. A lower limit for the K_ds for the TnI_{96-139} and TnI_{96-148} titrations were estimated from the determined off rate constants that best fit the observed spectra and the assumption that k_{on} could be no faster than the lower diffusion rate limit, $\sim 1 \times 10^8$ M^{-1} s^{-1} (63-65,68). The K_d was checked by manually changing the value, re-optimizing k_{off}, and observing if the resulting simulated peaks better matched the experimentally obtained spectra. In all cases the originally determined K_d yielded the best fit.

Table IV-1: Kinetics and energetics of TnI peptide binding to TnC.

Complex	k_{off} $(s^{-1})^a$ (Asp^{32}, Lys^{107})	K_d (μM)	$\Delta G^\circ_{binding}$ $(kcal\ mol^{-1})^d$	$\Delta G^{\ddagger}_{off}$ $(kcal\ mol^{-1})^e$ (Asp^{32}, Lys^{107})
TnC•TnI$_{96-131}$	400, 400	32 ± 16^b	-6.2 ± 0.3	14.1, 14.1
TnC•TnI$_{96-139}$	55, 75	$0.5 \rightarrow 1^c$	$-8.7 \rightarrow -8.3$	15.3, 15.1
TnC•TnI$_{96-148}$	40, 50	$0.4 \rightarrow 1^c$	$-8.9 \rightarrow -8.3$	15.5, 15.4

a - The degree of uncertainty for k_{off} is a factor of two. b - Reported value is for a 1:1 binding analysis. c - The range for the reported K_d is between the limit of accurate measurement (i.e. 1 μM) and the lower limit based upon an on rate constant less than or equal to the diffusion limit (i.e. ~1×10^8 $M^{-1}s^{-1}$). d – Calculated using $\Delta G^\circ = -RT \ln K_d$. Error reported for ΔG° (TnC•TnI$_{96-131}$) is half the difference in calculated ΔG° between the upper and lower limit of the reported K_d. e – Calculated using $\Delta G^{\ddagger}_{off} = -RT \ln [k_{off}h/kT]$

Backbone amide cross-peak resonance overlap prevented the use of chemical shift mapping (*63,69-71*) to completely identify the regions of TnC bound by the TnI peptides. This was due to the increased line width and number of cross-peaks from TnC as compared to previous studies using the N-terminal domain of TnC (*19,21*). The well-resolved residues provided sufficient information to show that when bound the two domains of TnC adopted line widths more representative of a 24 kDa molecule. This conclusion is made from the observed line widths of the N- and C- domains (Table IV-2 pg. 135), and predicted line widths based on the molecular weight of TnC and TnC complexes (*72*). As expected the N-terminal residues are relatively broad (Figure IV-3, panels A-C, G) at the beginning of the titration, presumably due to N-terminal dimerization (*73*). The C-terminal peaks lack the initial dimerization and thus only broaden upon peptide addition (Figure IV-3 panels D-F, and Table IV-2).
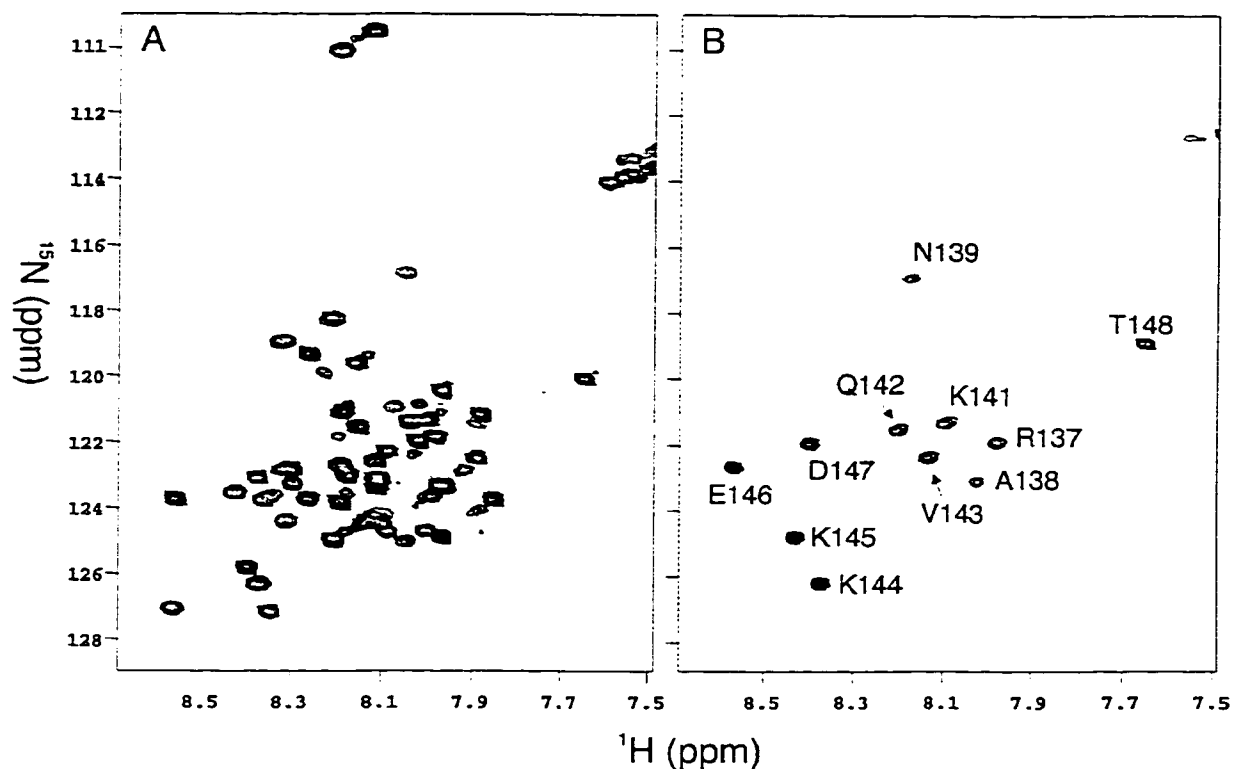
Figure IV-4

Contour plot of 2D-^{1}H,^{15}N-HSQC NMR spectra of ^{15}N labeled TnI$_{96-148}$ before (A) and after (B) addition of 1 equivalent of deuterated TnC. The threshold and vertical scale are identical between the two plots to show the change in line widths of TnI residues upon addition of protein. The eleven cross-peaks remaining in the spectra appear to be unperturbed by TnC binding and were assigned via TOCSY and NOESY NMR experiments. Broad poorly resolved resonances are observed at lower contour levels for (B). The one letter code is used to label assigned TnI residues in (B).

6. Assignment of Tocsy and Noesy Spectra of ^{15}N-TnI$_{96-148}$

To define which residues of TnI are interacting with TnC, ^{15}N-labeled TnI$_{96-148}$

was studied both free and when complexed with deuterated TnC. We have observed in

the proton spectrum of a shorter TnI peptide (residues 115-131) that the chemical shift

dispersion of amide resonances increased when the temperature was lowered from 30°C

to 5°C, and the pH lowered from 6.85 to 6.35 (data not shown). This indicated that some

intrinsic structure may form in the isolated peptide and this was tested with ^{15}N-labeled

TnI_{96-148}. Chemical shift changes in the one-dimensional ^1H and 2D-HSQC spectra were seen in isolated ^{15}N-labeled TnI_{96-148} when the temperature was reduced from 40 to 5°C, though line broadening severely affected the spectra (data not shown). Decreasing the pH from 6.85 to 6.25 did not significantly increase chemical shift dispersion.

The HSQC spectrum of ^{15}N-labeled TnI_{96-148} changed dramatically upon addition of TnC. Most of the peptide backbone amide resonances broadened, and rapidly disappeared (Figure IV-4, panels A and B). Line broadening is expected when the molecular weight of a species increases. Surprisingly, eleven peptide amide resonances remained sharp indicating a much smaller change in τ_{rot} (Figure IV-4, panel B) upon binding of TnC. These cross-peaks also experienced relatively small changes, if any, to their chemical shifts suggesting little or no change in environment upon protein binding. Two-dimensional versions of 3D-^{15}N-edited TOCSY and ^{15}N-edited NOESY spectra (Figure IV-5, panel A and B) of the TnI_{96-148} peptide complexed to TnC were taken in an effort to identify those peptide backbone amide residues relatively unperturbed by TnC binding. The NMR spin-systems of the unperturbed residues from TnI_{96-148} were identified from the TOCSY (Figure IV-5, panel A) experiments while the sequential order was established from the NOESY information (Figure IV-5, panel B). Spin-system information is degenerate for some amino acids (*i.e.* Asn and Asp have very similar TOCSY spectra), and therefore the known peptide amino acid sequence was used to identify degenerate residues that had NOE contacts to distinct amino acids (*e.g.* Glu[146] had short range NOEs to Lys[145] but not Lys[144] thus making the two degenerate Lysine residues assignable).
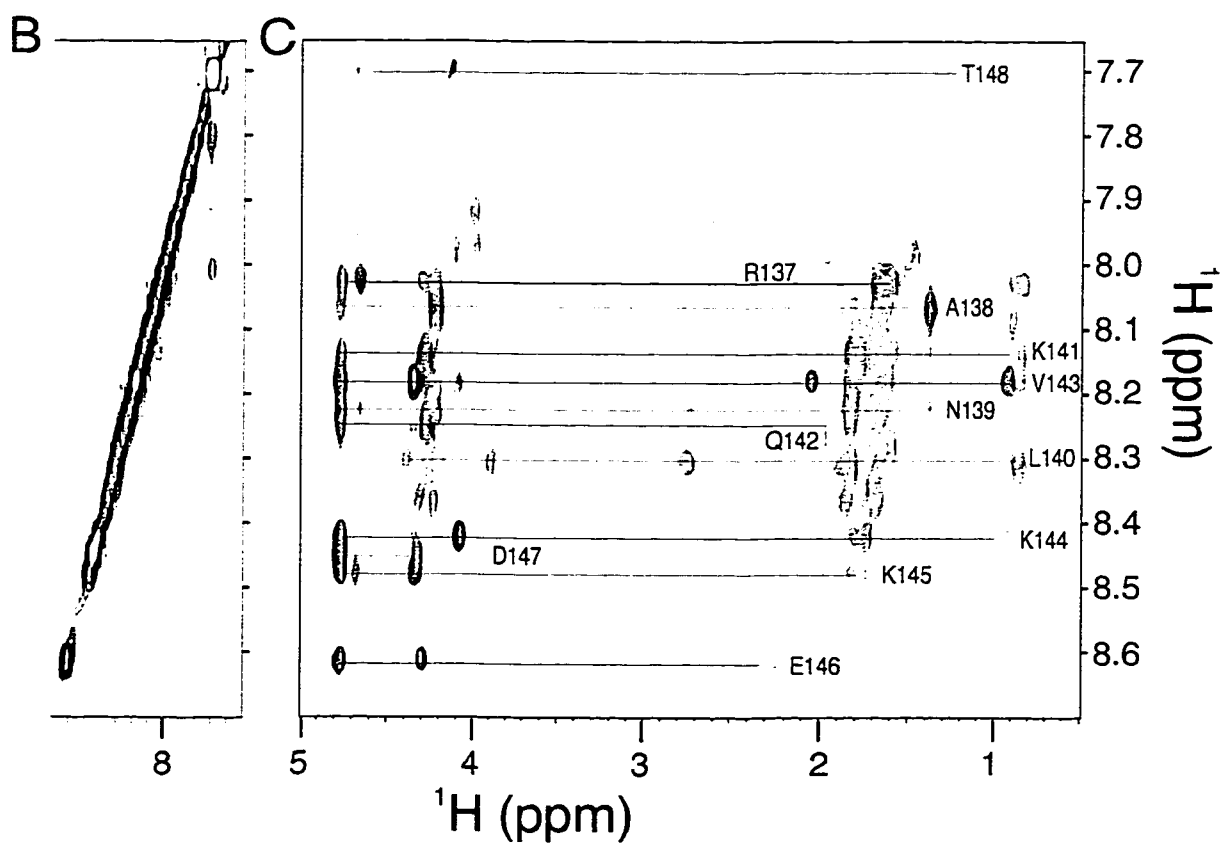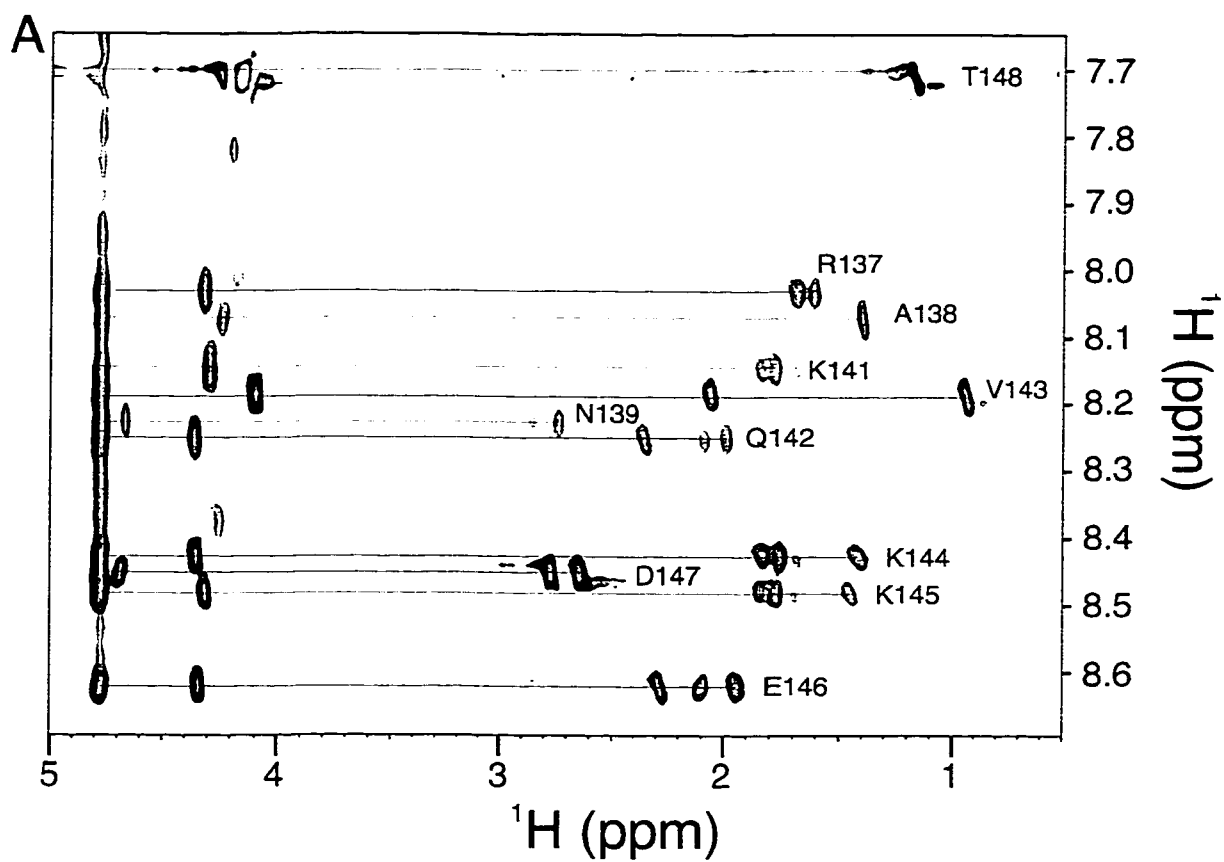
Figure IV-5

Expanded contour plots of two-dimensional, ^{15}N-edited (A) TOCSY and (B, C) NOESY spectra of ^{15}N-labeled TnI_{96-148} complexed to deuterated TnC. (A) and (C) show the aliphatic region of the TOCSY and NOESY spectra, respectively, while (B) shows the NOESY amide region. The lack of amide to amide cross-peaks (B) made sequential assignment dependent on accurate spin-system identification and aliphatic NOEs. The aliphatic NOEs also provided necessary information to assign degenerate spin systems such as Asn^{139}/Asp^{147} and Glu^{146}/Gln^{142}. Important NOESY contacts include the NOE of Lys^{141} to the methyl of Leu^{140}, and the similar contact of Lys^{144} to the methyl of Val^{143}. Thr^{148} could be assigned on its unusually intense cross-peaks, characteristic of a flexible C-terminal residue. Interestingly Leu^{140} only appears in the NOESY spectra. A total of ten unambiguous aliphatic NOEs allowed the deduction of the region of the TnI_{96-148} peptide not affected by TnC addition.

The eleven unperturbed residues have been assigned based on their individual spin

system and inter-residue NOEs to the last eleven residues of the C-terminal end of the

TnI_{96-148} peptide (Figure IV-6).

A.) N_{96}QKLF DLRGKFKRPP LRRVRMSADA
  MLKALLGSKH KVAMDLRANL KQVKKEDT$_{148}$

B.)

134 Met(50%)

121 Met(100%)

111 Leu(50%)

102 Leu(100%)

TnI
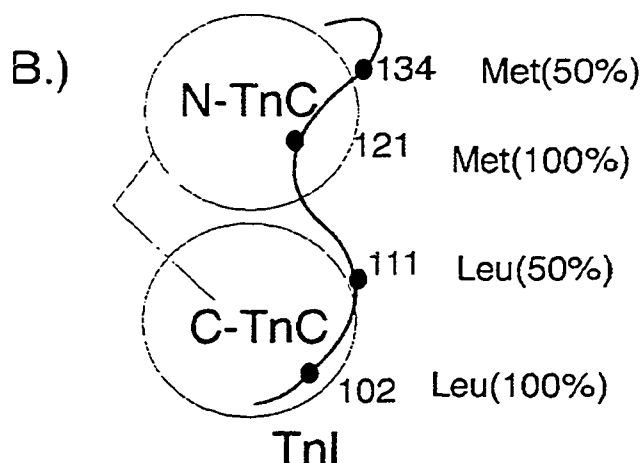
Figure IV-6

(caption on next page)

(Figure IV-6 cont.)

(A) Sequence of TnI residues 96 to 148 showing the eleven C-terminal residues (outline) not perturbed by TnC binding. Arg[137] is also shown outlined to indicate possible inclusion in this assignment (see text). Residues shown underlined and boldfaced indicate the positions of two leucines (residues 102 and 111) and Methionines (residues 121 and 134) labeled with ^{13}C in the synthetic ^{13}C-TnI$_{96-139}$ peptide. (B) Cartoon representation of the interaction of TnC with TnI. The ^{13}C-labeled amino acids are shown with their relative abundance.

An additional unperturbed amide resonance was tentatively assigned to Arg[137], but the possibility of this cross-peak belonging to Asn[96] (i.e. the N-terminal residue) could not be eliminated. The observed chemical shifts for the assigned TnI hydrogen atoms correspond to the random coil chemical shifts (56,74,75), indicating no defined secondary structure. Therefore the last eleven residues appear to be rotating freely (i.e. relatively short τ_c), and in a random coil in the presence or absence of TnC.

7. Monitoring of ^{13}C-TnI$_{96-139}$ upon addition of TnC

The ^{13}C-TnI$_{96-139}$ peptide (Figure IV-6) was complexed to TnC, and Figure IV-7 shows contour plots of the coupled ^{13}C-HSQC spectra of the ^{13}C-TnI$_{96-139}$ methionine and leucine methyl groups (panels A and C), respectively. In these plots, cross-peaks are split along the ^{1}H NMR axis by the ^{1}J$_{CH}$ coupling constant of ~138 Hz (~0.28 ppm) and 123 Hz for the Met and Leu residues, respectively. The two methionines (Panel A) of the free peptide are equivalent in ^{13}C NMR resonance frequencies but separated by 5 Hz in the ^{1}H NMR dimension. The 100% and 50% labeling for Met[121] and Met[134], respectively can be observed in the 1D trace taken through the cross-peaks at the position of the dotted line and displayed at the bottom of Panel A. The ^{1}H,^{13}C-HSQC spectra of each of the two methyl groups (also split by ^{1}J$_{CH}$) from each of the two leucine residues in the free and bound ^{13}C–TnI$_{96-139}$ peptides are shown in panels C and D, respectively.
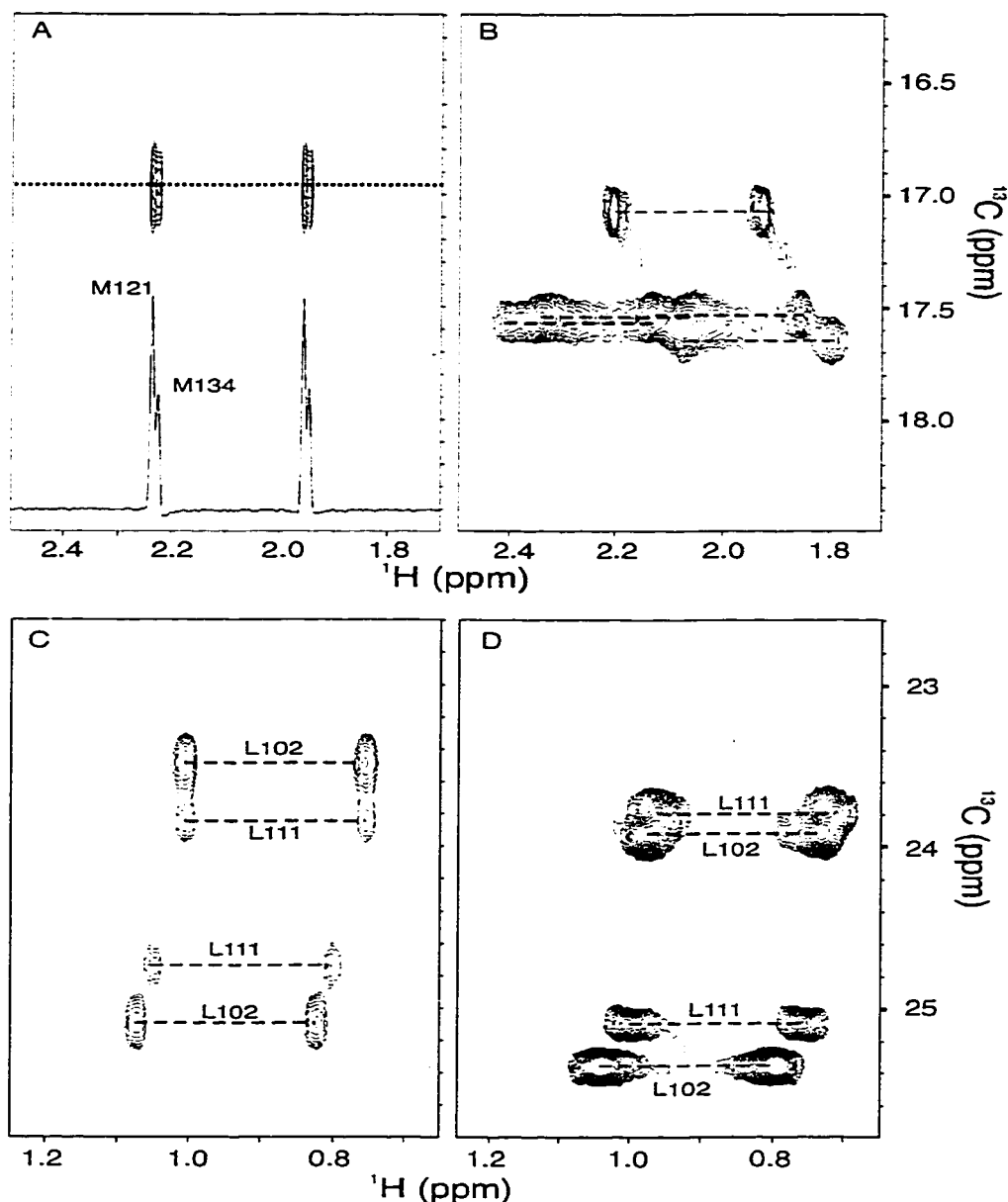
Figure IV-1

Contour plots of an expanded region of carbon coupled 2D-^{1}H,^{13}C-HSQC NMR spectra taken of [U-^{13}C]-(100% labeled) Leu^{102}, (50%) Leu^{111}, [^{13}CH$_3$]-(100%) Met^{121}, (50%) Met^{134}-TnI$_{96-139}$ free and bound to TnC. The spectral region for the methionine resonances is shown in (A) and (B) for free and bound TnI$_{96-139}$ peptide, respectively. The dotted line in (A) shows the position from which the 1D-trace of the ^{13}C-HSQC cross-peak (A bottom) was taken to display the pairs of coupled cross-peaks with the relative abundance. Panels (C) and (D) show the NMR spectral region for the leucine methyl groups of TnI$_{96-139}$ free and bound to TnC, respectively. Carbon decoupling in the directly detected dimension was not performed to allow extended acquisition and therefore resolution of the closely degenerate methionine methyl resonances. Dashed lines show coupled sets of cross-peaks. One-letter codes are used for the residues in the figure.

TnI leucine residues102 and 111 were 100% and 50% labeled with ^{13}C, respectively, and

the relative intensities are evident in both the free and bound spectra (Figure IV-7, panels

C and D, respectively). Most striking are the different behaviors for the spectra of Leu^{102}

and Leu^{111} (Panel D) versus Met^{121} and Met^{134} (Panel B) in the bound complex. For each

methyl group from Leu^{102} and Leu^{111}, there is only a single, coupled cross-peak, albeit

shifted and broadened due to the binding of TnC. However, residues Met^{121} and Met^{134}

(Figure IV-7, panel B) show at least 4 pairs of chemically shifted cross-peaks at ≈ 17.5

ppm (^{13}C NMR axis) with much broader line widths than that of the free peptide. Also

there is another sharp, but low intensity coupled cross-peak at ~17.05 ppm (^{13}C) which

corresponds to the proton chemical shift of Met^{134}. This implies that several different

states exist.

D. Discussion

The off rate and dissociation constants have been determined for three TnI

peptides interacting with TnC. Based on these dissociation constants and off rates we

have calculated the free energy of binding, and estimated the activation energy barriers

for both the forward and reverse reactions. We have also identified eleven C-terminal

residues in TnI_{96-148} that do not interact with TnC. The results indicate that residues

97–136 (and possibly 96 or 137) are directly interacting with TnC. Residues 138-148

(and possibly 137 or 96) do not appear to interact with TnC, nor does the presence or

absence of these extra TnI residues significantly reduce the affinity of complex

formation.

Table IV-2: NMR cross-peak line widths of TnC N- and C-terminal domain residues
before and after titration with TnI peptides.

Titration	TnC (Hz)	Complex (Hz)	Complex
	Asp^{32}, Lys^{107}	Asp^{32}, Lys^{107}	Mass (Da)[b]
TnI_{96-131}[c]	28, 20	25, 25	23416
TnI_{96-139}	24, 23	27, 31	23522
TnI_{96-148}	24, 21	28, 37	24701
	TnC (Hz)	TFE addition (Hz)	
	Ile^{37}, Ile^{113}	Ile^{37}, Ile^{113}	
TnC[a]	34, 26	26, 26	

[a] Results of Slupsky *et al.* (1995) (*73*) showing disruption of N-domain dimerization upon
addition of 13% TFE. Line widths are not directly comparable to the present data
because of differences in experimental and processing conditions. [b] the molecular weight
of unlabeled TnC is 18.2×10^3 g/mol. [c] TnC used in the TnI_{96-131} titration was labeled with
both ^{15}N and ^{13}C while the TnC in the TnI_{96-139} and TnI_{96-148} samples was only labeled with
^{15}N.

Removing residues 132-139 reduces the affinity of TnI for TnC, increases the

dissociation rate constant for the complex, and appears to reduce the ability of TnI to

restrict the two domains of TnC into a more constrained conformation. Partial

dimerization of TnC via the N-domain (73) of TnC is disrupted upon peptide addition as

is evident by slight narrowing of N-terminal TnC residues (Figure IV-3, panel G and

Table IV-2).

1. Energetics

Previous studies have shown that several regions of TnI have affinity for either, or

both, domains of TnC. TnI_{96-116} have been shown to bind ($K_d \approx 3 - 0.5 \, \mu M$) to the C-

terminal domain of TnC ((47), (76) and references therein) while the 115-131 region of

TnI has been shown to bind ($K_d \approx 20 \, \mu M$) to N-TnC (19,21,46,47). If we consider that

the TnI_{96-148} peptide binds simultaneously to both domains of TnC, and that the binding

free energy is the sum of the individual binding components, (i.e. the observed K_d is the

product of the individual K_ds for both domains, respectively) then one would expect to

see a dissociation constant for $TnI_{96-148}\bullet TnC$ in the 1-100 pM range. This is not the case

as we observe a K_d of ~ 500 nM. Further, the combination of an off rate constant in the

range of 40-75 s^{-1} and a dissociation constant in the picomolar range would require a k_{on}

of $1 \times 10^{13} \, M^{-1} \, sec^{-1}$, approximately 5 orders of magnitude faster than the diffusion limit

(63). The weaker observed binding (i.e. ~12-24 kcal mol^{-1}) may be a result of several

factors: 1.) the entropic cost of restricting the two domains of TnC, 2.) strain and/or

negative interactions in the TnI 'linker' region, 3.) shifting of either region of TnI in

relation to TnC (e.g. the 115-131 region of TnI_{96-139} and TnI_{96-148} may be binding in a

slightly different position relative to TnC than compared to $TnI_{115-131}$ bound to the isolated

N-TnC), 4.) the lack of C-terminal residues may disrupt secondary structure of binding

residues because of 'fraying' (77) or disordering. This end 'fraying' may also explain the

suspected Met^{134} 'free' species observed with $^{13}C-TnI_{96-139}$•TnC complex. Additionally, it

is possible that the observed TnI peptide off rates are for each individual domain of TnC

and not the whole molecule. This would require identical and non-cooperative binding of

the two regions of TnI to both domains of TnC which has not been reported. In general,

these kinds of concerns may be relevant when using peptides.

In previous NMR studies, no significant difference in binding strength was

observed when comparing the interaction of $TnI_{115-131}$ ($K_d = 24 \pm 4$ µM) and TnI_{96-148} (Kd

= 1 - 40 µM) with the N-domain of TnC (19,21), whereas we see interactions of TnI

residues 131-136 with TnC. As discussed above, if the regions of TnI that interact with

TnC shift when comparing binding to whole TnC and the isolated N-domain, then the

remaining residues (i.e. 131-136) could become more important. These residues may

also interact with an area of TnC other than the calcium regulated hydrophobic pocket.

There is some supportive evidence for this because inter-molecular NOE contacts were

observed in the TnI_{96-148}• N-TnC study on the side of TnC opposite that of the

hydrophobic pocket (termed the backside) (19,37,78). Recently the structure of the

cardiac equivalent of $TnI_{115-131}$ bound to the N-domain of cardiac TnC has been solved

and residues equivalent to 115-127 of skeletal TnI have been shown to bind in the

hydrophobic pocket of cardiac N-TnC (79,80). This information supports the idea that

residues 131-136 bind to TnC residues outside the hydrophobic pocket, or may suggest

that different TnI residues bind to TnC in the cardiac and skeletal systems. The 127-131

region of TnI is 100% identical over all compared species (fast skeletal chicken, quail,

rabbit, human, mouse, slow skeletal mouse, rabbit, human, and rat), suggesting that the

region is more than merely a structural loop (see (47) for a more detailed sequence

comparison). This does not necessarily require that 127-131 is actively involved in

specific TnC binding since this region may be important in the interaction with actin,

TnC, or both.

2. Mechanism and Models

There is ample evidence that TnC and TnI interact in an anti-parallel orientation.

Specifically, recent results show that TnI regions 115-131 and 96-115 bind to the N- and

C- terminal domains of TnC, respectively (see (2,19,21,76) and references therein). The

present results indicate that leucines 102 and 111 in the N-terminal portion of ^{13}C-TnI$_{96-139}$

bind in a single orientation while complexed to TnC. However, methionines 121 and 134

in the C-terminal portion of the ^{13}C-labeled peptide bind in multiple conformations. The

spectra show at least four pairs of broad cross-peaks shifted from the free peptide

resonance frequencies (Figure IV-7B) suggesting at least two bound environments for

each of the two methionine residues. Interestingly, the coupled cross-peak resonating at a

^{13}C chemical shift of 17.1 ppm has the same ^{1}H and ^{13}C chemical shift (within digital

resolution) of free Met^{134}, but is slightly broadened. This leads to the possibility that

Met^{134} may also exist in a random coil and relatively free conformation while the N-

terminal portion of the TnI peptide (containing Leu^{102} and Leu^{111}) is bound to the C-

domain of TnC. The number of bound peaks suggest that there may be up to three

conformations, described by two different binding models for Met^{121}/Met^{134} even when

the N-terminal region of the TnI peptide is 'tethered' to the C-domain of TnC. Two of

the simplest schemes are shown (Scheme 1 and 2).

$$Scheme\ 1 \qquad\qquad Scheme2$$

$$Peptide\overset{\rightarrow}{\leftharpoondown}Complex$$

$$\uparrow\downarrow \qquad\qquad or \qquad Peptide\overset{\rightarrow}{\leftharpoondown}Complex\overset{\rightarrow}{\leftharpoondown}Complex*$$
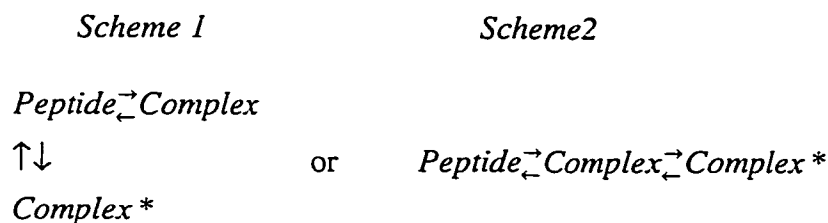
$$Complex*$$

In scheme 1, Complex and Complex* represent TnI_{96-139} 'tethered' to C-TnC via the 96-

115 TnI region, and subsequently binding in two distinct N-TnC sites. In scheme 2,

Complex and Complex* represent two kinetically relevant species, both of which are

tethered to C-TnC as in scheme 1 but with both Complex and Complex* (e.g.

representing different TnI peptide conformations) binding to a single site in N-TnC. This

is the first time that peptide promiscuity has been observed for TnI binding to TnC. It is

attractive to speculate that the three states are relevant to the three states shown to exist

for the regulation of the thin filament ((*81*) and references therein). In this situation

complex and complex* would be the TnC•TnI states corresponding to the 'closed' and

'open' states of the thin filament.

Previous binding studies have indicated a possible 1:2 binding stoichiometry of

TnI peptides to TnC attributed to affinities of the TnI peptides for the N- and C-terminal

domains of TnC, respectively (*47*), but was ruled out here because the TnC was present

in equimolar concentrations to TnI and only single bound cross-peaks were observed for

the leucine TnI resonances.

There are presently two models regarding the interaction of TnC and TnI. The

first model suggested separately by Olah *et al.* (*39*) and Ngai *et al.* (*50*) suggests that a

"switching mechanism" may exist in which TnI residues ~ 115-131 bind to the N-domain

of TnC in a calcium dependent fashion, and that the C-domain is bound alternately by

residues 96-115 and 1-40 of TnI (also known as Rp40) in the calcium saturated and apo

states, respectively. This model has the advantage that competition between residues 1-

40 and 96-115 in TnI might reduce the binding of TnI to calcium saturated TnC from the reported K_d 0.2 - 1.7 nM (82,83) to one more kinetically understandable in regards to observed rates of muscle regulation. The second model suggested by Vassylyev *et al.* and supported by others has the 1-40 region of TnI bound to the C-domain of TnC regardless of the presence or absence of calcium (2,23). The Vassylyev model also suggests that the inhibitory region of TnI adopts the NMR structure of the TnIp peptide bound to the C-domain of TnC reported by Campbell *et al.* (84), but instead of binding in the hydrophobic pocket of C-TnC makes few contacts to TnC in the presence or absence of calcium. The second model has been examined by two other groups in regards to TnT interactions (5) and resonance energy transfer studies (31). At present both models appear to be equally supported though neither model involves interactions of N-TnC with regions 131-136 of TnI. Our findings here suggest that TnI residues 97-136 (and 96 or 137) bind to both domains of TnC yet does not determine where interaction occurs in the C-domain of TnC.

In this study we have determined the dissociation and off rate constants of three TnI peptides with intact TnC in the calcium saturated state, and we have examined the NMR labeled ^{15}N-TnI$_{96-148}$ and ^{13}C-TnI$_{96-139}$ peptides when in complex with calcium saturated TnC. Our primary conclusion from this study is that TnI residues 97-136 (and 96 or 137) bind to whole TnC, and that residues ~138-148 do not interact with TnC. The residues reported here, that do not interact with TnC, were found by Tripet *et al.* to be important for binding to actin and for proper regulation of contraction. Additionally residues Leu^{102} and Leu^{111} show single bound conformations to TnC while Met^{121} and Met^{134} show multiple bound species. We would like to suggest that TnI residues 115-136 bind to the calcium saturated N-domain of TnC (in at least two conformations) with residues 131-136 possibly making "backside" contacts with N-TnC, and that residues ~97-115 bind to C-TnC.

E. References

1. Tobacman, L. S. (1996) *Annu. Rev. Physiol.* **58**, 447-481

2. Farah, C. S., and Reinach, F. C. (1995) *FASEB J.* **9**, 755-767

3. Potter, J. D., and Johnson, J. D. (1982) in *Calcium and Cell Function* (Cheung, W. Y., ed) Vol. 2, pp. 145-169, Academic Press, Inc.

4. Leavis, P. C., and Gergely, J. (1984) *CRC Crit. Rev. Biochem.* **16**, 235-305

5. Malnic, B., Farah, C. S., and Reinach, F. C. (1998) *J Biol Chem* **273**, 10594-601

6. Head, J. F., and Perry, S. V. (1974) *Biochem. J.* **137**, 145-154

7. Syska, H., Wilkinson, J. M., Grand, R. J. A., and Perry, S. V. (1976) *Biochem. J.* **153**, 375-387

8. Li, M. X., Gagné, S. M., Tsuda, S., Kay, C. M., Smillie, L. B., and Sykes, B. D. (1995) *Biochemistry* **34**, 8330-8340

9. Herzberg, O., and James, M. N. G. (1988) *J. Mol. Biol.* **203**, 761-779

10. Satyshur, K. A., Rao, S. T., Pyzalska, D., Drendal, W., Greaser, M., and Sundaralingam, M. (1988) *J. Biol. Chem.* **263**, 1628-1647

11. Rao, S. T., Satyshur, K. A., Greaser, M. L., and Sundaralingam, M. (1996) *Acta Crystallographica Section D* **52**, 916-922

12. Strynadka, N. C. J., Cherney, M., Sielecki, A. R., Li, M. X., Smillie, L. B., and James, M. N. G. (1997) *J. Mol. Biol.* **273**, 238-255

13. Houdusse, A., Love, M. L., Dominguez, R., Grabarek, Z., and Cohen, C. (1997) *Structure* **5**, 1695-1711

14. Gagné, S. M., Tsuda, S., Li, M. X., Smillie, L. B., and Sykes, B. D. (1995) *Nature Struct. Biol.* **2**, 784-789

15.   Gagné, S. M., Li, M. X., and Sykes, B. D. (1997) *Biochemistry* **36**, 4386-4392

16.   Slupsky, C. M., and Sykes, B. D. (1995) *Biochemistry* **34**, 15953-15964

17.   Spyracopoulos, L., Li, M. X., Sia, S. K., Gagné, S. M., Chandra, M., Solaro, R. J., and Sykes, B. D. (1997) *Biochemistry* **36**, 12138-12146

18.   Sia, S. K., Li, M. X., Spyracopoulos, L., Gagné, S. M., Liu, W., Putkey, J. A., and Sykes, B. D. (1997) *J. Biol. Chem.* **272**, 18216-18221

19.   McKay, R. T., Pearlstone, J. R., Corson, D. C., Gagné, S. M., Smillie, L. B., and Sykes, B. D. (1998) *Biochemistry* **37**, 12419-30

20.   Gagné, S. M., Li, M. X., McKay, R. T., and Sykes, B. D. (1998) *Biochem. Cell Biol.* **76**, 301-12

21.   McKay, R. T., Tripet, B. P., Hodges, R. S., and Sykes, B. D. (1997) *J. Biol. Chem.* **272**, 28494-28500

22.   Vassylyev, D. G., Takeda, S., Wakatsuki, S., Maeda, K., and Maeda, Y. (1998) *Biophys. J.* **74**, A53

23.   Vassylyev, D. G., Takeda, S., Wakatsuki, S., Maeda, K., and Maeda, Y. (1998) *Proc Natl Acad Sci U S A* **95**, 4847-52

24.   Nelson, M. R., and Chazin, W. J. (1998) *Protein Sci.* **7**, 270-282

25.   Ikura, M., Clore, G. M., Gronenborn, A. M., Zhu, G., Klee, C. B., and Bax, A. (1992) *Science* **256**, 632-638

26.   Meador, W. E., Means, A. R., and Quiocho, F. A. (1992) *Science* **257**, 1251-5

27.   Meador, W. E., Means, A. R., and Quiocho, F. A. (1993) *Science* **262**, 1718-21

28. Rayment, I., Rypniewski, W. R., Schmidt-Base, K., Smith, R., Tomchick, D. R.,
     Benning, M. M., Winkelmann, D. A., Wesenberg, G., and Holden, H. M. (1993)
     Science **261**, 50-58

29. Houdusse, A., and Cohen, C. (1995) *Proc. Natl. Acad. Sci. U.S.A.* **92**, 10644-
     10647

30. Olah, G. A., and Trewhella, J. (1994) *Biochemistry* **33**, 12800-12806

31. Luo, Y., Wu, J.-L., Gergely, J., and Tao, T. (1997) *Biochemistry* **36**, 11027-11035

32. Tripet, B. P., Van Eyk, J. E., and Hodges, R. S. (1997) *J. Mol. Biol.* **271**, 728-750

33. Tao, T., Scheiner, C. J., and Lamkin, M. (1986) *Biochemistry* **25**, 7633-7639

34. Leszyk, J., Grabarek, Z., Gergely, J., and Collins, J. H. (1990) *Biochemistry* **29**,
     299-304

35. Ngai, S.-M., Sönnichsen, F. D., and Hodges, R. S. (1994) *J. Biol. Chem.* **269**,
     2165-2172

36. Kobayashi, T., Grabarek, Z., Gergely, J., and Collins, J. H. (1995) *Biochemistry*
     34, 10946-10952

37. Jha, P. K., Mao, C., and Sarkar, S. (1996) *Biochemistry* **35**, 11026-11035

38. Kobayashi, T., Leavis, P. C., and Collins, J. H. (1996) *Biochim. Biophys. Acta*
     1294, 25-30

39. Olah, G. A., Rokop, S. E., Wang, C.-L. A., Blechner, S. L., and Trewhella, J.
     (1994) *Biochemistry* **33**, 8233-8239

40. Stone, D. B., Timmins, P. A., Schneider, D. K., Krylova, I., Ramos, C. H. I.,
     Reinach, F. C., and Mendelson, R. A. (1998) *J Mol Biol* **281**, 689-704

41.   Farah, C. S., Miyamoto, C. A., Ramos, C. H. I., da Silva, A. C. R., Quaggio, R.

       B., Fujimori, K., Smillie, L. B., and Reinach, F. C. (1994) *J. Biol. Chem.* **269,**

       5230-5240

42.   Van Eyk, J. E., and Hodges, R. S. (1988) *J. Biol. Chem.* **263,** 1726-1732

43.   Van Eyk, J. E., Thomas, L. T., Tripet, B. P., Wiesner, R. J., Pearlstone, J. R.,

       Farah, C. S., Reinach, F. C., and Hodges, R. S. (1997) *J. Biol. Chem.* **272,** 10529-

       10537

44.   Leavis, P. C., Rosenfeld, S. S., and Gergely, J. (1978) *J. Biol. Chem.* **253,** 5452-

       5459

45.   Takeda, S., Kobayashi, T., Taniguchi, H., Hayashi, H., and Maéda, Y. (1997) *Eur.*

       J. Biochem. **246,** 611-617

46.   Pearlstone, J. R., and Smillie, L. B. (1995) *Biochemistry* **34,** 6932-6940

47.   Pearlstone, J. R., Sykes, B. D., and Smillie, L. B. (1997) *Biochemistry* **36,** 7601-

       7606

48.   Campbell, A. P., Cachia, P. J., and Sykes, B. D. (1991) *Biochem. Cell Biol.* **69,**

       674-681

49.   Ngai, S.-M., and Hodges, R. S. (1992) *J. Biol. Chem.* **267,** 15715-15720

50.   Ngai, S. M. (1994) *Synthetic peptide studies on troponin C-troponin I interaction,*

       Ph.D. Thesis, University of Alberta. **94FD NGA,** pgs. 156

51.   Talbot, J. A., and Hodges, R. S. (1979) *J. Biol. Chem.* **254,** 3720-3723

52.   Talbot, J. A., and Hodges, R. S. (1981) *J. Biol. Chem.* **256,** 2798-2802

53.   Gagné, S. M., Tsuda, S., Li, M. X., Chandra, M., Smillie, L. B., and Sykes, B. D.

       (1994) *Prot. Sci.* **3,** 1961-1974

54. Studier, F. W., Rosenberg, A. H., Dunn, J. J., and Dubendorff, J. W. (1990) *Methods Enzymol.* **185,** 60-89

55. Sambrook, J., Fritsh, E. F., and Maniatis, T. (1989) *Molecular Cloning: A Laboratory Manual,* 2nd Edition Ed., Cold Spring Harbor Laboratory Press, N.Y.

56. Wishart, D. S., Bigam, C. G., Yao, J., Abildgaard, F., Dyson, H. J., Oldfield, E., Markley, J. L., and Sykes, B. D. (1995) *J. Biomol. NMR* **6,** 135-140

57. Muhandiram, D. R., and Kay, L. E. (1994) *J. Magn. Reson.* **B103,** 203-216

58. Kay, L. E., Keifer, P., and Saarinen, T. (1992) *J. Am. Chem. Soc.* **114,** 10663-10665

59. Zhang, O., Kay, L. E., Olivier, J. P., and Forman-Kay, J. D. (1994) *J. Biomol. NMR* **4,** 845-858

60. Delaglio, F., Grzesiek, S., Vuister, G. W., Zhu, G., Pfeifer, J., and Bax, A. (1995) *J. Biomol. NMR* **6,** 277-293

61. Slupsky, C. M. (1995) *The NMR Solution Structure of Calcium-Saturated Skeletal Muscle Troponin C.,* PhD Thesis, University of Alberta. pgs. 352

62. Wüthrich, K. (1986) *NMR of proteins and nucleic acids.,* John Wiley & Sons, New York

63. Kilby, P. M., Van Eldik, L. J., and Roberts, G. C. K. (1997) *Protein Sci.* **6,** 2494-2503

64. Bayley, P. M., Findlay, W. A., and Martin, S. R. (1996) *Protein Sci* **5,** 1215-28

65. Torok, K., Cowley, D. J., Brandmeier, B. D., Howell, S., Aitken, A., and Trentham, D. R. (1998) *Biochemistry* **37,** 6188-98

66. Wolfram, S. (1996) *The Mathematica Book*, 3rd Ed. (Walsh, J., Beck, G., and Grohens, J., Eds.), Wolfram Media/Cambridge University Press, Cambridge

67. Slupsky, C. M., Reinach, F. C., Smillie, L. B., and Sykes, B. D. (1995) *Protein Sci.* **4**, 1279-1290

68. Brown, S. E., Martin, S. R., and Bayley, P. M. (1997) *J Biol Chem* **272**, 3389-97

69. Lee, A. L., Volkman, B. F., Robertson, S. A., Rudner, D. Z., Barbash, D. A., Cline, T. W., Kanaar, R., Rio, D. C., and Wemmer, D. E. (1997) *Biochemistry* **36**, 14306-14317

70. Rajagopal, P., Waygood, E. B., Reizer, J., Saier, M. H. J., and Klevit, R. E. (1997) *Protein Sci.* **6**, 2624-2627

71. Shuker, S. B., Hajduk, P. J., Meadows, R. P., and Fesik, S. W. (1996) *Science* **274**, 1531-1534

72. Li, M. X., Gagné, S. M., Spyracopoulos, L., Kloks, C. P. A. M., Audette, G., Chandra, M., Solaro, R. J., Smillie, L. B., and Sykes, B. D. (1997) *Biochemistry* **36**, 12519-25

73. Slupsky, C. M., Kay, C. M., Reinach, F. C., Smillie, L. B., and Sykes, B. D. (1995) *Biochemistry* **34**, 7365-7375

74. Wishart, D. S., and Sykes, B. D. (1994) *Methods Enzymol.* **239**, 363-392

75. Wishart, D. S., Sykes, B. D., and Richards, F. M. (1991) *J. Mol. Biol.* **222**, 311-333

76. Campbell, A. P. (1991) *NMR Studies of the Interactions Between Proteins in the Thin Filament of Muscle*, PhD Thesis, University of Alberta. pgs. 424

77. Ehrhardt, M. R., Urbauer, J. L., and Wand, A. J. (1995) *Biochemistry* **34**, 2731-8

78.   McKay, R. T. (1999) *Defining the Interactions of Troponin-C with Troponin-I by Nuclear Magnetic Resonance Spectroscopy,* Ph.D. Thesis, Univ. of Alberta. **Manuscript in Preparation,** pgs.

79.   Li, M. X., Spyracopoulos, L., and Sykes, B. D. (1998) *Biophys. J.* **74,** A51

80.   Li, M. X., Spyracopoulos, L., and Sykes, B. D. (1999) *Submitted to Biochemistry Jan. 21,1999*

81.   Schaertl, S., Lehrer, S. S., and Geeves, M. A. (1995) *Biochemistry* **34,** 15890-4

82.   Wang, C. K., and Cheung, H. C. (1985) *Biophys J* **48,** 727-39

83.   Ingraham, R. H., and Swenson, C. A. (1984) *J Biol Chem* **259,** 9544-8

84.   Campbell, A. P., and Sykes, B. D. (1991) *J. Mol. Biol.* **222,** 405-421

Chapter V: Interactions and Energetics

A. Introduction

This chapter will focus specifically on the E41A mutation of calcium saturated

sN-TnC (E41A), and the energetics of the 'opening' of the hydrophobic pocket in the

native and mutant proteins. The Glu^{41} to an Ala^{41} mutation of sN-TnC has been shown to

drastically reduce the affinity for calcium in site I (*1*), and to reduce the structural

opening (*i.e.* movement of the BC helices away from the NAD unit) associated with

calcium binding to the wild type protein (*2*). Based on this finding, Glu^{41} was suggested

to be the "ultimate" (*2*) fulcrum controlling the opening of sN-TnC. The hypothesis that

the exposure of approximately 500 $Å^2$ of hydrophobic surface area in sN-TnC was

regulated by a single glutamate residue forming an electrostatic (bidentate) bond to

calcium was unique. Another possibility is that the binding of calcium to each of the two

sites in sN-TnC results in the rearrangement of the hydrophobic core. TnC core residues

are homologous to other calcium-binding proteins wherein unfavorably tight packing

lowers the energetic barrier to opening (*3*). Binding of calcium may lower the barrier

further by causing subtle hydrophobic rearrangement favorable to opening and/or further

restriction of already entropically stressed residues. Glu^{41} would therefore be more

accurately described as necessary but not sufficient for structural opening in the absence

of other members of the troponin-C complex.

Very recently, in the highly homologous cardiac system, the addition of cardiac

TnI peptide corresponding to skeletal $TnI_{115-131}$ (*i.e.* $cTnI_{147-163}$) has been shown to result in

opening of the otherwise closed calcium saturated structure of cN-TnC ((*4*), and personal

communications). This strongly suggests that the binding of calcium does not necessarily

have to result in opening of the hydrophobic pocket for regulation of contraction to occur. Instead calcium would control the energy barrier to opening and subsequently allow or prevent the interactions with the inhibitory protein in a calcium dependent manner.

This chapter will present unpublished NMR spectroscopic data concerning the titration of ^{15}N-labeled E41A with unlabeled $TnI_{115-131}$ peptide. The purpose of this study was to determine if the mutation of Glu^{41} to Ala^{41} in sN-TnC was sufficiently energetically unfavorable to the 'opening' of the N-domain that the TnI peptide would no longer be able to bind. The final sections of this chapter will present a brief summary of the reported energetics involved in various ligands binding to several regions and mutants of TnC.

B. Experimental Procedures

1. E41A sN-TnC Protein

The cloning, expression and purification of [U-^{15}N]-E41A-sN-TnC was performed

as described previously (1) with the exception that the protein was subjected to an

additional step of RP-HPLC purification on a SynChropak semi-preparative C-8 column

(250 mm x 10 mm, 300 Å pore size) with adapted pre-column filter (0.2 µm). A and B

buffers were made from a (40x) stock of 200 mM ammonium acetate, and 10 mM EDTA

dissolved in HPLC grade H$_2$O at pH 6.5. The A buffer was made by diluting 25 ml of

stock buffer into 975 ml of HPLC water and adjusting the pH back to 6.5, then filtering

(0.2 µm pore size) to remove any particulate matter. The B buffer was made the same as

A buffer except that the 25 ml of stock was dissolved in 475 ml of HPLC water and 500

ml of HPLC grade acetonitrile (again adjusting the pH to 6.5 after dilution followed by

filtration). A single preparative column run consisted of ten to twenty crude protein

injections (2 ml/injection at approximately 1 mg of protein per ml) while running A

buffer (2ml/min). It was very important to allow the column to re-establish equilibrium

in between injections. This could be accomplished by monitoring the pH of eluted

solvent during injections, allowing a minimum of 2 min between injections, and

providing an additional 14 mins of A buffer wash before starting the AB gradient. The

AB gradient consisted of 12.5 mins at 4% A-B/min (i.e. gradient changed from 0 to

50%B) and then a slower gradient of 1% B/min for 50 minutes (i.e. 50% to 100% B, the

proteins of interest eluted during this period). The column was then maintained at 100%

B for 20 mins. At least two column washes (4% B/min for 25 mins per wash) were

needed to remove residual TnC from the column. Failure to wash the column would

result in contaminating subsequent preparative runs. Eluted protein was then

concentrated by freeze drying, and metals were removed in the presence of EDTA on a

G25 size exclusion column with ammonium bicarbonate buffer (see (5) and references

therein). The protein was repeatedly freeze dried until no further change to the pH was

detected. Amino acid analysis, mass spectroscopy, and analytical HPLC (at pH 2 using

standard TFA/acetonitrile methodology) were used to establish the composition,

concentration, mass, and purity of the sample, respectively.

2. NMR Spectroscopy on $E41A \cdot TnI_{115-131}$

All NMR sample volumes were 500 μL (90% H_2O and 10% D_2O), consisting

of 100 mM KCl, 10 mM D_3-imidazole, 0.01 % (v/v) NaN_3, and 0.1 mM 2,2-dimethyl-2-

silapentane-5-sulfonate (DSS, as internal standard). The reported pH was not corrected

for isotope effects, and the temperature of all NMR experiments was 30°C. The

$E41A \cdot TnI_{115-131}$ NMR sample consisted of the NMR stock buffer listed above with the

addition of 1.5 mM ^{15}N-E41A-sN-TnC, and 6 mM $CaCl_2$ for the titration (two equivalents

of calcium per metal binding site) with a pH of 6.7. The $CaCl_2$ concentration was

increased to 6 equivalents per calcium binding site (see Discussion and below) for the

relaxation experiments. Spectra were referenced according to Wishart et al. (6).

The first stock solution of $TnI_{115-131}$ contained 3 mg of peptide, dissolved in 55 μL

of the NMR buffer, and 5 μL were used for each of the first 11 additions. A second TnI

stock solution (75 μL at approximately the same concentration) of $TnI_{115-131}$ was prepared

for the final 3 addition points (25 μL per addition). The ratio of $TnI_{115-131}$ peptide to

E41A for each of the 14 titration points was 0, 0.12, 0.19, 0.27, 0.44, 0.50, 0.62, 0.55,

0.70, 0.77, 0.94, 1.38, 1.70, 2.13 and 2.50 to 1, respectively. Each point of the titration

was monitored by 1D-^{1}H, and 2D-^{1}H,^{15}N-HSQC NMR spectroscopy. After spectra were

acquired for each titration point, 5 µL of the NMR sample was set aside. From this

isolated portion of the sample, 3 separate 1 µL portions were used for amino acid

analysis. This technique resulted in a zero volume change for the first 11 additions. The

change in concentration of the E41A and TnI$_{115-131}$ peptide was accomodated for in the

dissociation constant calculations.

a.) 600 MHz relaxation

The relaxation data were acquired on a Unity 600 MHz spectrometer equipped

with a triple-resonance probe and z-axis actively shielded field gradients. The number of

acquired points (and sweep widths) for the ^{15}N-HSQC (7), ^{15}N-T$_1$, ^{15}N-T$_2$, ^{1}H-saturated

and non-saturated ^{15}N-NOE (8) are 1024 (8000 Hz), and 128^1 (1650.2 Hz) for the directly

and indirectly detected dimensions, respectively. The number of transients were 16, 8, 8,

32, and 32 for the listed experiments, also respectively. The relaxation delays were

11.1, 55.5, 122.1, 199.8, 277.5, 388.5, 499.5, 666, 888, and 1254.3 ms for the ^{15}N-T$_1$

experiment, and 16.2, 32.5, 48.8, 65.0, 81.3, 97.5, 113.8, 130.0, 146.3, and 162.6 ms for

the ^{15}N-T$_2$. The number of delay cycles for the ^{1}H-saturated NOE experiment was 596.

Delays between transients were 1.2, 3, 2, and 5 s for the T$_1$, T$_2$, and ^{1}H-saturated NOE

and non ^{1}H-saturated NOE experiments, respectively.

b.) 500 MHz relaxation

Additional relaxation data for the E41A•TnI$_{115-131}$ sample was acquired on a

Varian Unity Inova 500 MHz, also equipped with a 5mm triple resonance probe and z-

axis pulsed field gradients. The number of acquired points (and sweep widths) for the

^{15}N-T$_1$-pfg, ^{15}N-T$_2$-pfg, ^{1}H-saturated and non-saturated ^{15}N-NOE-pfg at 500 MHz were

896 (7000 Hz), and 128 (1500 Hz) for the directly and indirectly detected dimensions,

respectively. The number of transients were 8, 8, 32, and 32 for the listed experiments,

also respectively. The relaxation delays were 11.1, 55.5, 122.1, 199.8, 277.5, 388.5,

499.5, 666.0, 888.0, and 1254.3 ms for the ^{15}N-T$_1$ experiment, and 15.6, 31.3, 46.9, 62.6,

78.2, 93.8, 109.5, 125.1, 140.8, and 156.4 ms for the ^{15}N-T$_2$. The number of delay cycles

for the ^{1}H-saturated NOE experiment was 596. Delays between transients were 1.2, 3, 2,

and 5 s for the T$_1$, T$_2$, and ^{1}H-saturated NOE and non ^{1}H-satuated NOE experiments,

respectively.

All spectra were processed using NMRPipe (*9*) and analyzed using PIPP (*10*).

Directly and indirectly detected data were zero filled to twice the number of acquired

points and then apodized using a shifted sine bell before Fourier transformation.

---

[1] 256 points were acquired for the first 11 additions and 128 points were acquired for the last three.

C. Results

1.) Titration of E41A with TnI$_{115-131}$ peptide

We have monitored the effect of the addition of TnI$_{115-131}$ peptide to calcium

saturated ^{15}N-E41A protein to help derive the energetic contribution of Glu^{41} to the

opening of N-TnC. Figure V-1 shows the change in E41A backbone amide ^{1}H,^{15}N-

HSQC NMR cross-peaks upon addition of TnI$_{115-131}$.
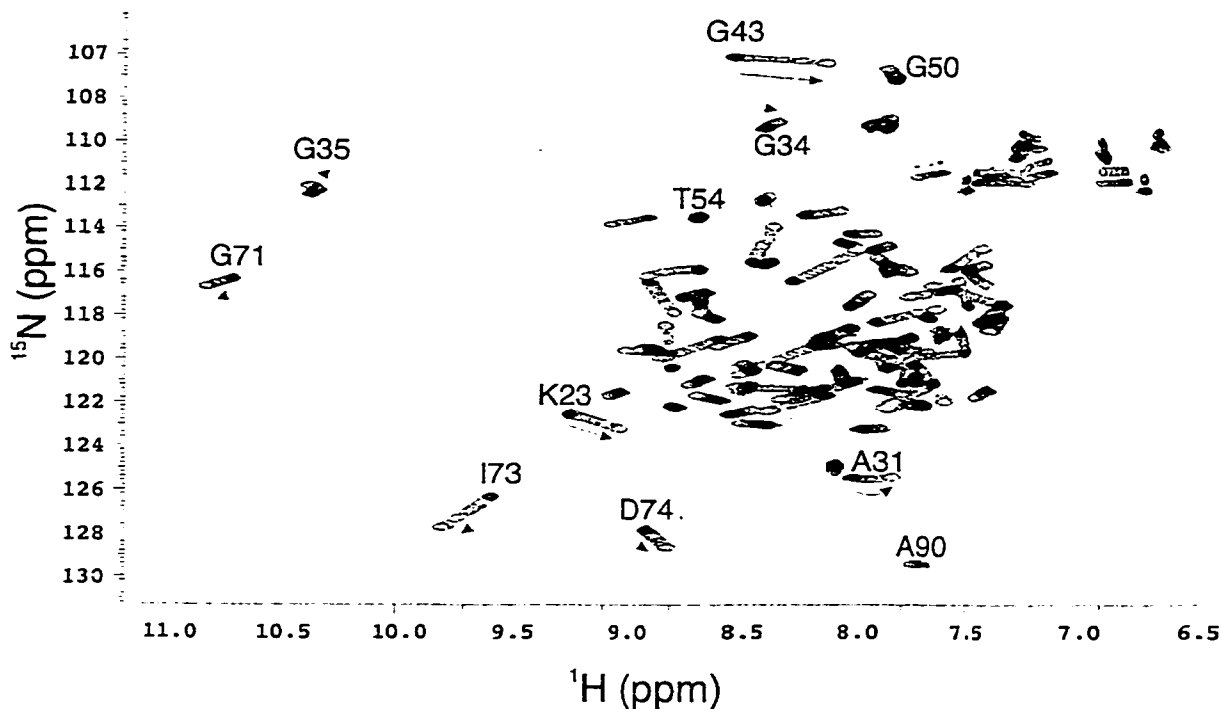
Figure V-1

Contour plots of the titration of calcium-saturated ^{15}N-labeled E41A-sN-TnC with
unlabeled TnI$_{115-131}$ monitored by 2D-^{1}H,^{15}N-HSQC NMR spectroscopy. E41A before
addition of peptide is shown with multiple contours while each addition of TnI$_{115-131}$ is
shown in single contour representation. Several E41A backbone amide cross-peaks are
labeled with the single letter amino acid code, and the arrow indicates direction of the
change in chemical shift.

From the observed E41A backbone amide $\Delta\delta_{total}$ (Figure V-2) a dissociation constant of

300 ± 100 µM was determined as described previously (*5,11,12*).

Ratio of TnI$_{115-131}$ to E41A
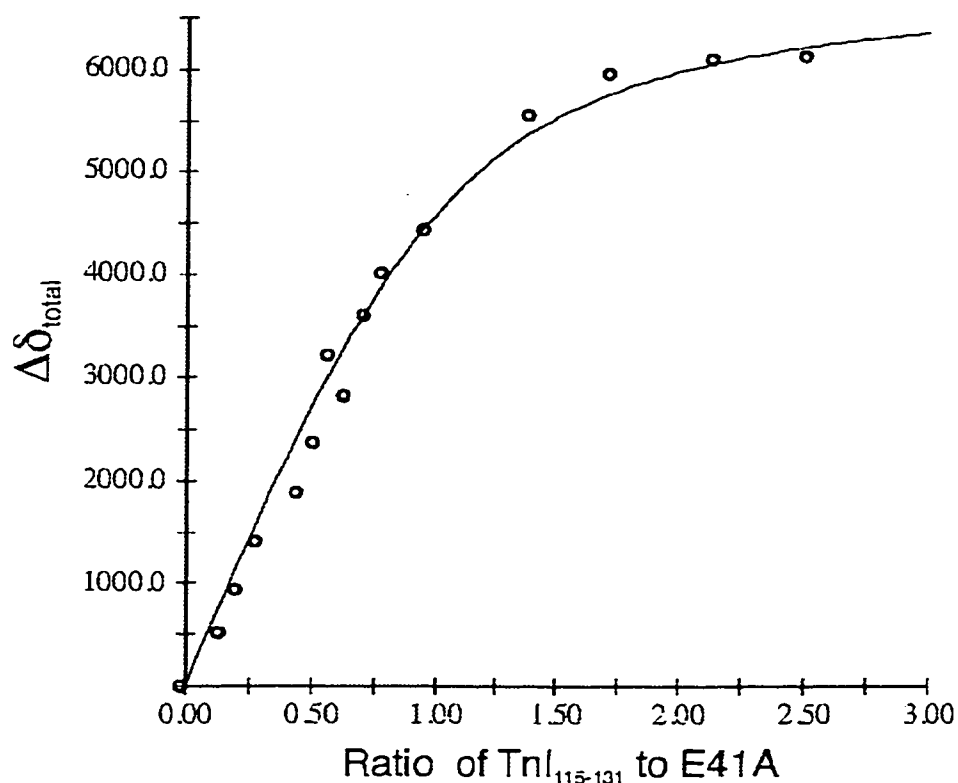
Figure V-2

Binding curve determined from two-dimensional HSQC NMR spectra for the titration of calcium-saturated E41A N-TnC with TnI$_{115-131}$. The $\Delta\delta_{total}$ for the 82 monitored E41A N-TnC backbone amide cross-peaks is shown for each addition of TnI$_{115-131}$. Residues Ser^{15}, Asp^{30}, Asp^{36}, Val^{45}, and Glu^{76} could not be followed due to spectral overlap. Pro^{53} could not be followed due to the lack of an amide hydrogen resonance, and residues Ala^{1}, Ser^{2} could not be followed due to rapid exchange. The determined dissociation constant was 300 ± 100 μM.

The dissociation constant for E41A•TnI$_{115-131}$ corresponds to an energy of binding of 4.8 ± 0.2 kcal/mol, and can be compared to the dissociation constant of 26 μM (energy of binding of 6.1 kcal/mol) for TnI$_{115-131}$•N-TnC as reported in Chapter II. The difference in energy of binding (1.3 kcal/mol) of TnI$_{115-131}$ to E41A and wild type N-TnC can be attributed to the contribution of Glu^{41}. The contribution could be direct binding energy to the TnI peptide and/or to the energy barrier of opening (see below).

2.) Change in Chemical Shift

The ^{1}H ($\Delta\delta_{HN}$), ^{15}N ($\Delta\delta_N$) and "total" ($\Delta\delta_{total}$, see (5)) change in chemical shift for

each residue of calcium saturated E41A upon addition of $TnI_{115-131}$ is presented in Figure

V-3, panels A-C, respectively. For comparison purposes, Figure V-3, panels D-F, G-I, J-

L, M-O, and P-R show the ^{1}H, ^{15}N, and total change in chemical shift for: E41A apo to

calcium saturated (*1*), sN-TnC apo to calcium (*13*), sN-TnC calcium saturated to $TnI_{115-131}$

bound (*5*), cardiac N-TnC apo to calcium (*1*), and cN-TnC calcium saturated to cardiac

$TnI_{147-163}$ (*4*), all respectively. The change in chemical shift for Glu^{41} in the native protein

was not found to respond significantly to the TnI peptide (Figure V-3, panels J-L).

However, Ala^{41} in the E41A protein **did** respond in a statistically different way to the

binding of $TnI_{115-131}$ (see Figure V-3, panel A-C and Discussion). The possibility of

residue 41 contributing directly to peptide binding is unlikely due to its position in both

the calcium-saturated E41A and sN-TnC molecules in relation to the expected site of

binding. The reduction in affinity for $TnI_{115-131}$ to E41A was therefore attributed to the

peptide forcing open the structure prior to binding. Additional information was needed to

support the assumption that $TnI_{115-131}$ binds in the same location in E41A as the native

protein (see Discussion).

Residue #

Residue #

Residue #

Residue #
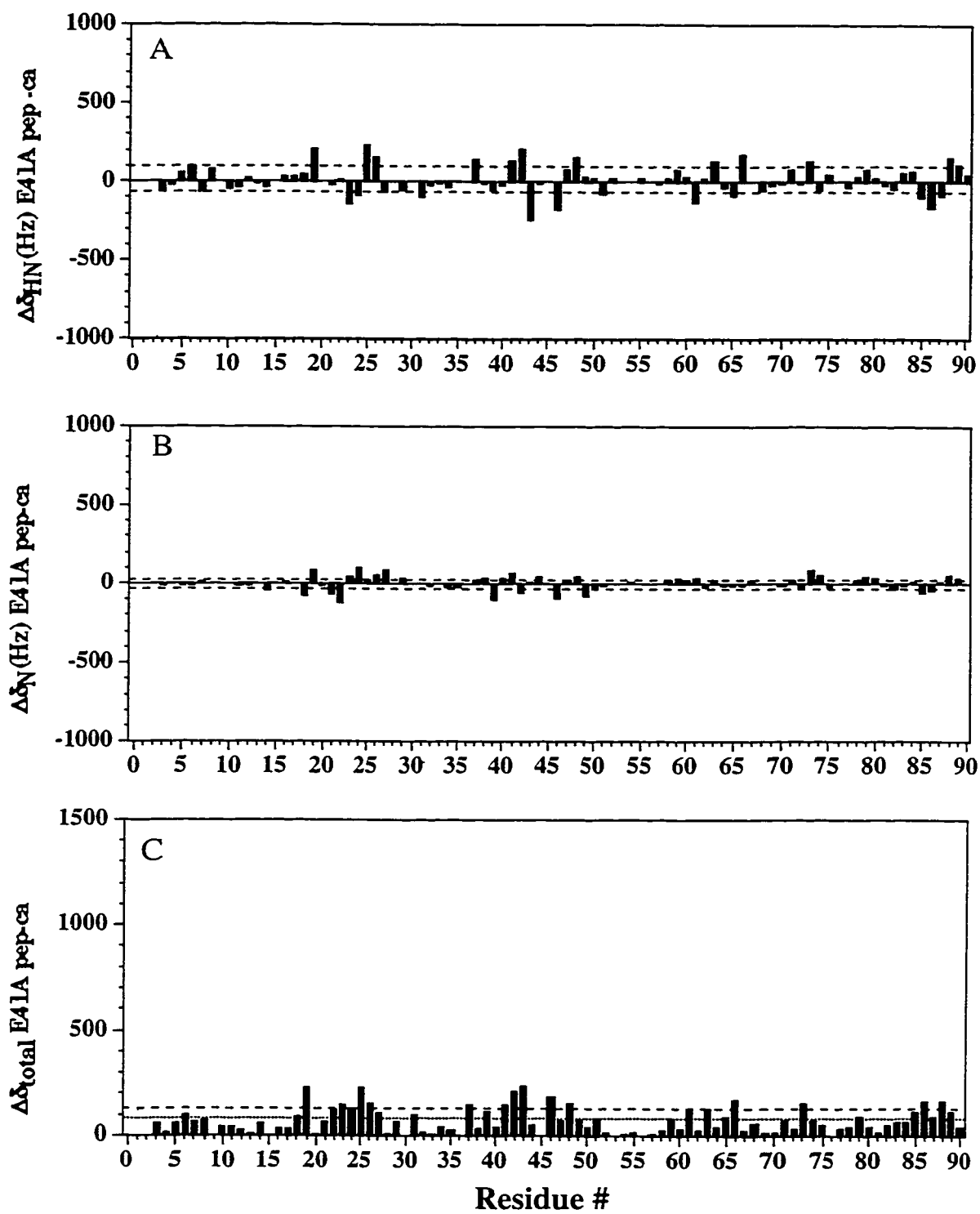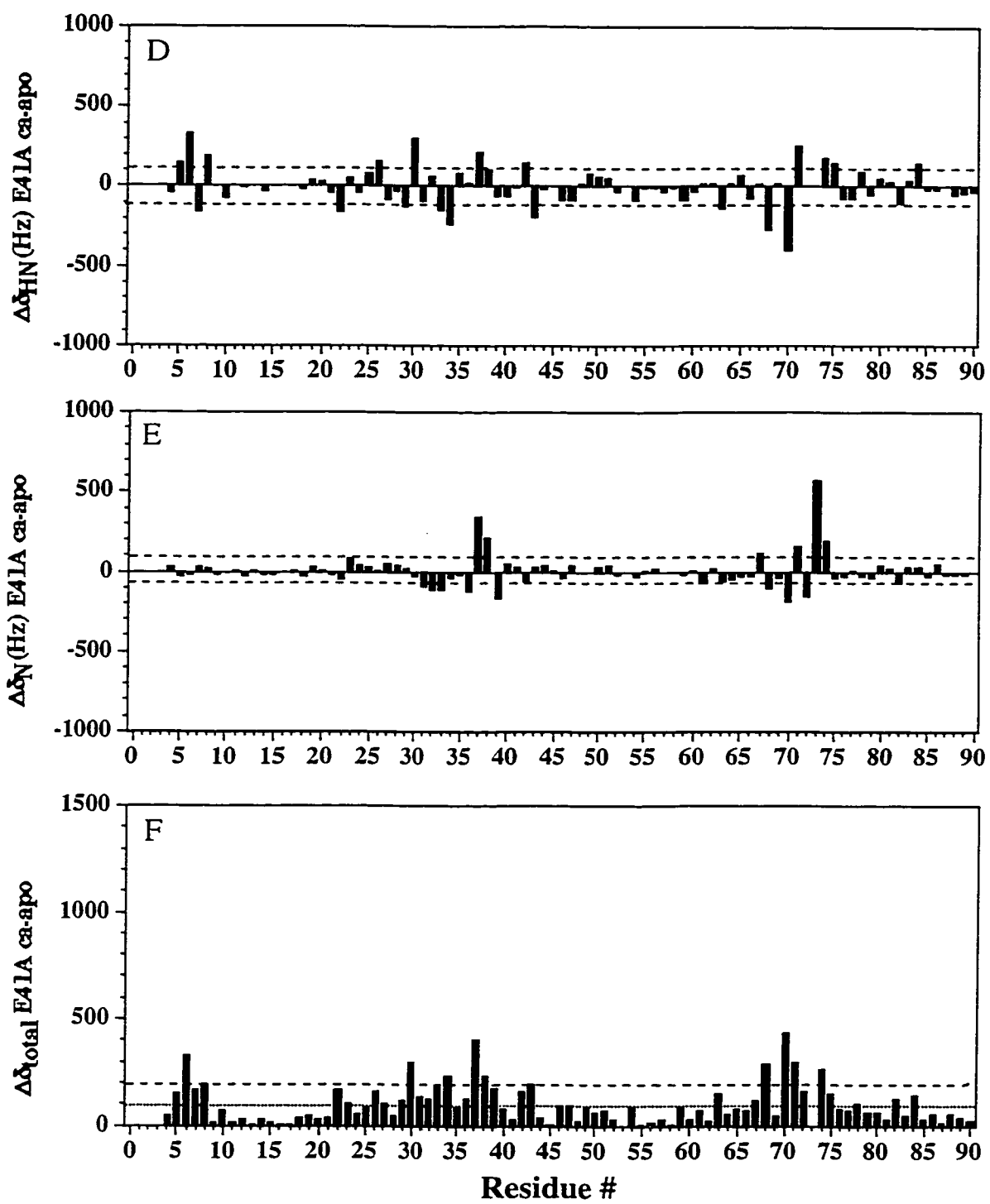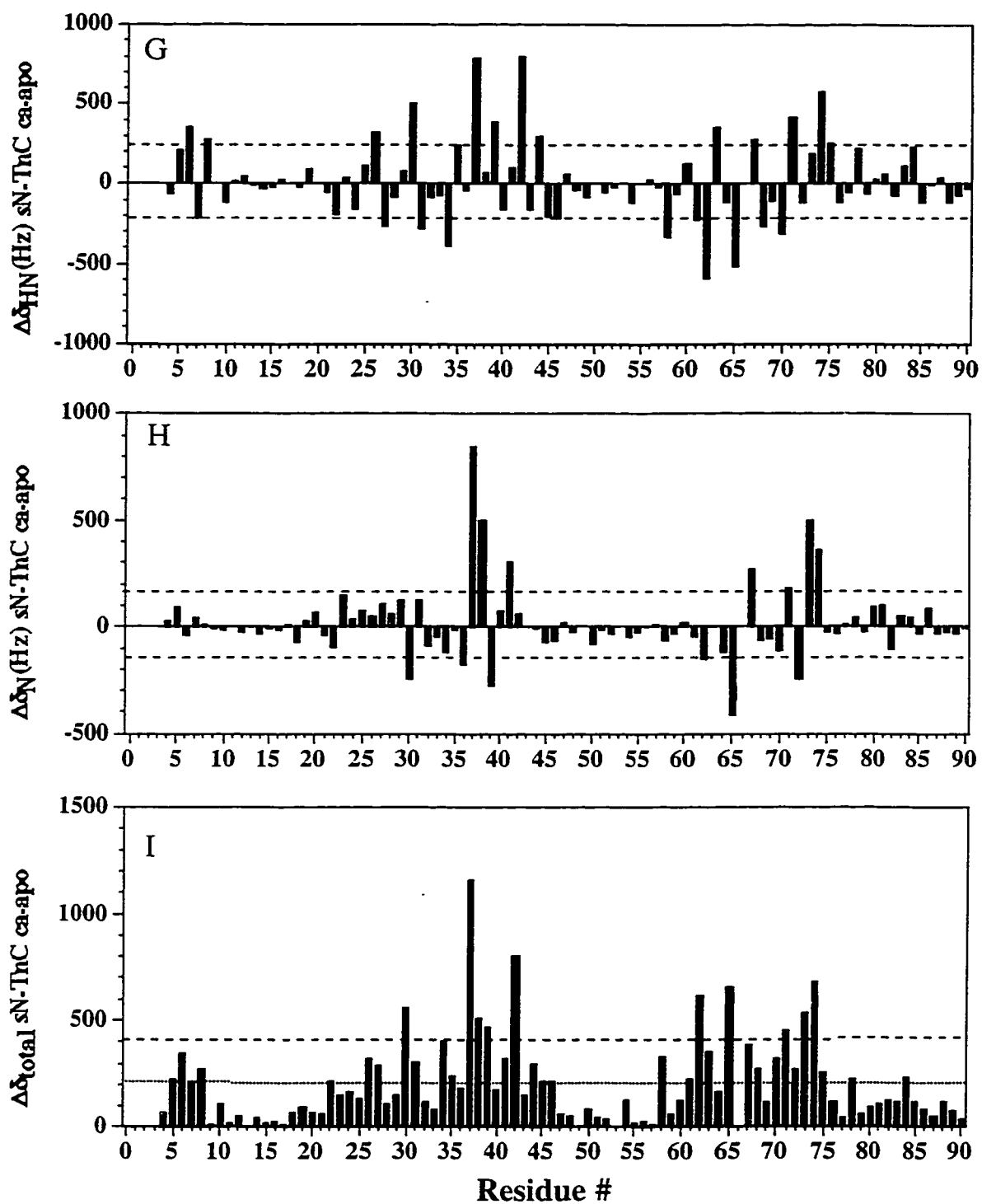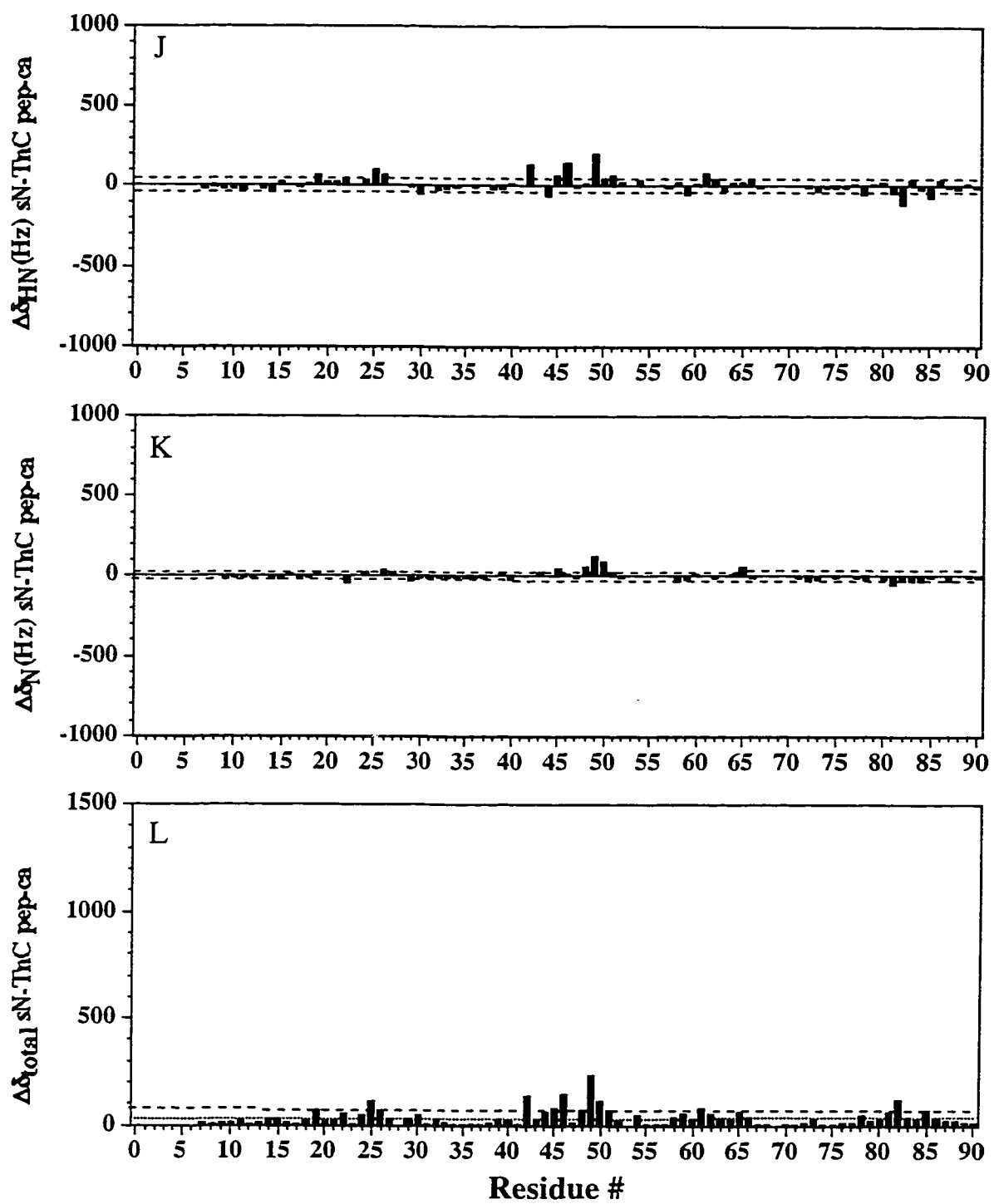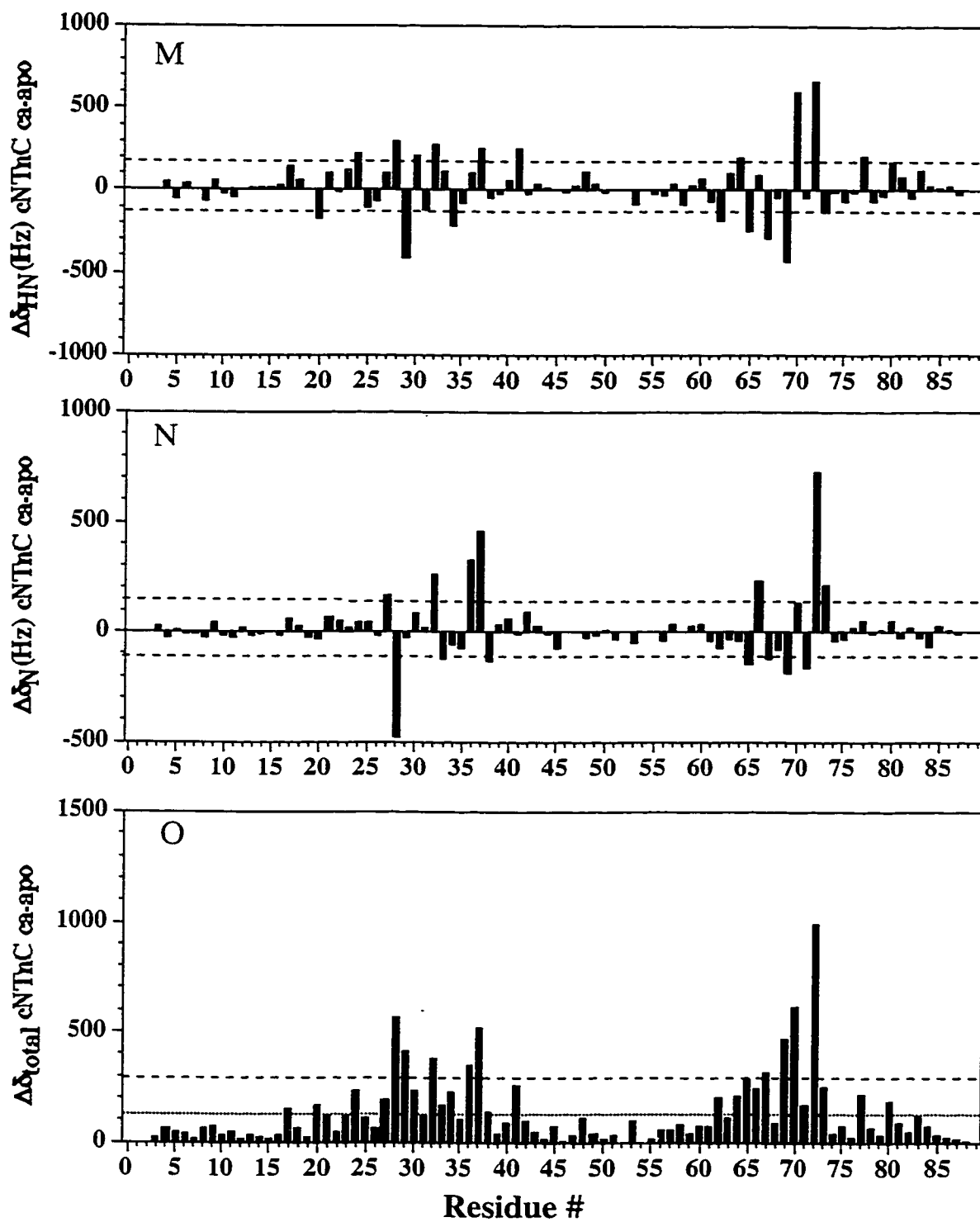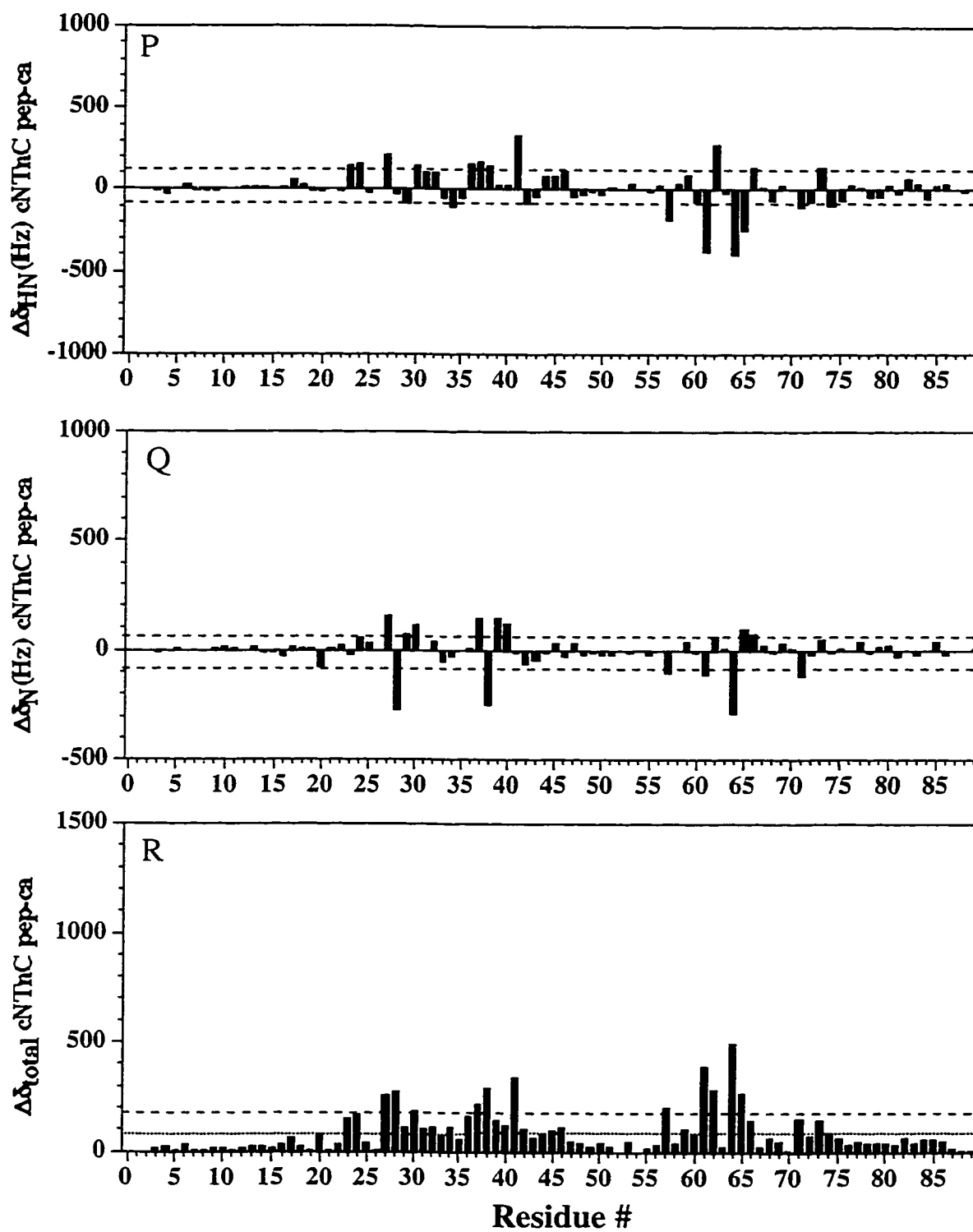
Figure V-3

Changes in chemical shifts for (A-F) E41A, (G-L) sN-TnC and (M-R) cN-TnC upon addition of (A-F, G-I, M-O) calcium, (A-C, J-L) $TnI_{115-131}$, or (P-R) $cTnI_{147-163}$. Reported changes for ^{15}N and ^{1}H are the chemical shifts of the calcium-saturated state minus the apo state or the peptide bound state minus the calcium-saturated, respectively. Average changes are indicated with a dotted line while one standard deviation is shown with a dashed line. Graphs are displayed at the same scale for comparison purposes.

3.) Chemical Shift Mapping

To determine the location of TnI peptide binding the change in chemical shifts

occurring in the native and E41A protein upon addition of $TnI_{115-131}$ peptide, was

compared (Figure V-3). From Figure 3, panel C (*i.e.* E41A response to $TnI_{115-131}$)

residues Ile^{19}, Lys^{23}, Ala^{24}, Ala^{25}, Phe^{26}, Ile^{37}, Glu^{41}, Leu^{42}, Glu^{43}, Met^{46}, Met^{48}, Ile^{61}, Asp^{66},

Ile^{73}, Met^{86}, and Glu^{88} were observed to experience statistically different changes in

chemical shift upon addition of $TnI_{115-131}$. These residues correspond very well with those

found to respond in sN-TnC upon $TnI_{115-131}$ addition, specifically residues[2] **Ile^{19}**, **Ala^{25}**,

Phe^{26}, **Leu^{42}**, Val^{45}, **Met^{46}**, Leu^{49}, Gly^{50}, **Ile^{61}**, and Met^{82}. Many of these residues are

buried in the calcium saturated E41A structure, and therefore supports the hypothesis that

$TnI_{115-131}$ binds in the hydrophobic pocket, and in a very similar location on both E41A

and sN-TnC.

The average magnitude and standard deviation of the change in chemical shift for all

the proteins compared is presented in Table V-1.

---

[2] **Bold** indicates residues that show statistically significant changes in chemical shift for both E41A and sN-TnC. Residues are included in this list only if they had statistically different chemical shifts for sN-TnC•$TnI_{115-131}$ under both salt conditions (5).

Table V-1: Change in NMR HSQC backbone amide cross-peak chemical shifts for E41A, sN-TnC and cardiac N-TnC upon addition of calcium followed by TnI peptide.

Protein/Complex	Average $\Delta\delta_{HN}$ (std)[a]	Average $\Delta\delta_N$ (std)	Average $\Delta\delta_{total}$ (std)
E41A Ca^{2+} to $TnI_{115-131}$ bound	9.5 (86)	2.5 (39)	75 (59)
sN-TnC Ca^{2+} to $TnI_{115-131}$ bound	10 (44)	3.2 (24)	35 (38)
cN-TnC Ca^{2+} to $cTnI_{147-163}$ bound[b]	9.4 (105)	-2.8 (69.5)	84 (95)
E41A apo[c] to Ca^{2+}	-0.7 (113)	3.5 (96)	98 (92)
sN-TnC apo[d] to Ca^{2+}	15 (237)	16 (162)	209 (200)
cN-TnC apo[e] to Ca^{2+}	24 (159)	12 (133)	132 (161)

[a] Values for the average and standard deviation are in Hz. An absolute value for the average was not calculated in order that the overall direction of change could be determined. For each $\Delta\delta_{HN}$ or $\Delta\delta_N$ the change in chemical shift was calculated as the chemical shift of the Ca^{2+} state minus the apo chemical shifts, or the peptide bound state minus the Ca^{2+} chemical shifts, respectively. For [b, c, d] and [e], data were taken from references (1,4,13) and (1), respectively.

The binding of peptide results in more downfield shifts for the amide hydrogen (as indicated by the average positive shifts), but there does not appear to be an overall correlation between binding of peptide, and the direction of chemical shift in the nitrogen chemical shift. There appears to be a lack of correlation for hydrogen $\Delta\delta$ regarding calcium binding, although positive shifts are observed for nitrogen. The most immediate observation from Table V-1 is that the greatest changes in chemical shift occur upon addition of calcium to the sN-TnC molecule. The change appears to be proportional to the large structural change, exposure, and solvation of the residues making up the hydrophobic pocket while E41A and cN-TnC do not 'open', but instead experience subtle rearrangement of the core residues. E41A has the smallest $\Delta\delta_{total}$ (98) upon addition of calcium out of the three systems monitored, though it is fairly close to that observed for

the cardiac protein. This corresponds well with E41A having the smallest change in tertiary structure as reported (2), however the change in chemical shifts (Figure V-3, panels D-F) also suggest that E41A is undergoing some rearrangement since the changes are not isolated to the active calcium binding site (*i.e.* site II). The general correlation between the magnitude of chemical shift and the degree of structural change is also apparent with the addition of $TnI_{115-131}$ to calcium saturated sN-TnC, since the addition of peptide caused relatively small changes in the N-domain structure when compared to the effect of calcium. The results indicate that both cardiac and E41A are responding similarly to the addition of calcium (compare the $\Delta\delta_{total}$ of 98 for E41A and 132 for cardiac in Figure V-3), and almost identically to the addition of peptide. Taken with the recent results by Li *et al.* (4), this again strongly indicates that the peptide is binding to an 'open' E41A.

4.) Relaxation data

The $^{15}N\text{-}T_1$, $^{15}N\text{-}T_2$ and (^1H),$^{15}N\text{-}NOE$ relaxation data for $^{15}N\text{-}E41A\bullet TnI_{115-131}$ are shown in Figure V-4, panels A-C, respectively. The average $^{15}N\text{-}T_1$ relaxation times at 500 and 600 MHz are 488 ± 6 ms and 591 ms ± 11, respectively[3]. The average times for $^{15}N\text{-}T_2$ relaxation at 500 and 600 MHz are 114 ± 2 and 116 ± 1 ms, respectively. The average NOE was 0.65 ± 0.01 and 0.71 ± 0.01 at 500 and 600 MHz, also respectively.

---

[3] The average error is reported.
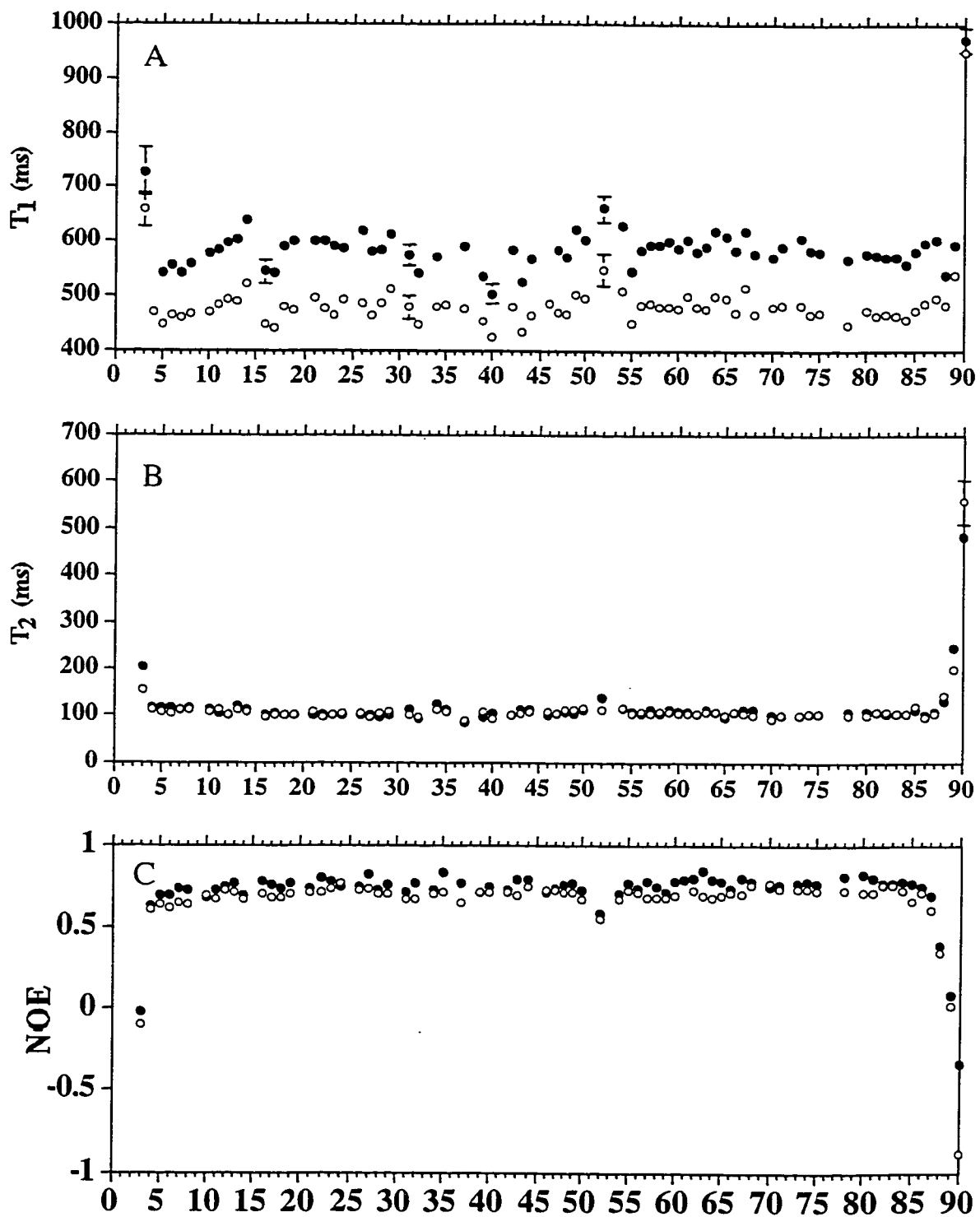
Figure V-4

(A) ^{15}N-T$_1$, (B) ^{15}N-T$_2$, and (C) (^{1}H)^{15}N-NOE relaxation data for calcium saturated ^{15}N-E41A-sN-TnC while complexed with TnI$_{115-131}$ and acquired at (o)500 and (•) 600 MHz, respectively. Positive and negative error bars are shown for all residues, but are smaller than the size of the symbol for almost all of the residues. Residues Ala^1, Ser^2 could not be followed due to rapid exchange, and Pro^{53} could not be monitored due to the lack of an amide hydrogen resonance. Residues Glu^9, Ser^{15}, Ala^{20}, Ala^{25}, Asp^{30}, Gly^{33}, Asp^{36}, Ser^{38}, Ala^{41}, Val^{45}, Gln^{51}, Gly^{69}, Thr^{72}, Glu^{76}, Glu^{77}, and Leu^{79} could not be monitored due to spectral overlap. Thr^4, Gly^{35}, and Met^{46} could not be followed during the T$_1$ experiments at 600 MHz and Ile^{61} could not be calculated from the 500 MHz spectra due to overlap. Please note that T$_1$ and T$_2$ change proportionally with internal motion for correlation times of the complexes studied.

Residues Met^3, Asn^{52}, Glu^{88}, Asp^{89}, Ala^{90} showed internal motion (*i.e.* NOE less than 0.6

and 0.65 at 500 and 600 MHz, respectively) that would affect the measured T$_1$ value.

The average T$_1$ at 500 and 600 MHz, excluding these residues, is 477 and 583,

respectively, while the average T$_2$ at 500 and 600 MHz changes to 105 ± 0.9 and 106 ± 1,

also respectively.

D. Discussion

The results presented in this chapter have demonstrated that $TnI_{115\text{-}131}$ binds to

E41A with a 1:1 stoichiometry, and with less affinity than to the native protein. The TnI

peptide has also been shown to bind in the hydrophobic pocket that is not exposed in the

calcium-saturated E41A protein. The decrease in binding affinity is attributed to the

remaining energetic cost of opening after core residues rearrange. In the closing section

of this chapter, I would like to compare the changes in chemical shifts for cardiac,

skeletal and the E41A mutant N-TnC, evaluate more closely the behavior of chemical

shift changes to site I of E41A, and examine the energetics involved in peptide binding to

the proteins discussed.

1.) Comparison of Changes in Chemical Shift

I have presented chemical shift maps for three N-TnC systems (*i.e.* cardiac,

skeletal and the E41A mutant, see Figure V-3), and have re-organized the data (Figure V-

5) for easier comparison. The first panel in Figure V-5 compares the magnitude of $\Delta\delta_{total}$

for each backbone amide of sN-TnC upon addition of calcium versus $TnI_{115\text{-}131}$. The vast

majority of the changes in chemical shift are greater for the addition of calcium as would

be expected from the larger structural change. Figure V-5, panels B and C show the same

comparison for the E41A mutant and cN-TnC proteins upon calcium and TnI peptide,

respectively. The change upon addition of calcium is much smaller when compared to

sN-TnC, while the effect of peptide addition is substantially larger for both E41A and

cN-TnC.

A $y = 0.014x + 29.718$

$\Delta\delta_{total}$ sN-TnC ca to peptide

$\Delta\delta_{total}$ N-TnC apo to ca

B $y = 0.099x + 64.281$

$\Delta\delta_{total}$ E41A ca to pep

$\Delta\delta_{total}$ E41A apo to ca

C $y = 0.189x + 58.572$

$\Delta\delta_{total}$ cNTnC ca to peptide

$\Delta\delta_{total}$ cNTnC apo to ca

$y=0.304x+37.211$

$\Delta\delta_{total}$ E41A apo to ca

$\Delta\delta_{total}$ sN-TnC apo to ca

$\Delta\delta_{total}$ sN-TnC apo to ca

$\Delta\delta_{total}$ E41A ca-pep

$y=0.577x + 56$

$\Delta\delta_{total}$ sN-TnC ca to pep

$\Delta\delta_{total}$ sN-TnC ca to pep
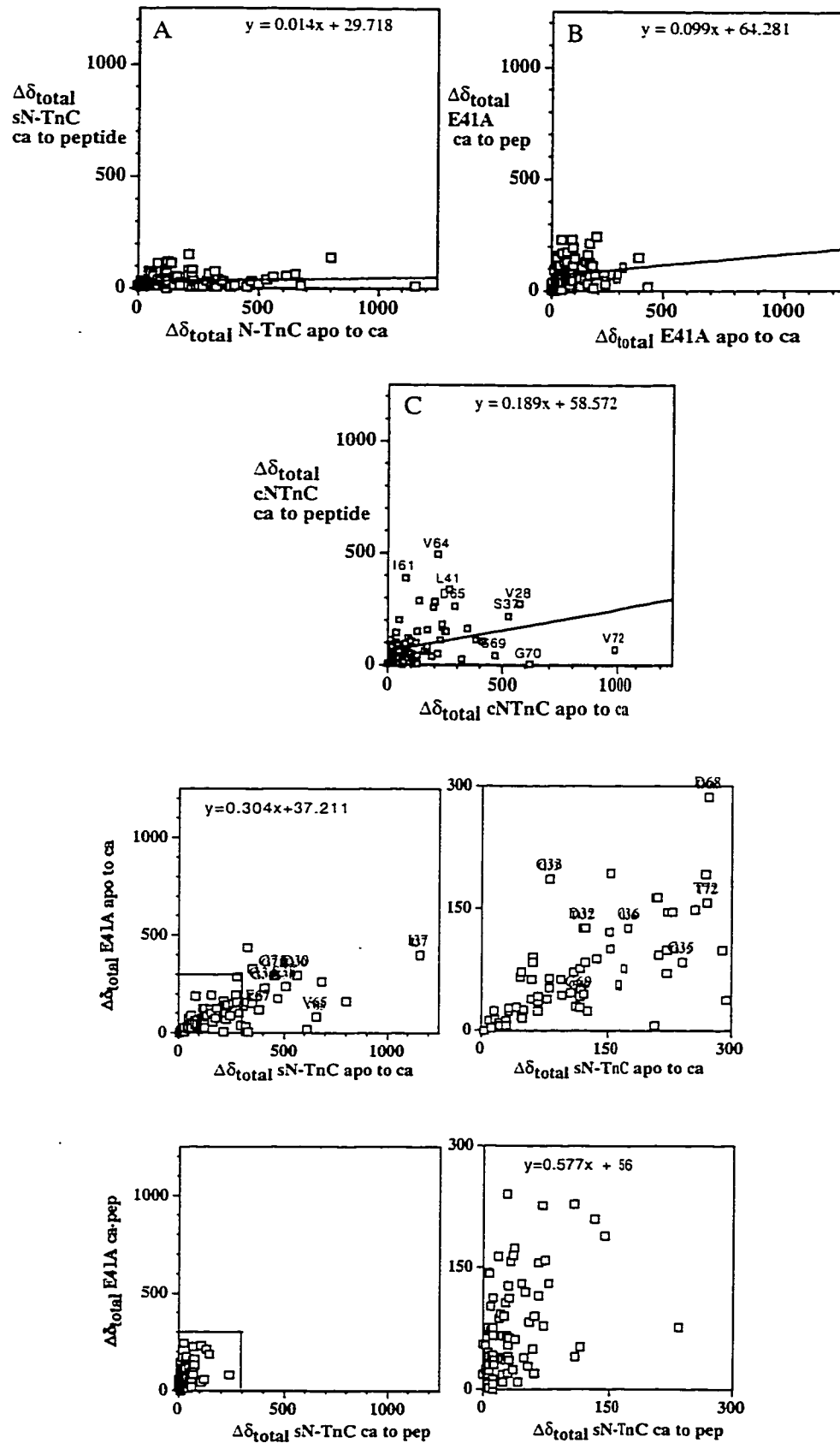
Figure V-5

Comparison of changes in total chemical shift for (A) sN-TnC, (B) E41A-sN-TnC, and (C) cN-TnC upon addition of calcium to the apo protein (*x-axis*) and peptide (TnI$_{115-131}$, cTnI$_{147-163}$ for the skeletal and cardiac system, respectively. *y-axis*). The linear fits for the data sets are shown (solid line) with the corresponding equation. Labels for cN–TnC are included in the one-letter amino acid code. (D) comparison of $\Delta\delta_{total}$ for E41A (*y-axis*) and sN-TnC (*x-axis*) with an expanded plot (boxed area) shown in (E). (F) shows a comparison of $\Delta\delta_{total}$ for peptide binding to E41A (*y-axis*) and sN-TnC (*x-axis*) with (G) showing an expanded region of (F) indicated by the box.

Interestingly, the change for several residues in cN-TnC upon calcium (*e.g.* Val^{72}, Gly^{70}) or peptide (*e.g.* Val^{64}, Ile^{61}) addition is larger than the corresponding change in E41A. This suggests that the cardiac regulatory domain may be even more predisposed to opening as supported by the tighter affinity of the cardiac system (*4*), and despite the even greater disabling of the first calcium-binding site. Figure V-5, panel D and E compare the effect of calcium binding to E41A and sN-TnC. The residues responding to calcium binding in both proteins are not restricted to one or both of the calcium binding sites (residues from sites I and II are labeled). This supports the proposed idea that structural re-arrangements are occurring in both proteins. Figure V-5, panel F and G show a similar comparison for TnI$_{115-131}$ binding to E41A and sN-TnC. Panel F demonstrates that the magnitude of $\Delta\delta_{total}$ upon addition of peptide is smaller than calcium, and that E41A is responding much more to peptide when compared to sN-TnC. The data suggests that E41A and cN-TnC are undergoing similar large structural changes when compared to sN-TnC upon addition of TnI peptide.

One of the overall conclusions of this chapter is that TnI$_{115-131}$ binds to an open E41A and that the reduction in affinity (compared to sN-TnC) is the energetic

contribution of Glu^{41}. However, as mentioned in the results section, Ala^{41} in the mutant

protein shows statistically different $\Delta\delta_{total}$ with the addition of peptide. The position of

Ala^{41} in relation to the proposed site of peptide interaction precluded Ala^{41} from directly

contributing to binding, but upon examining the change in chemical shifts of site I

(residues ~30-41) backbone amide cross-peaks some unique characteristics were

observed.

The same fast exchange line shapes were seen, but two 'events' were evident by

the non-linear change in chemical shift (e.g. Figure V-1, compare residues Gly^{35}, Ala^{31},

Gly^{34} to the behavior of Ile^{73} or Lys^{23}). I would like to suggest that the binding of peptide

not only opens the hydrophobic pocket, but also results in a structural change in site I that

allows calcium to bind more favorably despite the lack of Glu^{41}. This appears to be direct

proof of the coupling between structural changes associated with opening of the

hydrophobic pocket (i.e. peptide binding), and the formation of an active calcium binding

site I. A recent publication has reported that TnC affinity for calcium increases with the

addition of TnI peptides (see (14) and references therein). The ability of calcium to bind

in site I without the bidentate glutamate contribution would again support the proposal

that Glu^{41} provides only a small portion of the total calcium affinity (and thus the

regulatory mechanism) that results in skeletal muscle contraction.

2.) Relaxation Data

There are presently two systems, the highly homologous cardiac N-TnC in the

apo and calcium saturated forms (15) and E41A in the apo state (16), available for

comparison to the presented relaxation data (Figure V-4). The amount of calcium in the

$TnI_{115-131}$•E41A sample was increased to 6 equivalents of calcium per binding site for

comparison to previous relaxation studies (*16*). The cardiac system presents the most attractive comparison since the data was collected in the calcium saturated state and the system is probably more similar to the E41A mutant than to the native skeletal protein. The relaxation data for E41A indicates a general quenching of backbone motion upon addition of peptide when compared to apo sN-TnC and calcium-saturated cN-TnC. For cN-TnC and apo sN-TnC regions of mobility can be seen (*e.g.* calcium binding sites I and II involving residues 30-41 and 66-77 for skeletal and 29-40 and 65-76 in cardiac, respectively). However, for E41A bound to $TnI_{115-131}$ peptide the relaxation times appear much more uniform and even the terminal residues appear more restricted (e.g. residues 3, 4, 87, and 88 Figure V-4, panel B). The average $^{15}N\text{-}T_1$, $^{15}N\text{-}T_2$ and NOEs are smaller for the E41A•$TnI_{115-131}$ complex as expected (due to increased mol. wt.), but the magnitude of the reduction is greater than can be attributed to the change in mass (*i.e.* the mol. wt. changes by ~10% while the T_2 changes by > 20%). The relaxation rates suggests that the backbone amide bond vectors become more uniformly restricted in their local mobility. It is interesting that even backbone motions of flexible regions are 'frozen' by the addition of peptide. The final section of the discussion will deal with the energetic implications of the titrations presented in this and previous chapters.

3.) Energetics[4]

In addition to defining structural changes NMR can provide information on other angles of calcium regulation, specifically the kinetics and energetics of the interaction of TnC with ligands such as calcium and troponin-I. From the kinetic standpoint, it is important to determine whether or not the calcium-induced structural 'opening', and the

---

[4] Portions of the Energetics section have been published previously: Gagne, S.M., Li, M.X., McKay, R.T., and Sykes, B.D. Biochem. Cell. Biol. **76**, 302-312.

subsequent interaction with troponin-I, are kinetically competent to be a part of the

mechanism of muscle contraction. For example, fast twitch insect flight muscle must be

able to regulate contractions as fast as 600-1000 Hz. The value of k_{off} (3×10^2 s^{-1}) for the

TnI$_{115-131}$ peptide when in complex to sN-TnC is the same as the calcium off rate

determined by Potter and Johnson in the absence of TnI (17). Thus the steps of calcium

binding, opening, and TnI•TnC complex formation are all occurring on similar time

scales.

<div align="center">a.) The energy barrier to opening</div>

From the energetics standpoint, NMR has been used to determine the dissociation

constants for calcium binding to sN-TnC, E41A, and cN-TnC (1), as well as the

dissociation constants for the various peptides to both the regulatory domain and intact

TnC, and the cTnI$_{148-164}$•cN-TnC (18) complex. I have attempted to summarize the

reported energetics/kinetics data regarding TnC in Table V-2, and have included in the

table the data presented in this and the preceding chapters[5]. The data allows one to begin

to estimate the equilibrium constant for the 'closed' to 'open' conformational change, and

the energetics contribution of E41 to the mechanism. The binding of two equivalents of

calcium to sN-TnC is energetically favorable by a total of 14.6 kcal·mol^{-1} (Figure V-6).

---

[5] Caution must be taken when comparing data acquired from different techniques as conditions can vary
considerably. A single reference for CaM and parvalbumin have been included in the energetic table to
show that these two homologous systems differ from skeletal and cardiac TnC (and they from each other)
for binding of calcium. This strongly suggests that any assumption on the thermodynamic mechanism (i.e.
ΔH or ΔS driven) of interaction would be hazardous at best.

Table V-2: Summary of the reported Energetics involved in various ligands binding to regions of TnC.

Complex[a]	Temp. (°C)	K_a (M⁻¹)	K_d (μM)	k_{off} (s⁻¹)	k_{on} (M⁻¹s⁻¹)	ΔG (kcal/mol)	ΔH° kcal/mol	ΔS° cal/Kmol	Ref.
TnC•TnT (Apo, Mg²⁺, Ca²⁺)[b]	20					-9.0, -10.3, -10.6			(19)
TnI•TnT (Apo, Mg²⁺, Ca²⁺)	20					-9.2, ~9.2, ~9.2			(19)
TnC(TnT•TnI)[c] (Apo, Mg²⁺, Ca²⁺)	20					-8.7, -10.9, -13.5			(19)
TnC•TnI•TnT (Apo, Mg²⁺, Ca²⁺)	20					-16.8, -18.9, -21.6			(19)
TnI•TnC[d] (Ca²⁺, Mg²⁺)	25	1.7x10⁹, 1.2x10⁸							(20)
TnC•TnI[e] (EDTA, MG²⁺, Ca²⁺)	25	1.0x10⁶, 2.6x10⁷, 1.1x10⁹				-2.8 Apo-Mg²⁺ -4.4 Apo-Ca²⁺			(20)
TnI•TnC[f] (Apo, Mg²⁺, Ca²⁺)	20	6.67x10⁵, 4.58x10⁷, 5.58x10⁹				-7.8, -10.3, -13.1	7.5, 9.9, 16.2[g]	52.1, 68.9, 99.8	(21)[b]
TnI•TnC (Apo, Mg²⁺, Ca²⁺)	10	4.24x10⁵, 2.51x10⁷, 2.09x10⁹				-7.3, -9.6, -12.1			(21)
Ca•TnC[i]	20	2x10⁷, 2x10⁵							(21)

Complex[a]	Temp. (°C)	K_a (M^{-1})	K_d (μM)	k_{off} (s^{-1})	k_{on} (M^{-1}s^{-1})	ΔG (kcal/mol)	ΔH° kcal/mol	ΔS° cal/Kmol	Ref.
Ca•cTnC(siteII)[j]	25, 4		2-5, 2-8	na, 700-800	*2-4x10^8				(22)
2Ca from Tn			62±7						(23)
TnI from Tn[k]			16±4						(23)
4Ca•CaM	25					3.8			(24)[l]
1Ca•TR$_2$C	25	~10^6				-8.25	-1.75	21.7	(24)
2Mg•CaM	25					9.1			(24)
Ca•Parvalbumin	25					-17.9			(24)
Ca•TnC	25					-30.8, -13.3			(24)
Ca•cTnC	25					-4.6			(24)
Ca•EDTA	20-25					-14.5	-6.6	26	(24)
TnC•TnC	4		83[m]			*-5.17			(25)
ApoTnC•TnIp	25-30[n]	7.1x10^3	140						(26)
TnC•TnIp	25-30	6.7x10^4	15						(26)
Apo TnC	25					4.8[o]	41		(27)
Apo TnC$_{1-85}$ unfolding	25					2.6[m]	37.5		(27)
TnC$_{95-162}$ unfold unfolding	25					3.6[m]	17.1		(27)
Ca•N-TnC	30		16, 1.7[p]						(28)
Ca•E41A-N-TnC	30		1300, 15[q]						(1)
TnI$_{115-131}$•E41A	30		300 ±100			4.8 ± 0.2			(5)
TnI$_{115-131}$•N-TnC	30		26±6						(11)
TnI$_{96-148}$•N-TnC	30		1-40						(11)
TnI$_{96-131}$•TnC	30		32±16						(12)
TnI$_{96-139}$•TnC	30		0.5-1						(12)
TnI$_{96-148}$•TnC	30		0.4-1						(12)

Complex[a]	Temp. (°C)	K_a (M^{-1})	K_d (µM)	k_{off} (s^{-1})	k_{on} (M^{-1}s^{-1})	ΔG (kcal/mol)	ΔH° kcal/mol	ΔS° cal/Kmol	Ref.
TnI[147-163]•cN-TnC	30	154							(4)
TnI[104-115]•TnC	25		10-14[f]						(29)
Ca•(TnC•TnI[104-115])	20-25		1.2						(14)
Ca•(cTnC•cTnI[137-148])[g]	20-25		0.55						(14)
Opening Apo-F29W-N-TnC	-11[f]			2			-32	111	(30)
[a]F105W•TnI[96-116]	20		2.8±0.2						(31)
F29W•TnI[96-116]	20		20±2						(31)
F105W•TnI[96-148]	20		1.2±0.2						(31)
F29W•TnI[96-148]	20		0.03±0.02						(31)
F29W•TnI[104-116]	20		72±20						(31)
F105W•TnI[104-116]	20		75±5						(32)
[v]III/IV•TnI[104-115]	30		192±37						(33)
Apo-TnC•TnI[104-115] (^{19}F-Phe[106])	23		37±31						(34)
TnC•TnI104-115 (^{19}F-Phe[106])	23		48±18						(34)
Ca•TnC	25		~300						(17)

This chart excludes most of the information regarding homologous systems to avoid confusion. A single reference has been added (Forsén et al. see above) that includes parvalbumin and calmodulin to show the difference in driving force for binding between two similar proteins. Probes or "labels can significantly affect binding parameters between proteins" (35). Error ranges have been excluded were deemed insignificant (e.g. less than 5% of reported value) for space reasons. [a] an asterix indicates calculated values, not experimental. TnC is always skeletal unless otherwise stated (e.g. cN-TnC). [b] subject in parenthesis shows presence of ions for the free energy of binding respectively. Probe was IAE-DANS-TnC. [c] probe was IAE-Tnl. [d] IAE label on TnI. Temperature from personal communication. [e] DANZ label on TnC. [f] The values reported are for the IAE probe attached to TnC Cys[98] not the values of

the probe attached TnI Cys[133]. [g] It is important to note here that the reaction has both positive ΔH (enthalpically opposed, endothermic) and ΔS (entropically favored) and is therefore only spontaneous for temperatures *above* T=ΔH/ΔS. [h] Presence of the labels is shown to have an effect on affinities. [i] K_a is for two "classes" of calcium binding sites. [j] Protein conformational changes were much slower than the Ca^{2+} rates, k_D^{on} and k_D^{off} were 120-210 s^{-1} and 90-260 s^{-1} ($4°C$), respectively and were slowed by the use of IAANS probe on residue TnC Cys[35]. [k] After Ca^{2+} removal from low affinity (SiteI,II) sites in Tn complex. IAANS-TnI or ANS (noncovalently to TnC) was used as a probe. [l] Forsén *et. al.* (24) and references therein. [m] The value reported is lower than expected from other studies (36-39). [n] The temperature was not published. Reported value is from Dr. B. Sykes, personal communication. [o] Free energy of unfolding for apo-TnC, apo-TnC_{1-85} and calcium/magnesium saturated TnC_{95-162} could not be measured due to the mostly unstructured state of apo-C-TnC. The C-domain was estimated to be 95% unfolded at $25°C$. [p] For metal binding sites I and II, respectively. The error range of the reported Kd was ±10 and ±1 for sites I and II, also respectively. [q] Error ranges for the reported K_d were ± 500 for site I and ± 5 for site II. [r] Interestingly, they found only a single binding of the peptide to whole calcium saturated TnC. [s] Both CD ($25°$) and fluorescence ($20°$) were used. The original low affinity averaged K_ds were 2.5 mM for sTnC and 2 mM for cardiac. The cardiac peptide caused no change in C but an increase in affinity for calcium by fluorescence. The most stunning result was that addition of skeletal peptide to the cardiac protein caused a decrease in calcium affinity as if calcium binding was being blocked. [t] -11° at 2.2kbar (~2000 atmospheres). [u] F105W and F29W refer to the substitution introduced in both isolated C- and N-TnC, respectively. [v] III/IV refers to the III,IV heterodimer formed from synthetic peptides designed to mimic a pair of EF hand calcium-binding sites.

E41A   **cN-TnC**   **sN-TnC**
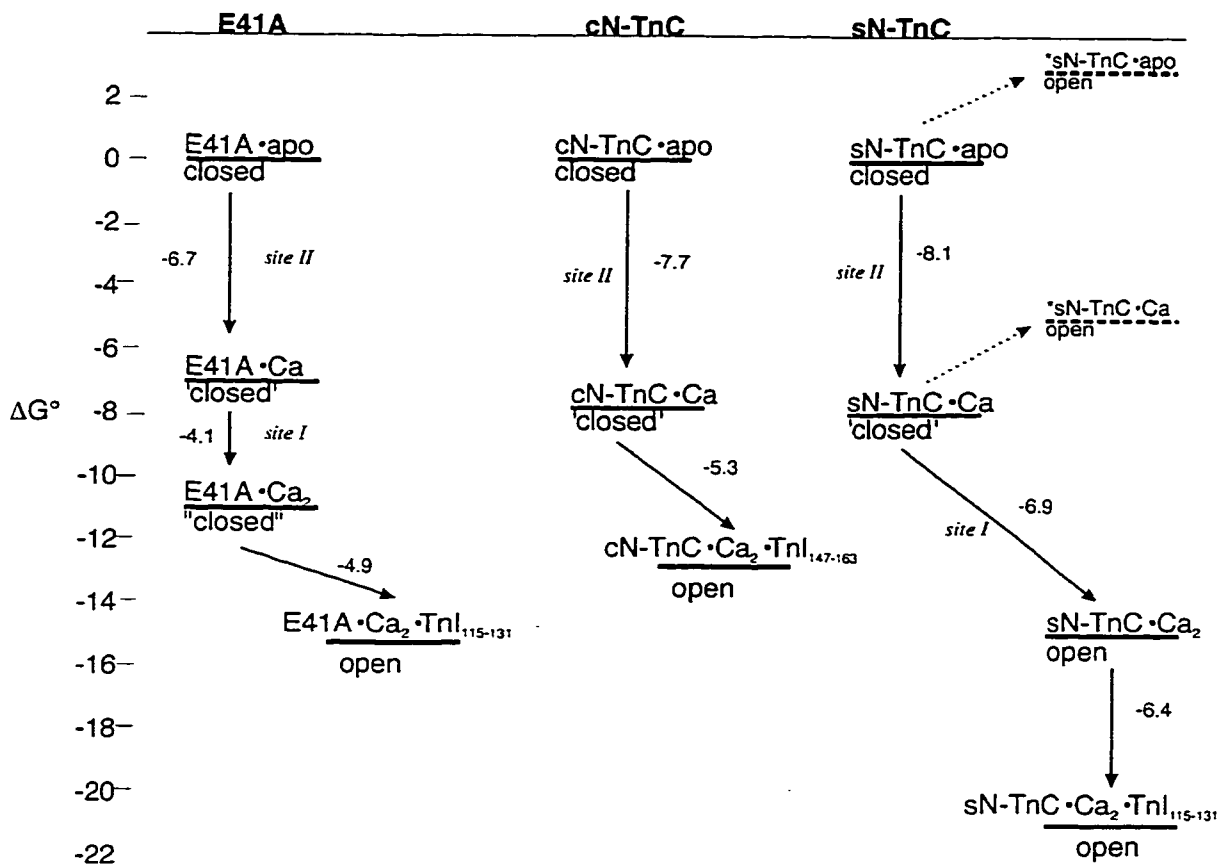

Figure V-6

Relative change in free energy (kcal/mol) of E41A sN-TnC, cN-TnC and native sN-TnC upon calcium or TnI peptide binding. The proteins were placed at zero free energy for ease of comparison of the state functions. The solid arrows mark pathways for which we have NMR-derived experimental data, while the dashed arrows indicate undetermined transitions. The use of closed, 'closed', and and "closed" indicates apo, single calcium-bound and two calcium-bound molecules (with any associated internal structural rearrangement), respectively.

This energy represents the favorable interaction of each bound calcium atom with the

residues making up both sites **I and II** (*i.e.* a single calcium ion does not just interact with

a single site), plus the unfavorable structural opening and resultant exposure of

hydrophobic residues. In comparison, binding of two equivalents of calcium to E41A,

which remains closed, is favorable by only 10.7 kcal·mol^{-1}. Therefore, the loss of the

-CH_2-CO_2^- portion of E41 costs a minimum of 4 kcal·mol^{-1} to calcium binding in sites I

and II (the two sites have been shown to be almost energetically inseparable (40,41)).

E41A may contribute much more if the rearrangements are large and unfavorable

therefore lowering the observed calcium affinity. Cardiac N-TnC binds one equivalent of

calcium, resulting in a total stabilization of cN-TnC by 7.7 kcal·mol^{-1}, and no structural

opening of the cardiac regulatory domain. The presence of the cTnI$_{147-163}$ peptide causes

cN-TnC to open. If the skeletal and cardiac peptides are assumed to have similar binding

intensity to the "open" conformation (of their respective proteins) then the reduction of

binding affinity reported for the cardiac TnI peptide would be a direct result of the energy

needed to open the calcium-saturated cN-TnC structure. The dissociation constant for

cTnI$_{147-163}$ binding to cN-TnC is 154 ± 10 µM which corresponds to 5.3 kcal·mol^{-1} and a

difference of 1.1 kcal·mol^{-1} when compared to the skeletal case. A barrier of opening of

1.1 kcal·mol^{-1} would suggest that ~16% of calcium saturated cN-TnC is open at any given

time with a kinetic rate of opening (assuming k$_{close}$ ~1x10^8 s^{-1}) in excess of 1.6 × 10^7 s^{-1}.

This is highly related to the data presented in this chapter regarding the E41A•TnI$_{115-131}$

complex which showed a $\Delta G°$ of -4.9 kcal/mol (K$_d$ of 300 ± 100 µM) or a difference

from the sN-TnC affinity of 1.5 kcal/mol. The change in chemical shifts and the

energetics data both suggest that more structural re-arrangement occurs for cN-TnC than

for E41A, and thus the energy barrier is lower[1] for the cardiac system. This is related to

the work done by Evenäs et al. on E140Q calmodulin (42). They found that calcium is

still bound tightly and established a dynamic equilibrium between the open and closed

---

[1] Assuming a similar unfavorable exposure of hydrophobic surface area.

states (~65% open corresponding to a $\Delta G°_{open}$ of -0.4 kcal·mol^{-1}) with an exchange rate of

$1-7 \times 10^4 s^{-1}$.

High-pressure fluorescence studies have estimated a 2 kcal·mol^{-1} barrier to

opening of apo F29W sN-TnC (*30*). However, this work found an exposure of 900-1600

A^2 which is 2 to 3 times the change found by NMR (*43*) and X-ray studies (*44*). The

authors state the possibility of concomitant high pressure, low temperature induced

denaturation. It remains to be determined whether the experimental $\Delta G°$ is the energy of

partial denaturation and subsequent exposure of the tryptophan residue, or a result of the

movement of the B/C helices from the NAD helical unit.

b.) Binary Interactions

A very interesting paper by Cheung *et al.* found that the affinities for the binary

complexes of troponin exceeded that of the tertiary complex (*19*). It was postulated in

the report that the weakened binary interactions were functionally related to regulation of

contraction (*i.e.* a measurement of the energetics involved in the 'on' or 'off' states).

Another explanation, especially in light of recent findings of multiple interactions, is that

the energies measured by Cheung *et al.* are the non-biologically specific interactions that

compete with the "proper" interactions present in the native troponin complex.

Specifically the affinities of TnC for TnI has been "tuned" by competing interactions

from other proteins. This statement is not meant to imply that these interactions are

unimportant or that they do not occur in the native complex. For example, if the

interactions in the binary complexes have to be broken to form the tertiary complex, then

the apparent tertiary affinity will be lower than a case where there are no energetic costs

involved. The exposed hydrophobic pockets of TnC and the heptad repeating units

occurring in TnC and TnI may unfortunately provide areas for non-biologically specific

interactions. All the interactions need to be elucidated before a full understanding of the

mechanism of regulation can be gained.

F. References

1. Li, M. X., Gagné, S. M., Spyracopoulos, L., Kloks, C. P. A. M., Audette, G., Chandra, M., Solaro, R. J., Smillie, L. B., and Sykes, B. D. (1997) *Biochemistry* **36**, 12519-25

2. Gagné, S. M., Li, M. X., and Sykes. B. D. (1997) *Biochemistry* **36**, 4386-4392

3. Kragelund, B. B., Jonsson, M., Bifulco, G., Chazin, W. J., Nilsson, H., Finn, B. E., and Linse, S. (1998) *Biochemistry* **37**, 8926-8937

4. Li, M. X., Spyracopoulos, L., and Sykes, B. D. (1999) *Submitted to Biochemistry Jan. 21,1999*

5. McKay, R. T., Tripet, B. P., Hodges, R. S., and Sykes, B. D. (1997) *J. Biol. Chem.* **272**, 28494-28500

6. Wishart, D. S., Bigam, C. G., Yao, J., Abildgaard, F., Dyson, H. J., Oldfield, E., Markley, J. L., and Sykes, B. D. (1995) *J. Biomol. NMR* **6**, 135-140

7. Muhandiram, D. R., and Kay, L. E. (1994) *J. Magn. Reson.* **B103**, 203-216

8. Farrow, N. A., Muhandiram, R., Singer, A. U., Pascal, S. M., Kay, C. M., Gish, G., Shoelson, S. E., Pawson, T., Forman-Kay, J. D., and Kay, L. E. (1994) *Biochemistry* **33**, 5984-6003

9. Delaglio, F., Grzesiek, S., Vuister, G. W., Zhu, G., Pfeifer, J., and Bax, A. (1995) *J. Biomol. NMR* **6**, 277-293

10. Garrett, D. S., Powers, R., Gronenborn, A. M., and Clore, G. M. (1991) *J. Magn. Reson.* **95**, 214-220

11. McKay, R. T., Pearlstone, J. R., Corson, D. C., Gagné, S. M., Smillie, L. B., and Sykes, B. D. (1998) *Biochemistry* **37**, 12419-30

12. McKay, R. T. (1999) *Defining the Interactions of Troponin-C with Troponin-I by Nuclear Magnetic Resonance Spectroscopy*, Ph.D. Thesis, Univ. of Alberta. **Manuscript in Preparation**, pgs.

13. Gagné, S. M., Tsuda, S., Li, M. X., Chandra, M., Smillie, L. B., and Sykes, B. D. (1994) *Prot. Sci.* **3**, 1961-1974

14. Van Eyk, J. E., Kay, C. M., and Hodges, R. S. (1991) *Biochemistry* **30**, 9974-9981

15. Spyracopoulos, L., Gagné, S. M., Li, M. X., and Sykes, B. D. (1998) *Biochemistry* **In Press**

16. Gagné, S. M., Tsuda, S., Spyracopoulos, L., Kay, L. E., and Sykes, B. D. (1998) *J. Mol. Biol.* **278**, 667-86

17. Potter, J. D., and Johnson, J. D. (1982) in *Calcium and Cell Function* (Cheung, W. Y., ed) Vol. 2, pp. 145-169, Academic Press, Inc.

18. Li, M. X., Spyracopoulos, L., and Sykes, B. D. (1998) *Biophys. J.* **74**, A51

19. Cheung, H. C., Wang, C. K., and Malik, N. A. (1987) *Biochemistry* **26**, 5904-7

20. Ingraham, R. H., and Swenson, C. A. (1984) *J Biol Chem* **259**, 9544-8

21. Wang, C. K., and Cheung, H. C. (1985) *Biophys J* **48**, 727-39

22. Hazard, A. L., Kohout, S. C., Stricker, N. L., Putkey, J. A., and Falke, J. J. (1998) *Protein Sci* **7**, 2451-9

23. Nishio, T., and Iio, T. (1983) *J Biochem (Tokyo)* **94**, 745-54

24. Forsén, S., Vogel, H. J., and Drakenberg, T. (1986) in *Calcium and Cell Function* Vol. VI, pp. 113-157, Academic Pres, Inc.

25.   Margossian, S. S., and Stafford, W. F. d. (1982) *J Biol Chem* **257**, 1160-5

26.   Cachia, P. J., Sykes, B. D., and Hodges, R. S. (1983) *Biochemistry* **22**, 4145-52

27.   Fredricksen, S. R., and Swenson, C. A. (1996) *Biochemistry* **35**, 14012-14026

28.   Li, M. X., Gagné, S. M., Tsuda, S., Kay, C. M., Smillie, L. B., and Sykes, B. D.
      (1995) *Biochemistry* **34**, 8330-8340

29.   Lan, J., Albaugh, S., and Steiner, R. F. (1989) *Biochemistry* **28**, 7380-7385

30.   Fogeul, D., Suarez, M. C., Barbosa, C., Jorge J. Rodrigues, J., Sorenson, M. M.,
      Smillie, L. B., and Silva, J. L. (1996) *Proc. Natl. Acad. Sci. U.S.A.* **93**, 10642-
      10646

31.   Pearlstone, J. R., Sykes, B. D., and Smillie. L. B. (1997) *Biochemistry* **36**, 7601-
      7606

32.   Pearlstone, J. R., and Smillie, L. B. (1995) *Biochemistry* **34**, 6932-6940

33.   Slupsky, C. M., Shaw, G. S., Campbell, A. P., and Sykes, B. D. (1992) *Protein
      Sci.* **1**, 1595-1603

34.   Campbell, A. P., Cachia, P. J., and Sykes, B. D. (1991) *Biochem. Cell Biol.* **69**,
      674-681

35.   Grabarek, Z., Leavis, P. C., Tao, T., and Gergely, J. (1984) *Biophys. J.* **45**, 261a

36.   Slupsky, C. M., Kay, C. M., Reinach, F. C., Smillie, L. B., and Sykes, B. D.
      (1995) *Biochemistry* **34**, 7365-7375

37.   Wang, C. L., Zhan, Q., Tao, T., and Gergely, J. (1987) *J Biol Chem* **262**, 9636-40

38.   Wang, C. K., Lebowitz, J., and Cheung, H. C. (1989) *Proteins* **6**, 424-30

39.   Murray, A. C., and Kay, C. M. (1972) *Biochemistry* **11**, 2622-7

40.   Tsalkova, T. N., and Privalov, P. L. (1983) *Mol Biol (Mosk)* **17**, 1042-7

41.   Tsalkova, T. N., and Privalov, P. L. (1985) *J Mol Biol* **181,** 533-44

42.   Evenas, J., Thulin, E., Malmendal, A., Forsén, S., and Carlstrom, G. (1997)

      Biochemistry **36,** 3448-3457

43.   Gagné, S. M., Tsuda, S., Li, M. X., Smillie, L. B., and Sykes, B. D. (1995) *Nature*

      Struct. Biol. **2,** 784-789

44.   Strynadka, N. C. J., Cherney, M., Sielecki, A. R., Li, M. X., Smillie, L. B., and

      James, M. N. G. (1997) *J. Mol. Biol.* **273,** 238-255

Chapter VI: Summary and Future

A great deal of information has been amassed since the inception of this thesis. For example, the structure of calcium-saturated skeletal troponin-C has been solved (*1*), confirmed and refined by additional techniques (*2,3*), and examined in detail (see (*4*) and references therein). There are published high resolution data for the cardiac homologue (*5*), and even for binary complexes (*6-8*). Other groups have continued to delineate the interacting regions of larger complexes, and to broaden studies to include other members of the thin filament (see (*9*) and references therein).

The first chapter of the thesis described the physical location, components, and present models surrounding the regulation of muscle contraction. Chapter II established the stoichiometry, location, thermodynamics, and kinetics of interaction between a TnI peptide and the regulatory domain of TnC. The location of binding was identified as the hydrophobic pocket, and the development of lineshape analysis for kinetic studies provided invaluable direction for the subsequent projects. In the third chapter the three-dimensional solution structure of the regulatory domain of TnC was solved while complexed to a TnI peptide capable of full inhibitory activity. The structure revealed subtle changes in TnC upon addition of peptide. This chapter also directly identified atoms of TnC that were within 5 Å of TnI, and confirmed that the regulatory domain of TnC and the larger TnI peptide interact through the hydrophobic pocket. A comparison was also done showing that different peptides interact with TnC in similar, but not completely identical manner. The fourth chapter expanded the study to include intact TnC and multiple TnI peptides. The chapter focused on the kinetics and energetics of TnC•TnI interaction, and also began to look directly at the TnI peptide instead of

indirectly via TnC. The exact residues of TnI$_{96-148}$ that did not interact with TnC were determined. Most importantly, more than one bound conformation of TnI while in complex with intact TnC was discovered.

The presence of multiple bound TnI conformations has broad implications. The difficulties experienced in determination of the bound N-TnC in Chapter III may be directly related. TnC could adopt a single or multiple similar structures when in complex with different forms of TnI, but even similar TnC structures would result in averaging of NOEs, slight changes in chemical shift, and add complexity to already challenging spectra analysis. Temperature, conditions, and/or concentrations may affect the relative populations of different TnC•TnI complexes. The existence of multiple bound TnI species might also account for difficulties experienced in our lab (and others) when attempting to determine the structure of TnI either isolated or in complex.

The last chapter focused on the role of Glu^{41} in the 'opening' of N-TnC. The energetics of complex formation between E41A N-TnC and a TnI peptide used in a previous study was determined, and the energetic contribution of Glu^{41} to 'opening' was derived. In addition, direct coupling between exposure of the hydrophobic pocket and formation of a favorable calcium binding site I (despite the mutation) was shown. The information presented supports the proposition that calcium binding causes structural rearrangement in TnC that lowers the energy barrier to exposure of the hydrophobic pocket.

Despite the amount of knowledge gained there are always new questions that arise from every discovery. I would like to conclude this thesis with ideas and suggestions that I have accumulated during the writing of this thesis.

The first project would involve solving the solution structure of intact TnC while in complex with TnI_{96-139}. The minimum peptide length would reduce the complexity of assignment and increase synthesis yield. The structure of TnC in the TnC•TnI complex is under debate (see Chapter I and IV) regarding the presence of an extended, semi-extended, or more compact TnC. The three-dimensional structure of both isolated domains of TnC while complexed to TnI has either been solved or is presently underway and therefore the difficulties involved in assignment would be minimal. Assignment of the backbone resonances for TnC residues in the central linker (*i.e.* central or D/E helix) should present immediate chemical shift index information regarding the presence of definable secondary structure. The acquisition of coupling constants in this region should also yield valuable structural data. It would also be interesting to determine the nature of interactions between the TnC linker and TnI residues.

Another useful experiment would be to determine if $TnI_{115-131}$ has a measurable affinity for apo-E41A. The peptide would be expected to behave similarly to the recently reported homologous cardiac system (see Chapters IV, V and (*8*)) in which the peptide is unable to bind the apo protein. However, this simple experiment may yield exciting and unexpected results.

Additional projects could include the elucidation of the region of TnI that interacts with the C-domain of TnC. Present work in our lab includes the exploration of the competition between N-terminal regions of TnI (e.g. Rp40 and TnI_{96-115}) and has resulted in re-examination of the models regarding regulation of muscle contraction. Interestingly, it has always been assumed that residue 96 of TnI was the terminal residue interacting with TnC. A study similar to the one performed in Chapter IV could explore

the N-terminal region of TnI capable of interacting with C-TnC by utilizing peptides of various lengths (*e.g.* residues 85-148, 96-148, 100-148) bound to labeled TnC. The use of specifically labeled TnI peptides could be used to explore the composition and possibility of multiple TnI structures while complexed to the C-domain of TnC.

The energetics of the troponin system have been explored (see Table V-2), but there is no information regarding direct measurement of ΔH or ΔS for the complexes involving the peptides presented in this work. Microcalorimetry could provide a great deal of this information as could NMR. NMR titrations of the presented complexes could simultaneously be performed at multiple temperatures thus allowing determination of the enthalpy and entropy. For example, at present we do not know the effect of raising the temperature on a TnC•TnI peptide complex. Spectra would be expected to improve due to decreasing τ_c. However, the spectra quality may also improve if complex formation is entropically driven (*i.e.* only favorable at higher temperatures)[1], or worsen if enthalpically driven.

The last idea I would like to suggest involves the use of a very specifically labeled TnI peptide and TnC. TnI_{96-139} would be synthesized as in Chapter IV with specifically ^{13}C-labeled methyl groups on residues suspected of interacting with TnC. TnC would also be specifically ^{13}C-labeled on residues shown previously to respond to TnI addition. The residues to be labeled would determine the type of auxotroph used for expression of TnC. Established edit/edit NMR experiments could then be used to determine the relative translational and rotational positions of the peptide in the complex via residues showing inter-molecule NOEs. This experiment would provide three-dimensional

---

[1] Table V-2 showed that TnI and TnC complex formation has been found to entropically driven.

structural information to facilitate previously proposed experiments, and would reveal if

peptide promiscuity (*i.e.* binding of peptide in a parallel and anti-parallel orientation)

exists in the TnC•TnI peptide systems.

I predict quite confidently that the troponin system will continue to provide an

ever-increasing number of exciting avenues for future work, and wish future students in

the lab all the best in their endeavors.

A. References

1.   Slupsky, C. M., and Sykes, B. D. (1995) *Biochemistry* **34**, 15953-15964

2.   Strynadka, N. C. J., Cherney, M., Sielecki, A. R., Li, M. X., Smillie, L. B., and James, M. N. G. (1997) *J. Mol. Biol.* **273**, 238-255

3.   Houdusse, A., Love, M. L., Dominguez, R., Grabarek, Z., and Cohen, C. (1997) *Structure* **5**, 1695-1711

4.   Gagné, S. M., Li, M. X., McKay, R. T., and Sykes, B. D. (1998) *Biochem. Cell Biol.* **76**, 301-12

5.   Sia, S. K., Li, M. X., Spyracopoulos, L., Gagné, S. M., Liu, W., Putkey, J. A., and Sykes, B. D. (1997) *J. Biol. Chem.* **272**, 18216-18221

6.   McKay, R. T., Pearlstone, J. R., Corson, D. C., Gagné, S. M., Smillie, L. B., and Sykes, B. D. (1998) *Biochemistry* **37**, 12419-30

7.   Vassylyev, D. G., Takeda, S., Wakatsuki, S., Maeda, K., and Maeda, Y. (1998) *Proc Natl Acad Sci U S A* **95**, 4847-52

8.   Li, M. X., Spyracopoulos, L., and Sykes, B. D. (1999) *Submitted to Biochemistry Jan. 21,1999*

9.   Malnic, B., Farah, C. S., and Reinach, F. C. (1998) *J Biol Chem* **273**, 10594-601

Appendix 1: Dissociation Constant Determination

[E] = protein conc.
[I] = peptide conc.
[EI] = complex conc.
[E_o] and [I_o] are initial protein and peptide conc., respectively.

$$K_d = [E][I]/[EI] \qquad\qquad E + I \underset{Kd}{\overset{Kel}{\rightleftharpoons}} EI$$

$$[EI] = [E_o] - [E] \qquad\qquad [E] = [E_o] - [EI]$$
$$[I] = [I_o] - [EI] \qquad\qquad [I] = [I_o] - [EI]$$
$$\therefore [I] = [I_o] - [E_o] + [E]$$

$\delta_{EI} = \delta_{bound}$ = chemical shift for the complex
δ_E = chemical shift for the protein
δ_I = chemical shift for the peptide
δ_{obs} = observed chemical shift
δ_{free} = chemical shift of unbound species
δ_{bound} = chemical shift of complex

$$^{1}\delta_{obs} - \delta_{free} = [EI]/[E_o]\delta_{EI}$$

$$[E_o](\delta_{obs} - \delta_{free})/(\delta_{bound}) = [EI]$$

$$\delta_{obs} = \delta_E [E]/[E_o] + \delta_{EI} [EI]/[E_o]$$

$$(\delta_{obs} - \delta_{free})/\delta_{bound} = [EI]/[E_o] = ([E][I])/(K_d[E_o]) = (([E_o]-[EI])([I_o]-[EI]))/(K_d[E_o])$$

$$z = \text{fraction bound} = [EI]/[E_o]$$

$$(\delta_{obs} - \delta_{free})/\delta_{bound} = ([E_o] -z[E_o])([I_o]-z[E_o])/K_d[E_o] = [EI]/[E_o] = z$$

$$z K_d = ([E_o][I_o] - z[E_o]^2 - z[E_o][I_o] - (z[E_o])^2)/ E_o$$

$$z K_d = [I_o] - z[E_o] - z[I_o] - z^2[E_o]$$
$$0 = [I_o] - z[E_o] - z[I_o] - z^2[E_o] - z K_d$$
$$0 = [I_o] - z ([E_o] + [I_o] + K_d) - z^2[E_o]$$

$$ax^2 + bx + c = 0 \qquad\qquad x = (-b \pm (b^2-4ac)^{0.5})/2a$$

$$(\delta_{obs} - \delta_{free})/\delta_{bound} = [EI]/[E_o] = -([E_o]+[I_o]+K_d) \pm ((([E_o]+[I_o]+K_d)^2-4[E_o][I_o])^{0.5})/(2E_o)$$

---

[1] Values for E_o, I_o, δ_{free}, δ_{obs}, and δ_{bound} are known.

Appendix 2: Example script used for line width analysis.

```
Definitions:

Reaction is of the type          E    +      I    <=>     EI

sites:              free                      bound
concentrations:Eo - EIIo - EIEI
dissociation constant = Kd = [E][I]/ [EI]
labels:                  A                     B

populations          pA =(Eo-EI)/Eo         pB=EI/Eo


lifetimes:           tauA=pA tauB/pB        tauB=1/koff

chemical shifts:     vA                     vB

linewidths           wA                     wB
```

(*   concentrations in mM   *)

Kd = 0.03;

EI := (((Eo + Io + Kd) -
        Sqrt[Eo Eo - 2 Eo Io + Io Io + 2 Eo Kd + 2 Io Kd + Kd Kd])/2);

pB := EI/Eo;

pA := (1 - pB);

(*   koff in sec -1   *)

tauB := 1/koff;

tau   := pA tauB;

vA = 130;   (*   shifts in Hz   *)

vB = 100;

dv := vA - vB;

Dv := 0.5 (vA + vB) - v;

wA = 10;   (*   linewidths in Hz   *)

wB = 20;

T2A := 1 / (Pi wA);

T2B := 1 / (Pi wB);

P := tau ((1/(T2A T2B)) - 4 Pi Pi Dv Dv + Pi Pi dv dv) + pB/T2B + pA/T2A;

Q := tau (2 Pi Dv - Pi dv (pA - pB));

R := 2 Pi Dv (1 + tau (1/T2A + 1/T2B)) + Pi dv tau (1/T2B -1/T2A) +
   Pi dv (pA - pB);

Int := (P (1 + tau (pB/T2A + pA/T2B)) + Q R)/ (P P + R R);

Appendix 3: Chemical Shifts of sN-Tnc in complex with TnI$_{96-148}$

1 ALA
CA   51.832
HA   4.142
CB   19.653
HB#   1.546
C   174.000
; 0.0
2 SER
CA   58.439
HA   4.527
CB   63.800
HB#   3.900
C   174.030
; 0.0
3 MET
N   999.999   # unknown
HN   999.999   # unknown
CA   56.135
HA   4.688
CB   34.060
HB1   999.999   # unknown
HB2   999.999   # unknown
CG   999.999   # unknown
HG1   999.999   # unknown
HG2   999.999   # unknown
CE   16.878
HE#   2.078
C   176.745
; 0.0
4 THR
N   115.893
HN   8.047
CA   61.375
HA   4.445
CB   70.480
HB   4.652
CG2   21.613
HG2# 1.191
C   175.105
; 0.0
5 ASP
N   123.022
HN   8.690
CA   57.415
HA   4.464
CB   40.375
HB1   2.639
HB2   2.739
CG   179.800
C   178.620
; 0.0
6 GLN
N   120.903

HN   8.888
CA   59.125
HA   4.102
CB   29.356
HB1   2.106
HB2   2.188
CG   35.458
HG1   2.352
HG2   2.505
CD   180.300
NE2   113.120
HE21 7.120
HE22 7.327
C   179.090
; 0.0
7 GLN
N   122.980
HN   7.823
CA   58.317
HA   3.939
CB   17.037
HB1   2.083
HB2   2.167
CG   33.490
HG#   2.423
CD   180.300   # predicted
NE2   112.470
HE21 7.230
HE22 7.560
C   177.825
; 0.0
8 ALA
N   124.392
HN   8.498
CA   55.080
HA   4.151
CB   18.296
HB#   1.479
C   180.995
; 0.0
9 GLU
N   120.633
HN   8.129
CA   59.122
HA   4.053
CB   29.927
HB#   2.087
CG   -5.340
HG1   2.202
HG2   2.375
CD   180.000   # predicted
C   178.755
; 0.0

10 ALA
N   123.942
HN   7.917
CA   55.533
HA   4.115
CB   18.381
HB#   1.409
C   179.130
; 0.0
11 ARG
N   116.234
HN   7.957
CA   59.685
HA   3.859
CB   30.484
HB#   1.834
CG   26.370   # predicted
HG1   1.660   # predicted
HG2   1.720   # predicted
CD   43.277
HD#   3.148
NE   999.999   # unknown
HE   999.999   # unknown
NH1   999.999   # unknown
HH11   999.999   # unknown
HH12   999.999   # unknown
NH2   999.999   # unknown
HH21   999.999   # unknown
HH22   999.999   # unknown
C   178.030
; 0.0
12 ALA
N   120.538
HN   7.679
CA   53.778
HA   4.232
CB   18.483
HB#   1.441
C   178.580
; 0.0
13 PHE
N   118.599
HN   7.656
CA   59.300
HA   4.436
CB   41.062
HB1   3.257
HB2   3.265
CE1   999.999   # unknown
CD1   999.999   # unknown
HD#   7.270   # predicted
HD1   7.290
HD2   7.310
HE#   7.380   # predicted
HE1   7.380   # predicted
HE2   7.390

CZ   999.999   # unknown
HZ   999.999   # unknown
C   175.625
HB#   3.247
; 0.0
14 LEU
N   118.897
HN   7.398
CA   53.732
HA   4.561
CB   45.273
HB1   1.526
HB2   1.948
CG   26.595
HG   2.090
CD1   28.252
HD1#   0.904
CD2   24.664
HD2#   1.098
C   175.980
; 0.0
15 SER
N   117.283
HN   7.754
CA   56.422
HA   4.622
CB   65.689
HB1   4.052
HB2   4.453
C   175.320
; 0.0
16 GLU
N   123.003
HN   9.124
CA   60.193
HA   4.017
CB   29.501
HB1   2.020
HB2   2.093
CG   36.755
HG1   2.383
HG2   2.443
CD   183.700   # predicted
C   179.640
; 0.0
17 GLU
N   120.695
HN   8.936
CA   60.130
HA   4.122
CB   29.225
HB1   1.968
HB2   2.083
CG   36.770
HG1   2.310
HG2   2.379

CD   184.400   # predicted
C   179.150
; 0.0
18 MET
N   121.289
HN   7.774
CA   58.410
HA   3.890
CB   33.162   # predicted
HB1   1.852   # predicted
HB2   2.060
CG   32.673   # predicted
HG1   2.413   # predicted
HG2   2.468   # predicted
CE   17.370
HE#   1.980
C   178.320
; 0.0
19 ILE
N   121.124
HN   8.333
CA   67.061
HA   3.755
CB   37.892
HB   2.049
CG1   28.872
HG11   1.049
HG12   1.695
CD1   13.703
HD1#   0.950
CG2   17.641
HG2#   1.221
C   177.630
; 0.0
20 ALA
N   121.872
HN   7.981
CA   55.335
HA   4.250
CB   17.924
HB#   1.555
C   180.265
; 0.0
21 GLU
N   121.611
HN   7.685
CA   58.280
HA   4.158
CB   29.092
HB1   1.960
HB2   2.080
CG   36.100   # predicted
HG1   2.180   # predicted
HG2   2.410   # predicted
CD   183.700   # predicted
C   178.825

; 0.0
22 PHE
N   119.953
HN   8.829
CA   60.560
HA   5.010
CB   37.787
HB#   3.518
CD1   999.999   # unknown
CD2   999.999   # unknown
HD#   7.200   # predicted
HD1   7.190   # predicted
HD2   7.190   # predicted
CE1   999.999   # unknown
CE2   999.999   # unknown
HE#   7.340   # predicted
HE1   7.340   # predicted
HE2   7.340   # predicted
CZ   999.999   # unknown
HZ   999.999   # unknown
C   178.650
; 0.0
23 LYS
N   125.229
HN   9.268
CA   58.557
HA   3.993
CB   31.251
HB#   1.960
CG   24.312
HG#   1.108
CD   26.941
HD1   0.255
HD2   1.404
CE   41.880
HE#   2.602
C   177.220
; 0.0
24 ALA
N   123.082
HN   7.656
CA   55.074
HA   4.245
CB   17.749
HB#   1.568
C   180.700   # predicted
; 0.0
25 ALA
N   123.007
HN   7.688
CA   53.870
HA   4.087
CB   18.463
HB#   1.762
C   177.900   # predicted
; 0.0

26 PHE
```
N      121.157      #  predicted
HN       8.882      #  predicted
CA      62.488
HA       3.217
CB      39.828
HB#      2.724
CD1    999.999      #  unknown
CD2    999.999      #  unknown
HD#      6.680      #  predicted
HD1      6.680      #  predicted
HD2      6.680      #  predicted
CE1    999.999      #  unknown
CE2    999.999      #  unknown
HE#      7.100      #  predicted
HE1      7.100
HE2      7.100      #  predicted
CZ     999.999      #  unknown
HZ     999.999      #  unknown
C      176.710
; 0.0
```
27 ASP
```
N      119.549
HN       8.489
CA      57.203
HA       4.222
CB      40.030
HB1      2.627
HB2      2.674
CG     179.800      #  predicted
C      177.920
; 0.0
```
28 MET
```
N      118.586
HN       7.460
CA      58.206
HA       4.107
CB      32.007      #  predicted
HB1      2.058      #  predicted
HB2      2.158      #  predicted
CG      33.030      #  predicted
HG1      2.408      #  predicted
HG2      2.625      #  predicted
CE      17.527      #  predicted
HE#      1.962      #  predicted
C      177.860
; 0.0
```
29 PHE
```
N      118.380
HN       7.718
CA      58.250
HA       4.195
CB      38.930      #  predicted
HB1      2.750
HB2      2.973
CD1    999.999      #  unknown
```

```
CD2    999.999      #  unknown
HD#      7.160      #  predicted
HD1      7.170      #  predicted
HD2      7.170      #  predicted
CE1    999.999      #  unknown
CE2    999.999      #  unknown
HE#    999.999      #  unknown
CZ     999.999      #  unknown
HZ     999.999      #  unknown
C      177.780
: 0.0
```
30 ASP
```
N      119.393
HN       7.998
CA      52.372
HA       4.508
CB      38.858
HB1      1.439
HB2      2.450
CG     178.800      #  predicted
C      176.640
: 0.0
```
31 ALA
```
N      130.327
HN       7.743
CA      55.063
HA       4.092
CB      19.442
HB#      1.440
C      179.100
; 0.0
```
32 ASP
```
N      114.183
HN       8.134
CA      52.896
HA       4.626
CB      39.953
HB1      2.746
HB2      3.132
CG     181.800      #  predicted
C      177.795
; 0.0
```
33 GLY
```
N      111.632
HN       8.028
CA      46.957
HA#      3.855
C      175.800
; 0.0
```
34 GLY
```
N      109.400
HN       8.137
CA      46.443
HA1      3.996
HA2      4.109
C      175.990
```

; 0.0
35 GLY
N   113.739
HN   10.722
CA   45.153
HA1   3.679
HA2   4.491
C   173.240
; 0.0
36 ASP
N   116.062
HN   7.752
CA   52.722
HA   5.140
CB   41.358
HB1   3.064
HB2   2.258
CG   179.400   # predicted
C   173.170
; 0.0
37 ILE
N   125.675
HN   9.572
CA   60.180
HA   4.952
CB   39.990
HB   1.824
CG1   27.129
HG1#   1.223
CD1   14.819
HD1#   0.444
CG2   17.882
HG2#   0.978
C   175.810
; 0.0
38 SER
N   123.864
HN   8.699
CA   56.036
HA   4.842
CB   66.624
HB1   4.034
HB2   4.513
C   175.765
; 0.0
39 THR
N   115.658
HN   9.171
CA   67.260
HA   3.825
CB   68.426
HB   4.199
CG2   23.352
HG2#   1.380
C   177.055
; 0.0

40 LYS
N   122.237
HN   7.894
CA   59.549
HA   4.139
CB   35.144
HB1   1.795
HB2   1.923
CG   24.642
HG1   1.421
HG2   1.517
CD   29.272
HD#   1.711
CE   42.050
HE#   3.017
C   180.030
; 0.0
41 GLU
N   122.691
HN   7.742
CA   59.030
HA   4.126
CB   29.840
HB1   2.360
HB2   999.999   # unknown
CG   35.800   # predicted
HG#   2.485
CD   180.000   # predicted
C   179.735
; 0.0
42 LEU
N   122.425
HN   8.759
CA   58.030
HA   4.013
CB   42.638
HB1   1.603
HB2   1.765
CG   26.672
HG   1.605
CD1   25.520   # predicted
HD1#   0.886
CD2   23.442
HD2#   0.835
C   178.770
; 0.0
43 GLY
N   106.866
HN   8.639
CA   48.345
HA1   4.012
HA2   3.598
C   175.400
; 0.0
44 THR
N   119.650

HN	7.935		
CA	67.219		
HA	3.922		
CB	69.106		
HB	4.348		
CG2	21.862		
HG2#	1.290		
C	176.540		
; 0.0			

45 VAL

N	122.664	
HN	7.392	
CA	66.624	
HA	3.580	
CB	31.552	
HB	1.936	
CG1	22.871	
HG1#	0.641	
CG2	21.265	
HG2#	0.337	
C	177.580	
; 0.0		

46 MET

N	118.390		
HN	8.354		
CA	59.525		
HA	4.000		
CB	32.070	#	predicted
HB1	1.818	#	predicted
HB2	2.068	#	predicted
CG	33.460		
HG1	2.510		
HG2	2.630		
CE	17.511		
HE#	1.923		
C	178.890		
; 0.0			

47 ARG

N	119.811		
HN	8.176		
CA	59.177		
HA	4.721		
CB	30.001		
HB1	1.948		
HB2	1.995		
CG	28.855		
HG1	1.810		
HG2	1.930		
CD	43.557		
HD#	3.226		
NE	86.000	#	predicted
HE	7.430	#	predicted
NH1	999.999	#	unknown
HH11	999.999	#	unknown
HH12	999.999	#	unknown
NH2	999.999	#	unknown

HH21	999.999	#	unknown
HH22	999.999	#	unknown
C	181.200		
; 0.0			

48 MET

N	124.347		
HN	7.867		
CA	58.976		
HA	4.245		
CB	32.512		
HB1	2.304		
HB2	2.367		
CG	32.986	#	predicted
HG1	2.615		
HG2	2.760		
CE	17.371		
HE#	2.247		
C	178.640		
; 0.0			

49 LEU

N	119.240	
HN	7.662	
CA	54.779	
HA	4.394	
CB	20.785	
HB#	1.885	
CG	-0.236	
HG	1.677	
CD1	22.867	
HD1#	0.814	
CD2	26.167	
HD2#	0.822	
C	177.300	
; 0.0		

50 GLY

N	108.174	
HN	7.837	
CA	45.787	
HA1	3.814	
HA2	4.252	
C	174.520	
; 0.0		

51 GLN

N	119.808		
HN	8.102		
CA	54.157		
HA	4.509		
CB	30.960		
HB1	1.658		
HB2	2.160		
CG	33.945		
HG1	2.125	#	predicted
HG2	2.198		
CD	180.000	#	predicted
NE2	113.610	#	predicted
HE21	7.000	#	predicted

HE22   7.300   # predicted
C   174.225
; 0.0
52 ASN
N   117.963
HN   8.677
CA   51.290
HA   5.163
CB   39.193
HB1   2.559
HB2   2.814
CG   178.100   # predicted
ND2   113.299
HD21   6.757
HD22   7.539
C   172.160
; 0.0
53 PRO
N   999.999   # unknown
CA   62.556
HA   4.791
CB   32.350
HB1   1.956
HB2   2.191
CG   999.999   # unknown
HG#   1.970
CD   50.112
HD1   3.282
HD2   3.655
C   177.815
; 0.0
54 THR
N   114.222
HN   8.666
CA   60.580
HA   4.456
CB   71.679
HB   4.753
CG2   22.217
HG2#   1.376
C   175.280
; 0.0
55 LYS
N   123.256
HN   8.819
CA   60.356
HA   3.903
CB   32.504
HB1   1.792
HB2   2.001
CG   25.025
HG#   1.499
CD   29.195
HD1   1.661
HD2   1.727
CE   42.530

HE#   3.055
C   178.340
; 0.0
56 GLU
N   118.353
HN   8.774
CA   60.597
HA   4.108
CB   18.465
HB1   1.955
HB2   2.092
CG   37.460
HG1   2.334
HG2   2.507
CD   184.600   # predicted
C   180.085
; 0.0
57 GLU
N   122.469
HN   7.755
CA   59.356
HA   3.990
CB   999.999   # unknown
HB1   999.999   # unknown
HB2   999.999   # unknown
CG   999.999   # unknown
HG#   2.363
CD   180.000   # predicted
C   179.390
; 0.0
58 LEU
N   121.065
HN   8.056
CA   58.280
HA   4.004
CB   21.422
HB#   2.130
CG   26.939
HG   1.805
CD1   23.789
HD1#   0.790
CD2   25.852
HD2#   0.879
C   178.565
; 0.0
59 ASP
N   119.562
HN   8.360
CA   57.472
HA   4.318
CB   39.999
HB1   2.646
HB2   2.721
CG   178.900   # predicted
C   178.995
; 0.0

60 ALA
N   123.353
HN   7.682
CA   55.066
HA   4.174
CB   18.422
HB#   1.506
C   180.270
: 0.0
61 ILE
N   121.532
HN   7.878
CA   65.407
HA   3.666
CB   38.175
HB   1.954
CG1   28.924   #   predicted
HG11   1.049   #   predicted
HG12   1.740
CD1   14.030
HD1#   0.810
CG2   17.556
HG2#   0.820
C   178.290
: 0.0
62 ILE
N   118.918
HN   7.530
CA   65.394
HA   3.425
CB   37.540
HB   1.982
CG1   29.294
HG11   0.978
HG12   1.741
CD1   12.884
HD1#   0.774
CG2   16.436
HG2#   0.692
C   177.760
; 0.0
63 GLU
N   119.230
HN   8.316
CA   59.387
HA   4.005
CB   29.933
HB1   2.082
HB2   2.169
CG   999.999   #   unknown
HG1   2.306
HG2   2.412
CD   180.000   #   predicted
C   178.290
; 0.0
64 GLU

N   116.378
HN   7.414
CA   58.992
HA   4.024
CB   999.999   #   unknown
HB1   2.017
HB2   2.180
CG   37.200   #   predicted
HG1   2.297
HG2   2.527
CD   184.600   #   predicted
C   178.110
; 0.0
65 VAL
N   108.269
HN   7.257
CA   61.057
HA   4.599
CB   33.175
HB   2.483
CG1   19.172
HG1#   0.893
CG2   21.965
HG2#   0.847
C   175.850
; 0.0
66 ASP
N   123.070
HN   7.718
CA   53.755
HA   4.708
CB   40.935
HB1   2.640
HB2   2.772
CG   180.000   #   predicted
C   177.305
; 0.0
67 GLU
N   128.720
HN   8.534
CA   59.362
HA   4.227
CB   21.277
HB1   2.038
HB2   2.242
CG   999.999   #   unknown
HG1   2.268
HG2   2.374
CD   180.000   #   predicted
C   176.960
; 0.0
68 ASP
N   116.022
HN   7.997
CA   52.549
HA   4.764

CB   40.370
HB1   2.771
HB2   3.133
CG   180.000   # predicted
C   177.685
; 0.0
69 GLY
N   110.220
HN   7.736
CA   47.273
HA1   3.892
HA2   3.816
C   175.340
; 0.0
70 SER
N   118.206
HN   8.553
CA   60.249
HA   4.233
CB   65.024
HB1   3.979
HB2   4.234
C   176.245
; 0.0
71 GLY
N   118.055
HN   10.991
CA   45.812
HA1   4.138
HA2   3.446
C   172.797
; 0.0
72 THR
N   108.934
HN   7.676
CA   58.294
HA   4.914
CB   73.818
HB   3.679
CG2   22.306
HG2#   1.037
C   173.615
; 0.0
73 ILE
N   126.189
HN   9.131
CA   60.562
HA   5.094
CB   40.715
HB   1.992
CG1   27.564
HG11   0.848
HG12   1.622
CD1   13.320
HD1#   0.848
CG2   18.174

HG2#   1.282
C   176.305
; 0.0
74 ASP
N   132.020
HN   9.517
CA   53.305
HA   5.282
CB   41.336
HB1   2.764
HB2   3.411
CG   178.700   # predicted
C   175.835
; 0.0
75 PHE
N   119.516
HN   8.793
CA   61.697
HA   3.468
CB   38.611
HB1   1.991
HB2   2.484
CD1   999.999   # unknown
HD#   6.690
HD1   6.680   # predicted
HD2   6.680
CE1   999.999   # unknown
HE#   7.090   # predicted
HE1   7.110
HE2   7.080
CZ   999.999   # unknown
HZ   999.999   # unknown
C   176.475
; 0.0
76 GLU
N   117.426
HN   7.754
CA   59.117
HA   3.791
CB   28.296
HB1   1.908
HB2   1.990
CG   36.080
HG#   2.351
CD   180.000   # predicted
C   180.300
; 0.0
77 GLU
N   120.545
HN   8.205
CA   58.076
HA   4.147
CB   29.890
HB#   1.970
CG   999.999   # unknown
HG1   2.340

HG2	2.453	
CD	180.000	# predicted
C	178.800	
; 0.0		
78 PHE		
N	123.245	
HN	8.822	
CA	61.337	
HA	3.996	
CB	40.085	
HB1	3.195	
HB2	3.487	
CD1	999.999	# unknown
CD2	999.999	# unknown
HD#	7.100	# predicted
HD1	7.100	# predicted
HD2	7.100	# predicted
CE1	999.999	# unknown
HE#	7.270	# predicted
HE1	7.280	# predicted
HE2	7.280	# predicted
CZ	999.999	# unknown
HZ	999.999	# unknown
C	177.305	
: 0.0		
79 LEU		
N	119.867	
HN	8.002	
CA	58.162	
HA	3.442	
CB	20.109	
HB1	0.880	
HB2	1.999	
CG	25.100	# predicted
HG	1.108	
CD1	26.027	
HD1#	0.563	
CD2	23.507	
HD2#	0.604	
C	179.145	
; 0.0		
80 VAL		
N	119.977	
HN	7.282	
CA	67.284	
HA	3.270	
CB	31.202	
HB	2.431	
CG1	21.467	
HG1#	0.831	
CG2	24.059	
HG2#	1.072	
C	178.180	
; 0.0		
81 MET		
N	120.975	

HN	7.900	
CA	59.432	
HA	3.685	
CB	33.472	
HB1	1.976	
HB2	2.160	# predicted
CG	31.587	
HG1	2.180	# predicted
HG2	2.448	
CE	17.441	
HE#	1.797	
C	178.310	
; 0.0		
82 MET		
N	118.197	
HN	8.041	
CA	56.230	
HA	4.076	
CB	32.498	
HB1	0.850	
HB2	1.393	
CG	32.983	# predicted
HG1	1.083	
HG2	1.560	# predicted
CE	999.999	# unknown
HE#	999.999	# unknown
C	179.165	
; 0.0		
83 VAL		
N	122.251	
HN	8.432	
CA	67.255	
HA	3.651	
CB	31.531	
HB	2.041	
CG1	21.653	
HG1#	0.667	
CG2	24.438	
HG2#	1.174	
C	178.170	
; 0.0		
84 ARG		
N	120.535	
HN	8.103	
CA	58.060	
HA	4.030	
CB	30.122	
HB#	1.823	
CG	27.460	# predicted
HG1	1.570	
HG2	1.790	# predicted
CD	43.698	# predicted
HD#	3.010	
NE	85.700	# predicted
HE	7.190	# predicted
NH1	999.999	# unknown

```
HH11    999.999      #  unknown
HH12    999.999      #  unknown
NH2     999.999      #  unknown
HH21    999.999      #  unknown
HH22    999.999      #  unknown
C       178.710
; 0.0
85 GLN
N       117.465
HN        7.492
CA       57.514
HA        4.197
CB      999.999      #  unknown
HB1     999.999      #  unknown
HB2       2.140      #  predicted
CG       33.500      #  predicted
HG1       2.390      #  predicted
HG2       2.470      #  predicted
CD      179.500      #  predicted
NE2     111.890      #  predicted
HE21      6.725      #  predicted
HE22      7.370      #  predicted
C       177.905
; 0.0
86 MET
N       120.070
HN        7.970
CA       59.397
HA        4.010
CB       30.110
HB1       2.140
HB2       2.365      #  predicted
CG       32.478      #  predicted
HG1       2.687      #  predicted
HG2       2.870      #  predicted
CE       17.392
HE#       2.250
C       179.365
; 0.0
87 LYS
N       121.040
HN        8.056
CA       58.042
HA        4.164
CB       33.193
HB1       1.692
HB2       1.803
CG       25.543
HG1       1.219
HG2       1.357
CD      999.999      #  unknown
HD1     999.999      #  unknown
HD2     999.999      #  unknown
CE      999.999      #  unknown
HE1     999.999      #  unknown
HE2     999.999      #  unknown
```

```
C       177.325
; 0.0
88 GLU
N       121.356
HN        7.857
CA       57.425
HA        4.230
CB       30.298
HB1       2.026
HB2       2.096
CG       36.420
HG1       2.291
HG2       2.360
CD      180.000      #  predicted
C       176.595
; 0.0
89 ASP
N       122.122
HN        8.084
CA       54.643
HA        4.649
CB       41.508
HB1       2.649
HB2       2.797
CG      180.600      #  predicted
C       175.020
; 0.0
90 ALA
N       130.339
HN        7.601
CA       54.156
HA        4.130
CB       20.168
HB#       1.385
C       170.540
; 0.0
```

```
# Total atoms in shift file    :   1026
# Atoms assigned in shift file :   832   ( 81.0916
)
# Atoms unknown in shift file  :   80
```